Defining the Chemical and Molecular Mechanisms of Cytotoxicity Induced by the Endoperoxide Class of Antimalarials

This thesis is submitted in accordance with the requirements of the University of Liverpool for the degree Doctor of Philosophy

By

James William Firman

February 2015

Declaration

This thesis is the result of my own work. The material contained within has not been presented, nor is currently being presented, either wholly or in part for any other degree or qualification.

James William Firman

This research was carried out in the Department of Chemistry and the Department of Pharmacology and Therapeutics at the University of Liverpool, and at the MRC Toxicology Unit, Leicester.

Acknowledgements

I would like to offer sincere thanks to my supervisors in acknowledgement of the assistance and direction which they have provided over the course of this project. I must first express my gratitude to Dr Amy Chadwick, whose support and guidance has proven invaluable from the very first day. This appreciation is extended towards Prof. Kevin Park and Prof. Marion MacFarlane, the input and perspectives of whom have served great utility throughout.

Recognition must be afforded to the many others whose help and expertise have further facilitated the progression of this research. I would like particularly to confer thanks to Prof. Kelvin Cain and Dr Xiao-Ming Sun, to Dr Chandra Pidathala and Prof. Paul O'Neill and to Dr Ian Copple. Their combined aid has been of great benefit.

This experience has been made all the more memorable on account of the friends with whom I have been fortunate enough to make acquaintance over the duration of study. Amongst many, special thanks are reserved for Phil, Luke, Oisin, Bhav, Jon, Mike, Jack, George, William, Mariama and Claire, in recognition both of the laughter and of the deep, spiritual conversation which they have provided.

I must finish by thanking all of those folks back home and further afield who have given me their encouragement and companionship, both over the preceding four years and also beyond. Particular appreciation is kept for Joe, Dave, Micheal, Sam, Tom, and for anybody who has ridden with the CTC. I would like finally to show my immense gratitude towards my family – my grandad and most notably my mum – for the continued support afforded towards my endeavours, both academic and otherwise.

Contents

Abstract

Artemisinin-derived endoperoxide drugs find widespread employment as frontline treatment against malaria. Although evidence of their potential to express toxicity within a clinical setting remains limited, outcomes derived from animal studies attest their ability to induce neurological and developmental toxicity in mammalian systems. Activity is further demonstrated *in vitro* within rapidly proliferating human cells – most notably those belonging to immortalised, cancer-derived lines – with significant cytotoxic effects being observed upon drug treatment across a range of settings. It is believed that these find their origin through a mechanism dependent upon Fe(II)-mediated reduction of the endoperoxide bridge functionality, culminating in molecular bioactivation and the subsequent formation of carbon-centred free radical species which in turn, owing to their great reactivity, impart deleterious effects upon cellular functioning. Evidence suggests that dysfunction of the mitochondrion and the formation of reactive oxygen species (ROS) are key stages in the route through which artemisinin derivatives are able to induce death.

The characteristics of artesunate-stimulated impact upon mitochondrial functioning are examined. It is demonstrated that culturing of cells in the presence of galactose enhances cytotoxic potential within the HeLa line. The magnitude of this variation in sensitivity is indicative that targeting of the mitochondrion affords a route through which activity is mediated. Falls in cell viability are further preceded by declines in ATP production, providing evidence that disruption of oxidative phosphorylation occurs as an early event in the route towards death. Studies performed on mitochondrial bioenergetic function using the Seahorse XF analyser indicate that artesunate imparts dose-dependent and time-dependent decreases in respiratory reserve capacity and oxidative phosphorylation coupling efficiency, whilst stimulating a switch towards glycolytic energy production.

Attempts to delineate the root causes of these effects are focused upon examining the relationship between oxidative stress, Fe(II) content and mitochondrial performance. The mitochondrially-localised antioxidant tiron and the lysosomal Fe(II) chelator desferrioxamine are shown to induce substantial cytoprotective effects against artesunate within the HeLa line. Evidence derived from Seahorse XF analysis indicates strongly that these outcomes are related to the capacity of both compounds to abrogate drug impact upon the functions of the mitochondrion. It can thus be posited that mitochondrial damage has its origins in the emergence of oxidative stress, with Fe(II) content acting as key determinant in its progression. The outcomes of further examinations performed within the ρ^0 HeLa line suggest an origin for ROS emergence independent of the respiratory chain.

In order to test the hypothesis that artemisinin derivatives might induce direct peroxidation of the mitochondrial phospholipid cardiolipin, the impact of a cytochrome c peroxidase inhibitor TPP-IOA is examined on the response of HeLa and HL-60 cells towards artesunate treatment. Results indicate that the inhibitor has variable effects upon cardiolipin oxidation state and subsequent cell survival, leaving doubt as to the true validity of such a connection. As a further study, the cytotoxic capacities of a range of novel artemisinin-derived anticancer agents and wholly synthetic tetraoxane and trioxolane antimalarials are given assessment.

In conclusion, it can be stated that the outcomes of the studies performed in this thesis emphasise the importance of mitochondrial liability towards the progression of artemisinin-induced cell death. Further insights into the mechanistic routes through which drug administration contributes, *via* oxidative stress and free Fe(II) content, to the defective functioning of the organelle have been achieved.

Publications

Papers

Copple, I.M., Mercer, A.E., **Firman, J.W.**, Donegan, G., Herpers, B., Wong, M.H.L., Chadwick, J., Bringela, A.D., Cristiano, M.L.S., van de Water, B., Ward, S.A., O'Neill, P.M., Park, B.K. Examination of the cytotoxic and embryotoxic potential and underlying mechanisms of next-generation synthetic trioxolane and tetraoxane antimalarials. *Mol. Med.* 2012, 18 (7), 1045-1055.

La Pensee, L., Sabbani, S., Sharma, R., Bhamra, I., Shore, E., Chadwick, A.E., Berry, N.G., **Firman, J.W.**, Araujo N.C., Cabral, L., Cristiano, M.L.S., Bateman, C., Janneh, O., Gavrila, A., Wu, Y., Hussain, A., Ward, S.A., Stocks, P.A., Cosstick, R., O'Neill, P.M. Artemisinin–polypyrrole conjugates: Synthesis, DNA binding studies and preliminary antiproliferative evaluation. *ChedMedChem***.** 2013, 8 (5), 709-718.

List of Abbreviations

2-DG	2-Deoxyglucose
ACT	Artemisinin-based combination therapy
ALA	Aminolevulinic acid
APAF-1	Apoptotic protease activating factor 1
BSA	Bovine serum albumin
$CDCl_3$	Deuterated chloroform
CoQ_{10}	Ubiquinone
DCC	*N,N*-Dicyclohexylcarbodiimide
DCFH-DA	Dichloro-dihydro-fluorescein diacetate
DCM	Dichloromethane
DDM	n-Dodecylmaltoside
DFO	Desferrioxamine
DHA	Dihydroartemisinin
DHE	Dihydroethidium
DMAP	Dimethylaminopyridine
DMEM	Dulbecco's Modified Eagle's Medium
DMF	*N,N*-Dimethylformamide
DMSO	Dimethylsulphoxide
DPI	Diphenyleneiodonium
ECAR	Extracellular acidification rate
EGTA	Ethylene glycol tetraacetic acid
EPR	Electron paramagnetic resonance
FACS	Fluorescence activated cell sorting
FBS	Foetal Bovine Serum
FCCP	Carbonyl cyanide-p-trifluoromethoxyphenylhydrazone
FSC	Forward scatter
HB27	Immortalised breast cancer-derived cell line
HBSS	Hanks' balanced salt solution
HeLa	Immortalised cervical carcinoma-derived cell line
Hep G2	Immortalised hepatocellular carcinoma-derived cell line
HEPES	(4-(2-Hydroxyethyl)-1-piperazineethanesulphonic acid
HL-60	Immortalised promyelocytic cancer-derived cell line
IC_{50}	Half-maximal inhibitory concentration
INT	Iodonitrotetrazolium chloride
Jurkat	Immortalised T-lymphoblastic cell line
LC-MS	Liquid chromatography-mass spectrometry
MMP	Matrix metalloproteinase
Molt-4	Immortalised T-lymphoblastic cell line
MOPS	3-(N-morpholino)propansulphonic acid
MP-1	Microperoxidase-11
MTT	3-(4,5-Dimethylthiazol-2-yl)-2,5-diphenyltetrazolium bromide

NAO	Nonyl acridine orange
NCI	National Cancer Institute (USA)
NMR	Nuclear magnetic resonance
Nrf2	Nuclear factor erythroid 2-related factor
OCR	Oxygen consumption rate
PBMC	Peripheral blood mononuclear cell
PfATPase6	Plasmodium Falciparum ATPase 6
PFDHA	10*β*-(*p*-Fluorophenoxy)dihydroartemisinin
PI	Propidium iodide
RCF	Relative centrifugal force
ROS	Reactive oxygen species
RPMI	Roswell Park Memorial Institute medium
RT	Room temperature
SD	Standard deviation from the mean
SDH	Succinate dehydrogenase
SDS	Sodium dodecyl sulphate
SERCA	Sarco/endoplasmic reticulum Ca^{2+}-ATPase
SSC	Side scatter
TEMPOL	4-Hydroxy-2,2,6,6-tetramethylpiperidin-1-oxyl
TMRE	Tetramethylrhodamine ethyl ester
VEGF	Vascular endothelial growth factor
WHO	World Health Organisation

Chapter One

General Introduction

1.1. Introduction

Artemisinin-derived endoperoxide drugs are routinely employed as frontline treatment in the fight against malaria. Their use in combination regimens provides highly effective therapy against parasite strains displaying resistance to other drug classes (WHO, 2010). Despite their high therapeutic efficacy and excellent safety profile within a clinical setting, concerns regarding their administration have emerged as a consequence of evidence outlining their ability to induce toxicity across animal models (Efferth *et al.*, 2010). It has now become established that these compounds possess significant levels of activity against proliferating mammalian cells, such as those found within cancer cell lines (Firestone *et al.*, 2009). Research has demonstrated that such effects occur as a consequence of an ability to induce the formation of reactive oxygen species (ROS) and apoptotic cell death through a mechanism held to be dependent upon mitochondrial dysfunction (Mercer *et al.*, 2011; Mercer *et al.*, 2007). Within this chapter, current understanding as to the route through which these drugs are believed to impact upon cell function shall be given detailed review, in order to provide background and context for the studies into the mechanistic aspects of their activity which shall be presented in this thesis.

1.2. Discovery of Artemisinin

Artemisinin **(1)**, known alternatively as qinghaosu, is a sesquiterpene lactone compound characterised by the presence of an endoperoxide bridge functionality. Occurring naturally within the leaves of the wormwood *Artemisia annua*, it has for millennia been used in Chinese folk medicine for the treatment of fevers and other maladies (Cui *et al.*, 2009). Its employment against malaria has been described in literature dating back to the fourth century AD, with the purported efficacy of *Artemisia annua* preparations being attested in

numerous medical manuscripts. The earliest modern, scientific assessments into the clinical antimalarial effectiveness of the plant were performed during the late 1960s as part of a scheme by the Chinese government to develop novel modes of treatment for the disease. Having emerged as the lead amongst an array of other traditional therapies examined, by 1972 work performed by the group of Tu YouYou had led to the identification, characterisation and isolation of artemisinin as the active antiparasitic compound (Tu, 2011). Purified directly from leaves at a low initial yield, its promising activity in early *in vivo* investigations led to its eventual employment in a clinical setting.

1.3. Artemisinin the Antimalarial

1.3.1. Disease Profile of Malaria

Malaria is a disease which occurs as a consequence of infection by protozoal parasites of the genus *Plasmodium*. Carried and transmitted by mosquitoes, it constitutes a major health risk across the tropical and subtropical regions throughout which it is endemic. It is estimated that in excess of 200 million cases are reported annually worldwide, with roughly half a million of these culminating in fatality (WHO, 2010). Instances of malaria are classified as either severe or uncomplicated, with progression of the disease dictated through factors related both to the general health status of the patient and to the identity of the parasite responsible for the infection. Severe malaria is associated overwhelmingly with the species *P. falciparum*, which constitutes the most prevalent *Plasmodium* form. *P. malariae*, *P. ovale*, *P. knowlesi* and *P. vivax* are encountered with smaller frequency, and result generally in a milder, uncomplicated variety of the illness.

Typically, the anopheles mosquito functions as the transmission vector for *Plasmodium*. Entry into man results from the bite of the female as it takes up a blood meal, injecting the

parasite within its saliva. Development of the condition occurs alongside the changes associated with the parasitic life cycle following transferral to the bloodstream. At the earliest phase, infective sporozoites locate to hepatocytes, where they reproduce asexually to form merozoites. The release of these merozoites precedes their entry into ethyrocytes, where they commence a multiplication process culminating in the destruction of the cell and a continuation of the cycle of infection and reproduction. Symptoms of malaria are usually noted 7 – 14 days following initial infection, passing first through stages of general malaise and illness before developing into characteristic paroxysmal fevers. In instances of severe disease, complications including anaemia, cerebral malaria and renal failure – any of which may be fatal – are often observed within the patient.

1.3.2. Antimalarial Treatment

Quinine, a naturally-occurring alkaloid prevalent in the bark of *Cinchona*, was the earliest antimalarial to find common use within the West. Its structure forms the basis of the class of synthetic agents referred to as quinolines, which contain the widely-employed antimalarials chloroquine, mefloquine and amodiaquine. Their common mechanism of action is believed to be centred upon disruption of the parasite feeding process within red blood cells (Foley *et al.*, 1998). The degradation of haemoglobin is necessary for the obtaining of amino acids required for growth, although the toxicity of haem Fe(II) towards *Plasmodium* warrants the crystallisation of this species into non-toxic hemozoin. Quinolines act to prevent the formation of this hemozoin, causing parasite death through the eventual harmful accumulation of haem Fe(II) (Loria et al., 1999).

The safety, efficacy and cost-effectiveness of chloroquine led to its emergence as frontline treatment against malaria. A growth in parasite resistance contributed to a fall in the effectiveness of both this and other quinoline compounds, prompting the development of

combination therapies centred upon drug classes with variant mechanisms of action (Hyde, 2002). Favourable treatment outcomes have been witnessed upon the co-administration of antifolates such as sulphadoxine and pyrimethamine, and although resistance to this combination has itself developed, it continues to find use alongside other agents (WHO, 2010). An alternative route through which treatment might be used in order to lower the threat of acquiring malaria is that of suppressive prophylaxis (Freedman, 2008). Regimens incorporating drugs such as the tetracycline antibiotic doxycycline, which act upon the parasite erythrocytic phase, are administered over a period extending both prior to and following the risk of disease exposure.

1.3.3. The Development of Artemisinin as Antimalarial Therapy

Although artemisinin had been identified for its antimalarial efficacy by the early 1970s, knowledge of its discovery was slow to emerge from out of the closed Chinese state. Difficulties associated with the poor solubility of the isolated compound across water-based and organic-based systems spurred within China the development of the semi-synthetic derivatives which have since found widespread clinical use (Klayman, 1985). Functionalisation of dihydroartemisinin (DHA) **(2)**, formed from lactone reduction of the natural product, led to the creation of the familiar drugs artemether **(3)**, arteether **(4)** and artesunate **(5)** (Meshnick *et al.*, 1996). Metabolism of these compounds *in vivo* occurs primarily through means of oxidation mediated by cytochrome P450 enzymes CYP 2B6 and CYP 3A4, serving to yield DHA as the active antiparasitic agent (Aweeka *et al.*, 2008). Rapid rates of clearance are apparent within man, with elimination occurring at half-lives typically of the order 2 – 5 hours (Benakis *et al.*, 1997). Levels of plasma protein binding are observed to be elevated, with the bound drug fraction estimated to account for greater than 90% of that in general circulation (Sidhu *et al.*, 1997). Administration of the drugs may proceed through oral, rectal or intramuscular routes. Artesunate, furthermore, owing to its

enhanced water solubility, may be given intravenously within a sodium salt formulation. Capable of providing rapid action against severe *P. Falciparum* malaria when delivered in such a manner, it remains generally the preferred treatment option in instances where acute remedy is required (Newton *et al.*, 2006).

Twenty years following the initial characterisation of artemisinin, reports into its properties had spread outside of China. During the mid-1990s, the first-generation derivatives were assessed in large-scale trials by European drug companies for their potential employment upon the global market (Faurant, 2011). Although they were shown to be highly effective in monotherapy, it was apparent that enhanced clinical efficacy and reduced sensitivity towards parasite resistance could be attained through their use in combination with other drugs. Numerous artemisinin combination therapy (ACT) regimens have since been developed, exploiting the varying modes of antimalarial action across several other therapeutic classes (Sinclair *et al.*, 2009). Artesunate is recommended for use alongside either of the quinolines mefloquine or amodiaquine, and it may also be administered accompanied by the antifolate combination sulphadoxine-pyrimethamine (Eastman *et al.*, 2009). Artemether and lumefantrine, as well as dihydroartemisinin and piperaquine, have also found clinical employment. Such partnerships exploit the comparatively lengthy half-lives of the compounds accompanying artemisinin in order to facilitate the advancement of dosing regimens which typically function to enable successful therapeutic resolution following three-day treatment courses (Nosten *et al.*, 2007).

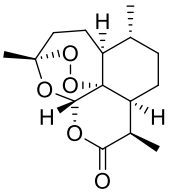

1

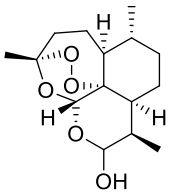

2

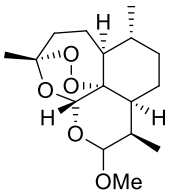

3

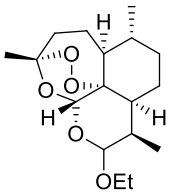

4

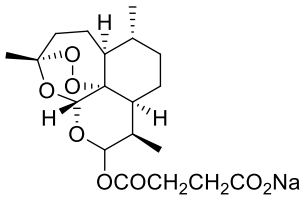

5

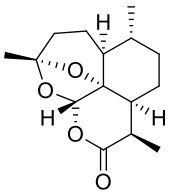

6

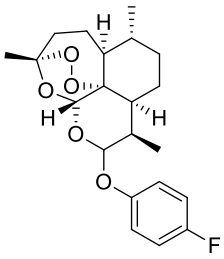

7

ACT is now considered the first line of treatment against *P. Falciparum* malaria. Artemisinin derivatives have been found to exhibit a general absence of clinical toxicity in man, accompanied by a high level of efficacy against parasite strains displaying broad resistance towards other drug classes (Park *et al.*, 1998; WHO, 2010). Whilst isolated reports of localised resistance have emerged in the literature, confinement of their use to combination strategies has prevented the emergence of significant spread.

1.3.4. Mechanism of Artemisinin Antimalarial Action

Although the precise mechanism through which artemisinin exerts its antiparasitic effects has not been definitively established, it is apparent that the presence of the endoperoxide bridge is a necessary feature for its activity (O'Neill *et al.*, 2004). It has been demonstrated

conclusively, through studies performed with compounds such as deoxyartemisinin **(6)**, that removal of this functionality deprives the compound of antimalarial properties (Klayman, 1985). It is commonly held that sources of chelatable and haem-bound Fe(II) are responsible for activating the molecule through reduction of the bridge, inducing the structural changes which lend it biological action (Mercer, 2009).

A number of potential routes through which artemisinin might induce the onset of parasite death have been identified. Research has demonstrated the ability to target several areas of *Plasmodium* function, ranging from the activities of enzymes such as the Sarco/endoplasmic reticulum Ca^{2+}-ATPase (SERCA) PfATP6, to pathways related to the detoxification of haem (O'Neill *et al.*, 2010b). Elevated oxidative stress and dysfunction of the mitochondrion have been observed additionally in several studies (Firestone *et al.*, 2009). It is currently uncertain as to whether antimalarial activity is mediated through impact upon a single target, or whether it arises as a consequence of simultaneous action upon several. It is widely believed that the mechanism of drug action is dependent upon Fe(II) activation. The relationship between the chemistry of artemisinin bioactivation and therapeutic activity shall now be considered with reference to each of its postulated targets. Alternative, Fe(II)-independent theories as regards to drug action also exist within the literature. A consideration of these shall additionally be presented

1.3.4.1. Endoperoxide Bioactivation and Carbon-Centred Radical Species

The endoperoxide bridge is identified as the key pharmacophoric and toxicophoric group within artemisinin-derived compounds. It has traditionally been held that the formation of reactive carbon-centred radicals is of central importance towards antiparasitic activity. Studies into its chemistry have elucidated routes through which Fe(II)-mediated reduction induces bioactivation of the molecule and the formation of free radical species (Fig. 1.1.)

(Haynes *et al.*, 1996; Wu *et al.*, 1998). Interaction of Fe(II) with the bridge may commence through association between the metal ion and either of the two constituent oxygen atoms. Reaction with oxygen 1 has been shown to proceed *via* the oxyl radical intermediate **(1a)**, before a rearrangement through C-C scission culminates in the generation of the primary carbon-centred radical **(1b)**. Alternatively, it has been demonstrated that the initial interaction between Fe(II) and oxygen 2 grants formation of the oxyl radical **(1d)**, which furnishes secondary carbon-centred radical species **(1e)** courtesy of 1,5 hydrogen-shift. In each instance, further progression to the stable products **(1c)** and **(1f)** is possible. Many of the proposed intermediates in these mechanisms have been identified through electron paramagnetic resonance (EPR) studies employing spin-traps (O'Neill *et al.*, 2000).

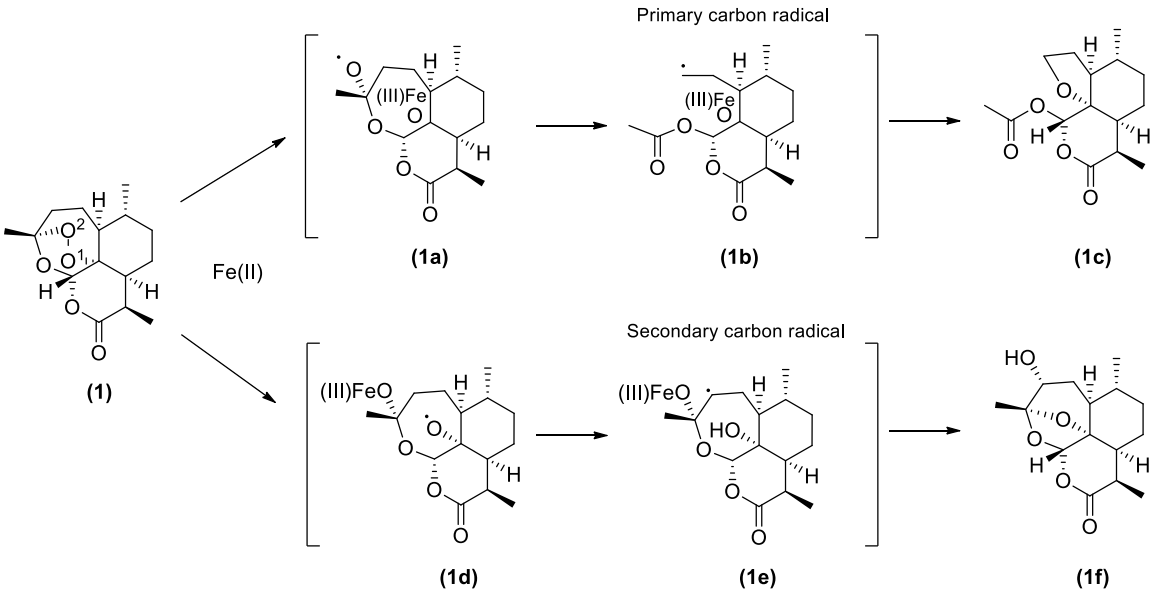

Figure 1.1. Proposed mechanism carbon-centred radical formation through Fe(II)-mediated endoperoxide bridge bioactivation. Adapted from Mercer *et al.*, 2007.

Although it was initially believed that haem Fe(II) within the parasitic food vacuole functioned as the reducing source for these degradations, the antagonistic effect of the

chelator desferrioxamine (DFO) towards antimalarial activity has suggested an additional activatory role for free Fe(II) (Stocks *et al.*, 2007).

1.3.4.2. Endoperoxide Bioactivation and the Open Peroxide Model

As an alternative to the carbon radical theory, it has been postulated that endoperoxide bridge activation proceeds *via* a mechanism reliant upon ionic ring opening. According to this hypothesis, Fe(II) functions as a Lewis acid, donating an electron to either of the constituent oxygen atoms and initiating the splitting of the bridge (Fig. 1.2.) (Haynes *et al.*, 2007; Haynes *et al.*, 1999; Olliaro *et al.*, 2001). The resulting zwitterion **(1g)** may react with a water molecule, generating reactive hydroperoxide species **(1h)** capable of direct oxidation of protein residues. It is additionally forwarded that such an intermediate may participate in Fenton-style reactions to produce quantities of the hydroxyl radical OH•. Further decomposition routes culminate in the formation of the secondary carbon-centred radical **(1e)** and the deoxyartemisinin **(1i)**.

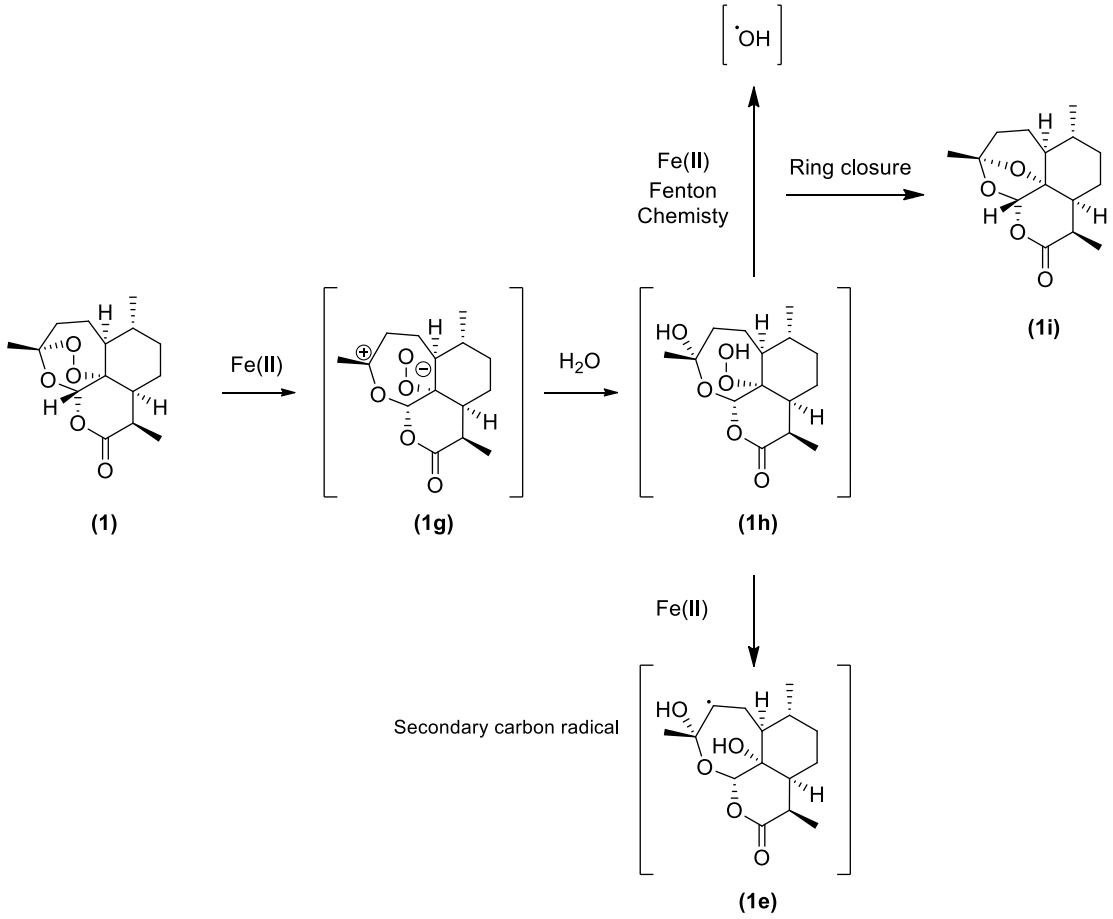

Figure 1.2. Bioactivation of the endoperoxide bridge and subsequent radical formation in the open peroxide model. Adapted from O'Neill *et al.*, 2010.

Along with the carbon-centred radical species described previously, these decomposition products are hypothesised as being involved in the process of parasite killing. Their reactivity is believed to afford them the ability to alkylate biologically active molecules, inducing alterations in structure which render them and the pathways dependent upon them dysfunctional (O'Neill *et al.*, 2010b).

1.3.4.3. Artemisinin and Haem Targets

The formation of haem-artemisinin adducts has been demonstrated to occur in biomimetic, *in vitro* and *in vivo* systems (Cazelles *et al.*, 2001; Robert *et al.*, 2005; Yang *et al.*, 1994).

Structural modifications arising from drug alkylation are identified at the α, β and δ carbon atoms of the haem prosthetic group (Robert *et al.*, 2001). Whilst this evidence attests to the capacity of artemisinin-derived radical species to form molecular conjugates, it does not provide indication that such modifications are of direct pharmacological relevance. Accordingly, whilst a link between haem adduction and the inhibition of hemozoin formation might appear feasible, conclusive evidence supporting such a hypothesis has yet to be produced. Adduct formation is further known to occur in parasite haemoproteins, including catalase and cytochrome c, although once again consequences as regards to drug activity remain undefined (Yang *et al.*, 1994).

1.3.4.4. Artemisinin and Thiol Targets

An ability to induce the alkylation of thiol groups has been confirmed, prompting examination into interaction between artemisinin and cysteine-containing proteins (Wu *et al.*, 2003). The adduction of albumin has been demonstrated, mediated through drug interaction with both cysteine and amino residues (Yang *et al.*, 1993). Interference with the function of the papain cysteine proteases, employed by parasites for the purposes of haemoglobin degradation, has additionally been identified as a means through which antimalarial activity might be exerted (Liu *et al.*, 2011b).

1.3.4.5. PfATP6 and Artemisinin

PfATP6, the parasitic analogue of the endoplasmic reticulum calcium ATPase SERCA, is recognised as a target for artemisinin. An ability to inhibit the activity of the enzyme was demonstrated through a study in which expression of the coding gene was amplified within frog eggs (Eckstein-Ludwig *et al.*, 2003). Abrogation of drug inhibitory effects was achieved

through the co-administration of the iron chelator DFO, suggesting Fe(II) activation as a required mechanistic feature. The relevance of any artemisinin-induced impairment in PfATP6 function towards parasitic survival remains unclear. Whilst altered calcium homeostasis has been observed within *Toxoplasma gondii*, effects upon endoplasmic reticulum morphology have been shown to be considerably smaller than those induced through the more potent SERCA inhibitor thapsigargin (Jones-Brando *et al.*, 2006; O'Neill *et al.*, 2010b). More recent evidence has cast additional doubts over the ability of artemisinin to fully affect enzymatic function, ensuring that any potential role for it in explaining antimalarial efficacy remains controversial (Arnou *et al.*, 2011).

1.3.4.6. Artemisinin-Induced Oxidative Stress

Increases in oxidative stress have been indentified upon artemisinin treatment. As shall be discussed later, it is well established that the formation of ROS is central to the mechanism of cytotoxicity in mammalian systems (Mercer *et al.*, 2010). Varying hypotheses regarding means of onset and importance towards parasite killing have been posited. Following the initial observation of a link between drug administration and the emergence of lipid peroxidation, it has been suggested that such modifications might produce deleterious effects upon the parasite through inducing injury within the food vacuole (Berman *et al.*, 1997; del Pilar Crespo *et al.*, 2008). A potential chemical explanation for this event has been ventured courtesy of a proposed mechanism reliant upon carbon-centred radical-mediated hydrogen abstraction at unsaturated lipid chains, culminating in the formation of peroxides upon interaction with oxygen (Fig. 1.3.) (O'Neill *et al.*, 2004).

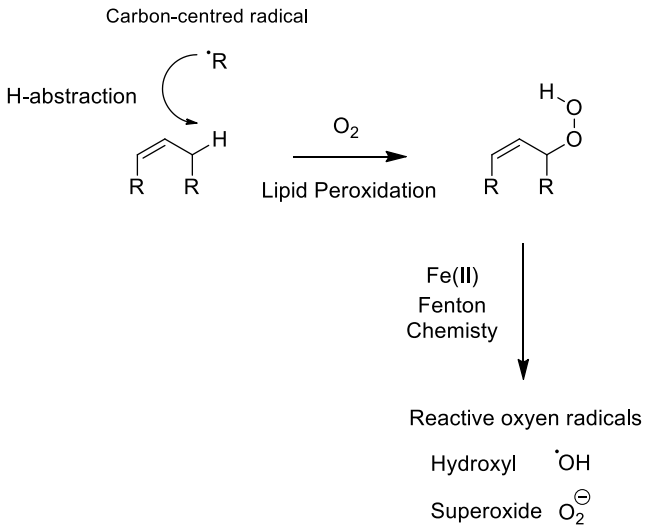

Figure 1.3. Peroxidation of lipids through artemisinin-derived radical species. Adapted from O'Neill *et al.*, 2004.

The open peroxide model of Fe(II) activation, discussed previously, also provides insight into a route through which the production of ROS might arise. Aside from involvement in the alkylation of amino acid residues, it is theorised that the hydroperoxide **(1h)** participates in Fenton reactions alongside Fe(II), generating the extremely reactive hydroxyl radical (O'Neill *et al.*, 2010b).

1.3.4.7. Radical-Independent Theories of Artemisinin Activity

An alternative theory as to the mode of action of artemisinin has been presented, which eschews the conventional hypotheses regarding the importance of bioactivation and the generation of reactive radical species, and emphasises ability to induce enhanced oxidative stress levels through an Fe(II)-independent mechanism (Haynes *et al.*, 2004). It holds that antiparasitic activity is derived from drug interference with the functioning of cofactors necessary for the maintenance of redox homeostasis. Specifically, this is believed to be mediated through a direct oxidation of the reduced flavins, such as $FADH_2$, which are required for the regeneration of the antioxidant glutathione (Haynes *et al.*, 2011). A

tentative chemical mechanism along which this might progress with artemether in a biomimetic setting is outlined in Figure 1.4. It is proposed that depletion of reduced antioxidant stock results in the inability of parasitic cells to detoxify ROS, causing eventual death. Evidence supporting this supposition is derived from biomimetic studies, which outline the capacity of artemisinin to induce the direct oxidation of the antimalarial drug leucomethylene blue (Haynes *et al.*, 2010). It is noted that Fe(II) is not essential for any such reaction to occur, prompting the suggestion of alternative activation mechanisms.

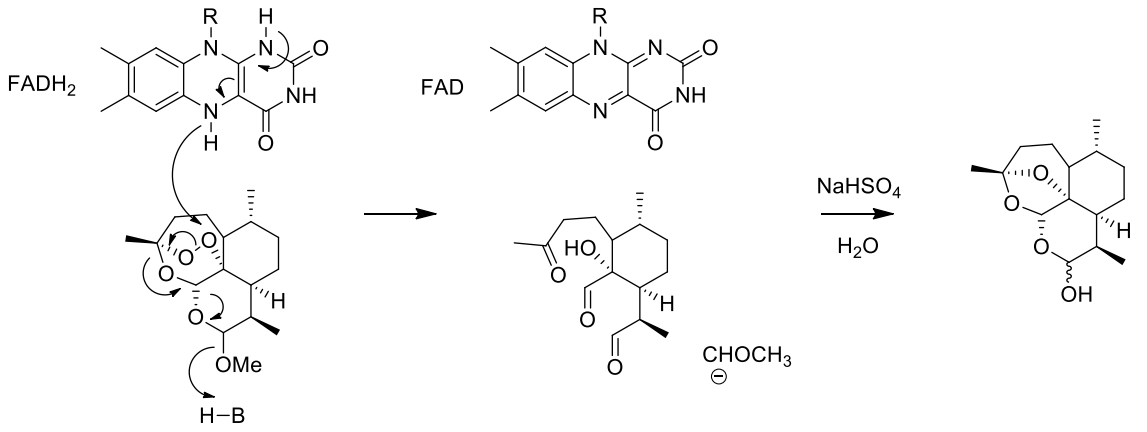

Figure 1.4. Suggested mechanism through which direct, artemether-induced oxidation of the reduced cofactor $FADH_2$ might occur within a biomimetic environment. Adapted from Haynes *et al.*, 2010.

In this model, the formation of carbon-centred radicals is not believed to be relevant towards the mechanism of drug activity. Fe(II)-mediated degradation of artemisinin is considered a side reaction, with its products possessing no pharmacological impact (Haynes *et al.*, 2004). It is held that the enhancement of parasiticidal effects in the presence of Fe(II) derives from its participation in Fenton chemistry, and is a product of a growth in existing levels of ROS. Although chemical studies point to the feasibility of Fe(II)-independent routes

to artemisinin activity, evidence supporting the tenets of this hypothesis has yet to emerge in either *in vitro* or *in vivo* systems.

1.3.4.8. Artemisinin and the Mitochondrion

Morphological alterations to the parasitic mitochondrion have been observed upon drug administration, suggesting a function for the organelle either as a source of artemisinin activation or as a target for its effects (Golenser et al., 2006; Jiang et al., 1985). The mitochondrion itself is recognised as the primary site for the generation of ROS, and it has been demonstrated that its depolarisation occurs in both parasitic and yeast models upon artesunate and DHA treatment through a mechanism reliant upon oxidative damage and the presence of Fe(II) (Li *et al.*, 2005; Wang *et al.*, 2010). Whether the formation of ROS might itself have a mitochondrial origin remains a topic of controversy, with the reports conflicting as to the capability of the drugs to induce defective functioning within the constituent complexes of electron transport chain. Despite the lack of definitive evidence, impairment can be considered a theoretical possibility owing to the prevalence of haemoproteins and Fe(II)-S clusters within this system. Owing to inconsistent study outcomes, it has yet to be established conclusively if such events are an early occurrence in the induction of cell death, or if they arise instead downstream subsequent to initial functional defects occurring elsewhere (del Pilar Crespo *et al.*, 2008).

1.4. The Activity of Artemisinin in Mammalian Cells

Artemisinin and its derivatives are identified as possessing activity across a range of mammalian systems. Their ability to impart deleterious effects upon both cellular and broader physiological functioning has been attested over an array of studies both *in vitro* and *in vivo*. The potential for these compounds to exert cytotoxicity effects was first demonstrated in investigations assessing their activity against Ehrlich ascites tumour cells (Woerdenbag *et al.*, 1993). Low micromolar IC_{50} values were noted for each drug examined, with the cytotoxicity of the semi-synthetic compounds DHA, artemether, arteether and artesunate each greater than that of their parent. Further examination confirmed that such effects were, as with antimalarial properties, dependent upon the presence of the endoperoxide bridge (Beekman *et al.*, 1997). Early hypotheses as to the mechanisms through which drugs effects were being exerted suggested that the inhibition of cell growth was of primary importance (Beekman *et al.*, 1996).

1.4.1. In-Vivo Artemisinin Toxicity

1.4.1.1. Artemisinin and Neurotoxicity

Neurotoxicity arising from artemisinin treatment has been noted to occur across animal models. Prolonged administration in dogs, rats, mice and monkeys is associated with the emergence of potentially fatal damage to the central nervous system (Brewer *et al.*, 1994; Toovey, 2006). *In vivo* studies performed within neuronal cell lines have outlined the onset of ROS generation, associated with mitochondrial dysfunction, as occurring in response to dosing with the drugs (Schmuck *et al.*, 2002). The potential for a link between artemisinin and onset of neurotoxicity within man has remained controversial (Efferth *et al.*, 2010).

Isolated reports of ataxia and ototoxicity in response to malaria treatment have not been credited as providing definitive evidence of the ability of the drugs to impair neurological function, since cerebral malaria may form a confounding factor in the establishment of such a relationship (Newton *et al.*, 2000). Mild, reversible impairment of auditory function following employment in combination with lumefantrine is identified across several clinical studies, albeit inconsistently (Hutagalung *et al.*, 2006; Toovey, 2006),

1.4.1.2. Artemisinin and Developmental Toxicity

Persistent reports of embryotoxicity in animal studies have prompted the World Health Organisation (WHO) to recommend that the use of artemisinin derivatives be forbidden in mothers during the opening trimester of pregnancy (WHO, 2006). Artemisinin treatment has been found to be associated with the emergence of teratogenicity, embryo death and resorption in rats, rabbits and monkeys (Clark *et al.*, 2008; Clark *et al.*, 2004). Observation of anatomical defects within these impaired embryos revealed abnormalities in skeletal and cardiovascular development, with such effects being noted alongside an absence of toxicity in the mothers. Further *in vitro* studies performed in cultured rat embryos have allowed for a closer assessment of the routes through which the drugs affect development. The administration of DHA was found to impact significantly upon the process of haematopoiesis within the yolk sac, leading to depletion of embryonic erythrocytes (Longo *et al.*, 2006; White *et al.*, 2006). It is hypothesised that defects such as the malformation of the skeletal and the cardiovascular systems might arise as a consequence of the anaemia and hypoxia occurring subsequent to the lowering of red blood cell population (D'Alessandro *et al.*, 2007). These embryonic erythrocytes are cells rich in both haem and in free Fe(II), identifying them as potential sites for artemisinin activation.

The toxicity witnessed in these systems has yet to be found to translate to humans within a clinical setting. Studies, albeit limited in scope, have indicated that the artemisinin derivatives retain a highly favourable safety profile, both in the mother and in the baby, throughout each stage of pregnancy (McGready *et al.*, 1998; McGready *et al.*, 2001). Larger patient samples, however, shall be required to verify absolutely that such effects are genuine prior to any relaxation of restrictions.

1.4.2. Cytotoxic Effects of Artemisinin against Cancer Cell Lines

Prompted by the initial investigations outlining the ability of artemisinin derivatives to induce death in selected cancer cells, a large-scale screening programme organised by the American National Cancer Institute (NCI) aimed to provide a wider assessment of their properties across a complete range of lines. Activity was demonstrated against leukaemia, lung, melanoma, colon, prostate, ovarian, and breast cancer cells, with the most sensitive again displaying IC_{50} values within the low micromolar range (Efferth *et al.*, 2001).

Since the emergence of these findings, artemisinin derivatives have been tested for their cytotoxic profiles against an array of immortalised lines. Mechanistic studies have outlined their abilities to promote apoptotic cell death, arrest proliferation and prevent metastasis, whilst further inducing the inhibition of angiogenesis (Singh *et al.*, 2004). In the process of performing these acts, the drugs have been shown to be associated with a diverse range of deleterious effects upon cellular functions. These are known to include the initiation of cell cycle arrest through cyclin reduction, the suppression of neovascularisation through VEGF receptor downregulation, the activation of pro-apoptotic mediators and the emergence of oxidative stress (Firestone *et al.*, 2009).

1.5. Mechanistic Aspects of Artemisinin Activity in Mammalian Cells

Attempts to elucidate the mechanistic route through which artemisinin induces toxicity across mammalian systems have highlighted both the aspects of cellular function impacted by their administration, and the factors responsible for mediating their progression. It is believed that, through means analogous to those within their antiparasitic mode of action, Fe(II) activation of the endoperoxide bridge produces reactive species accountable for promoting cellular dysfunction (Mercer, 2009). Research has identified that cell death, occurring through apoptotic and necrotic mechanisms, is stimulated through pathways dependent upon both the induction of mitochondrial damage and on the emergence of oxidative stress (Firestone *et al.*, 2009; Mercer *et al.*, 2011). A discussion of the current understanding which exists regarding the relationship between drug treatment and the onset factors contributing to each of these events shall now be presented.

1.5.1. Artemisinin and Cell Death

Studies within cancer cell lines have attested to the ability of artemisinin derivatives to induce termination through both apoptotic and necrotic routes. Prior to considering this evidence, a definition and overview of each of these two primary modes of death will be given.

1.5.1.1. Necrotic Cell Death

Necrotic death is characterised by its procession through a system of loosely-regulated signalling pathways stimulated as a consequence of sudden, external insult to cellular

integrity (Vanlangenakker *et al.*, 2008). Its onset may be initiated courtesy of a variety of stressors, including common external instigators such as physical trauma, ischaemia and temperature extremes, and further internal sources typically related to activation of the immune system. Cells are observed to pass through an early phase of swelling, related to a dysfunction of the mechanisms of ionic regulation (Golstein *et al.*, 2007). This culminates in irregular membrane blebbing and leakage of cell contents, typically resulting in the activation of an inflammatory response and the spread of death to neighbouring areas.

1.5.1.2. Apoptotic Cell Death

Apoptosis is a form of programmed death moderated under internal cellular regulation. Its activation may arise as a consequence of physiological or pathological stimuli, and it is implicated in the progression of a range of developmental processes and disease states (Taylor *et al.*, 2008). In contrast to the disorder and lack of regulation which characterises the progression of necrosis, apoptosis occurs through a series of well-defined signalling pathways culminating in cellular degradation and clean phagocytic removal of debris. The internal and external alterations in cellular morphology which occur over the course of apoptosis have been identified and characterised (Krysko *et al.*, 2008). A series of complex signalling cascades, themselves under the regulation of an array of hormones, growth factors and pro-apoptotic sensors, are accountable for mediating the activity of the caspase effector proteins responsible for the commencement of cell breakdown.

The pathways which culminate in the activation of apoptosis may be broadly catergorised as proceeding along either “intrinsic” or “extrinsic” routes. A summary of key stages present within each course is provided in Figure 1.5. The regulatory role of the mitochondrion is central to the intrinsic pathway of apoptosis (Wang et al., 2009). Initiation of this process typically occurs in response to stresses such as oxidative and chemical

damage, DNA insult and the effects of radiation. Increases in mitochondrial permeability prompt the release of a variety of pro-apoptotic factors from the inner membrane into the cytosol, including cytochrome c, which moves to form, alongside apoptotic protease activating factor 1 (APAF-1), the body know as the apoptosome responsible for caspase activation (Tait *et al.*, 2010). Alternatively, apoptosis can proceed through the extrinsic pathway (Elmore, 2007). In this pathway, activation of caspases is initiated through the binding of unique pro-apoptotic extracellular death ligands to respective surface death receptors.

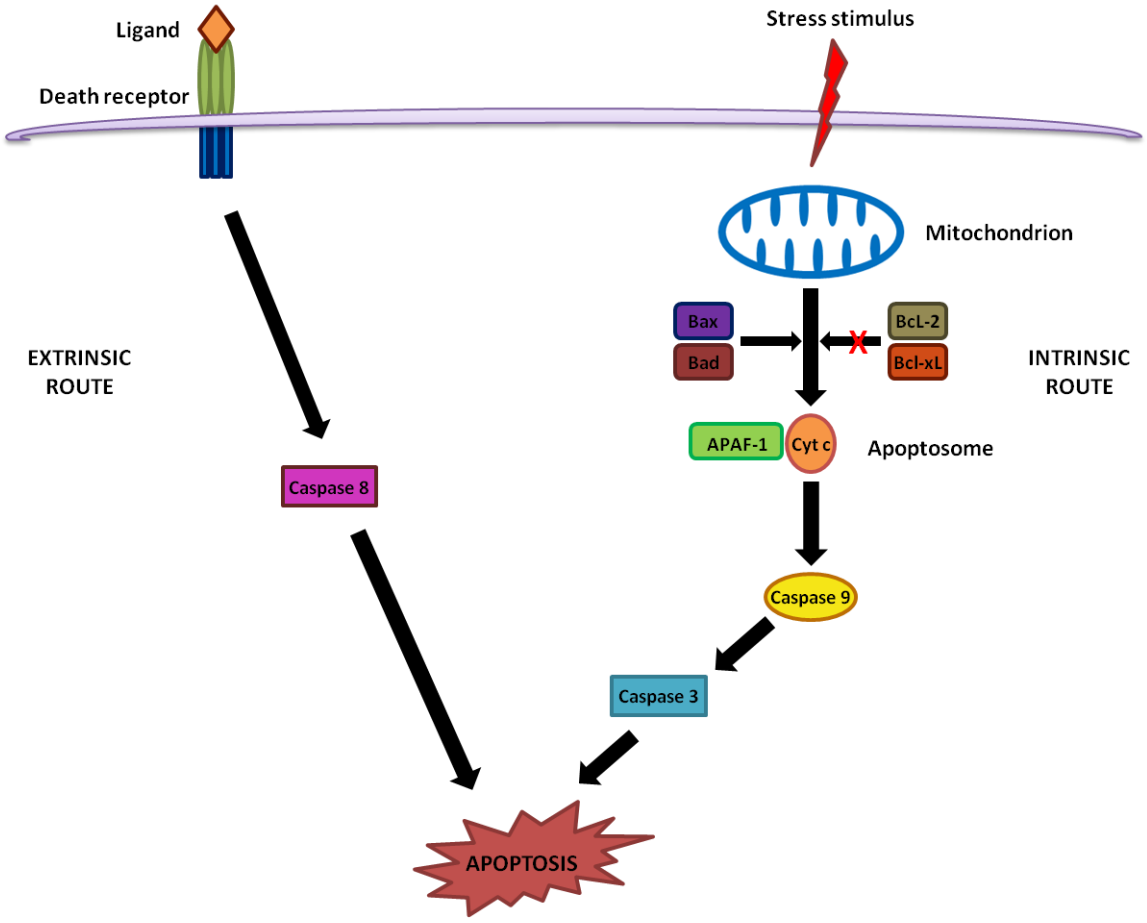

Figure 1.5. Scheme outlining primary stages within the pathways mediating apoptotic cell death.

1.5.1.3. Mechanistic Aspects of Artemisinin-Induced Cell Death

Research has indicated that artemisinin is capable of inducing cell death along both apoptotic and necrotic pathways. It is stimulation of the mitochondrially-regulated intrinsic apoptotic pathway which is identified as being the dominant mechanism across the great majority of systems examined (Firestone *et al.*, 2009). Evidence for its primacy is derived from the outcomes of studies which have established the induction of pro-apoptotic events occurring in response to drug treatment in cancer lines. Cell cycle arrest, inferred through increased populations within the G2/M and sub-G_0/G_1 phases, has been demonstrated (Morrissey *et al.*, 2010; Steinbrueck *et al.*, 2010). This is shown to occur alongside stimulation of pro-apoptotic Bax expression, release of cytochrome c and the activation of caspases (Anyasor *et al.*, 2009; Hou *et al.*, 2008). Support for involvement of the extrinsic pathway is less substantial. Limited upregulation in death receptor expression has been observed within prostate cancer lines, although the direct relevance of this remains at this time uncertain (He *et al.*, 2010). Necrosis is reported under selected conditions. Within the HeLa ρ^0 line, notable for its lack of functioning electron transport chain, cell death in response to artesunate treatment proceeds *via* a predominantly necrotic mechanism (Mercer *et al.*, 2011). It is believed that this is a function of the inability of these cells to efficiently undergo apoptosis, a factor which itself derives from deficiencies in their capacity to generate the quantities of ATP required for initiation of such processes.

1.5.2. Iron and Artemisinin Cytotoxicity

Theories into the mode of action of artemisinin derivatives in human cells are centred, as they are in parasitic systems, upon an iron activation hypothesis. Through methods analogous to those employed in assessing its necessity for antimalarial action, studies have

demonstrated that the presence of the endoperoxide bridge is a key requirement for the emergence of cell death (Efferth *et al.*, 2001). It is believed that the enhanced sensitivity of cancer cells towards artemisinin treatment occurs as a function of their reliance upon the maintenance of elevated intracellular iron concentrations (Mercer *et al.*, 2011). Correlations between levels of cytotoxicity and the modulation of iron content within these systems have been witnessed, providing further evidence for the existence of such a connection. It shall be necessary to present an overview of some of the more relevant actions of iron within cells, including the routes through which it is handled and metabolised, in order that context for future discussions regarding its relevance towards artemisinin activity might be provided.

1.5.2.1. The Cellular Functions of Iron

Iron possesses numerous functions which are central to the performance of many essential cellular processes (Cairo *et al.*, 2006). Its ability to exist in a variety of oxidation states lends it great utility as a mediator of redox pathways. For these roles, it is generally found either assembled into haem proteins, or bound up within Fe-S clusters. Haem is a key constituent of a myriad of enzymes and other proteins which are involved within an array of vital processes, and as such is present within electron transport molecules, metabolic catalysts of the cytochrome P-450 family, catalase antioxidant enzymes and in the haemoglobin oxygen transport mechanism (Warren, 2009). As a constituent of Fe-S clusters, iron is central to the regulation of additional redox routes, most notably within complexes I and II of the electron transport chain (Lill *et al.*, 2000).

Despite the necessity of iron for the maintenance of cell function, its reactivity can render it responsible for deleterious effects should it be present in excessive quantities. These are known to arise primarily as a product of an ability to generate highly reactive species,

including the $OH^{\bullet}$ hydroxyl radical, upon interaction with hydrogen peroxide (Thomas *et al.*, 2009). Termed the Fenton reaction, its mechanism proceeds according to the following equation:

$$Fe^{2+} + H_2O_2 \rightarrow Fe^{3+} + OH^{\bullet} + OH^{-}$$

As a consequence, it is necessary that cellular iron concentrations be regulated tightly in order to prevent the accumulation of excess. Free iron possesses the greatest potential for the stimulation of indiscriminate ROS formation, and as such metal ions are contained predominantly within bound states alongside transport or storage proteins (Galaris *et al.*, 2008). Within serum, iron remains conjoined to the glycoprotein transferrin, in which it is taken up into cells at transferrin receptors through a mechanism of endocytosis. Having entered, it becomes a constituent of the aggregate of free or weakly-bound iron termed the "labile iron pool" or "chelatable iron pool", in which it usually remains until it is either assembled into haemoproteins or taken up into storage in combination with ferritin (Hentze *et al.*, 2004).

It is this chelatable iron pool which is implicated as having major involvement in the formation of ROS (Kakhlon *et al.*, 2002). Iron in its unbound form is found in various compartments across the cell, with notable concentrations present within the cytosol, the mitochondrion, the nucleus and the lysosome. It is the latter, a body rich in hydrolytic enzymes and responsible for the breakdown of a broad range of biomolecules, which is distinguished by its particularly high content of the metal (Kurz *et al.*, 2008). This arises particularly as a consequence of its action as the site for haemoprotein degradation, and as such implicates it in the emergence of iron-related oxidative stress.

1.5.2.2. Iron Content and Cellular Artemisinin Susceptibility

Owing to its necessity for the construction of enzymes central to the processes of cell growth, metabolism and DNA synthesis, the tendency of cancer cells to undergo continuous active proliferation lends them a requirement for an enhanced internal concentration of iron (Kwok *et al.*, 2002). Cellular uptake of the metal is controlled through membrane transferrin receptors, which are responsible for internalising transferrin-bound iron courtesy of an endocytotic route. Elevated manifestation of the transferrin receptor is typically found to occur upon the surface of cells involved in multiplication (Steegmann-Olmedillas, 2011). In a direct comparison between the activities of artemisinin derivatives across immortalised lymphocytic and non-proliferating peripheral blood mononuclear cells (PBMC), it was revealed that the former display a much heightened degree of sensitivity towards drug effects (Mercer *et al.*, 2011). The cancer line studied, the HL-60, is particularly notable for both its susceptibility towards artemisinin-induced death and its elevated levels of transferrin receptor expression.

The modulation of iron content through exogenous routes has been shown to impact upon cell sensitivity towards artemisinin administration. Increasing the presence of iron through co-treatment with holotransferrin was observed to produce a heightened susceptibility towards DHA across both molt-4 leukaemic cells and the HB27 breast cancer-derived line (Lai *et al.*, 1995; Singh *et al.*, 2001). Mirroring the findings from both HL-60 and Jurkat studies, this effect was absent in their non-proliferating counterparts.

1.5.2.3. Haem-Iron and Artemisinin Activity

With evidence strongly suggesting a relationship between cellular iron and sensitivity towards artemisinin toxicity, research has sought to ascertain the identity of the metal source responsible for the mediation of bioactivation and related effects. The role of haem-Fe(II) as the key mediator of cytotoxic effects has been identified through studies assessing the impact of modulators of haem biosynthesis upon drug response in cancer cells (Mercer *et al.*, 2011; Mercer *et al.*, 2010). It was demonstrated that the addition of the haem precursors aminolevulinic acid (ALA), protoporphyrin-IX and transferrin-bound iron produced enhanced susceptibility towards artemisinin derivatives in sensitive cell lines whilst simultaneously stimulating haem formation. Co-treatment with the ALA synthase inhibitor succinyl acetone conversely reduced both cellular haem content and propensity towards cytotoxicity, whilst concurrently negating the formation of degradation products associated with bioactivation.

In the model of artemisinin antiparasitic activity, it is suggested that the ability to form adducts with haem is a determinant of pharmacological activity. Accordingly, defective haemoprotein functioning resulting from alkylation has been forwarded as a factor responsible in the induction of cytotoxic effects (Mercer, 2009; Mercer *et al.*, 2011). Owing to the role of haem units within enzymes responsible for the maintenance of redox processes, such as those found within the constituent complexes of the electron transport chain, it is posited that links might exist between reactivity with haem and the emergence of ROS formation.

1.5.2.4. Artemisinin and Iron-Mediated Free Radical Species Formation

It is hypothesised that the importance of iron towards the progression of artemisinin-induced cancer cell death stems from its ability to spur the formation of reactive carbon-

centred radical species through reduction of the endoperoxide bridge. Evidence derived from LC-MS studies has identified chemical species formed through the degradation of the artemisinin derivative 10*β*-(*p*-fluorophenoxy)dihydroartemisinin (PFDHA) **(7)** following incubation in HL-60 cells, indicating time-dependent drug activation occurring courtesy of a route which bears similarities to that observed within parasitic systems (Mercer, 2009; Mercer *et al.*, 2007). It is hence rational to suggest that the chemical mechanism behind bioactivation remains conserved across these settings. The observation that succinyl acetone protects against cytotoxicity whilst simultaneously reducing bioactivation suggests the presence of a link between activation, radical formation and the induction of cell death (Mercer *et al.*, 2011). As discussed previously, haem alkylation is proposed as being one route through which the cytotoxic mechanism might potentially be mediated.

1.5.3. Artemisinin and the Mitochondrion

It is interaction between artemisinin derivatives and the mitochondrion which is ultimately identified as being key to determining the response of cells towards treatment with the drugs. Evidence exists outlining the potential of the organelle to function as both a primary source for drug activation, and as the principal target for subsequent toxic impact. The emergence of reactive oxygen species formation and the induction of apoptotic cell death – processes both associated intimately with impact upon mitochondrial functions – have been demonstrated consistently across cell studies.

1.5.3.1. Drug-Induced Mitochondrial Dysfunction

Dysfunction of the mitochondrion is implicated as being of mechanistic relevance to the toxicity of a variety of drug classes. An overview of the key structural features possessed by the body is presented in Figure 1.6. The outer phospholipid bilayer membrane encases an

inner equivalent, which in turn surrounds the protein-dense matrix. It is this internal membrane which holds the substituent complexes of the electron transport chain. Situated between inner and outer membranes stands the intermembrane space, a region which folds into the matrix to form structures referred to as cristae. Mitochondrial liability has become associated with the deleterious impact of xenobiotics upon the functioning of targets ranging from the cardiovascular, hepatic, renal and central nervous systems, to skeletal muscle and the maintenance of lipid distribution (Dykens, 2008). Mechanisms through which drugs might impart damage to the operation of mitochondrial activities are numerous and varied. Many important cellular processes lie under the control of the organelle, with two of the most prominent being ATP generation through oxidative phosphorylation and the aforementioned regulation of intrinsic apoptosis (Newmeyer *et al.*, 2003). Deleterious impact upon the operation of the former has the potential to bear a significant general effect upon general cellular function.

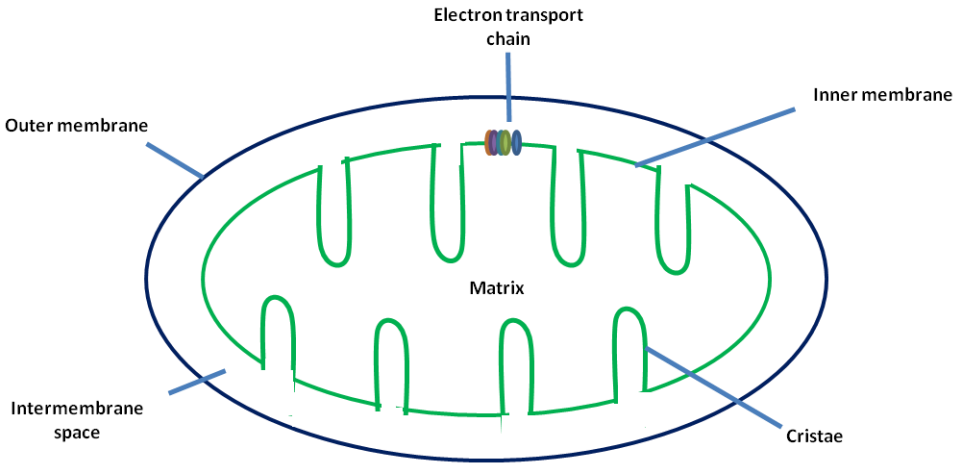

Figure 1.6. Overview of the key topographical features of the mitochondrion.

Acting as the dominant route towards ATP production, the process of oxidative phosphorylation is dependent upon the release of energy occurring through the series of consecutive redox reactions which collectively form the electron transport chain

(Huttemann *et al.*, 2007). Structurally, the electron transport system is composed of four redox-active complexes situated within the inner membrane of the mitochondrion. Passage of electrons occurs from donor to acceptor molecules, culminating in releases of energy which are in turn utilised for the extrusion of protons from inside the matrix and out into the intermembrane space (Fig. 1.7.) (Huttemann *et al.*, 2008). This imbalance in proton distribution creates an electrochemical gradient, referred to as the mitochondrial membrane potential, which hence drives the creation of ATP at ATP synthase.

The initial phase in the electron transport procedure is the oxidation by complex I (NADH dehydrogenase) of NADH. This process results in the transferral of two electrons to the carrier molecule ubiquinone (CoQ_{10}) and the movement of four protons into the intermembrane space. Ubiquinone is simultaneously fed by complex II (succinate dehydrogenase), which donates a pair of electrons accrued from succinate oxidation. The reduction of ubiquinone, fed through both sources, furnishes ubiquinol, which hence proceeds to function as a donor to complex III (cytochrome *bc*1 complex). Participation in the Q-cycle at this complex leads to the transferral of electrons to two units of the haemoprotein cytochrome c, alongside the net translocation of four protons from out of the matrix. At complex IV (cytochrome c oxidase), one electron is removed from each of four reduced molecules of cytochrome c. They are transferred, accompanied by four protons, to one molecule of oxygen – which functions as a terminal electron acceptor – culminating in the formation of water. Four further protons are simultaneously relocated into the intermembrane area. ATP synthase utilises the proton gradient to catalyse the phosphorylation of ADP, acting as the primary source for cellular ATP generation (Huttemann *et al.*, 2007).

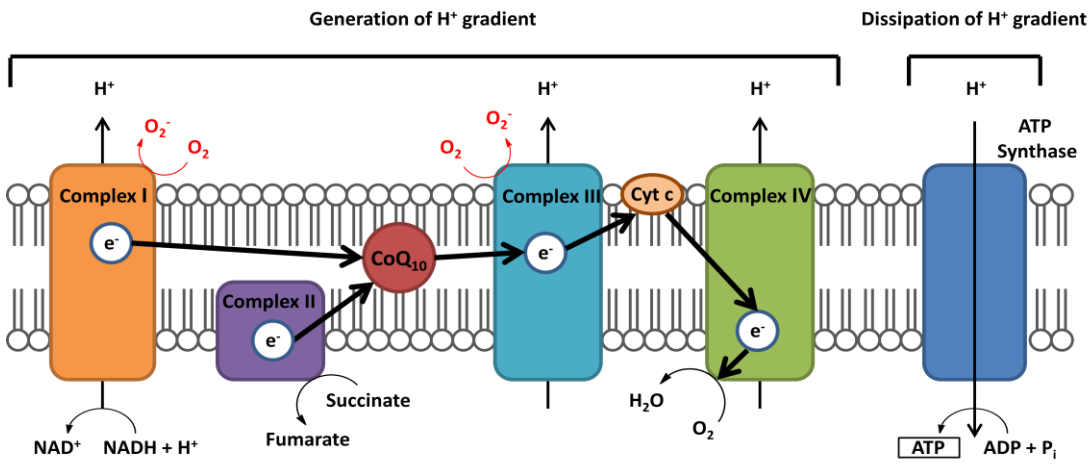

Figure 1.7. Diagram outlining the physiological functioning of the electron transport chain. Sites of ROS generation are highlighted in red.

The inequitable distribution of protons about the membrane culminates in the establishment of an electrochemical gradient. The associated potential difference of this, termed $\Delta\Psi_m$, stands between 180-200 mV (Dykens, 2008). The maintenance of such dispersal is essential in order that the production of ATP might proceed freely through the oxidative route. The requirement for oxygen to act as the final acceptor for electrons ensures that its continued consumption by cells is a necessity. Accordingly, it is owing to this process that the mitochondrion itself is accountable for approximately 90% of total cellular oxygen demand (Nathan *et al.*, 1999). Under physiological conditions, consumption of oxygen remains "coupled" to the establishment of $\Delta\Psi_m$ and hence to the generation of ATP.

Defective functioning of this system results in the generation of ATP becoming "uncoupled" from cellular oxygen uptake, resulting in a greatly reduced efficiency of energy production. This might arise either from the modification of any of the complexes which constitute the electron transport mechanism, from agents which act to compromise the integrity of the inner membrane or from a depletion of the substrates required to feed the redox chain (Dykens, 2008; Fosslien, 2001). Causes behind these effects include the specific inhibition of

enzymes, the sequestering of redox cofactors and also generalised damage occurring as a consequence of ROS production (Kirkinezos *et al.*, 2001; Neustadt *et al.*, 2008). Heightened oxidative stress generally finds its source in damage to the functioning of the electron transport chain, ensuring the common existence of a close link between mitochondrial injury and the elevation of ROS formation.

As has been discussed previously, mitochondrial damage stimulates apoptosis through the intrinsic pathway (Firestone *et al.*, 2009). Events which are known to occur alongside the onset of this process include the collapse of the mitochondrial membrane potential, the cessation of ATP production, and the permeabilisation of the outer membrane. The latter ultimately culminates in pore formation and the release of cytochrome c, initiating caspase activation and subsequent cell death. This pathway can be stimulated through events occurring outside of the mitochondrion, such as external ROS generation and the emergence of lysosomal dysfunction (Boya *et al.*, 2008).

1.5.3.2. Mechanistic Aspects of Artemisinin-Induced Mitochondrial Dysfunction

Evidence strongly suggests that dysfunction of the mitochondrion is a key stage in the mechanism through which artemisinin derivatives exert their cytotoxic effects. The production of ROS is observed within cancer cells upon drug treatment, with the protective effects afforded by the upregulation of cellular oxidative stress defence mechanisms and the co-administration of exogenous antioxidant agents indicating that damage arising from this is a major contributing factor towards the progression of cell death. Their emergence is witnessed to occur prior to the onset of toxic effects, identifying them as early mediators of response (Mercer *et al.*, 2011). Owing the position of the mitochondrion as the primary site

for pathological ROS generation, it is posited that artemisinin administration impacts upon the redox processes within. Studies performed in HeLa ρ^0 cells indicate that the absence of a functioning electron transport chain leads to a reduction ROS levels, conferring relative resistance to cytotoxic effects. Accordingly, damage to this system is implicated as being a route through which deleterious impact might be mediated (Firestone *et al.*, 2009). Events occurring alongside the defective oxidative phosphorylation functioning, including the collapse of the mitochondrial membrane potential and the cessation of ATP production have further been reported.

Attempts to rationalise these findings on a chemical level have been modelled primarily upon the iron activation hypothesis. Haem is believed to function as a source for endoperoxide bridge reduction, inducing decomposition of the artemisinin molecule and the formation of reactive carbon-centred radicals (Mercer *et al.*, 2007; Zhang *et al.*, 2009). Modification of proteins occurring as a consequence of alkylation by these species is posited as leading to their defective functioning, although definitive evidence for the significance of this has yet to be presented. It is additionally highly likely that the role of iron in the propagation of ROS through Fenton chemistry is additionally of great mechanistic relevance (O'Neill *et al.*, 2010b).

1.5.4. Reactive Oxygen Species in Artemisinin Cytotoxicity

The term reactive oxygen species is given to any chemically reactive molecule formed as a consequence of oxygen metabolism. Despite possessing physiological roles relating to cell signalling and pathogen defence, their tendency towards indiscriminate reaction with proteins and lipids ensures that their presence in elevated quantities is detrimental towards the functioning of the cell. The formation of ROS is strongly implicated as playing a central role within the mechanism of artemisinin-induced cell death (Firestone *et al.*, 2009). Studies

have shown that cell treatment with artemisinin derivatives results in increases in ROS levels, the abrogation of which can lend cytoprotective effects (Mercer *et al.*, 2011). The relationship between enhanced oxidative stress and the toxicity of DHA was first demonstrated in a study assessing impact of treatment upon immortalised cervical cancer cells (Efferth *et al.*, 2007). It was soon discovered that such an effect was general to many lines, and occurred alongside the onset of both necrotic and apoptotic cell death.

The effects of antioxidants have indicated that oxidative stress is an important causative factor in artemisinin cytotoxicity. ROS scavengers including tiron have been shown to greatly reduce drug impact upon cell viability, whilst an inverse correlation between susceptibility to toxicity and the expression levels of enzymes involved in endogenous defence mechanisms such as catalase, superoxide dismutase and glutathione-S-transferase has been shown to exist (Efferth, 2006; Mercer *et al.*, 2011). Despite such evidence strongly suggesting causality between ROS induction and the emergence of toxicity, a definitive route through which their formation is initiated has yet to be established (O'Neill *et al.*, 2010b). Owing to the importance of ROS towards the mechanism of action of artemisinin and its derivatives, it shall be necessary to explore the pathways through which they might be generated. An overview processes implicated in their production shall be given, so that consideration of the possible routes through which the drugs exert toxicity might be made.

1.5.4.1. Routes towards the Formation of Reactive Oxygen Species

ROS may be formed at many points within the cell, with their generation occurring as by-product across an array of systems. Under physiological circumstances, production is offset by the actions of cellular antioxidants, which act to convert oxygen radicals into more inert species and hence minimise potential for deleterious interactions (Vertuani *et al.*, 2004). These compounds, including glutathione, melatonin and ubiquinol, are essential towards

the maintenance of cellular health (Rizzo *et al.*, 2010). Should formation of ROS exceed the capability of the cell to neutralise them, then the system is said to exist under a condition of "oxidative stress"(Halliwell, 2007). The superoxide anion, O_2^-, generated through the one-electron reduction of molecular oxygen, is of particular importance owing to the tendency towards its formation within the mitochondrion. Its generation may occur in cells through a process of indirect electron leakage, or through the actions of selected oxidase and reductase enzymes. The equation for its formation is:

$$O_2 + e^- \rightarrow O_2^-$$

1.5.4.2. Reactive Oxygen Species and the Electron Transport Chain

It is established that the great majority of ROS generated within cells have their origin within the mitochondrion – a factor generally attributed to the role which the organelle possesses as the site of oxidative phosphorylation (Murphy, 2009). It is accepted, therefore, that injuries to mitochondrial processes are heavily associated with elevated oxidative stress. The electron transport chain, which holds the central role within the generation of ATP through the aforementioned pathway, is identified as the leading foundation for the generation of ROS occurring under both general physiological and pathological conditions.

The physiology of the electron transport system is outlined in Section 1.5.3.1. Despite the general efficiency of the pathway, electron leakage at various points within the chain is associated with ROS formation. Complex I and complex III are acknowledged as the primary sources of superoxide generation under physiological conditions (Le Bras *et al.*, 2005). As such, defective functioning within these systems occurring through pathological means is linked closely to the elevated expression of ROS (Turrens, 2003). Compounds such as the complex I inhibitor rotenone and the complex III inhibitor antimycin are known to induce oxidative stress and resultant cell death through specific action at sites within these bodies.

1.5.4.3. Reactive Oxygen Species Independent of the Electron Transport Chain

Although the electron transport chain is identified as being the dominant point of ROS generation within cells, numerous alternative sources unconnected with the machinery of oxidative phosphorylation are known to exist. It is understood that enzymes within the mitochondrion have the potential to produce significant quantities of ROS, either as a function of the physiological roles or as a consequence of defective operation (Dykens, 2008; Tahara *et al.*, 2009). Amongst these are the matrix oxidoreductase α-ketoglutarate dehydrogenase, the inner membrane-bound *sn*-glycerophosphate dehydrogenase and the outer-membrane-located cytochrome *b5* reductase and monoamine oxidase (Andreyev *et al.*, 2005).

Sources external to the mitochondrion include NADPH oxidase, located within the plasma membrane, xanthine oxidase, and nitric oxide synthase (Bedard *et al.*, 2007; Papi *et al.*, 2008). ROS in significant quantities are generated within the endoplasmic reticulum, and might also arise within the lysosomal compartment as a consequence of its elevated free iron content (Galaris *et al.*, 2008). Furthermore, oxidative stress occurring peripheral to the mitochondrion is capable of inducing damage to the functioning of the organelle, spurring the additional production of ROS through a mechanism termed “ROS-induced ROS release” (Zorov *et al.*, 2006).

1.5.4.4. Mechanistic Aspects of Artemisinin-Induced Reactive Oxygen Species Formation

As previously alluded to, the production of ROS is intimately connected with the induction of cytotoxic effects arising as a consequence of artemisinin treatment. The mechanistic routes through which the emergence of oxidative stress is mediated following drug administration remain largely unknown. Owing to the established relationship between

mitochondrial dysfunction and the onset of ROS formation, it is plausible to suggest the existence of a close association between the oxidative stress stimulated by artemisinin derivatives, and impact imparted by the compounds upon the processes mediated within the organelle. The ρ^0 HeLa line, which respires solely through glycolysis on account of the defective functioning of its electron transport chain, exhibits significant resistance towards the effects of the drugs (Chevallet *et al.*, 2006; Mercer *et al.*, 2011). Such an outcome is postulated as being linked with reduced incidence of ROS formation arising secondary to the bypassing of oxidative respiration, thus suggesting that artemisinin-induced interference with the operation of the electron transport system forms a dominant route through which oxidative stress is stimulated. The theorised contribution of reactive carbon-centred radicals towards drug-induced deficiencies in the operation of cellular systems provides a feasible mechanism towards the mediation of such impact.

It is further possible that cellular ROS might arise as a consequence of an oxidant function derived from the chemistry of the endoperoxide moiety (Haynes *et al.*, 2010). Several mechanisms through which this might be mediated within parasitic systems have been postulated, with the most prominent being discussed within Section 1.3.4.7. Should such pathways, dependent upon interference with the redox status of flavin cofactors, possess significance towards the pharmacological activity of the compounds, conservation of relevant processes within mammalian cells may influence the progression of cytotoxic effects.

1.6. Rationale for Study

1.6.1. Artemisinin Derivatives Assessed

Over the course of the studies constituting this thesis, a variety of endoperoxide compounds originating from several drug classes shall be examined for their activity profiles within cell systems. Assessment into the mechanistic aspects of artemisinin function within cancer cells will be performed using the first-generation, semi-synthetic derivative artesunate. This compound finds widespread employment across clinical settings, and has further been utilised in an assortment of examinations into the general cytotoxic effects of the drug class *in vitro*. Additional investigations shall make use of DHA, and the related derivative PFDHA. The latter is noted for its enhanced metabolic stability, and has been developed for use in assessment of drug bioactivation through LC-MS methods (Mercer *et al.*, 2011; Mercer *et al.*, 2007).

Research into the development of novel endoperoxide forms has been prompted owing to concerns regarding the toxicity and cost-effectiveness of the artemisinin derivatives in current general use (Ridley, 2002). An array of wholly synthetic compounds have been tested and developed over the preceding decades, with investigations into their antiparasitic profiles suggesting that many possess activities comparable to or greater than those of the traditional artemisinin-based agents (Jefford, 2007). The 1,2,4-trioxolane and 1,2,4,5-tetraoxane classes, illustrated respectively by OZ277 **(8)** and its derivative **(9)**, have exhibited notable promise as regards to their progression towards clinical utility (Uhlemann *et al.*, 2007). As such, the cytotoxic potentials of novel antimalarial candidates belonging to these series, synthesised by the group of Prof. Paul O'Neill, shall each be examined in order that the mechanistic aspects of their actions within mammalian systems might be elucidated. Further investigations have sought to explore the feasibility for exploiting

artemisinin activity against cancer cell lines as the basis for the development of a range of new compounds intended for employment as anticancer treatment (Chaturvedi *et al.*, 2010; O'Neill *et al.*, 2010a). Common design strategy has centred upon construction of hybrid classes, such as those exemplified by the artemisinin-acridine assembly **(10)**, in order that cell killing potential relative to the lone endoperoxide be enhanced (Jones *et al.*, 2009). Several compounds belonging to a series of novel DHA-polypyrrole conjugates are hence examined for their impact upon cellular function.

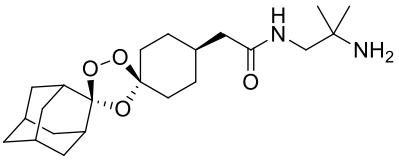

(8)

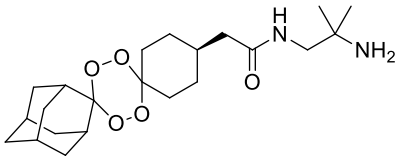

(9)

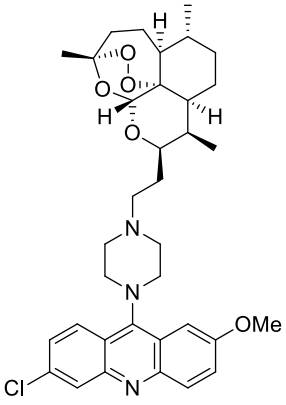

(10)

1.6.2. Cell Lines Examined

The activities of the aforementioned endoperoxides shall be determined across a variety of immortalised cell lines. The HeLa cell, derived from a cervical cancer tumour, is employed widely as a model in the *in vitro* assessment of xenobiotic function. It has accordingly found use in previous studies examining the cytotoxic profiles of artemisinin compounds, across which it is noted to display sensitivity towards effects of the drugs (Chen *et al.*, 2003;

Mercer *et al.*, 2011). As has been alluded to previously, the sustained culturing of HeLa cells in the presence of ethidium bromide has the effect of depleting the mitochondria of their DNA, preventing the assembly of a functioning electron transport chain and forcing reliance for ATP generation upon the glycolytic pathway (Chevallet *et al.*, 2006; Mercer *et al.*, 2011). Utilisation of this ρ^0 line can allow for direct assessment of the importance of the electron transport mechanism towards the progression of cytotoxic impact arising from drug treatment.

Owing to their great sensitivity towards an array of artemisinin-derived and synthetic endoperoxide classes, further assessments of cytotoxic potential shall be performed within promyelocytic leukaemic HL-60 cells (Efferth *et al.*, 2001; Mercer *et al.*, 2007). In addition, the Hep G2 hepatocellular carcinoma line, which constitutes an established vehicle for the assessment of toxic activity, shall be employed in selected assessments. Culturing techniques intended to heighten the sensitivity of cancer cells towards the impact of mitochondrial toxins shall further utilised for the same purposes.

1.7. Aims of Thesis

The discussion presented within this chapter has served to provide account of the historical, clinical and mechanistic perspectives related to the activity profiles of artemisinin and its derivatives across both pharmacological and toxicological settings. Concerns over the potential of the compounds in current use to impart developmental and neurological toxicity in clinical settings remain persistent, prompting examination into the routes through which such effects are mediated. Research has indicated the ability to induce significant, selective cytotoxic effects against sensitive, proliferating mammalian cells. It is widely believed that this impact is mediated through a mechanism reliant upon activation of the endoperoxide bridge, occurring as a direct consequence of interaction with sources

of Fe(II). ROS production has been identified as a key stage in the progression of cell death, a phenomenon which is held to occur alongside the onset of mitochondrial dysfunction and the activation of intrinsic apoptosis.

The impact of artemisinin upon the metabolic functioning of the mitochondrion has yet to be fully assessed, and neither have the sources of oxidative damage been conclusively elucidated. It shall be the intention of the research performed within this thesis to provide a deeper insight into the effects held by drugs upon the health of the organelle, further examining the roles of iron and oxidative damage in the determination of such a response. It is acknowledged that the long-term future of endoperoxide compounds as frontline antimalarial treatment lies in the successful development of novel synthetic classes. Accordingly, assessment into of the cytotoxic profiles of newly developed synthetic and semi-synthetic experimental derivatives shall be made. In order to achieve these aims, a variety of *in vitro* techniques employing immortal cancer cell lines shall be employed. The ultimate aim of these studies shall be to develop current our understanding of the mechanism through which cytotoxicity proceeds, so that this might in turn contribute towards the future safer use of the drugs and to a clearer view of how their chemistry relates to their cellular activity.

Chapter Two

Investigation into the Function of Mitochondrial Liability within the Development of Artemisinin Cytotoxicity

2.1. Introduction

It is established that the mitochondrion holds involvement in the mechanism through which endoperoxide compounds exert cytotoxicity in cancer cell lines (Mercer *et al.*, 2011). Although the effects of drug treatment have been documented across several studies, comparatively little is known regarding the nature of the interactions which underpin their activity within this body. This chapter shall be focused upon testing the hypothesis that cell death induced through the artemisinin derivative artesunate occurs through a mechanism reliant upon direct targeting of the organelle. In order to achieve this, response to treatment shall be examined across Hep G2 and HeLa cells sensitised towards mitochondrial toxins through culturing in the absence of glucose. These studies shall be complemented by an assessment of mitochondrial bioenergetic function performed using techniques developed for the Seahorse extracellular flux (XFe) analyser, in order that a more complete view regarding their bearing upon respiration might be attained.

Deleterious impact upon the physiological function of the mitochondrion is a defining feature of the mechanism of action through which artemisinin-derived compounds impart their cytotoxic influence within mammalian cells. The collapse of the mitochondrial membrane potential, the generation of ROS and the onset of intrinsic apoptosis are events which are noted to occur uniformly across a variety of cancer lines upon treatment with this class (Firestone *et al.*, 2009). Studies have further indicated that ρ^0 HeLa cells, which do not possess a functioning electron transport chain and hence lack an ability to produce ATP through oxidative phosphorylation, exhibit reduced sensitivity towards drug effects (Mercer *et al.*, 2011). The primary chemical and molecular basis behind these observations, combined with their relevance towards any toxicity which may be observed in a clinical setting, remain largely undefined.

Studies into this area have typically been performed *in vitro* within immortalised, cancer-derived cell lines. A key area in which these cells differ with respect to both those found in living systems and those maintained in primary culture is that of their bioenergetic profiles. Whilst it is typical of cells under general physiological conditions to generate ATP primarily and preferentially through oxidative phosphorylation within the mitochondrion, it is characteristic of cancer cells that they derive their energy almost exclusively through glycolytic routes (Moreno-Sanchez et al., 2007; Pedersen, 1978). This observation may be explained through the phenomenon referred to as the Crabtree Effect, whereby cells undergoing rapid proliferation are capable, dependent upon conditions and substrate availability, of switching their primary source of metabolism between oxidative and glycolytic routes (Dakubo, 2010). It is theorised that the prevalence of glycolytic respiration within cancer cells arises through their adaptation towards growth within the hypoxic environments common across many tumour types.

A consequence of this preference for glycolysis and concurrent reduced reliance upon oxidative phosphorylation is that the sensitivity of many commonly employed lines towards the effects of compounds exerting toxicity through activity within the mitochondrion is often greatly reduced (Xu *et al.*, 2005). In order that these cells might be modified towards the provision of a more physiologically relevant model for assessment of mitochondrial toxins in otherwise resistant systems, effective methods allowing for the circumvention of the Crabtree Effect have been developed (Marroquin *et al.*, 2007). The culturing of the hepatic carcinoma-derived Hep G2 cell in the presence of galactose, with the simultaneous exclusion of glucose, has been shown to inhibit the glycolytic generation of ATP, and hence force derivation of energy through solely mitochondrial means (Rossignol et al., 2004). The increased dependence upon the organelle in order to ensure cell survival ensures that susceptibility towards mitochondrially toxic compounds is enhanced. This state stands in

direct contrast to that witnessed within ρ^0 HeLa cells, which are capable of respiring exclusively through the route of glycolysis.

This technique has been increasingly employed as a means of screening for mitochondrial activity in drugs which display cytotoxic effects (Dykens *et al.*, 2008a; Dykens *et al.*, 2008b). It is methods adapted from it that shall be utilised within the forthcoming studies in order to investigate the profile of artesunate with regards to action upon the organelle. Both cytotoxicity, investigated using the MTT assay, and ATP content, examined using the CellTiter-Glo kit, shall be compared across cells cultured under each set of conditions. Full time courses shall be run for the assessment of these parameters, so that onset the progression of drug action may be observed. Furthermore, cellular oxygen consumption shall be measured using the Seahorse XFe analyser so that any variations in bioenergetic function might be monitored. These studies shall be performed in the Hep G2 cells, which have classically been employed in determining response to potential mitochondrial toxins through the methods described, before being expanded to the more sensitive HeLa line.

The generation of ATP through oxidative phosphorylation is one of the primary functions of the mitochondrion, and interference with this process is heavily indicative of impairment to the integrity of the body. Since it is established that maintaining the performance of this process is accountable for approximately 90% of total cellular oxygen consumption, methods for determining the variation in atmospheric oxygen levels in the environment of cells have found extensive use in the assessment of mitochondrial health (Nathan *et al.*, 1999). Classically, apparatus such as the Clark oxygen electrode has been utilised in order to monitor respiratory capability (Diepart *et al.*, 2010). The development of XFe technology has allowed for the simultaneous measurement of oxygen consumption (OCR) and extracellular acidification rates (ECAR), facilitating the assessment of oxidative and glycolytic performance with greatly improved levels of sensitivity (Dranka *et al.*, 2011).

In this chapter, the Seahorse XFe unit shall be employed so that respiratory function in HeLa cells may be examined in response to artesunate administration. Using mitochondrial and glycolytic stress test techniques, the bioenergetic performance of the mitochondrion is determined with reference to several parameters indicative of physiological activity. These are quantified through monitoring variations in OCR and ECAR associated with the addition of compounds known to impact upon the progress of respiration. Through this, it is possible to ascertain the efficiency at which oxidative phosphorylation is coupled to oxygen consumption in drug-treated cells, whilst simultaneously measuring the total respiratory capacity and basal respiratory levels (Hill *et al.*, 2009). Assessment of the impact of drug treatment upon these indicators allows for insight into the identity of the defects in mitochondrial performance induced, thus allowing for greater elucidation of their role towards the greater mechanism of cytotoxicity. Experiments are performed over full drug concentration and time courses, so that the relationship between the onset of mitochondrial dysfunction and the emergence of accompanying cell death might be studied in full. It is intended that, through these assessments, the hypothesis that artemisinin derivatives hold function as direct mitochondrial toxins can be granted thorough examination.

2.2. Materials and Methods

2.2.1. Materials

Dulbecco's Modified Eagle's Medium (DMEM), L-glutamine, penicillin/streptomycin solution, galactose, trypsin-EDTA solution (0.25%), (4-(2-Hydroxyethyl)-1-piperazineethanesulphonic acid (HEPES), sodium pyruvate, Hanks' balanced salt solution (HBSS), glucose, MTT, *N,N*-dimethylformamide (DMF), sodium dodecyl sulphate (SDS), MTT, oligomycin, rotenone, FCCP, artesunate and all additional solvents were purchased from Sigma-Aldrich (Poole, Dorset, UK). Foetal bovine serum (FBS) was purchased from Life Technologies (Paisley, UK). Nunc cell culture plates and flasks were purchased from Thermo Scientific (Loughborough, UK). Seahorse XFe96 Analyser, XF Cell Mito Stress Test Kits, XF Glycolysis Stress Test Kits, XFe96 FluxPaks, XF96 V3 PET Cell Culture Microplates, XFAssay Medium, and XFe Calibrant were purchased from Seahorse Bioscience (Boston, USA). CellTiter-Glo Luminescent Cell Viability Assay Kit was purchased from Promega (Southampton, UK). HeLa and Hep G2 cells were acquired from the European Collection of Cell Cultures (Salisbury, UK).

2.2.2. Cell Culture and Experimental Preparation

HeLa cells were cultured in high-glucose DMEM, with supplemental FBS (10% v/v), L-glutamine (1% v/v), sodium pyruvate (1% v/v) and penicillin/streptomycin solution (1% v/v). Hep G2 cells were cultured in high-glucose DMEM, with supplemental FBS (10% v/v), sodium pyruvate (1% v/v), HEPES (0.5% v/v) and penicillin/streptomycin solution (1% v/v). All cells were incubated at 37°C, in humidified air containing 5% CO_2. Cell counting was performed using a haemocytometer under a light microscope (Leica DME, Leica Microsystems, Milton Keynes, UK).

2.2.3. Preparation and Treatment of Cells in Galactose-containing Media

The tendency of cells within cancer-derived lines to preferentially derive ATP through glycolysis ahead of oxidative phosphorylation has been attributed to the Crabtree effect (Moreno-Sanchez *et al.*, 2007). Studies have shown that the culturing of cells in galactose-containing media, to the exclusion of glucose, can induce the cessation of glycolytic ATP production, and hence increase greatly reliance upon oxidative phosphorylation and the mitochondrion (Marroquin *et al.*, 2007). Cells respiring under these conditions display greater sensitivity towards mitochondrial toxins than those which continue dependence upon glycolysis, allowing for their use in the screening of compounds potentially exerting cytotoxicity through mitochondrion-dependent means.

HeLa cells were reconstituted in glucose-free DMEM supplemented with dialysed FBS (10% v/v), L-glutamine (2% v/v), sodium pyruvate (1% v/v), penicillin/streptomycin solution (1% v/v) and galactose (1 mM). Cells were washed in media three times in order to remove traces of glucose, before being added to relevant culture plates and left to adhere for a minimum period of 4 h prior to drug treatment. Hep G2 cells were reconstituted in glucose-free DMEM supplemented with dialysed FBS (10% v/v), L-glutamine (2% v/v) HEPES (2% v/v), sodium pyruvate (1% v/v), penicillin/streptomycin solution (1% v/v) and galactose (1 mM). Cells were washed in media three times in order to remove traces of glucose, before being added to relevant culture plates and left to adhere for a minimum period of 4 h prior to drug treatment.

2.2.4. Assessment of Cell Viability using the MTT Assay

The MTT assay is employed as a means of determining the viability of cells. It utilises the ability of mitochondrial reductase enzymes, which function only in living cells, to induce the reduction of the yellow tetrazolium compound 3-(4,5-dimethylthiazol-2-yl)-2,5-diphenyltetrazolium bromide (MTT) to an insoluble purple formazan salt. There is a direct proportionality between amount of formazan formed and quantity of living cells present, with the colour change accompanying this transformation used as a basis for the spectrophotometric determination of cell viability (Mosmann, 1983).

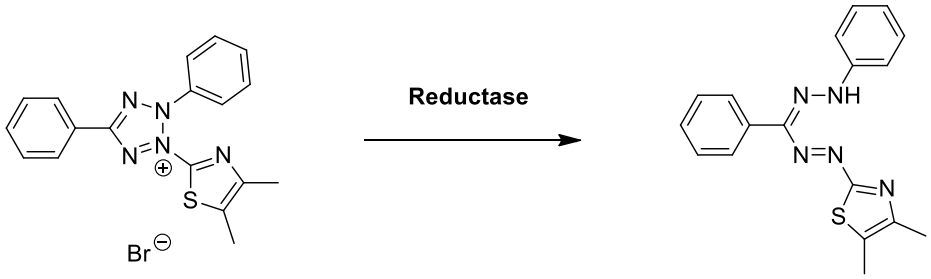

Tetrazole (Yellow) **Formazan (Purple)**

HeLa or Hep G2 cells (5 x 10^3/well) were plated, in triplicate, into flat-bottomed, 96-well plates, and left to adhere overnight. Cells were subsequently exposed to concentrations of drug ranging from 0.1 µM to 1000 µM, dependent upon the nature of the assay, and incubated for time periods of up to 72 h. Upon the completion of incubation, 20 µL of MTT solution (5 mg/ml in HBSS) was added to each well. Following a further 2 h incubation at 37°C, 200 µL of a lysis buffer (20 % w/v SDS, 50 % w/v DMF) was added to each well, and a further 4 h incubation at 37°C performed. Absorbance of each well was read on a plate reader (Dynex MRX, Magellan Bioscience, Worthing, UK), using a test wavelength of 570 nm and a reference wavelength of 590 nm. Results are expressed as a percentage of absorbance relative to untreated vehicle control, with IC_{50} derived from curves plotted using the GraFit Software (Erithacus Software, Surrey, UK).

2.2.5. Luminescent Analysis of Cellular ATP Content

Cellular ATP content was determined through use of the commercial CellTiter-Glo Luminescent Cell Viability Assay kit. The function of the assay is reliant upon the luciferase-dependent oxidation of a beetle luciferin substrate, resulting in the formation of oxyluciferin with the accompanying emission of light. The activity of the luciferase enzyme is proportional to the quantity of ATP present, allowing for ATP content to be inferred from detected luminescence

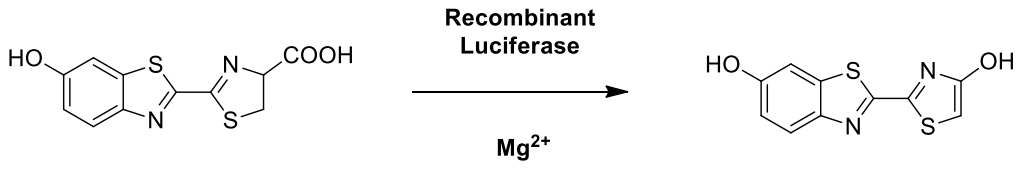

Beetle Luciferin

+ ATP
+ O_2

Oxyluciferin

+ AMP
+ PP_i
+ CO_2
+ Light

The kit was used according to the protocol provided by the manufacturers. HeLa or Hep G2 cells (5 x 10^3/well) were plated, in triplicate, into flat-bottomed, 96-well plates, before being left to adhere overnight. Cells were subsequently exposed to concentrations of drug ranging from 0.1 µM to 1000 µM, dependent upon the nature of the assay, and incubated at 37°C for time periods of up to 72 h. Following incubation, cells were treated with 20 µL of reconstituted Cell-TiterGlo reagent, before 100 µL of the reagent/media mixture was transferred to white-walled 96-well plates. After having been shaken for a period of 5 minutes, plates were read on a luminescence spectrophotometer (Varioskan Flash, Thermo Scientific, Loughborough, UK) at an absorbance wavelength of 560 nm. Results are expressed as a percentage of absorbance relative to untreated vehicle control, with IC_{50} derived from curves plotted using GraFit Software.

2.2.6. Seahorse XF Analysis of Oxygen Consumption and Extracellular Acidification Rates

OCR and ECAR were measured using the Seahorse XFe96 Analyser. The unit quantifies these parameters simultaneously through determining the variations in fluorescence intensity in two probes, one of which displays sensitivity towards oxygen concentration, and the other towards proton content. Measurements are made in assay medium located above a cell monolayer positioned on the surface of each well, and are typically repeated over seven-minute intervals for the duration of the experiment. The use of unbuffered DMEM allows for fluctuations in pH associated with variation in the rate of glycolysis, represented through ECAR, to be measured (Dranka *et al.*, 2011).

Typically, HeLa or Hep G2 cells (2.5 x 10^4/well) were plated in 96-well XF Cell Culture Microplates, and left to adhere overnight. HeLa cells and Hep G2 cells grown in high-glucose DMEM and adhered on 96-well XF Cell Culture Microplates had their media replaced with unbuffered minimal DMEM supplemented with L-glutamine (1% v/v), sodium pyruvate (1% v/v) and glucose (4.5 g/L). HeLa and Hep G2 cells grown in galactose-containing DMEM and adhered on 96-well XF Cell Culture Microplates had their media replaced with unbuffered minimal DMEM supplemented with L-glutamine (2% v/v), sodium pyruvate (1% v/v) and galactose (1 mM). Cells were then incubated at 37°C in a 0% CO_2 environment for a period of 1 h. XFe96 FluxPaks were prepared separately: 200 µL XF Calibrant Solution was added to each well on the day prior to the performance of the assay, ahead of overnight incubation at 37°C in 0% CO_2.

2.2.7. Direct Infusion

Artesunate was added to the injection port of a hydrated XFe96 FluxPak. Following injection, measurement of OCR and ECAR was performed over a 2 h period.

2.2.8. Mitochondrial Stress Test

The mitochondrial stress test allows for the assessment and quantification of mitochondrial bioenergetic function through determining cellular OCR and ECAR responses to the sequential addition of compounds impacting upon the function of oxidative phosphorylation (Hill *et al.*, 2012). Cells are initially treated with the ATP synthase inhibitor oligomycin, in order to bring about a cessation of oxidative energy generation and hence abolish oxygen consumption unrelated to proton leak. The addition of the ionophoric inner mitochondrial membrane permeabiliser carbonyl cyanide-p-trifluoromethoxyphenylhydrazone (FCCP) dissipates the membrane potential and produces a theoretical maximal OCR, before rotenone inhibits oxygen consumption related to the activity of complex I.

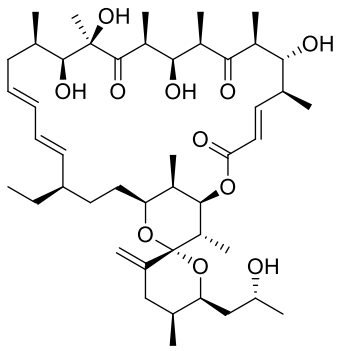

Oligomycin A

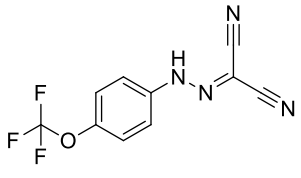

FCCP

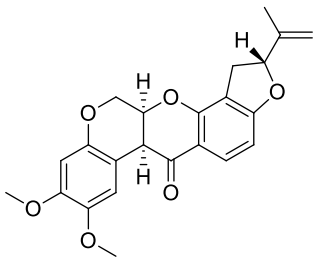

Rotenone

HeLa cells plated on an XF Cell Culture Microplate (2.5 x 10^4/well) and dosed with artesunate (1 – 100 µM) were incubated at 37°C for periods between 0 and 24 h. Culture media was replaced with unbuffered DMEM, as described in Section 2.2.6. Oligomycin (1.5

µM), FCCP (0.4 µM) and rotenone (1 µM) were placed respectively in injection ports A, B and C on a hydrated XFe96 FluxPak, ahead of calibration. Cellular OCR and ECAR were recorded at seven minute intervals over twelve cycles, with the injection of oligomycin, FCCP and rotenone occurring following the third, sixth and ninth intervals. Normalisation was performed with respect to cell number, which was determined using a haemocytometer following conclusion of recording.

2.2.9. Glycolytic Stress Test

Determining ECAR response to the addition of compounds stimulating and inhibiting rates of glycolysis allows for cellular glycolytic function to be assessed. Cells in glucose-free media are treated first with a saturating concentration of glucose, in order to stimulate glycolysis. Subsequent addition of oligomycin prevents oxidative ATP generation, hence increasing glycolytic rate to a maximal level. The introduction of the final compound, 2-deoxyglucose (2-DG), induces the cessation of glycolysis and limits ECAR to that associated with non-glycolytic mechanisms.

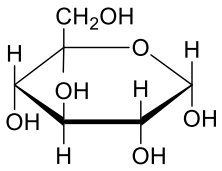

Glucose

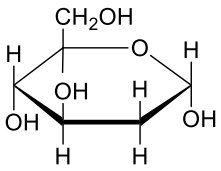

2-Deoxy-glucose

HeLa cells plated on an XF Cell Culture Microplate (2.5 x 10^4/well) and dosed with artesunate (5 – 50 µM) were incubated at 37°C for 24 h. Culture media was replaced with unbuffered, glucose-free DMEM, as described in Section 2.2.6. Glucose (10 mM), oligomycin (1.5 µM) and 2-DG (100 mM) were placed respectively in injection ports A, B

and C on a hydrated XFe96 FluxPak, ahead of calibration. Cellular OCR and ECAR were recorded at seven minute intervals over twelve cycles, with the injection of glucose, oligomycin and 2-DG occurring following the third, sixth and ninth intervals. Normalisation was performed with respect to cell number, which was determined using a haemocytometer following conclusion of recording.

2.2.10. Statistical Analysis

All values are expressed as a mean, ± standard deviation (SD) as represented through error bars on graphs. Following the assessment of data normality using the Shapiro-Wilk test, the Student's paired-t-test was employed in order to determine significance. In the event of non-normality, the Mann-Whitney U test was instead used for this purpose. Results were deemed significant when p-value was smaller than 0.05. Significance is represented as: * equivalent to $P < 0.05$, ** equivalent to $P < 0.01$ and *** equivalent to $P < 0.001$.

2.3. Results

2.3.1. Artesunate Toxicity and Mitochondrial Liability

2.3.1.1. Hep G2 Cells

2.3.1.1.1. Sensitivity of Galactose-Cultured and Glucose-Cultured Cells towards Rotenone Treatment

In order to verify that Hep G2 cells cultured in galactose exhibited heightened sensitivity towards mitochondrial toxins relative to those grown in glucose, the response to the complex I inhibitor rotenone was examined across both variants. Cells grown under either set of conditions were treated with rotenone for 24 h, before levels of cell viability were ascertained using the MTT assay. It was demonstrated that galactose-cultured cells exhibited greatly enhanced susceptibility towards rotenone-induced cytotoxicity (Table 2.1.), with relevant IC_{50} values calculated from the dose-response curves outlined in Figure. 2.1. This augmented response towards compounds impacting upon the functioning of the organelle indicates an increased reliance upon mitochondrial ATP production.

T (h)	IC_{50} (µM)	
	Glucose	Galactose
24	> 10	0.027 ± 0.009

Table 2.1. IC_{50} values of glucose-cultured and galactose-cultured Hep G2 cells dosed with rotenone. Cytotoxicity was determined using the MTT assay. Results are shown as the mean of three independent experiments, ± SD.

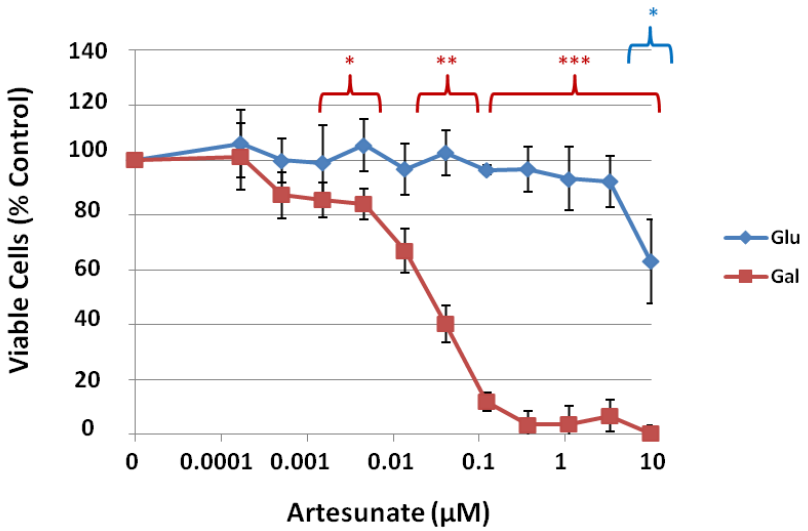

Figure 2.1. Representative traces outlining dose-response relationships in glucose-cultured and galactose-cultured Hep G2 cells upon artesunate treatment. Cells were exposed to 0 – 10 µM artesunate for a period of 24 h, before viability was ascertained using the MTT assay. Values are expressed as percentage of live cells relative to vehicle control, and are presented as the mean of three independent experiments, ± SD. * represents $p < 0.05$, ** represents $p < 0.01$ and *** $p < 0.001$, as determined through the paired t-test.

2.3.1.1.2. Response of Galactose-Cultured and Glucose-Cultured Cells towards Artesunate Treatment

Glucose-cultured and galactose-cultured Hep G2 cells were examined for their response to treatment with artesunate. Investigation into dose-response was performed following 24, 48 and 72 h incubation, with the MTT assay employed in order to determine the viability. Small differences, none statistically significant, were witnessed between IC_{50} values obtained after 24 and 48 h drug treatment (Table 2.2.).

T (h)	IC_{50} (µM)		p
	Glucose	Galactose	
24	94.7 ± 10.6	79.7 ± 26.2	> 0.05
48	48.0 ± 4.80	40.6 ± 1.97	> 0.05
72	28.8 ± 5.80	28.7 ± 2.70	> 0.05

Table 2.2. IC_{50} values of glucose-cultured and galactose-cultured Hep G2 cells dosed with artesunate. Cytotoxicity was determined using the MTT assay. Results are shown as the mean of three independent experiments, ± SD. $p < 0.05$ denotes statistical significance, as determined through the paired t-test.

2.3.1.1.3. Effect of Artesunate upon Oxygen Consumption Rate in Galactose-Cultured and Glucose-Cultured Cells

The Seahorse XFe96 analyser was used in order to assess the impact of artesunate upon mitochondrial respiratory function in Hep G2 cells. Glucose-cultured or galactose-cultured cells were dosed *in situ* with 500 µM artesunate, before OCR and ECAR responses were recorded over a period of 2 h. Drugged cells exhibited a gradual and significant decrease in levels of OCR, which had fallen to 78% and 74% of control values in glucose-cultured and galactose-cultured lines respectively following 120 minutes of exposure (Fig. 2.2. A). There was no significant variation in response between the two cell types. ECAR was observed to spike immediately upon drug administration over both cell varieties, before entering into decline (Fig. 2.2. B). The magnitude of this initial increase was substantially greater in the galactose-grown line, reaching 800% of control quantity at its maximum extent. After 2 h of measurement, ECAR had fallen to 73% and 79% of control respectively in the glucose-cultured and galactose-cultured varieties. Variation in response between types did not achieve significance.

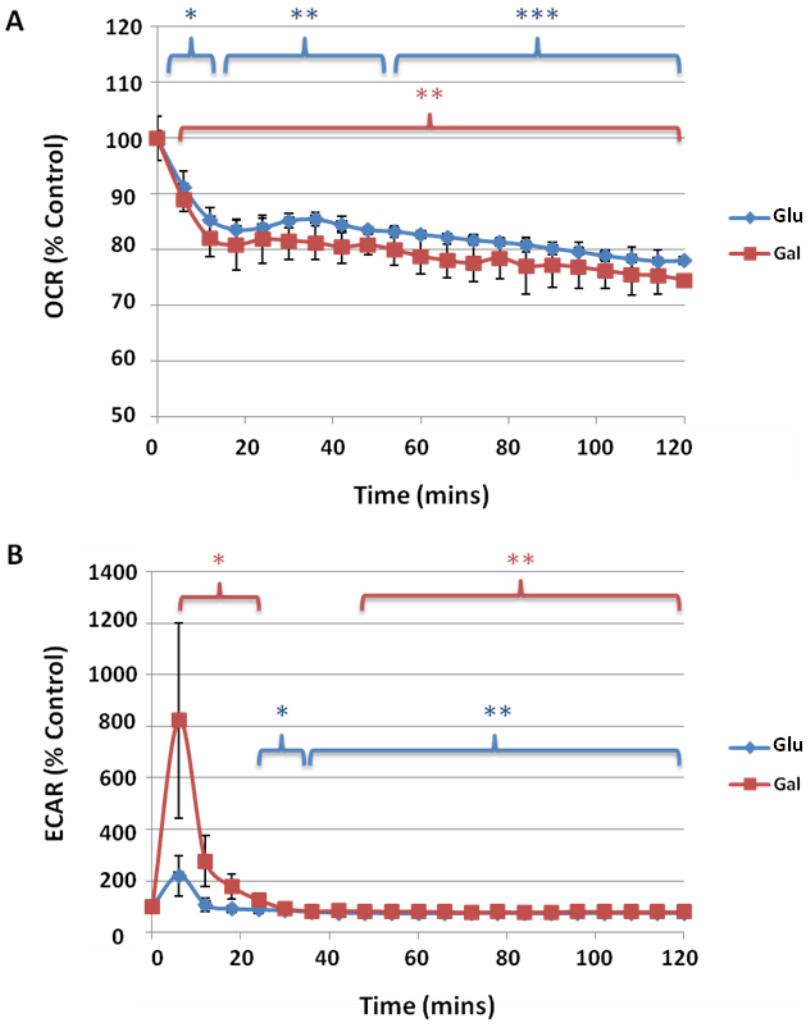

Figure 2.2. Cellular oxygen consumption and extracellular acidification rates in glucose-cultured and galactose-cultured Hep G2 cells responding to artesunate treatment. Cells were treated with 500 µM artesunate before variations in OCR **(A)** and ECAR **(B)** were measured over a 2 h period. Values are expressed as percentage of OCR relative to vehicle control, and are presented as the mean of three independent experiments, ± SD. * represents $p < 0.05$, ** represents $p < 0.01$ and *** $p < 0.001$, as determined through the paired t-test.

2.3.1.2. HeLa Cells

2.3.1.2.1. Sensitivity of Galactose-Cultured and Glucose-Cultured Cells towards Rotenone Treatment

HeLa cells cultured in either glucose-containing or galactose-containing media were treated with rotenone for 24 h, before their viability was examined using the MTT assay. Similar to

the pattern observed in the Hep G2 line, galactose-cultured cells exhibited a far greater sensitivity towards the cytotoxic effects of the compound (Table 2.3.).

T (h)	IC_{50} (µM)		p
	Glucose	Galactose	
24	0.24 ± 0.054	0.0038 ± 0.0023	0.0072

Table 2.3. IC_{50} values of glucose-cultured and galactose-cultured HeLa cells dosed with rotenone. Cytotoxicity was measured using the MTT assay. Results are shown as the mean of three independent experiments, ± SD. $p < 0.05$ denotes statistical significance, as determined through the paired t-test.

2.3.1.2.2. Response of Galactose-Cultured and Glucose-Cultured Cells towards Artesunate Treatment

Glucose-cultured and galactose-cultured HeLa cells were treated with artesunate, with dose-response relationships examined using the MTT assay following 6, 16, 24, 48 and 72 h incubation. Significant deviation between the sensitivity of the cell types to the drug is apparent at 16, 24 and 48 h (Table 2.4.).

T (h)	IC_{50} (µM)		p
	Glucose	Galactose	
6	> 1000	> 1000	-
16	193 ± 15.6	129 ± 2.60	0.0082
24	77.3 ± 5.92	24.8 ± 8.41	0.0095
48	27.1 ± 3.18	9.70 ± 0.98	0.0048
72	15.0 ± 2.31	10.0 ± 4.45	> 0.05

Table 2.4. IC_{50} values of glucose-cultured and galactose-cultured HeLa cells dosed with artesunate, obtained using MTT assay. Results are shown as the mean of three independent experiments, ± SD. $p < 0.05$ denotes statistical significance, as determined through the paired t-test.

2.3.1.2.3. ATP Content in Galactose-Cultured and Glucose-Cultured Cells following Artesunate Treatment

The impact of artesunate administration upon ATP levels in glucose-cultured and galactose-cultured HeLa cells was determined using the CellTiter-Glo luminescent ATP content assay. Variation in ATP abundance between cells was found to be significant following 16 and 24 h treatment (Table 2.5.).

T (h)	IC_{50} (µM)		p
	Glucose	Galactose	
6	> 1000	> 1000	-
16	210 ± 27.1	14.7 ± 10	0.0014
24	47.6 ± 9.3	5.37 ± 1.2	0.0092
48	13.5 ± 2.60	12.6 ± 0.20	> 0.05
72	16.3 ± 2.40	12.1 ± 1.50	> 0.05

Table 2.5. IC_{50} values of glucose-cultured and galactose-cultured HeLa cells dosed with artesunate, obtained using ATP content assay. Results are shown as the mean of three independent experiments, ± SD. $p < 0.05$ denotes statistical significance, as determined through the paired t-test.

The time-dependence of the IC_{50} values assayed through MTT and ATP content assays, as outlined in Table 2.4. and Table 2.5., is displayed graphically in Figure 2.3. A fall in ATP levels is shown to precede cytotoxicity in glucose-cultured (Fig. 2.3 A) and galactose-cultured (Fig. 2.2. B) HeLa cells. The extent of this effect is greater within the latter variety.

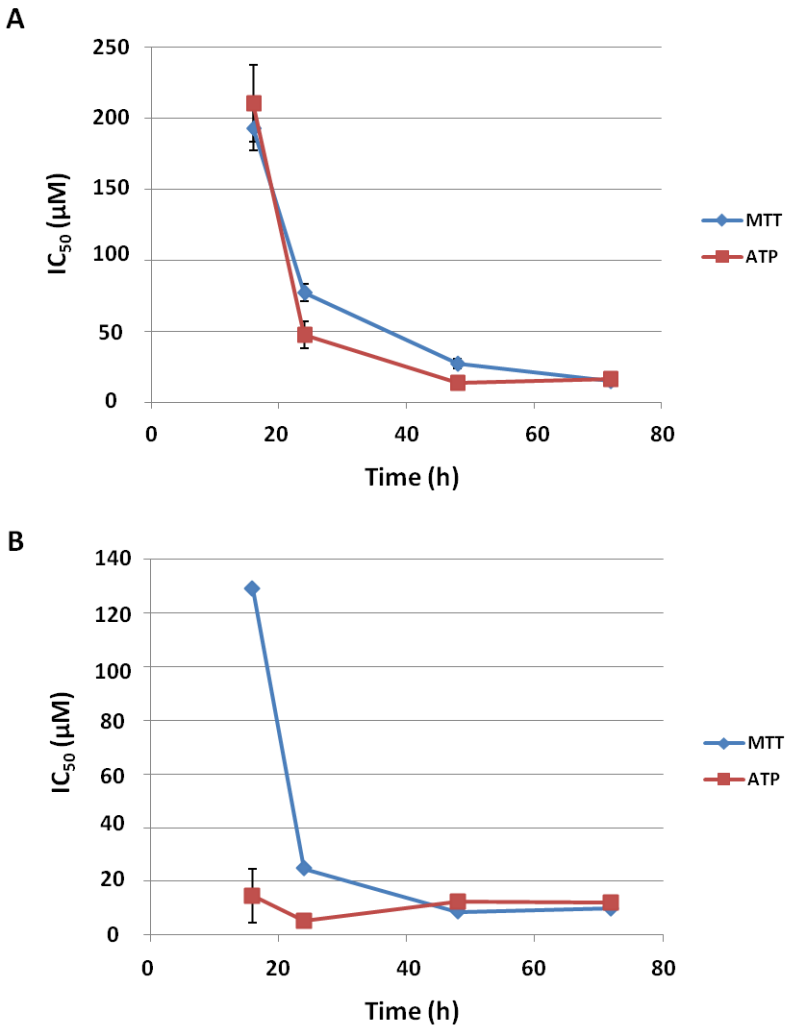

Figure 2.3. Time-dependence of IC_{50} values obtained through MTT and ATP content assays. HeLa cells cultured in glucose **(A)** and galactose **(B)** were exposed to artesunate for over time periods ranging from 6 – 72 h. Results are shown as the mean of three independent experiments, ± SD.

2.3.1.2.4. Effect of Artesunate upon Oxygen Consumption Rate in Galactose-cultured and Glucose-cultured Cells

The Seahorse XFe96 analyser was used in order to assess the impact of artesunate upon mitochondrial respiratory function in HeLa cells. Glucose-cultured or galactose-cultured cells were dosed *in situ* with 50 µM artesunate, before OCR response was recorded across a period of 2 h. OCR had fallen to 78% and 77% of control values in glucose-cultured and galactose-cultured cells respectively following 120 minutes of exposure (Fig. 2.4. A). ECAR

increased initially upon drug exposure within each cell type, growing to 250-300% of control levels at its greatest extent (Fig. 2.4. B). Levels subsequently fluctuated, before reaching 66% and 67% of control in the glucose-cultured and galactose-cultured cells respectively upon 2 h treatment.

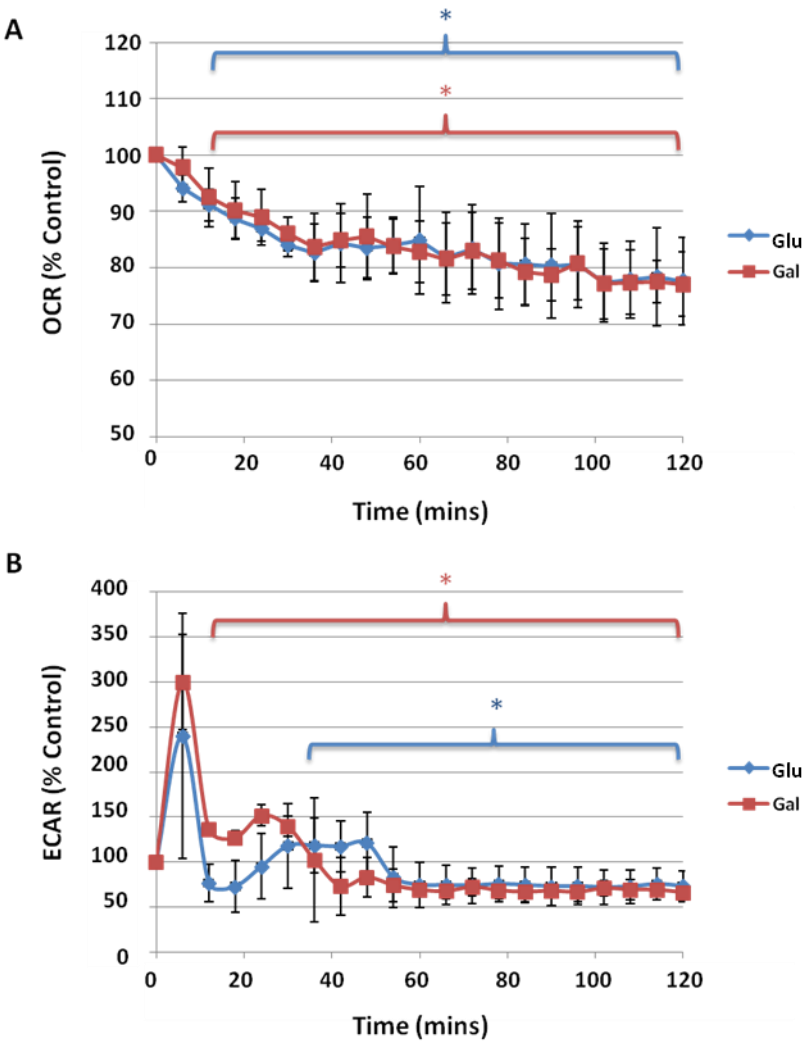

Figure 2.4. Cellular oxygen consumption and extracellular acidification rates in glucose-cultured and galactose-cultured HeLa cells responding to artesunate treatment. Cells were treated with 50 µM artesunate before variations in OCR **(A)** and ECAR **(B)** were measured over a 2 h period. Values are expressed as percentage of OCR or ECAR relative to vehicle control, and are presented as the mean of three independent experiments, ± SD. * represents $p < 0.05$, as determined through the paired t-test.

2.3.2. Impact of Artesunate upon Mitochondrial Bioenergetic Function

2.3.2.1. The Mitochondrial Stress Test

The mitochondrial function of HeLa cells in response to artesunate treatment was examined using the Seahorse XFe analyser. Through determining variation in OCR and ECAR associated with the addition of compounds known to impact upon structures associated with oxidative phosphorylation, it is possible to examine several parameters indicative of mitochondrial health. A model trace, outlining the typical OCR response of cells to the addition of compounds over the course of a stress test, is displayed in Figure 2.5. It is typical for a set of twelve OCR or ECAR measurements to be made over a period of 80 minutes, with a seven minute equilibration and mixing cycle occurring between each.

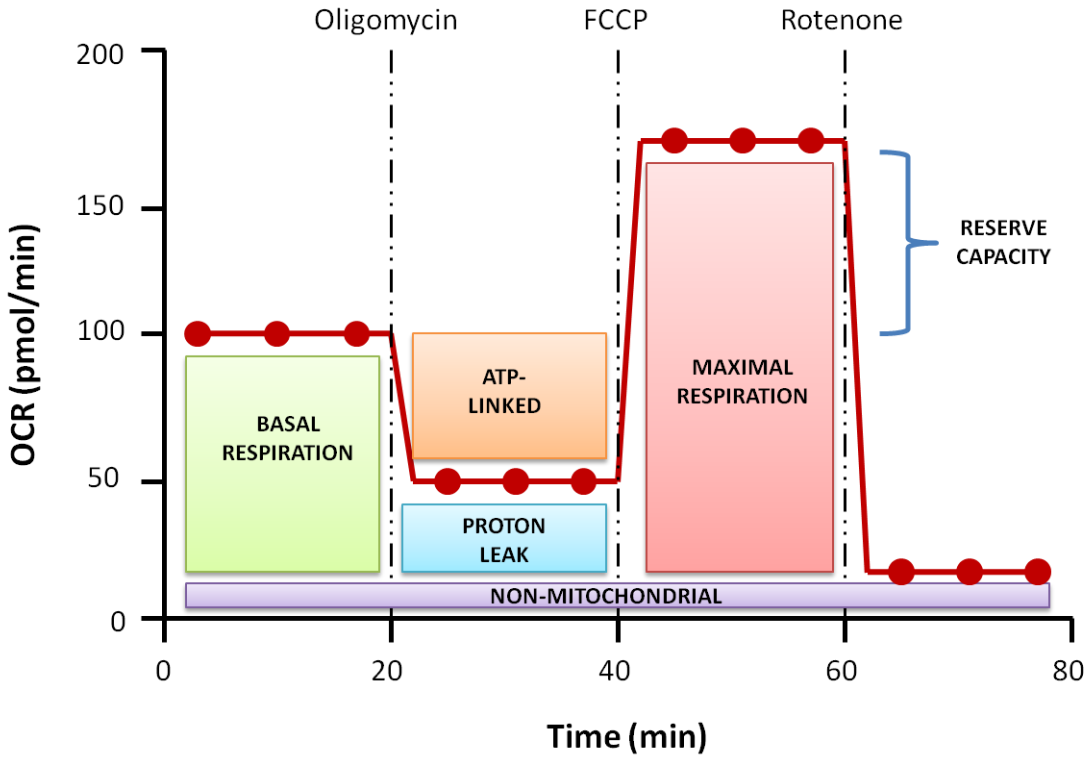

Figure 2.5. Idealised OCR trace displaying parameters discernible during the course of the mitochondrial stress test. OCR response to the sequential addition of oligomycin, FCCP and rotenone is outlined.

Three measurements are made corresponding to levels of basal cellular respiratory oxygen consumption, prior to the injection of the first compound. The addition of the ATP synthase inhibitor oligomycin has the effect of blocking oxidative phosphorylation, thus removing all oxygen consumption associated with the generation of ATP. A fall in OCR is witnessed to occur, the magnitude of which is dependent upon the extent of remaining consumption unrelated to oxidative ATP synthesis. Typically, this OCR can be attributed both to the passive leakage of protons across the inner mitochondrial membrane, and also to non-mitochondrial respiration.

FCCP is an ionophoric compound, which permeabilises the inner membrane of the mitochondrion to the passage of protons, and thus induces a collapse in membrane potential. The removal of the proton gradient uncouples oxygen consumption from ATP production, leading to an increase in OCR to levels approaching their theoretical maximum. The complex I inhibitor rotenone, which suspends predominant oxygen consumption through the electron transport chain, reduces OCR to that occurring primarily through non-mitochondrial routes. Experimental OCR traces displayed Figure 2.6. outline the variations in response to oligomycin and FCCP administration in control cells (Fig. 2.6. A), and in those treated with 50 μM artesunate (Fig. 2.6. B), for a period of 24 h. Increased proton leak and decreased maximal respiration are clearly evident in the latter. Figure 2.7. displays the corresponding variations in ECAR, with growth in basal glycolytic rate readily apparent.

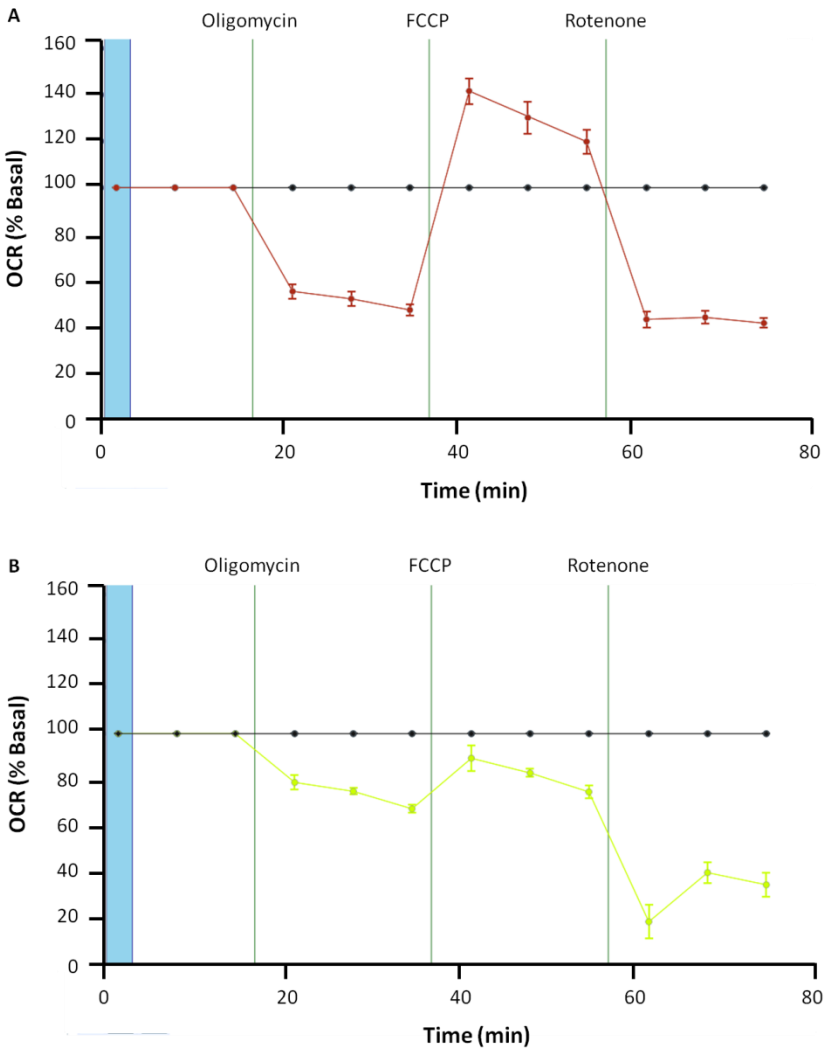

Figure 2.6. Representative experimental OCR traces derived from mitochondrial stress tests. OCR response to the sequential addition of oligomycin, FCCP and rotenone is outlined in control **(A)** and 50 µM artesunate-treated **(B)** HeLa cells following 24 h incubation.

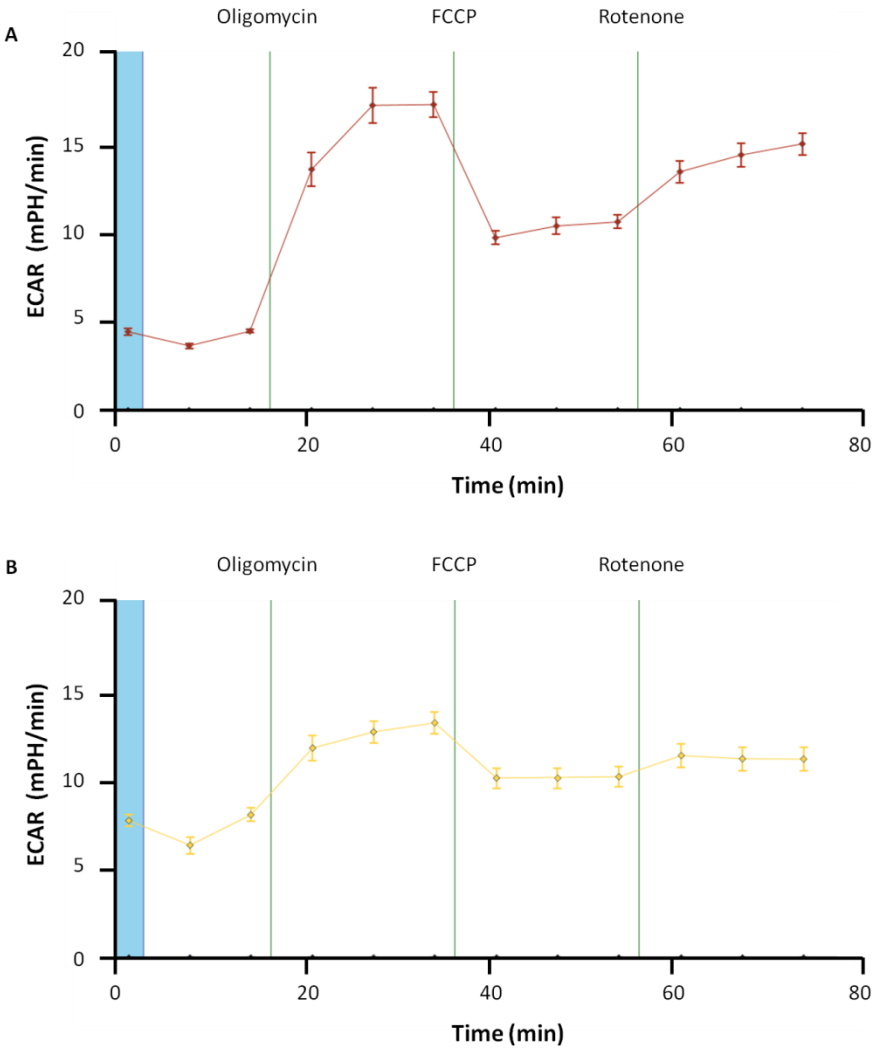

Figure 2.7. Representative experimental ECAR traces derived from mitochondrial stress tests. ECAR response to the sequential addition of oligomycin, FCCP and rotenone is outlined in control **(A)** and 50 µM artesunate-treated **(B)** HeLa cells following 24 h incubation.

2.3.2.1.1. Effects of Artesunate upon Basal Oxygen Consumption Rate

Basal OCR was measured in HeLa cells following 24 h treatment with artesunate over concentrations ranging from 1 to 100 µM (Fig. 2.8. A), and with 20 µM artesunate across times ranging from 0 to 24 h (Fig. 2.8. B). No significant variations in OCR levels were seen with respect to either concentration or to time.

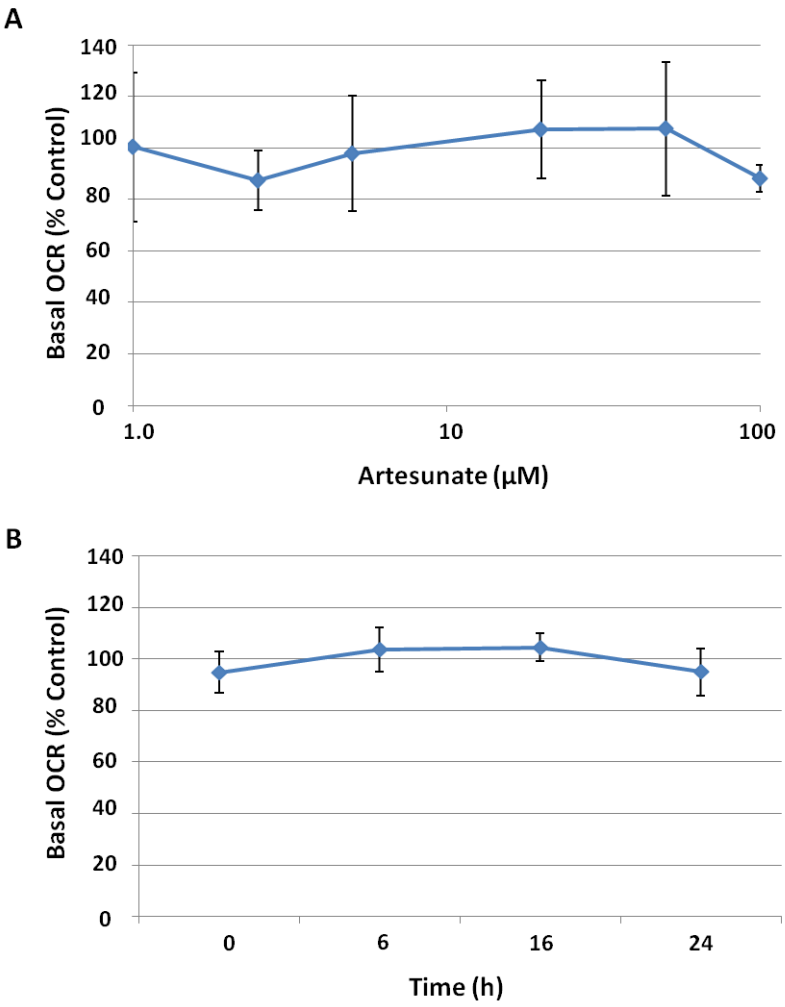

Figure 2.8. Effects of artesunate upon basal oxygen consumption rate. HeLa cells were treated for 24 h with artesunate in concentrations ranging from 1 – 100 µM **(A)** and with 20 µM artesunate over time courses ranging from 0 – 24 h **(B)**. Values are expressed as percentage of normalised OCR relative to vehicle control, and are presented as the mean of three independent experiments, ± SD.

2.3.2.1.2. Impact of Artesunate upon Mitochondrial Coupling Efficiency

The efficiency of oxidative coupling and ATP production may be inferred through determining the proportion of OCR linked to the generation of ATP, relative to that attributable to proton leak. As outlined in Figure 2.5., the addition of oligomycin induces reduction in OCR from basal levels, with that which remains assignable to both the leak of protons and to non-mitochondrial respiration.

If *u* is OCR following oligomycin addition, *b* is basal OCR and *n* is non-mitochondrial OCR, the coupling efficiency *CE* can be determined through the equation:

$$CE = 1 - \frac{(u - n)}{(b - n)}$$

So that as incidence of proton leak increases, coupling efficiency falls. Treatment of HeLa cells with artesunate for 24 h over concentrations from 1 to 100 µM (Fig. 2.9. A) induced a significant decrease in the efficiency of coupling, with levels falling to 60% of those in vehicle control. Dosing with 20 µM artesunate (Fig. 2.9. B) resulted in significant reductions following 16 and 24 h incubation.

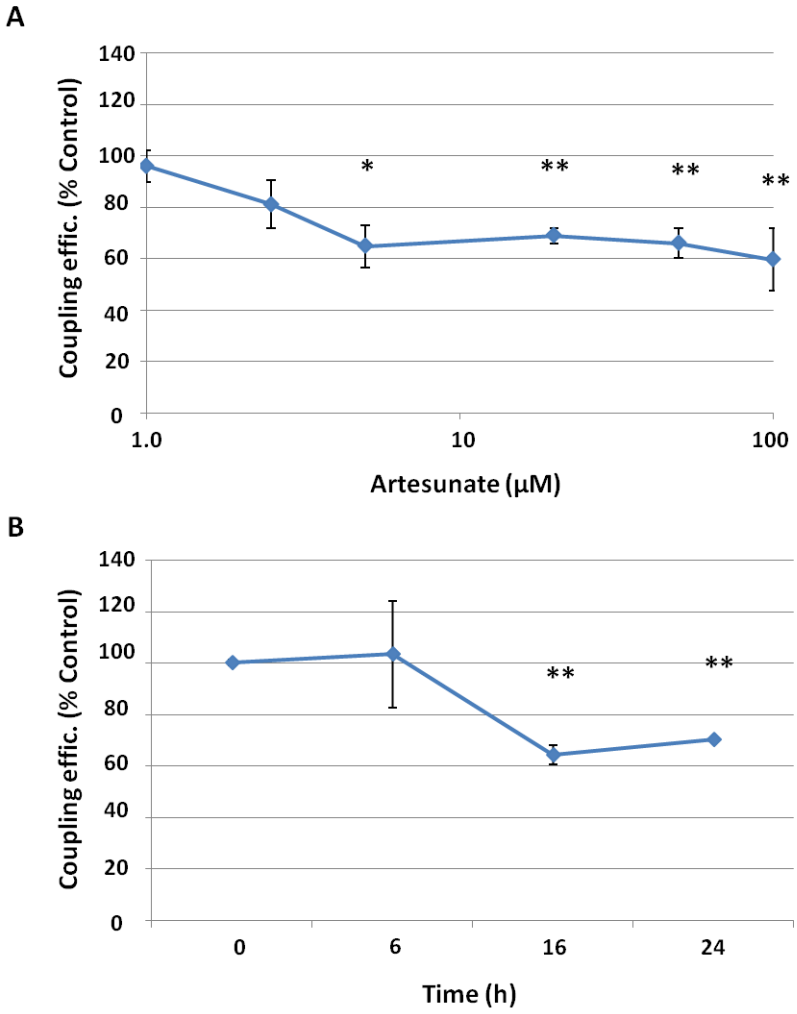

Figure 2.9. Impact of artesunate upon mitochondrial coupling efficiency. HeLa cells were treated for 24 h with artesunate in concentrations ranging from 1 – 100 µM **(A)** and with 20 µM artesunate over time courses ranging from 0 – 24 h **(B)**. Values are expressed as percentage of normalised OCR relative to vehicle control, and are presented as the mean of three independent experiments, ± SD. * represents $p < 0.05$ and ** $p < 0.01$, as determined through the paired t-test.

2.3.2.1.3. Effect of Artesunate upon Mitochondrial Reserve Capacity

It is typical that cells respire and consume oxygen under resting conditions at rates far smaller than those of which they are capable under instances of increased bioenergetic demand. The maximal respiratory capacity of a cell can be determined through examining the magnitude of the OCR increase induced through addition of the ionophore FCCP, a compound which collapses proton gradient and uncouples ATP production. If *m* is OCR

following FCCP addition, *b* is basal OCR and *n* is non-mitochondrial OCR, reserve capacity *RC* can be determined through the equation:

$$RC = \frac{(m-n)}{(b-n)}$$

A significant, steady and dose-dependent decrease in HeLa cell reserve capacity occurred upon 24 h artesunate treatment (Fig. 2.10. A), with values falling to 40% of control at the maximal 100 µM concentration. Time-dependence was additionally evident, with significant falls in response to 20 µM artesunate apparent following 16 and 24 h (Fig. 2.10. B).

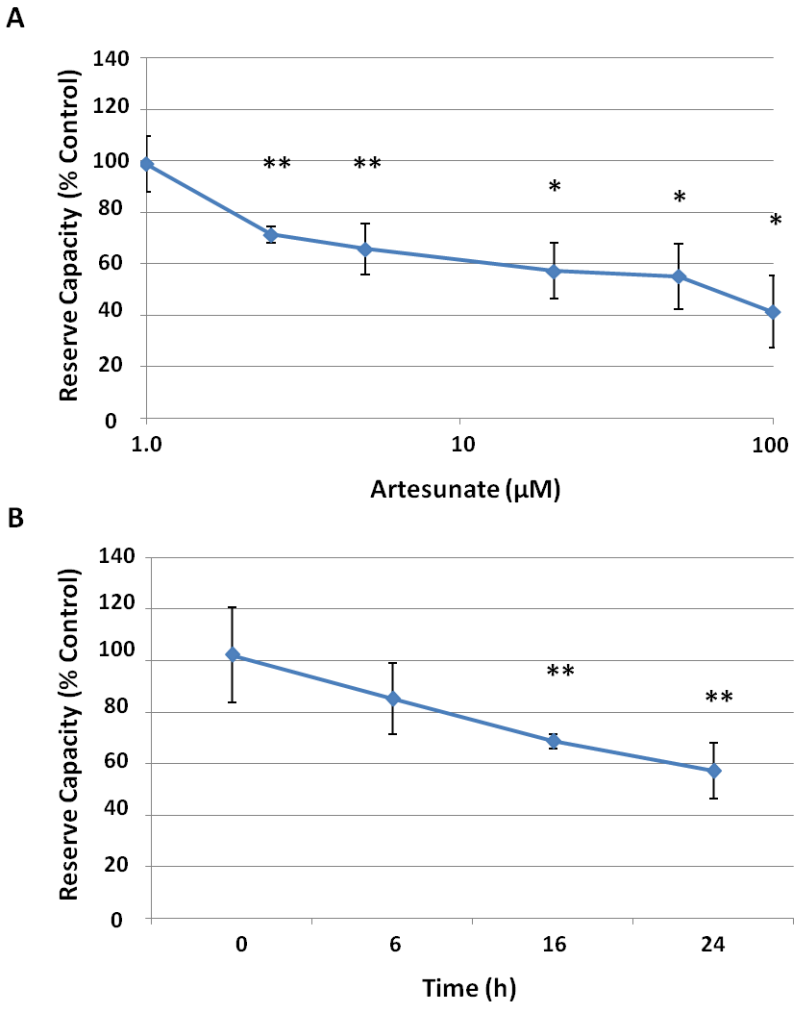

Figure 2.10. Effect of artesunate upon mitochondrial reserve capacity. HeLa cells were treated for 24 h with artesunate in concentrations ranging from 1 – 100 µM **(A)** and with 20 µM artesunate over time courses ranging from 0 – 24 h **(B)**. Values are presented as the mean of three independent experiments, ± SD. * represents $p < 0.05$ and ** $p < 0.01$, as determined through the paired t-test.

2.3.2.1.4. Effect of Artesunate upon Basal Extracellular Acidification Rate

Rates of cellular glycolysis are determined through measuring media acidification (ECAR) stimulated though increased proton production. Basal ECAR is recorded prior to addition of oligomycin. HeLa cells treated with 1 – 100 µM artesunate for a period of 24 h exhibit significant, dose-dependent increases in levels of basal acidification up to 50 µM, before falling to those of control (Fig. 2.11. A). Cells dosed with 20 µM artesunate display a time-dependent growth in ECAR, which becomes significant following 16 and 24 h (Fig. 2.11. B).

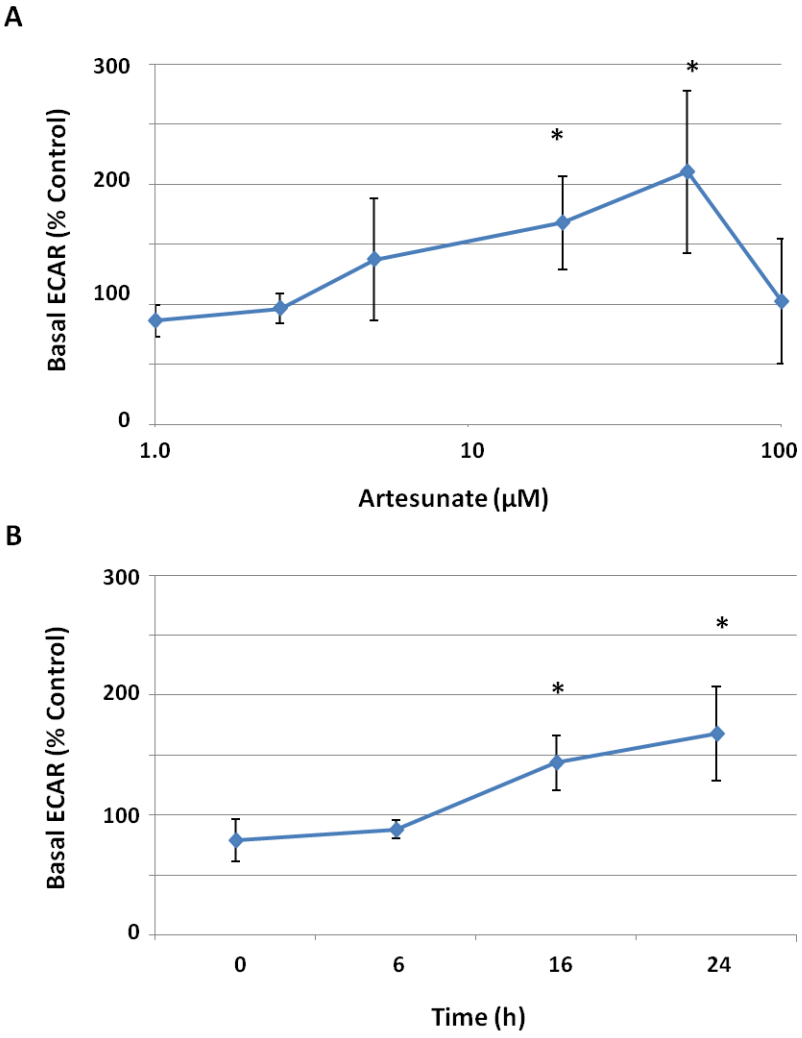

Figure 2.11. Effect of artesunate upon basal extracellular acidification rate. HeLa cells were treated for 24 h with artesunate in concentrations ranging from 1 – 100 µM **(A)** and with 20 µM artesunate over time courses ranging from 0 – 24 h **(B)**. Values are presented as the mean of three independent experiments, ± SD. * represents $p < 0.05$, as determined through the paired t-test.

2.3.2.2. Glycolytic Stress Test

The Seahorse XFe analyser was used in order to determine the glycolytic capacity of HeLa cells in response to artesunate treatment. ECAR variation resulting from the sequential addition of compounds impacting upon the progression of glycolysis enables such functions to be quantified. An idealised ECAR trace taken over the course of a typical glycolytic stress test is outlined in Figure 2.12. Twelve ECAR measurements are generally made over a period of 80 minutes, with a seven minute equilibration and mixing period occurring between each.

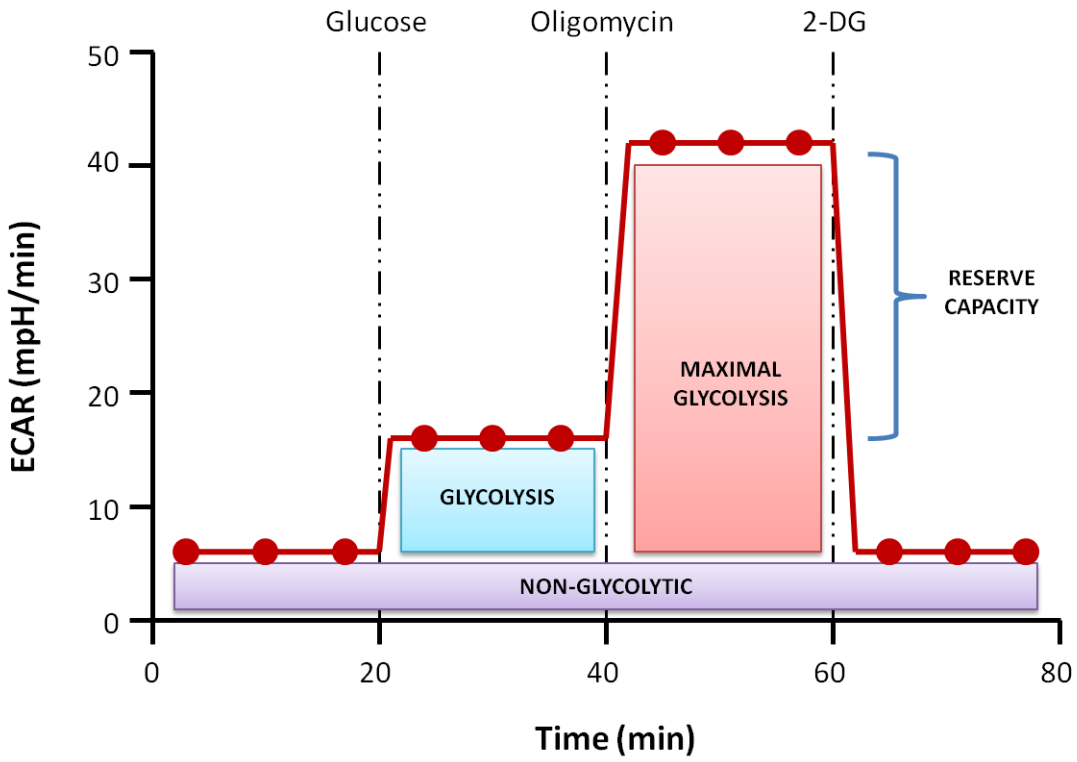

Figure 2.12. Idealised ECAR trace displaying parameters discernible during the course of the glycolytic stress test. ECAR response to the sequential addition of glucose, oligomycin and 2-DG is outlined.

Culture media is replaced with glucose-free DMEM, before the introduction of glucose stimulates basal glycolysis. Maximal levels are attained through addition of oligomycin – a compound inhibiting ATP synthase and hence shifting energy production from oxidative phosphorylation. The final compound added, 2-DG, blocks glycolysis, reducing remaining ECAR to that arising from non-glycolytic sources. Experimental OCR traces displayed Figure 2.13. outline the response to administration of these compounds both in control cells (Fig. 2.13. A) and in those treated with 50 µM artesunate (Fig. 2.13. B) for a period of 24 h. Increased proton leak and decreased maximal respiration are clearly evident in the latter.

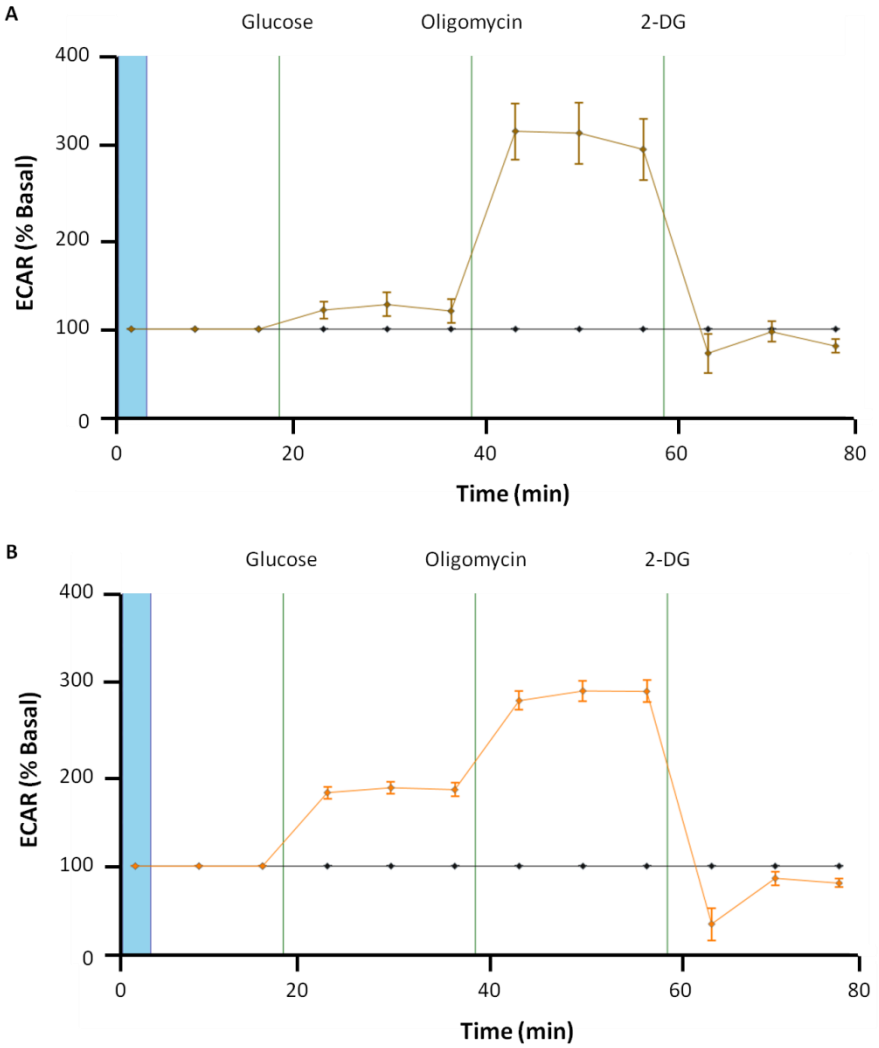

Figure 2.13. Representative experimental ECAR traces derived from glycolytic stress tests. ECAR response to the sequential addition of glucose, oligomycin and 2-DG is outlined in control **(A)** and 50 µM artesunate-treated **(B)** HeLa cells incubated for a period of 24 h.

2.3.2.2.1. Impact of Artesunate upon Glycolytic Reserve Capacity

The glycolytic reserve capacity of a cell may be inferred from the relative magnitude of the ECAR response following addition of oligomycin.

If *o* is ECAR level following oligomycin addition, *g* is glucose-stimulated ECAR and *n* is non-glycolytic ECAR, glycolytic reserve *GR* is given by the equation:

$$GR = \frac{(o - n)}{(g - n)}$$

Following 24 h treatment with 50 µM artesunate, a significant, dose-dependent decrease in the glycolytic reserve capacity of HeLa cells is noted (Fig. 2.14.).

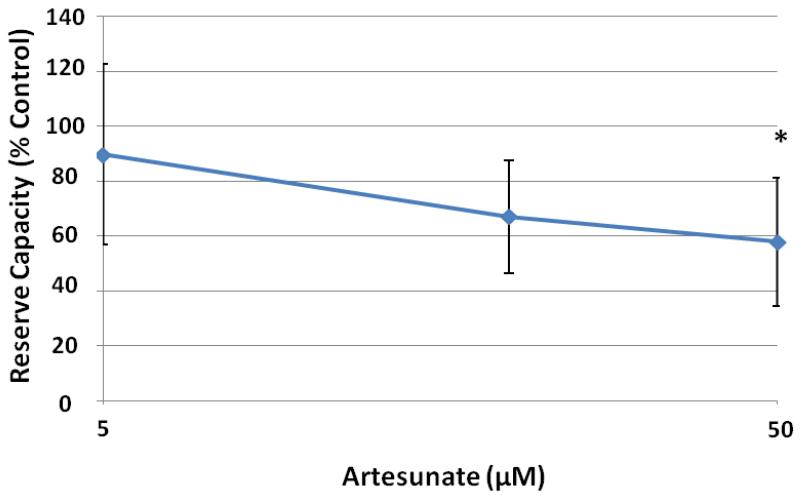

Figure 2.14. Impact of artesunate upon glycolytic reserve capacity. HeLa cells were treated for 24 h with artesunate in concentrations ranging from 5 – 50. Values are expressed as percentage of normalised ECAR relative to vehicle control, and are presented as the mean of three independent experiments, ± SD. * represents $p < 0.05$, as determined through the paired t-test.

2.4. Discussion

The activity of artesunate has been examined with respect to its functions as a mitochondrial toxin. Studies into its effects across cells sensitised towards mitochondrial liability through galactose culturing have indicated a tendency towards enhanced cytotoxicity, albeit with variability dependent upon cell line and length of treatment. It was generally observed that the sensitivity of cervical carcinoma-derived HeLa cells towards artesunate was greater than that of the hepatocellular Hep G2 line – an effect which was found to occur uniformly irrespective of culture conditions. This may be understood with reference to the bioenergetic profile of the Hep G2 cells, which possess elevated glycolytic capacity and hence a relative general resistance to the effects of mitochondrially toxic compounds (Marroquin *et al.*, 2007). Their choice as the initial cell line in which to investigate artesunate toxicity through galactose culture was made owing to their prevalence across studies performed within the literature.

No significant variation was noted between the artesunate IC_{50} values obtained through the MTT assay in glucose-cultured and galactose-cultured Hep G2 cells over all incubation time points examined (Table 2.2.). Although this response would appear inconsistent when viewed alongside the existing evidence testifying to the role of endoperoxides as mitochondrial toxins, it has been noted that compounds such as tamoxifen, doxorubicin and imipramine, which are further known disrupters of mitochondrial function, possess near-identical cytotoxicity profiles within both glucose-cultured and galactose-grown Hep G2 cells (Dykens *et al.*, 2008b; Marroquin *et al.*, 2007). In these instances, it is theorised that their action in the mitochondria forms only a single facet of the mechanism through which they induce cell death, with effects upon other areas of cellular function being of considerable additional importance (Will *et al.*, 2014).

Repetition of this experiment within the more sensitive HeLa line produced a greater general variance in the response between glucose-cultured and galactose cultured cells, with significant differences in MTT-defined IC_{50} value noted following 16, 24 and 48 h artesunate treatment (Table 2.4.). The magnitude of this variation was greatest at the 24 and 48 h points, at which galactose-cultured cells were observed to possess a three-fold greater sensitivity to the effects of the drug relative to those grown in glucose. The relevance of the extent of such disparities in susceptibility has been subject to discussion, with consensus across the literature generally holding a difference of at least two-fold to three-fold in the Hep G2 line to be indicative of a compound possessing mitochondrial liability (Swiss *et al.*, 2013; Will *et al.*, 2014). Variations observed at the 24 and 48 h treatment would place artesunate within this range, although a lack of corresponding data within the literature from HeLa cells makes comparison imperfect. Contrast is noted with respect to the effects witnessed in response to the direct mitochondrial toxin rotenone, which exhibits sixty-fold greater activity within the galactose-cultured cells (Table 2.3.).

Examination into artesunate effects upon ATP content in HeLa cells was performed using the luciferase-based CellTiter-Glo assay. Galactose-cultured cells displayed greatly enhanced sensitivity following 16 h and 24 h incubation, with fourteen-fold and nine-fold decreases in IC_{50} witnessed respectively relative to those grown in glucose (Table 2.5.). These differences had abated after 48 and 72 h, at which points there was almost no variability between types. It was generally observed that diminished ATP levels preceded a fall in MTT-detected cell viability, although such an effect was most prominent in galactose-cultured cells up to 24 h and in glucose-cultured cells between 24 and 48 h. A fall in ATP content occurring prior to cell death suggests that drug-induced disruption to ATP synthesis is causative in cytotoxicity, whilst the more pronounced nature of this within galactose-grown cells indicates that action upon mitochondrial energy generation serves additional importance (Fig. 2.3.).

Cellular bioenergetic function was impacted through artesunate treatment. Use of the Seahorse XFe analyser allowed for a broad investigation of the respiratory profile of HeLa cells to be performed, outlining the consequence of drug effects upon the activity of the mitochondrion. Full concentration and time-courses for stress test experiments were obtained for 0 – 24 h drug incubation, so that the onset of mitochondrial dysfunction could be related to the emergence of cytotoxicity. Evidence obtained suggests that artesunate imparts deleterious effects upon the performance of oxidative phosphorylation. Whilst no significant impact upon basal OCR level was noted with respect either to concentration of drug or to length of treatment (Fig. 2.8.), clear dose-dependent and time-dependent increases in basal ECAR were apparent until the dropping-off at heightened concentration (Fig. 2.11.). Elevation in ECAR is indicative of a growth in glycolytic respiration rate – an effect which is apparent as a compensatory mechanism in cells possessing compromised capacity to generate ATP through oxidative means. Nevertheless, the maximal glycolytic capacity of the cell, ascertained through the glycolytic stress test, fell steadily with artesunate dose (Fig. 2.14.). This signifies that supplementation of ATP through increased shift towards glycolysis grows increasingly unsustainable at higher drug concentration, enabling swifter depletion of energy and enhanced resultant levels of cell death.

Coupling efficiency of ATP production is inferred through determining the extent of proton leak across the inner mitochondrial membrane. The pumping of protons from the matrix into the intermembrane space is mediated through the four complexes constituting the electron transport chain, with the resultant gradient utilised for the purpose of ATP generation through ATP synthase. Whilst the non-productive diffusion of protons back across the inner membrane is found to occur at a basal rate under physiological conditions, significant increases are associated with dysfunctions in oxidative phosphorylation (Divakaruni *et al.*, 2011; Jastroch *et al.*, 2010). It is observed from stress test data that coupling efficiency decreases in a manner which is dependent upon artesunate dose and

length of incubation, falling to approximately 60% of control value in response to 5 µM treatment following 24 h, and 20 µM following 16 h (Fig. 2.9.). No further fall beyond the 60% minimum is witnessed, despite the continued decline in cell viability with respect to dose and time beyond those points.

A factor commonly associated with diminished coupling and enhanced proton leak is damage to the electron transport chain complexes or to the inner mitochondrial membrane (Hill *et al.*, 2012). There are an array of mechanisms through which this might occur in response to drug treatment, ranging from generalised oxidative stress to specific, targeted inhibition and modification of individual enzymes and proteins. The existing evidence regarding the activity of endoperoxide compounds within cells suggests several routes through which they might potentially induce functional modifications impacting adversely upon the progression of oxidative phosphorylation. It is hypothesised that the Fe(II)-mediated formation of carbon-centred radicals is key to both cytotoxic and pharmacological mechanisms of action, with the reactivity of these species affording them potent ability as alkylating agents (Mercer, 2009; Mercer *et al.*, 2010). Modification of haem in the presence of artemisinin has been demonstrated through biomimetic and *in vitro* studies, with structural changes noted within a variety of enzymes (Selmeczi *et al.*, 2004; Yang *et al.*, 1994). It is known that haemoproteins are a common feature within electron transport chain complexes, leading to a proposed route whereby defective complex function resulting from alkylation might contribute towards ROS formation (Mercer *et al.*, 2011). It has not been established, however, whether these structural alterations have the ability to impact significantly upon the activity of the proteins, prompting certain authors to doubt their relevance towards drug cytotoxic and antiparasitic action (Haynes *et al.*, 2013; Haynes *et al.*, 2011; Haynes *et al.*, 2004).

The mitochondrial reserve capacity relates to the spare respiratory potential possessed by a cell. Under instances of increased bioenergetic demand, the ability of the mitochondrion to increase rate of energy generation in order to match heightened requirements can act as a key determinant of its facility to overcome stress (Dranka *et al.*, 2011). Reduction in reserve capacity is associated with a diminished capacity to respond in such conditions – postulated as holding relationship with decreases in mitochondrial mass – with a total depletion culminating in death (Hill *et al.*, 2012). Experimentally, it is OCR response to the addition of the ionophoric uncoupler FCCP which is employed in order to determine the magnitude of maximal respiration, with reserve capacity inferred through relating this value to the basal and non-mitochondrial constituents of OCR. It was found that steady decreases in this parameter were witnessed with respect to both artesunate dose and incubation time, declining to a minimum value of 40% following 100 µM treatment over a 24 h period (Fig. 2.10.). It is understood that the extent of the reserve capacity is determined through the general efficiency of oxidative phosphorylation, a factor which is dependent upon the degree of respiratory coupling. Combined with the corresponding data outlining the reduction in coupling efficiency, its fall provides further evidence suggesting the presence of damage to the electron transport system. Whilst dysfunction might result from specified complex inhibition, as discussed earlier, it can arise additionally as a consequence of general oxidative stress. The effects of elevated ROS levels are well known to be deleterious towards an array of processes within cells, and it has been established that structural changes resulting from lipid peroxidation and protein modification may be causative of these (Fiers *et al.*, 1999; Imlay, 2003; Kowaltowski *et al.*, 1999). Studies have associated the induction of ROS with reduced reserve capacity across several cell systems, suggesting that damage resulting from oxidative stress can impact upon the ability of the cell to respond to further insult (Dranka *et al.*, 2010; Hill *et al.*, 2009; Perron *et al.*, 2013). The resulting cycle of ever-increasing oxidative damage would lead to a further diminished ability to restore

cell functions, resulting ultimately in its death. The source of this stress with respect to artesunate cytotoxicity remains to be elucidated, although this shall be granted further investigation in due course.

The relationship between the onset of artesunate cytotoxicity and the progression of mitochondrial dysfunction can be examined up to 24 h. No indication of bearing upon cell viability, reserve capacity or coupling efficiency is evident following 6 h treatment. Impact upon each of these parameters emerges only following 16 h incubation, before progressing further at 24 h. It can be observed that decline in mitochondrial function occurs alongside decrease in cell viability – strongly suggesting that drug impact upon the performance of the mitochondrion is a key determinant of cytotoxicity. This correlation is also witnessed to occur with respect to dose across the 1 – 100 μM range at a single, 24 h incubation period. The *in situ* dosing of glucose-cultured and galactose-cultured cells with a single, elevated drug dose produced only modest declines in OCR following 2 h exposure, which appears commensurate with the lack of substantial toxicity noted at this point (Fig. 2.4.). Contrasts must be made with the outcomes obtained from the studies performed by Dykens *et al.*, in which profound, sustained decreases in OCR – accompanied with commensurate increases in ECAR – were noted to occur over identical time-spans upon the administration of the mitochondrially-active compounds rotenone and nefazodone (Dykens *et al.*, 2008b).

When combined, the data presented within this chapter indicates that impact upon the bioenergetic profile of the mitochondrion is a key feature of the route through which artesunate is able to impart cytotoxic effects. Defective mitochondrial functioning, witnessed in terms of a diminished efficiency of oxidative phosphorylation and an accompanying increased reliance upon glycolytic respiration, is found to occur alongside cell death. Variations in sensitivity to the drug across galactose-cultured and glucose-cultured cell lines imply that increased dependence upon mitochondrial ATP production is

associated with heightened susceptibility towards toxicity. However, the relatively modest magnitude of these differences relative to direct mitochondrial toxins such as rotenone would suggest that non-mitochondrial activity is also a contributing factor towards their mechanism of action. In order to define the route through which defects arise, detailed investigation into the factors affecting their emergence shall follow.

Chapter Three

Examination into the Contributory Roles of Oxidative Stress and Free Iron within the Emergence of Artemisinin-Stimulated Cell Death

3.1. Introduction

In establishing the mechanistic routes through which artesunate induces the emergence of mitochondrial dysfunction, consideration must be given both to the initial interactions which underpin susceptibility towards the effects of the drug, and to the consequences which these later possess regarding physiological activity within the cell. Evidence strongly suggests that the cytotoxic impact of artemisinin is related intimately to its ability to stimulate the onset of ROS formation (Firestone *et al.*, 2009). Whilst knowledge of the pathways underpinning such an occurrence remains incomplete, it is widely accepted that cellular iron possesses roles within both the early bioactivation of the compound, and within the propagation of oxidative stress (Mercer *et al.*, 2010). The intention of this chapter is to examine the hypothesis that the iron-mediated generation of ROS forms an essential stage in the emergence of defective mitochondrial bioenergetic functioning. Particular focus shall be given to examination of the impact that the modulation of oxidative stress and iron levels has upon the respiratory activity of the organelle. This work shall be accompanied by further investigations centred upon elucidation of the cellular origins of such events.

It is acknowledged that there exists a variety of mechanisms through which aberrant functioning of the mitochondrion might arise as a consequence of drug treatment (Dykens, 2008). Studies have demonstrated that the administration of artemisinin derivatives in cancer cells is accompanied by substantial impact upon the operation of several physiological processes mediated at the organelle, associated with impairment of bioenergetic activity, efficiency of oxidative phosphorylation and energy generation linked to reduction in ATP production capacity, collapse of the mitochondrial membrane potential, and the eventual initiation of cell death through the intrinsic apoptotic pathway (Mercer *et al.*, 2011). The outcomes of examinations performed within the previous chapter suggest

that the origin of these defects might arise from the effects of drug action at both mitochondrial and non-mitochondrial sites.

A theme common across many studies performed assessing the activities of artemisinin derivatives within mammalian systems is an observed ability to impart the induction of oxidative stress. It has been noted that the time-dependent and dose-dependent generation of ROS occurs upon administration of the compounds across an array of cancer cell lines (Firestone *et al.*, 2009). ROS prevalence is heavily associated with the progression of cytotoxicity, with the capacity for antioxidant compounds to abrogate oxidative stress linked closely to cytoprotective effect (Mercer *et al.*, 2011). The impact of oxidative damage upon the functioning of cellular systems may be widespread and substantial. Such effects typically arise as a product of the structural modifications occurring subsequent to interaction between reactive oxyl radicals and biomolecules including phospholipids, DNA, Fe-S clusters and haemoproteins (Apel *et al.*, 2004). As a consequence of central role which many of these elements play within physiological processes occurring in the organelle, it is hypothesised that the effects of ROS impart substantial impact upon mitochondrial function and morphology.

Oxidative stress is characterised by the elevated production of ROS ahead of levels which can be safely detoxified through the actions of endogenous antioxidant pathways(Apel *et al.*, 2004). Such an occurrence may arise owing to the defective operation of a variety of systems across the cell predisposed which are towards their formation. Many appropriate sites are situated within the mitochondrion – a body identified as the primary cumulative source for ROS generation (Murphy, 2009). It is accepted that the great majority of these ROS have their origin in the initial conversion of molecular oxygen to the superoxide radical, which occurs as a consequence of electron leakage from the electron transport chain (Dykens, 2008). Accordingly, damage to the machinery associated with the maintenance of

oxidative phosphorylation is linked closely with emergence of oxidative stress (Turrens, 2003). In addition, a variety of alternative ROS-producing systems are known to exist within the organelle. Amongst these stand enzymes such as monoamine oxidase, aconitase and cytochrome *b5* reductase (Andreyev *et al.*, 2005).

Sources of ROS external to the mitochondrion are further acknowledged as possessing roles significant towards both physiological and pathological processes (Orient *et al.*, 2007). Enzymes such as xanthine oxidase and NADPH oxidase are capable of generating quantities of superoxide as part of immune response to pathogens (Papi *et al.*, 2008; Segal *et al.*, 2012). Its production may further be associated with the activities of cytochrome P450, cyclooxygenase and nitric oxide synthase enzymes. ROS emerging from these sources have potential to impact across all areas of the cell, including within the mitochondrion (Li *et al.*, 2013). It is feasible, therefore, that defective operation within these systems might have potential to function as an indirect route towards the initiation of mitochondrial damage and dysfunction.

Irrespective of source, interactions occurring between ROS and cellular iron, such as those outlined in Section 1.5.2.1., Chapter 1, are noted as being of central importance towards both the progression of oxidative stress and to the deleterious effects imparted by the reactive molecules upon the structural and functional integrity of cell systems (Galaris *et al.*, 2008). ROS possess an ability to instil substantial damage to iron-containing elements, such as haem units and Fe-S clusters, present across many proteins possessing essential roles within both mitochondrial and non-mitochondrial processes (Davies, 1990). It is hypothesised that enzymatic inactivation arising through this route might be accountable for the dysfunction of, amongst other systems, the complexes involved within the electron transport chain (Cortes-Rojo *et al.*, 2011). Alongside direct damage to protein structure, it is further acknowledged that ROS-iron interaction serves to stimulate propagation of

oxidative stress (Thomas *et al.*, 2009). Free, unbound Fe(II) is relevant within this pathway, owing to its ability to participate alongside hydrogen peroxide in the generation of the hydroxyl radical through Fenton chemistry (Kakhlon *et al.*, 2002). The concentration of free iron is found to be significant at points within the mitochondrial matrix and the lysosomal bodies. Owing to their position as sites at which the degradation of iron-containing proteins largely occurs, the latter are particularly notable for their elevated content (Kurz *et al.*, 2011). Modulation of levels within through use of loaders or chelators is accordingly associated with alleviation of oxidative stress and a diminished likelihood of progression towards cell death in response to drug treatment (Hamacher-Brady *et al.*, 2011).

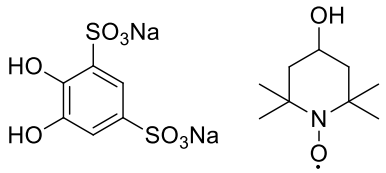

Tiron **TEMPOL**

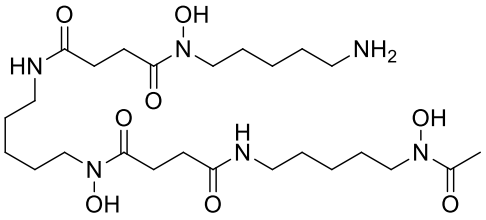

DFO

The studies presented in this chapter are intended to provide a greater mechanistic insight into the relationship between ROS formation and onset of mitochondrial damage in the context of artesunate treatment, and hence examine the hypothesis that defective bioenergetic function arises as a consequence of iron-associated oxidative damage towards the organelle. The impacts of the antioxidant ROS scavengers tiron and 4-hydroxy-2,2,6,6-tetramethylpiperidin-1-oxyl (TEMPOL) upon the response of HeLa cells towards drug administration are examined, with particular focus being given to their influence on cell survival and mitochondrial function. Bioenergetic performance shall be monitored once

again using the Seahorse XFe unit. In order that the contribution of unbound iron might be examined, the lysosomal chelator DFO shall be dosed alongside the artesunate derivative, and its ability to modulate drug effects upon ROS production, cell viability and mitochondrial activity assayed. Further investigation shall seek to elucidate the importance of the electron transport chain towards the generation of superoxide, whilst additionally determining the potential relevance of extra-mitochondrial ROS sources in the emergence of oxidative stress.

3.2. Materials and Methods

3.2.1. Materials

Uridine, bovine serum albumin (BSA), sucrose, mannitol, ethylene glycol tetraacetic acid (EGTA),magnesium chloride, magnesium sulphate, potassium phosphate monobasic, potassium phosphate dibasic, ammonium acetate, sodium succinate, tiron, TEMPOL, DFO, diphenyleneiodonium (DPI), metyrapone, allopurinol, indomethacin, DHE, NADH, CoQ_1, DDM, potassium cyanide, potassium ferricyanide, cytochrome c, iodonitrotetrazolium chloride (INT) and all additional solvents were purchased from Sigma-Aldrich (Poole, Dorset, UK). 3-(N-morpholino)propansulphonic acid (MOPS) was purchased from Fisher Scientific (Loughborough, UK). MitoSOX was purchased from Life Technologies (Paisley, UK). Bradford assay reagent was purchased from Bio-Rad (Hertfordshire, UK). PFDHA was synthesised by the group of Prof. Paul O'Neill (University of Liverpool, Liverpool, UK). HeLa ρ^0 cells were donated by Dr Edward Bampton (Medical Research Council Toxicology Unit, Leicester, UK).

3.2.2. Cell Culture and Experimental Preparation

HeLa cells were cultured and maintained according to the protocol outlined in Section 2.2.2., Chapter 2. HeLa ρ^0 cells were cultured in DMEM, with supplemental FBS (10% v/v,) sodium pyruvate (1% v/v), uridine (1% v/v) and penicillin/streptomycin solution (1% v/v). All cells were incubated at 37°C, in humidified air containing 5% CO_2.

3.2.3. Isolation of Mitochondria

Mitochondria were isolated from rat liver using a protocol adapted from that of Will *et al.* (Will *et al*., 2006). Wistar rats were sacrificed, before their liver was removed, diced and

suspended in a buffer containing 210 mM mannitol, 70 mM sucrose, 5 mM HEPES, 1 mM EGTA and 0.5% w/w BSA. The resulting mixture was homogenised prior to centrifugation (10 minutes, 700*g*), after which the supernatant was filtered and centrifuged once more (10 minutes, 14000*g*) to yield a mitochondria-rich pellet. This was resuspended in buffer, before being centrifuged (10 minutes, 10000*g*) and suspended in an alternative buffer composed of 210 mM mannitol, 70 mM sucrose, 10 mM magnesium chloride, 5mM potassium phosphate dibasic, 10 mM MOPS and 1 mM EGTA. Protein content of this mitochondrial suspension was assayed using the method of Bradford (Bradford, 1976).

3.2.4. Analysis through Flow Cytometry

Cells were analysed using the BD FACSCanto II flow cytometer (BD, Oxford, UK), upon which was running the FACSDiva software. Forward scatter (FSC) and side scatter (SSC) parameters, alongside voltage threshold, were adjusted so that a population of viable cells could be obtained to the exclusion of debris (Fig. 3.1.). A minimum of $1x10^4$ cells were analysed for each sample, with fluorescence output measured in the appropriate channels.

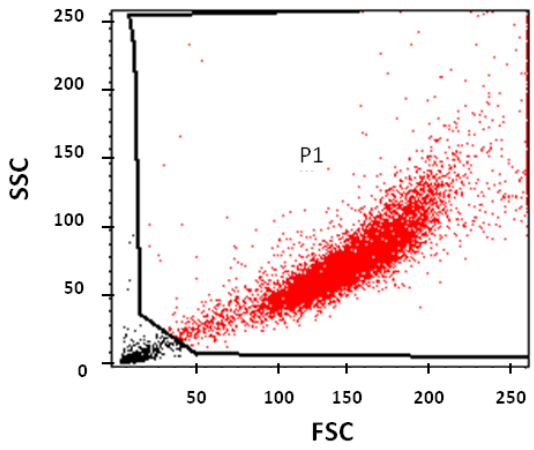

Figure 3.1. Representative dotplot displaying population of untreated HeLa cells. The exclusion of debris through gating is outlined. Viable cells appear within area "P1".

3.2.5. Detection of Cellular Reactive Oxygen Species through use of Dihydroethidium

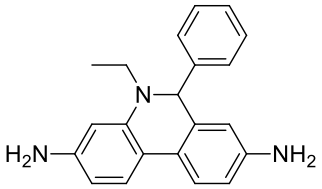

Dihydroethidium

Dihydroethidium (DHE) is a fluorescent compound which may be employed in flow cytometric protocols for the detection of ROS (Peshavariya *et al.*, 2007). Interaction with products such as hydrogen peroxide, superoxide, peroxynitrite and the hydroxyl radical leads to the formation of oxidised ethidium and hydroxyethidium derivatives, the presence of which may be monitored in combination following excitation at a wavelength of 488 nm. HeLa cells (2 x 10^5) were drug-treated for a period of 24 h before undergoing preparation for analysis through flow cytometry. Having been washed with HBSS and centrifuged (1000*g*), the remaining cell pellet was resuspended in 0.5 ml DHE solution (final concentration 500 µM), before incubation was carried out at 37°C for a period of 10 minutes. Performance of assay upon the flow cytometer followed immediately.

3.2.6. Measurement of Total Mitochondrial Reactive Oxygen Species using MitoSOX

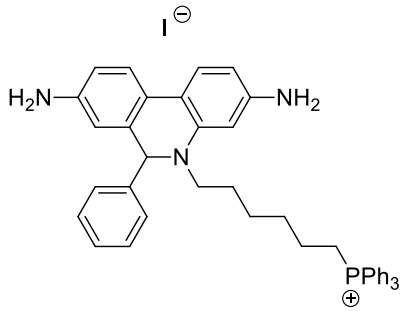

Mitosox

MitoSOX is a fluorescent dye which functions as a mitochondrially-targeted derivative of DHE. As with its parent compound, the formation of oxidised ethidium and hydroxyethidium derivatives, the combined prevalence of which may be detected following excitation at a wavelength of 488 nm, occurs upon interaction with reactive species such as hydrogen peroxide, superoxide, peroxynitrite and the hydroxyl radical (Zielonka *et al.*, 2010). HeLa cells (2 x 10^5) were treated with drug for a period of 24 h prior to being readied for employment upon the flow cytometer. Following addition of MitoSOX (final concentration 1 µM), incubation was performed at 37°C for 10 minutes before cells were washed with HBSS and centrifuged (1000*g*) to produce a pellet. This was subsequently resuspended in 0.5 ml HBSS, with samples then being analysed immediately through flow cytometry.

3.2.7. Measurement of Mitochondrial Superoxide using MitoSOX

The generation of a characteristic hydroxyethidium derivative arises as a function of superoxide-mediated oxidation at the functionalised DHE moiety (Zhao *et al.*, 2003). As such, detection of this species allows for the specific quantification of superoxide presence.

Experimentally, this is achieved through monitoring fluorescence at the distinctive excitation and emission wavelengths of 396 nm and 579 nm (Robinson *et al.*, 2006). HeLa and HeLa ρ^0 cells (1 x 10^5), were plated, in duplicate, into 24-well plates. Following artesunate dosing, incubation was performed for a period of 24 h. Upon completion, 5 µL MitoSOX solution (final concentration 1 µM) was added to each well, before a further incubation for 10 minutes at 37°C. Cells were subsequently washed wish HBSS and centrifuged (1000*g*), producing a pellet which was resuspended in 300 µL HBSS. 100 µL aliquots of this solution were plated, in duplicate, into a white 96-well plate, before MitoSOX fluorescence was read (excitation 396 nm, emission 579 nm) on the Varioskan Flash reader (Thermo Scientific, Loughborough, UK). The remaining solution was sonicated to produce cell lysates, the protein content of which was determined using the method of Bradford. (Bradford, 1976). Fluorescence was ultimately normalised towards protein abundance.

3.2.8. Assessment of Cell Viability using the MTT Assay

Cell viability within the HeLa line was ascertained through use of the MTT assay, as detailed in Section 2.2.4., Chapter 2.

3.2.9. Determination of Mitochondrial Bioenergetic Function through the Seahorse XF Stress Test

The impact of artesunate, and assorted modulators of its activity, upon the mitochondrial functioning of HeLa cells was examined on the Seahorse XFe 96 unit through means of the mitochondrial stress test, according to the protocols described in Section 2.2.8., Chapter 2.

3.2.10. Analysis of Drug Bioactivation using an LC-MS Method

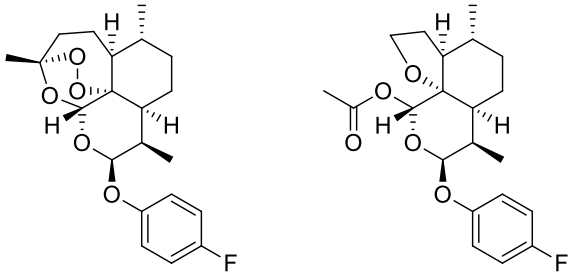

PFDHA **PFDHA THF Acetate**

Bioactivation of the DHA derivative PFDHA was quantified using an existing LC-MS method (Mercer *et al.*, 2011; Mercer *et al.*, 2007). The degradation of PFDHA and the formation of its THF acetate isomer occur as a consequence of Fe(II)-mediated reduction of the endoperoxide bridge. The quantity of each compound present may be determined through monitoring transitions corresponding to characteristic fragmentation patterns. In order to prepare samples for analysis, cells (1 x 10^6) were incubated in the presence of 25 µM PFDHA and 10 µM DFO. Following incubation, 4 nmol artesunate was added as an internal standard, and cells were extracted using chloroform (3 x 3 ml), before combined extracts were dried over anhydrous magnesium sulphate. Debris was removed through filtration, and solvent *in vacuo*, to yield final samples which were dissolved in 100 µL methanol prior to analysis. Standards were produced to enable the quantification of materials recovered (0.025 – 50 nmol), and these were ran before and following samples.

LC-MS was performed using the 4000 QTRAP (AB Sciex, Warrington, UK). Separation was attained using the Agilent ZORBAX Eclipse XDB-C8 column (150 mm x 3.9 mm, Agilent Technologies, Santa Clara, USA), with an eluent of methanol and 10 mM ammonium acetate (70:30, v/v) delivered at a flow rate of (rate). The machine was operated in positive ion mode, with an ion spray voltage of + 5.0 kV. Back pressure for collision gas was 2 p.s.i.,

curtain gas 20 p.s.i., nebuliser gas 30 p.s.i. and turbo gas 65 p.s.i.. Nitrogen was used for all purposes.

Parameter	PFDHA	THF acetate	Artesunate
Fragmentation transition	396.0 to 163.0	396.0 to 266.7	402.1 to 163.1
Declustering potential (V)	6	21	21
Focusing potential (V)	370	370	370
Entrance potential (V)	8	5	12
Collision energy (V)	17	30	30
Collision cell entrance potential (V)	14	19	18.6
Collision cell exit potential (V)	10	14	26
Dwell time (s)	200	100	200

Table 4.1. Parameters for the LC-MS quantification of PFDHA and THF-acetate.

3.2.11. Assessment of Electron Transport Chain Complex Activity

The functioning of the constituent complexes composing the respiratory chain was measured using a series of spectrophotometric methods (Frazier *et al.*, 2012). Isolated mitochondria, obtained using the protocol described in Section 3.2.3., were suspended in relevant assay buffers before alterations in the absorbance related to characteristic reaction substrates was monitored through use of a spectrophotometer (Cary 4000, Varian Inc., USA).

3.2.11.1. Complex I

Decreases in NADH oxidation, a process which proceeds through the pathway outlined in the equation below, are diagnostic of defective operation at complex I.

$$NADH + H^+ + CoQ_1 \rightarrow NAD^+ + CoQ_1\text{-}H_2$$

Monitoring the extent of NADH prevalence, achieved through determining characteristic absorbance at 340 nm, facilitates assessment of activity. Isolated mitochondria, treated *in situ* with 1 mM artesunate, were suspended in assay buffer containing 50 mM potassium phosphate monobasic, 50 mM NADH, 1 mM KCN, 10 mM antimycin A, 0.1% (w/v) BSA and 50 mM CoQ_1. NADH depletion was measured over a 5 minute period, with rate in the presence of artesunate normalised towards that of vehicle control.

3.2.11.2. Complex II

Activity of complex II is assayed through measuring decreases in absorbance at 280 nm associated with the reduction of CoQ_1.

$$Succinate + CoQ_1 \rightarrow Fumarate + CoQ_1\text{-}H_2$$

Isolated mitochondria, treated *in situ* with 1 mM artesunate, were suspended in assay buffer containing 50 mM potassium phosphate monobasic, 10 mM sodium succinate, 1 mM potassium cyanide, 10 mM antimycin A and 2.5 mM rotenone. Addition of CoQ_1 at a final concentration of 50 mM initiated reaction, which was subsequently monitored for 5 minutes. Normalisation of detected rate was performed towards vehicle control.

3.2.11.3. Complex III

Complex III activity may be determined through detecting increased absorbance characteristic of the formation of reduced cytochrome c, as measured at 550 nm, upon stimulation with reduced CoQ_1.

$$DB\text{-}H_2 + \text{Cytochrome c (ox)} \rightarrow DB + \text{Cytochrome c (red)}$$

To an assay buffer composed of 50 mM potassium phosphate monobasic, 1 mM n-dodecylmaltoside (DDM), 1 mM KCN, 2.5 mM rotenone, and 0.1% (w/v) BSA was added 0.1 mM reduced DB and 1 mM artesunate. Cytochrome c at a final concentration of 15 µM was introduced to initiate reaction, which was recorded for 5 minutes. Detected rate was subsequently normalised towards vehicle control.

3.2.11.4. Complex IV

Complex IV performance is assayed through monitoring decrease in the prevalence of reduced cytochrome c. This is again measured at 550 nm.

$$\text{Cytochrome c (red)} + O_2 \rightarrow \text{Cytochrome c (ox)} + H_2O$$

To a 50 mM solution of potassium phosphate monobasic was added mitochondrial suspension dosed *in situ* with 1 mM artesunate. Reduced cytochrome c to a final concentration of 15 µM was introduced to commence reaction, which was read for 3 minutes prior to its termination with potassium ferricyanide. Normalisation of detected rate was performed towards vehicle control.

3.2.12. Measurement of Complex II Activity

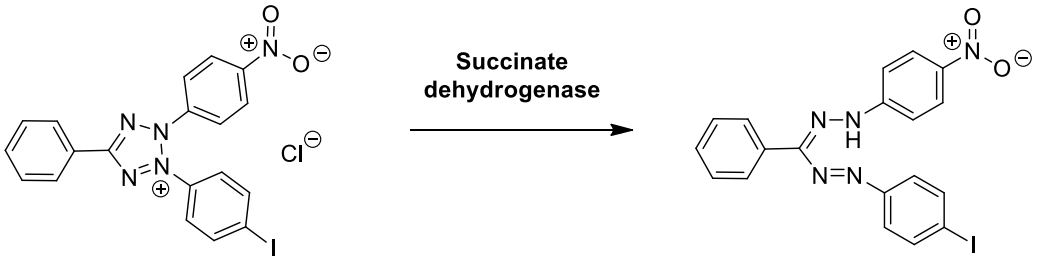

Iodonitrotetrazolium chloride **Formazan**

The activity of Complex II was measured in isolated mitochondria using a spectrophotometric method derived from that of Green and Narahara (Armstrong *et al.*, 2010; Green *et al.*, 1980). Complex II, alternatively known as succinate dehydrogenase (SDH) reduces INT to a formazan compound, the absorbance of which may be monitored at 458 nm following alcohol extraction. 0.1 ml of mitochondrial suspension obtained through the route described in Section 3.2.3. (0.5 mg protein) was added to 0.4 ml of reaction mixture containing 50 mM sucrose, 50 mM sodium succinate, 10 mM potassium phosphate monobasic and 0.8 mM INT. Having been dosed with 0 – 1000 µM artesunate, samples were incubated at 37°C for 30 minutes. Following this period, 1.5 ml ethanol was added to each tube, and samples were left on ice for a further 15 minutes. Centrifugation was subsequently performed (5 minutes, 1000*g*), before the absorbance was 1 ml of resultant supernatant was determined at 458 nm (Varioskan Flash, Thermo Scientific, Loughborough, UK).

3.2.13. Statistical Analysis

Data is presented and analysed in line with the protocols described in Section 2.2.10., Chapter 2.

3.3. Results

3.3.1. Impact of Antioxidants upon Cellular Response to Artesunate Treatment

3.3.1.1. Mitochondrial Reactive Oxygen Species

3.1.1.1.1. Effects of Tiron upon Artesunate-Induced Mitochondrial Reactive Oxygen Species

Mitochondrial ROS prevalence was examined through use of flow cytometry and the MitoSOX dye. MitoSOX is a derivative of DHE localised towards the mitochondrion through the affixing of a charged triphenylphosphonium functionality. The polycyclic compound becomes oxidised upon contact with cellular ROS, producing cationic ethidium and hydroxyethidium derivatives which emit red fluorescence upon intercalation within DNA. Their presence might be quantified through monitoring emission stimulated as a consequence of excitation at 488 nm. Owing to spatial containment inside the organelle, the scope of ROS detection remains confined within. Representative histograms displaying fluorescence distribution in vehicle control (Fig. 3.2. A) and 100 µM artesunate-dosed HeLa cells (Fig. 3.2. B) outline the increases in fluorescence associated with heightened ROS abundance.

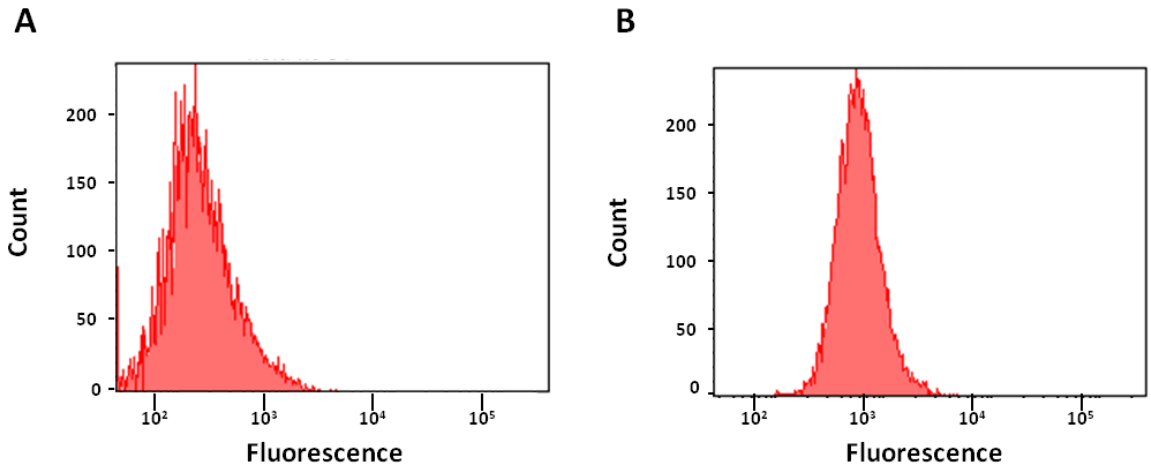

Figure 3.2. Representative histograms outlining variation in MitoSOX fluorescence between control and drug-treated HeLa cells. The distribution of MitoSOX fluorescence is displayed in untreated control **(A)** and 100 µM artesunate-dosed HeLa cells **(B)** following 24 h incubation.

HeLa cells were co-treated with 50 and 100 µM artesunate and 2 mM tiron for a period of 24 h. The antioxidant was able to impart significant reductions in levels of ROS, with detected quantities falling from 200 – 250% of control values in solely drug-treated cells to ~ 150% on co-dosing (Fig. 3.3.).

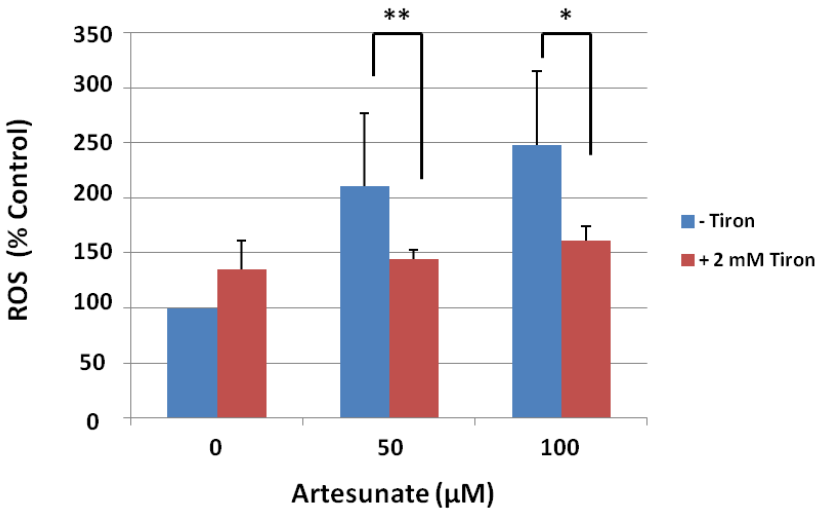

Figure 3.3. Effects of tiron upon artesunate-induced mitochondrial reactive oxygen species. HeLa cells were co-treated with 50 – 100 µM artesunate and 2 mM tiron for a period of 24 h. Mitochondrial ROS levels were determined through monitoring variation in MitoSOX fluorescence using flow cytometry. Values are expressed as percentage fold-increase relative to vehicle control, and are presented as the mean of three independent experiments, ± SD. * represents $p < 0.05$ and ** $p < 0.01$, as determined through paired t-test.

3.3.1.1.2. Impact of TEMPOL upon Artesunate-Stimulated Mitochondrial Reactive Oxygen Species

HeLa cells were dosed with 50 and 100 µM artesunate alongside 2 mM TEMPOL for a period of 24 h, prior to assessment of mitochondrial oxidative stress using flow cytometry and the MitoSOX dye. The antioxidant was able to impart significant reductions in the quantities of drug-stimulated ROS detected within the organelle (Fig. 3.4.).

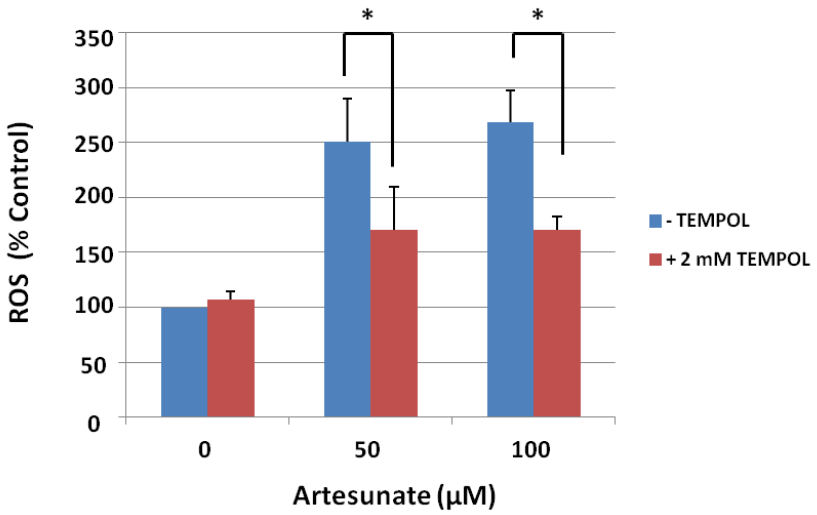

Figure 3.4. Impact of TEMPOL upon artesunate-induced mitochondrial reactive oxygen species. HeLa cells were co-treated with 50 – 100 µM artesunate and 2 mM TEMPOL for a period of 24 h. Mitochondrial ROS levels were determined through monitoring variation in MitoSOX fluorescence using flow cytometry. Values are expressed as percentage fold-increase relative to vehicle control, and are presented as the mean of three independent experiments, ± SD. * represents $p < 0.05$, as determined through paired t-test.

3.3.1.2. Cytotoxicity

3.3.1.2.1. Protective Impact of Tiron against Artesunate Cytotoxicity

The ability of tiron to impact upon the susceptibility of HeLa cells towards artesunate treatment was investigated using the MTT assay. Significant increases in viability following 24 h were noted on the co-administration of 2 mM tiron alongside 50 and 100 µM artesunate, with the presence of the antioxidant preserving the survival of ~ 90% of cells (Fig. 3.5.).

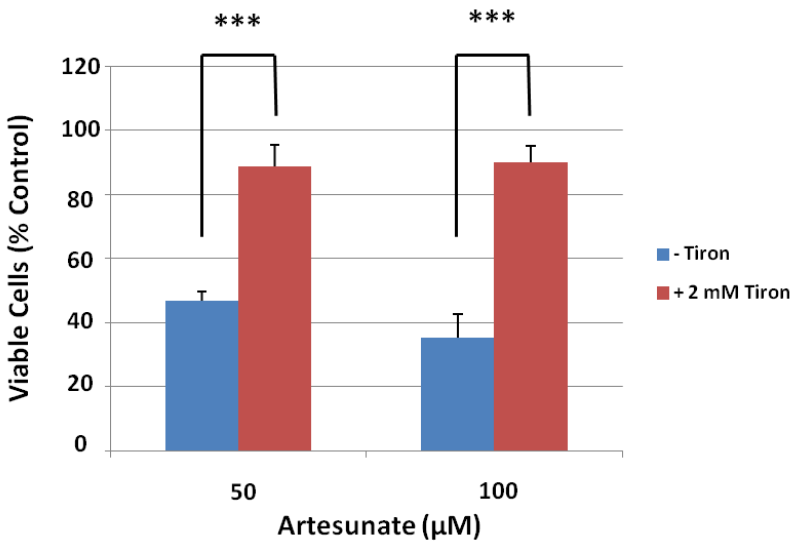

Figure 3.5. Protective impact of tiron against artesunate cytotoxicity. HeLa cells were co-treated with 50 – 100 µM artesunate and 2 mM tiron for a period of 24 h. Cytotoxicity was measured using the MTT assay. Values are expressed as percentage fold-change relative to vehicle control, and are presented as the mean of three independent experiments, ± SD. *** represents $p < 0.001$, as determined through paired t-test.

3.3.1.2.2. Protective Effects of TEMPOL against Artesunate Cytotoxicity

TEMPOL was additionally tested for its cytoprotective capability against artesunate toxicity within HeLa cells. Cells were co-treated with 50 or 100 µM artesunate alongside 2 mM TEMPOL for a period of 24 h, before viability was ascertained using the MTT assay. Whilst the antioxidant was able to significantly abrogate drug-induced impact upon cell survival, effects were not as profound as those witnessed upon the co-administration of tiron (Fig. 3.6.).

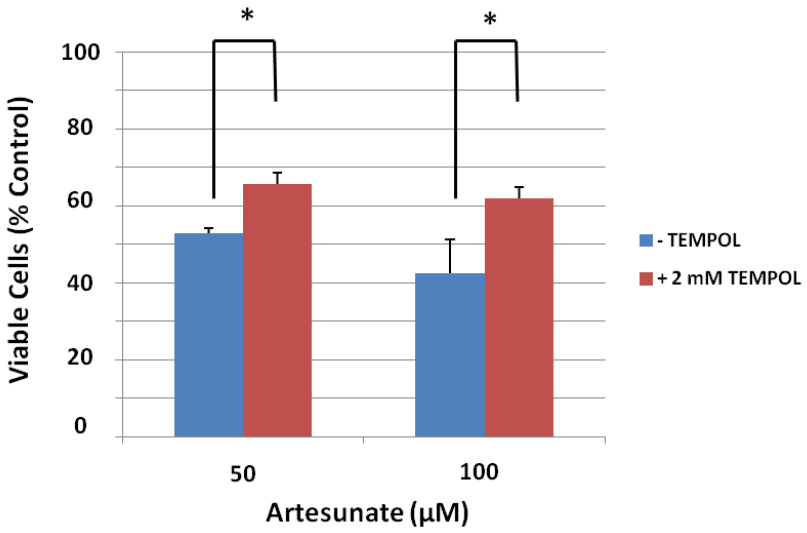

Figure 3.6. Protective effects of TEMPOL against artesunate cytotoxicity. HeLa cells were co-treated with 50 – 100 µM artesunate and 2 mM TEMPOL for a period of 24 h. Cytotoxicity was measured using the MTT assay. Values are expressed as percentage fold-change relative to vehicle control, and are presented as the mean of three independent experiments, ± SD. * represents $p < 0.05$, as determined through paired t-test.

3.3.1.3. Cellular Reactive Oxygen Species

3.3.1.3.1. Impact of Tiron upon Artesunate-Induced Cellular Reactive Oxygen Species

Levels of oxidative stress within the whole cell were determined through flow cytometry using the DHE dye. DHE is the parent compound of MitoSOX, and owing to its lack of specific localisation, possesses the capacity to quantify ROS abundance across the cell body. Activity arises as a consequence of the formation of cationic ethidium and hydroxyethidium derivatives upon contact with ROS – the fluorescence of which may be monitored following excitation at 488 nm. Representative traces outline patterns of fluorescence observed within vehicle control (Fig. 3.7. A) and 100 µM artesunate-treated HeLa cells (Fig. 3.7. B). Increased emission associated with greater prevalence of ROS is clearly evident within the latter.

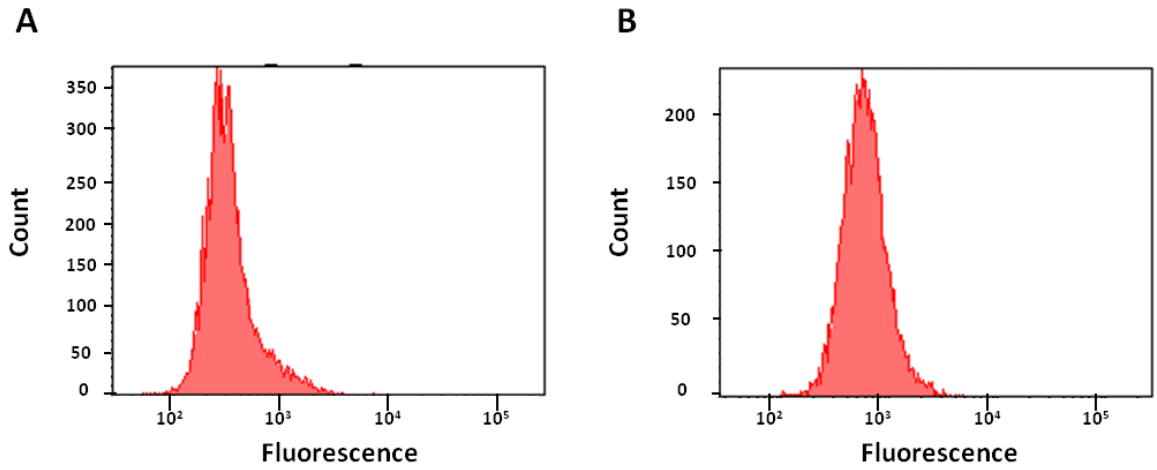

Figure 3.7. Representative histograms outlining variation in DHE fluorescence between control and drug-treated HeLa cells. The distribution of DHE fluorescence is displayed in untreated control **(A)** and 100 µM artesunate-dosed HeLa cells **(B)** following 24 h incubation.

50 and 100 µM artesunate and 2 mM tiron were administered together for 24 h in HeLa cells, prior to the flow cytometric determination of mitochondrial ROS levels. Addition of the ROS scavenger led to a significant attenuation of oxidative stress within the organelle, mirroring effects observed within the mitochondrion (Fig. 3.8).

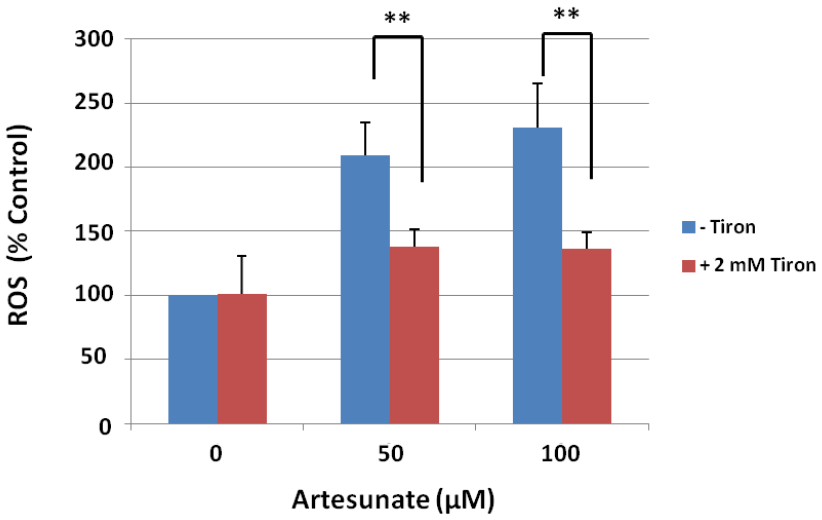

Figure 3.8. Impact of tiron upon artesunate-induced cellular reactive oxygen species. HeLa cells were co-treated with 50 – 100 µM artesunate and 2 mM tiron for a period of 24 h. Cellular ROS levels were determined through monitoring variation in DHE fluorescence using flow cytometry. Values are expressed as percentage fold-increase relative to vehicle control, and are presented as the mean of three independent experiments, ± SD. ** represents $p < 0.01$, as determined through paired t-test.

3.3.1.4. Mitochondrial Bioenergetic and Respiratory Function

3.3.1.4.1. Impact of Tiron upon Artesunate-Induced Mitochondrial Dysfunction

The capacity for tiron to modulate the impact of artesunate upon the bioenergetic functioning of the mitochondrion was ascertained through use of the Seahorse XF mitochondrial stress test. Employment of the methods described in Section 2.2.8., Chapter 2 has allowed for determination of both the reserve capacity and coupling efficiency in HeLa cells responding to treatment with drug and antioxidant.

Cells were again dosed with 2 mM tiron alongside either 50 or 100 µM artesunate. Following 24 h incubation, the stress test was performed and the relevant parameters were quantified. Co-administration of the antioxidant imparted significant protective effect against artesunate-induced reductions in mitochondrial coupling efficiency (Fig. 3.9. A) and reserve capacity (Fig. 3.9. B). In each instance, normalised values approached those found in untreated controls.

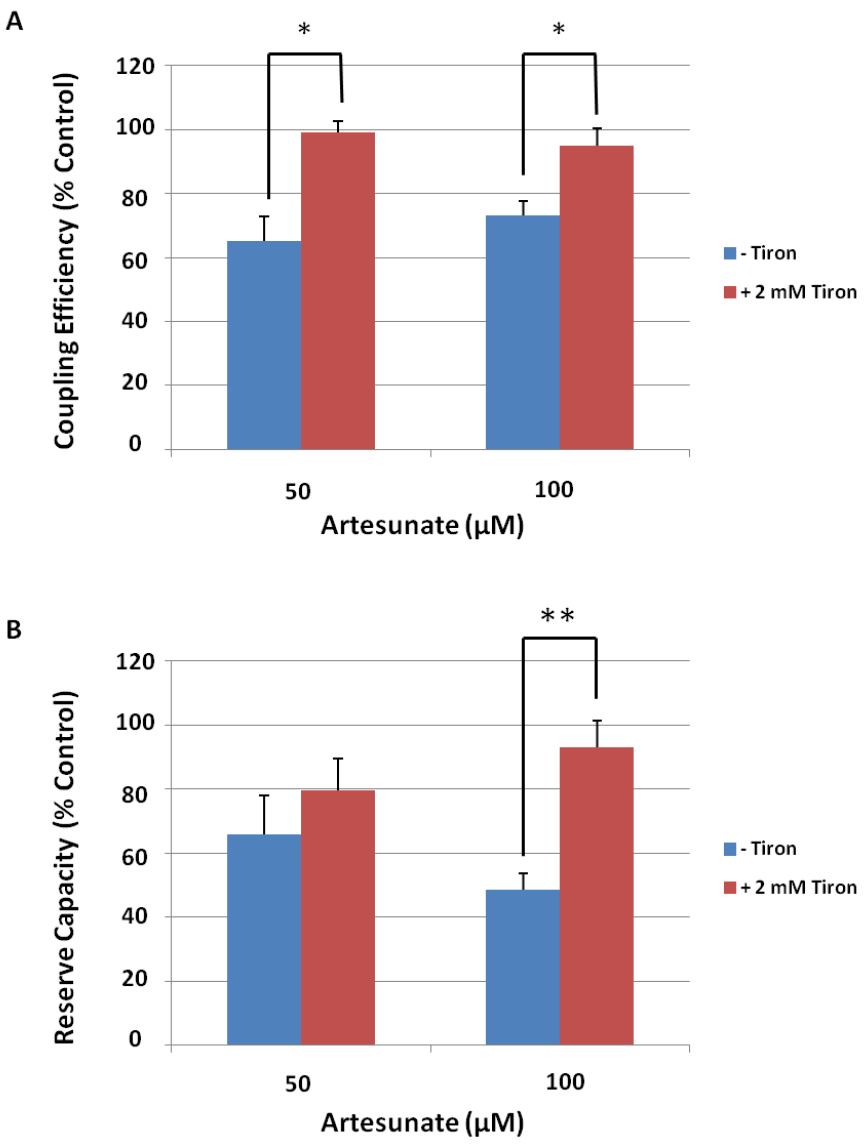

Figure 3.9. Impact of tiron upon artesunate-induced mitochondrial dysfunction. HeLa cells were treated for 24 h with 50 – 100 µM artesunate and 2 mM tiron, before coupling efficiency **(A)** and reserve capacity **(B)** were determined using the XF mitochondrial stress test. Values are expressed as percentage of normalised OCR relative to vehicle control, and are presented as the mean of three independent experiments, ± SD. * represents $p < 0.05$ and ** $p < 0.01$, as determined through paired t-test.

3.3.2. The Mitochondrial Origin of Reactive Oxygen Species Formation

3.3.2.1. Influence of the Electron Transport Chain upon Superoxide Formation

The contribution of the electron transport mechanism towards the artesunate-stimulated formation of mitochondrial superoxide was examined through monitoring variation in MitoSOX fluorescence arising in response to drug treatment across HeLa and HeLa ρ^0 cells. Specific detection of the prevalence of superoxide was achieved through detecting solely formation of the hydroxyethidium oxidation product at excitation wavelength 396 nm and emission wavelength 579 nm. Cells of each line were treated with 50 and 100 µM artesunate for a period of 24 h, before levels of the species were ascertained. It was revealed that, although results between lines did not achieve significance, higher prevalence was found within the HeLa cells (Fig. 3.10.). Such an outcome suggests that the electron transport chain is linked with maximal ROS expression. Significant quantities of superoxide were nevertheless detected relative to control upon drug treatment within the ρ^0 line, indicating that artesunate retains capacity to induce elevated formation of superoxide within these bodies even in the absence a functioning respiratory pathway.

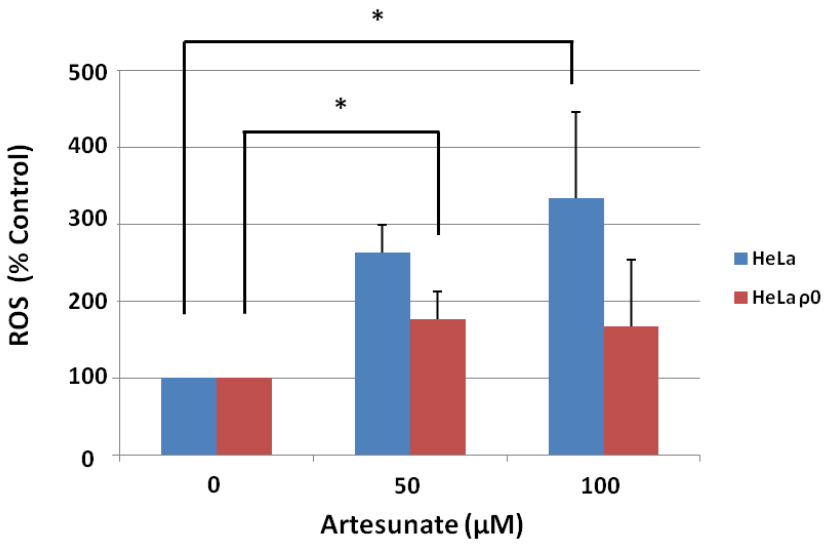

Figure 3.10. Influence of the electron transport chain upon superoxide formation. HeLa and HeLa ρ^0 cells were treated with 50 and 100 μM artesunate for a period of 24 h. Mitochondrial ROS levels were determined through monitoring variation in MitoSOX fluorescence. Values are expressed as percentage fold-increase relative to vehicle control, and are presented as the mean of three independent experiments, ± SD. * represents $p < 0.05$, as determined through paired t-test.

3.3.2.2. Effects of Artesunate upon the Activities of Complexes Constituting the Electron Transport Chain

The impact of artesunate administration upon the activities of complexes within the electron transport chain was determined in isolated mitochondria through use of relevant spectrophotometric methods. Significant yet partial inhibition of complex II was noted to occur upon treatment with 1 mM artesunate, with function being reduced to approximately 60% of that of vehicle control (Fig. 3.11.). Effects upon the operation of other constituents were observed to be minimal.

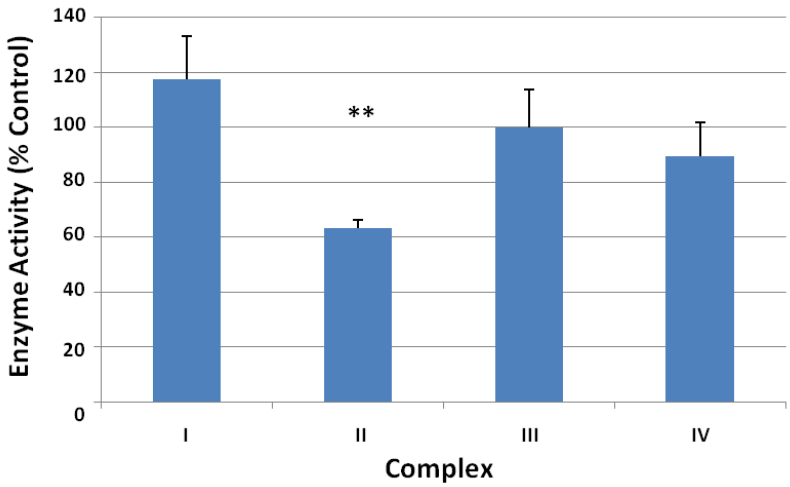

Figure 3.11. Effects of artesunate upon the activities of complexes constituting the electron transport chain. Isolated rat liver mitochondria were treated with 1 mM artesunate. Complex function was determined using relevant spectrophotometric methods. Values are expressed as percentage fold-change relative to vehicle control, and are presented as the mean of three independent experiments, ± SD. ** represents $p < 0.01$, as determined through paired t-test.

3.3.2.3. Impact of Artesunate upon Complex II Function

The ability of artesunate to induce defective functioning of complex II was further examined through monitoring drug-induced variation in absorbance attributed to the formazan product formed as a consequence of enzymatic reduction of INT in isolated mitochondria. Mitochondria prepared from rat liver were suspended in reaction mixture containing succinate and INT, before being dosed with 0 – 1000 µM artesunate. Following a 30 minute period of incubation, conclusion of the assay revealed that the presence of drug was able to reduce activity to a minimum of 65% of vehicle control value (Fig. 3.12.). Such extent of inhibition correlates with that detailed in Section 3.3.2.2.

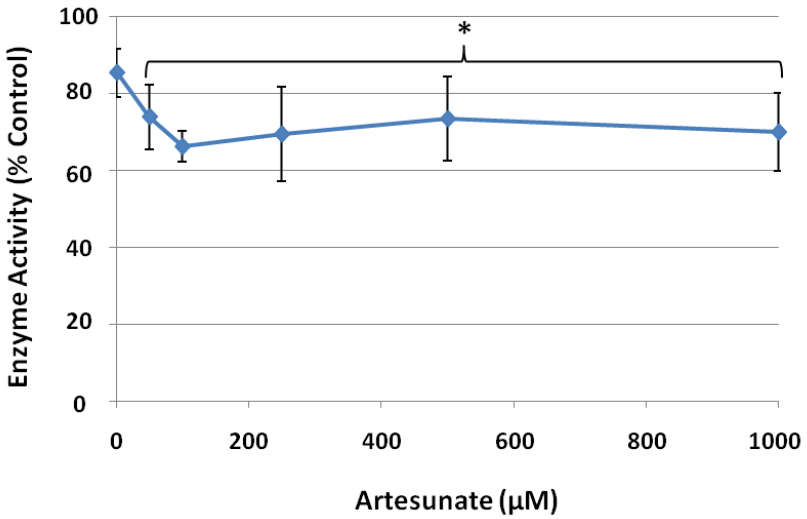

Figure 3.12. Impact of artesunate upon complex II function. Isolated rat liver mitochondria were treated with 0 – 1000 µM artesunate. Following 30 minutes incubation, SDH activity was determined using a spectrophotometric method. Values are expressed as percentage fold-change relative to vehicle control, and are presented as the mean of three independent experiments, ± SD. * represents $p < 0.05$, as determined through paired t-test.

3.3.3. Non-Mitochondrial Reactive Oxygen Species and Artesunate Cytotoxicity

In order to examine the potential relevance of extra-mitochondrial ROS upon the progression of artesunate-induced toxicity, the roles of several enzymes implicated in possessing significance as sites for superoxide generation were examined for their impact in determining cell response to drug treatment. HeLa cells were co-treated with artesunate alongside compounds known to function as inhibitors of these systems, in order that their contribution towards ROS production and the progression of cell death might be ascertained. The effects of inhibitors of NADPH oxidase, cytochrome P450, xanthine oxidase and cyclooxygenase – DPI, metyrapone, allopurinol and indomethacin respectively – were examined for their activities with respect to modulating artemisinin toxicity.

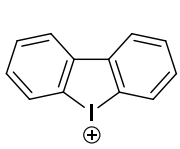

DPI

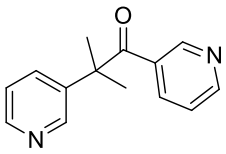

Metyrapone

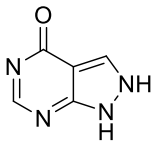

Allopurinol

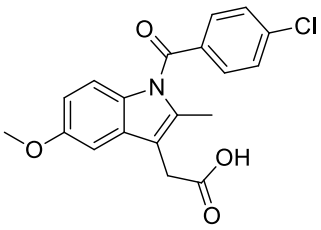

Indomethacin

3.3.3.1. Impact of Enzyme Inhibitors upon Cell Viability

Prior to their employment in assays alongside artesunate, the cytotoxicity of the inhibitors alone was examined. HeLa cells were treated for 24 h with 0 – 1000 µM of each compound, before cell viability was determined using the MTT assay. DPI exhibited significant impact upon survival at concentrations greater than 0.5 µM (Fig. 3.13. A), metyrapone at greater than 300 µM (Fig. 3.13. B), indomethacin in excess of 100 µM (Fig. 3.13. C) and allopurinol exceeding 300 µM (Fig. 3.13. D).

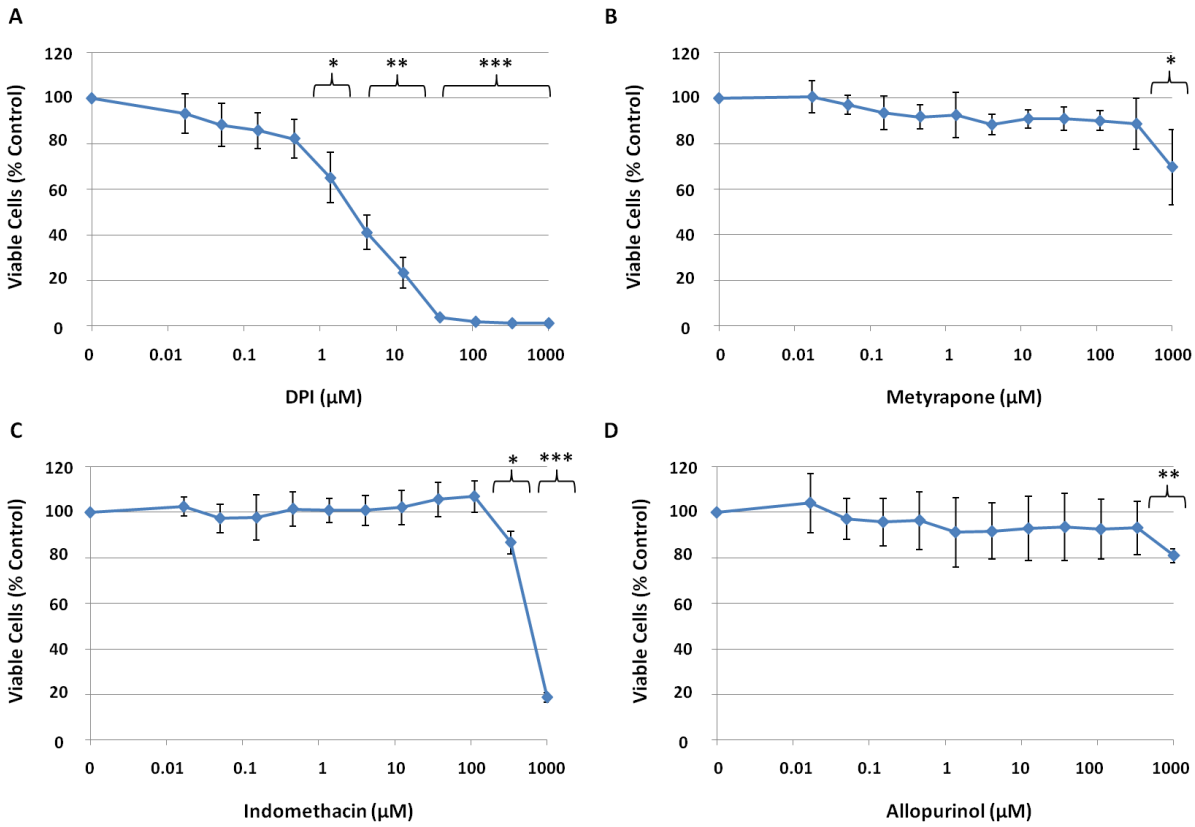

Figure 3.13. Impact of enzyme inhibitors upon cell viability. HeLa cells were treated for a period of 24 h with 0 – 1000 µM DPI **(A)**, metyrapone **(B)**, indomethacin **(C)** and allopurinol **(D)**. Cytotoxicity was measured using the MTT assay. Values are expressed as percentage fold-change relative to vehicle control, and are presented as the mean of three independent experiments, ± SD. * represents $p < 0.05$, ** $p < 0.01$ and *** $p < 0.001$ as determined through paired t-test.

3.3.3.2. Protective Effects of Enzyme Inhibitors upon Artesunate-Stimulated Cytotoxicity

The ability of each inhibitor to modulate the impact of artesunate-induced cytotoxicity in HeLa cells was determined through use of the MTT assay. Cells were treated for 24 h with 50 or 100 µM artesunate and either 0.5 µM DPI (Fig. 3.14. A), 250 µM metyrapone (Fig. 3.14. B), 100 µM indomethacin (Fig. 3.14. C) or 300 µM allopurinol (Fig. 3.14. D). DPI was able to induce a mild yet significant protective effect in response to 100 µM artesunate, whereas all other compounds exerted no notable alterations.

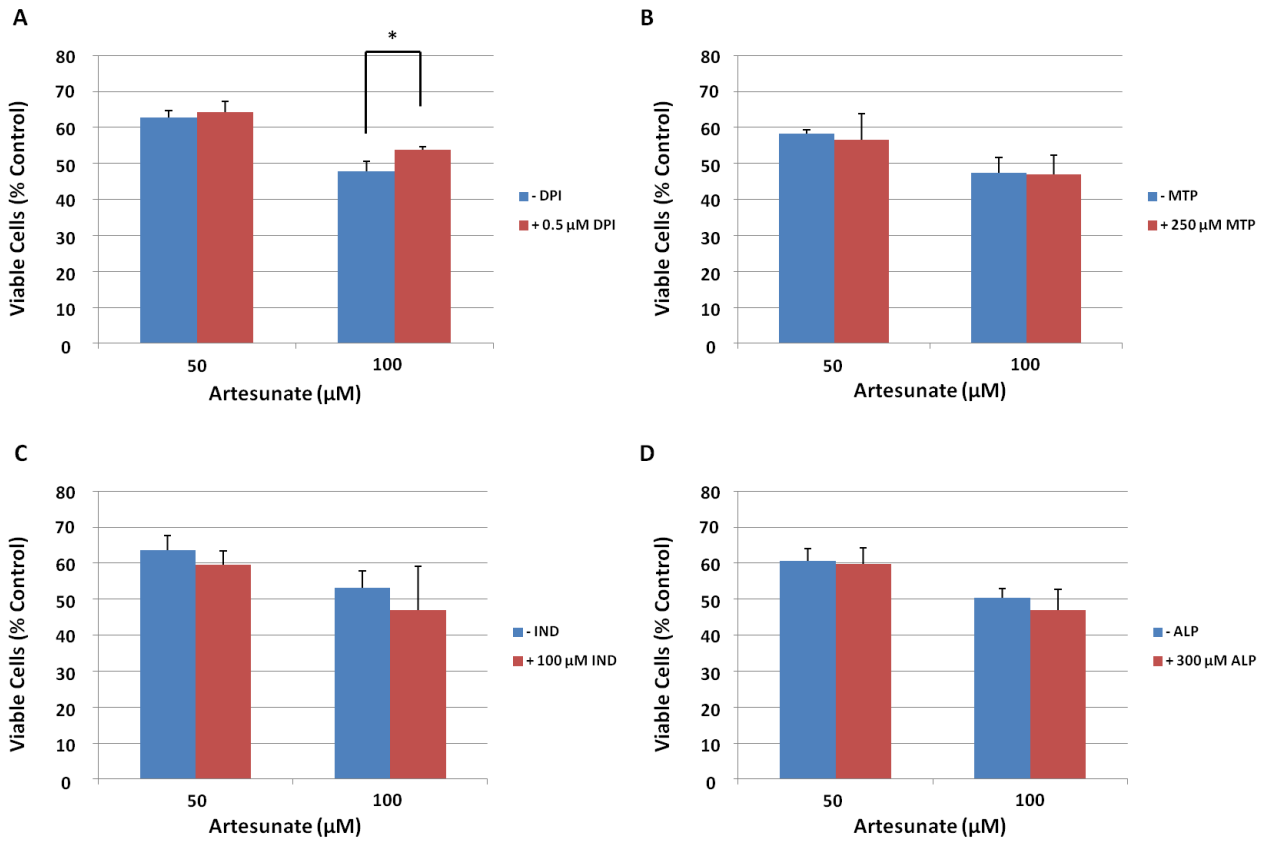

Figure 3.14. Protective effects of enzyme inhibitors upon artesunate-stimulated cytotoxicity. HeLa cells were co-treated for 24 h with 50 – 100 μM artesunate and 0.5 μM DPI **(A)**, 250 μM metyrapone **(B)**, 100 μM indomethacin **(C)** and 300 μM allopurinol **(D)**. Cytotoxicity was measured using the MTT assay. Values are expressed as percentage fold-change relative to vehicle control, and are presented as the mean of three independent experiments, ± SD. * represents $p < 0.05$, as determined through paired t-test.

3.3.3.3. Impact of Enzyme Inhibitors upon the Prevalence of Cellular Reactive Oxygen Species

The effect of the inhibitors upon the formation of cellular ROS emerging through artesunate treatment was examined using DHE. Either 0.5 μM DPI (Fig. 3.15. A), 250 μM metyrapone (Fig. 3.15. B), 100 μM indomethacin (Fig. 3.15. C) or 300 μM allopurinol (Fig. 3.15. D) was administered alongside 50 or 100 μM artesunate in HeLa cells prior to 24 h treatment. No significant impact upon level of drug-stimulated oxidative stress was evident across each compound.

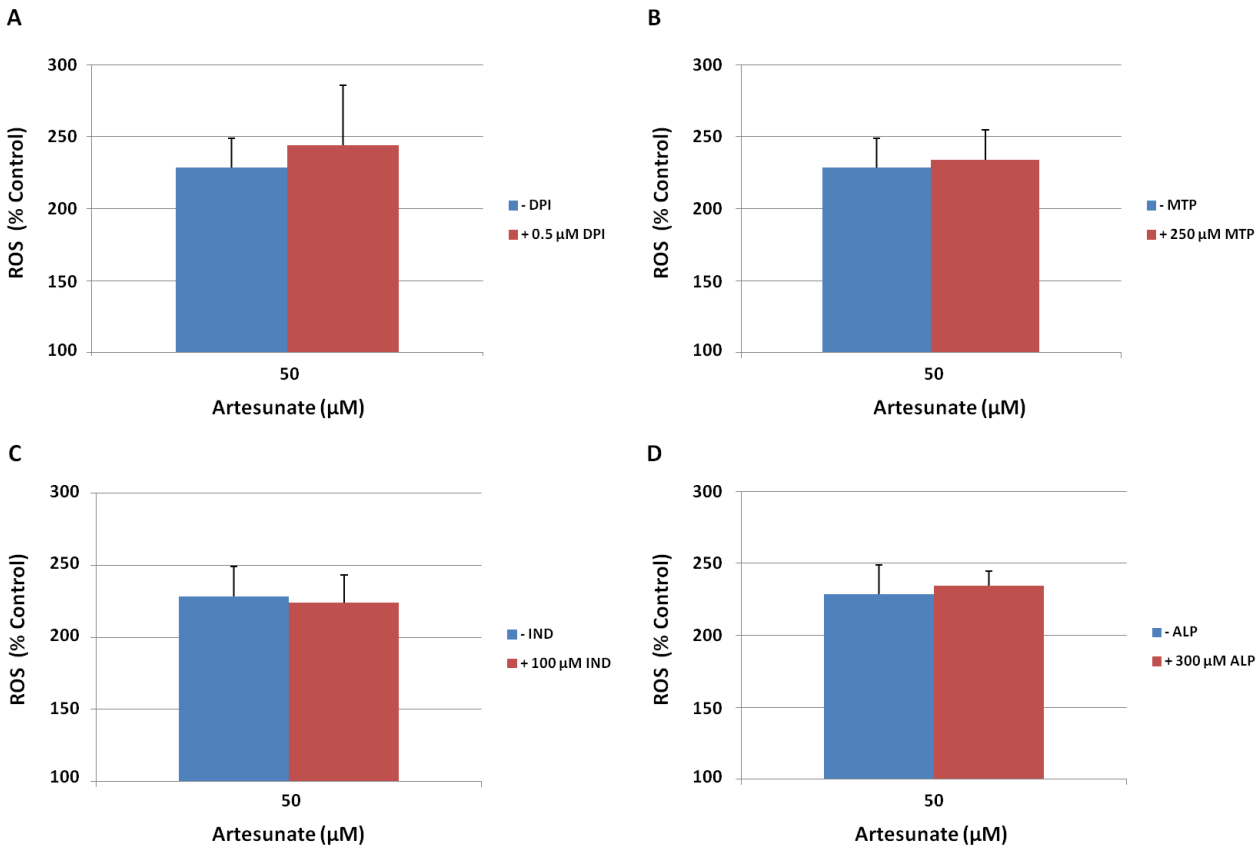

Figure 3.15. Impact of enzyme inhibitors upon the prevalence of cellular ROS. HeLa cells were co-treated for 24 h with 50 – 100 μM artesunate and 0.5 μM DPI **(A)**, 250 μM metyrapone **(B)**, 100 μM indomethacin **(C)** and 300 μM allopurinol **(D)**. Cellular ROS levels were determined through monitoring variation in DHE fluorescence using flow cytometry. Values are expressed as percentage fold-change relative to vehicle control, and are presented as the mean of three independent experiments, ± SD.

3.3.4. Effects of Iron-Chelator DFO upon Cellular Response to Artesunate Treatment

3.3.4.1. Cytotoxicity of DFO towards HeLa Cells

Prior to its employment in assays alongside artesunate, the cytotoxicity of DFO within HeLa cells was examined using the MTT assay. Cells were treated for 24 h with DFO in concentrations ranging from 0 – 1000 μM. Viability did not decrease beneath 70% of control values, even at elevated dose (Fig. 3.16.).

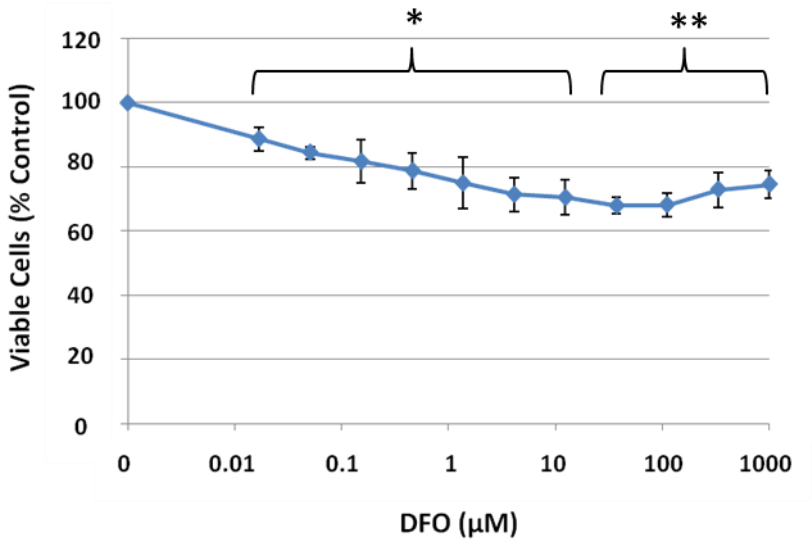

Figure 3.16. Cytotoxicity of DFO towards HeLa cells. HeLa cells were treated with 0 – 1000 μM DFO for a period of 24 h. Cytotoxicity was measured using the MTT assay. Values are expressed as percentage fold-change relative to vehicle control, and are presented as the mean of three independent experiments, ± SD. * represents $p < 0.05$ and ** $p < 0.01$, as determined through paired t-test.

3.3.4.2. Capacity of DFO to Impact upon Artemisinin Bioactivation

Fe(II) reduction of the endoperoxide bridge culminates in the structural rearrangement of parent artemisinin compounds to furnish stable isomeric products through mechanisms proceeding *via* the formation of reactive radical intermediates. The bioactivation of PFDHA can be monitored through means of an established LC-MS method quantifying the degradation of parent compound alongside the emergence of its THF acetate isomer (Fig. 3.17.).

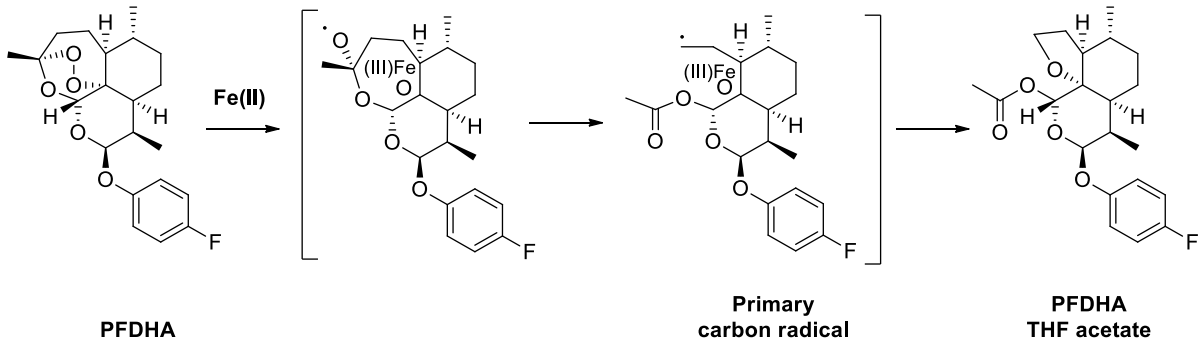

Figure 3.17. Mechanism of THF acetate formation through Fe(II)-mediated PFDHA degradation.

Characterisation of the levels of PFDHA and THF acetate present in samples extracted from cells following co-incubation with DFO is achieved through monitoring respectively the fragmentation transitions 396.0 to 163.0 (Fig. 3.18. A) and 396.0 to 266.7 (Fig. 3.18. B). Extraction efficiency is determined through ascertaining the quantity of internal standard artesunate (Fig. 3.18. C, transition 402.1 to 163.1) recovered following isolation. In order to enable quantification of the materials present in absolute molar values, reference is made to standard curves constructed for each particular compound.

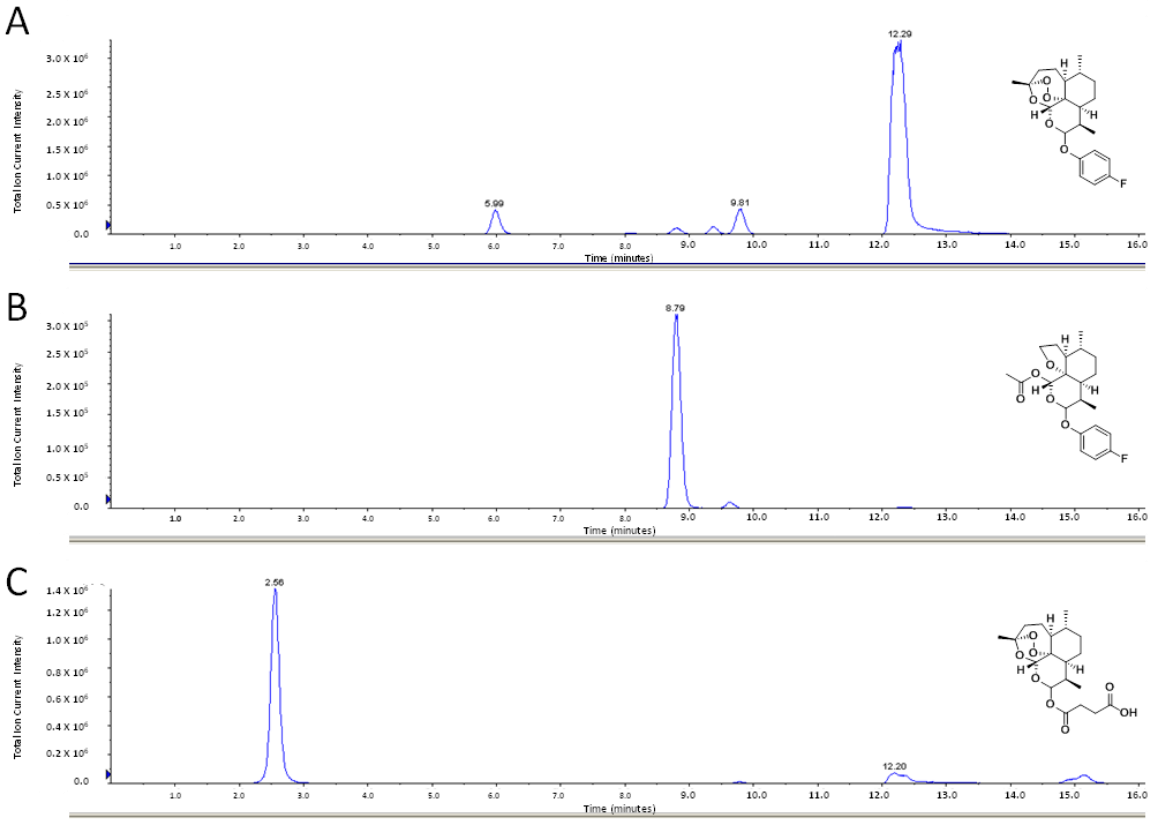

Figure 3.18. Representative selected-ion chromatogram traces detailing retention patterns for monitored fragmentation transitions. Traces correspond to the transitions PFDHA 396.0 to 163.0 **(A)**, PFDHA THF-acetate 396.0 to 266.7 **(B)** and artesunate 396.0 to 166.7 **(C)**.

HeLa cells were co-incubated with 25 µM PFDHA and 10 µM DFO for a period of 24 hours, prior to organic extraction. Upon LC-MS analysis, it was observed that the presence of the

chelator imparted significant increase in the proportion of recovered starting material (Fig. 3.19. A) and decrease in the fraction of detected THF acetate (Fig. 3.19. B). Such an outcome illustrates the facility to DFO to protect against Fe(II)-mediated endoperoxide bridge bioactivation.

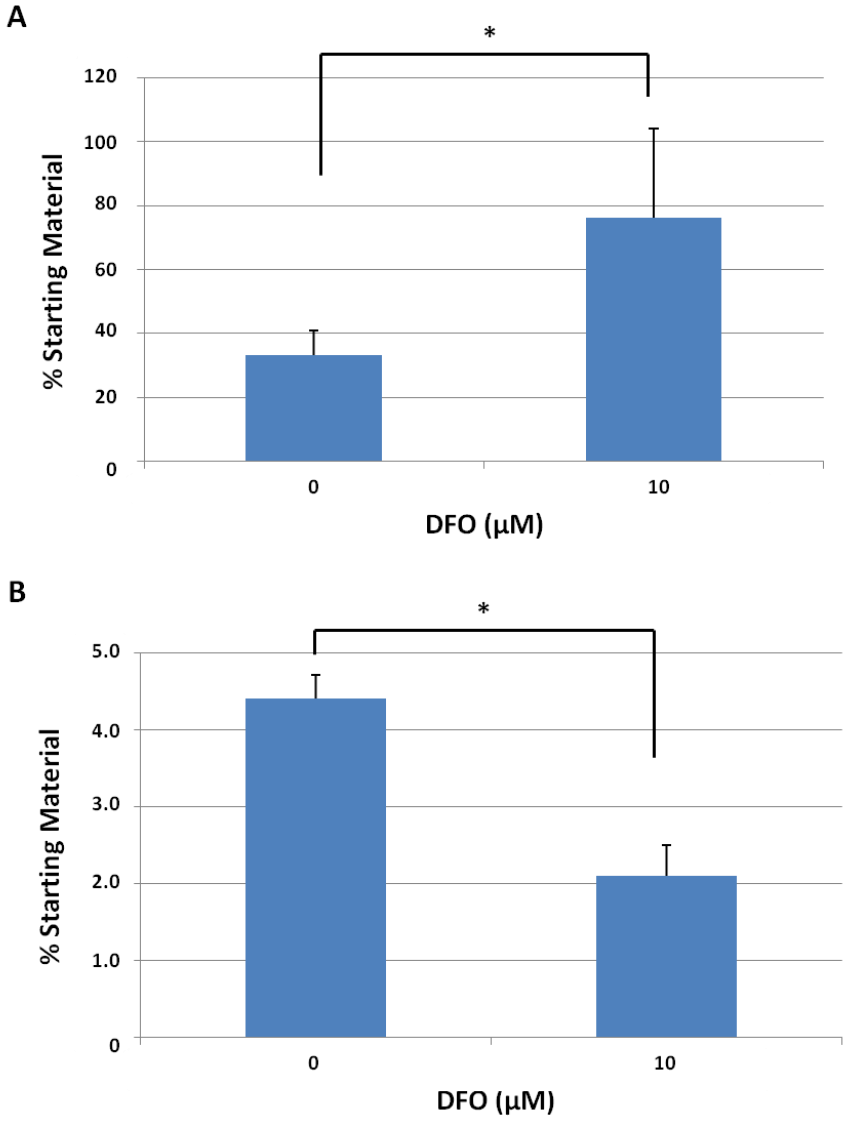

Figure 3.19. Capacity of DFO to impact upon artemisinin bioactivation. HeLa cells were co-treated with 25 µM PFDHA and 10 µM DFO for a period of 24 h, before quantities of recovered parent compound **(A)** and THF acetate isomer **(B)** were determined. Values are expressed in terms of the quantity of PFDHA and THF acetate retrieved as a percentage of starting material, and are presented as the mean of three independent experiments, ± SD. * represents $p < 0.05$, as determined through paired t-test.

3.3.4.3. Impact of DFO upon Artesunate-Induced Mitochondrial Reactive Oxygen Species

The ability of DFO to impact upon levels of artesunate-induced ROS within the mitochondrion was examined through flow cytometry using the MitoSOX dye. HeLa cells were co-treated for 24 h with 50 or 100 µM artesunate alongside 10 µM DFO, before quantification was performed. Significant reductions in ROS levels were evident owing to administration of the chelator, with fold-changes relative to vehicle control falling to approximately 140% from the 200 – 220% observed in solely artesunate-treated cells (Fig. 3.20.).

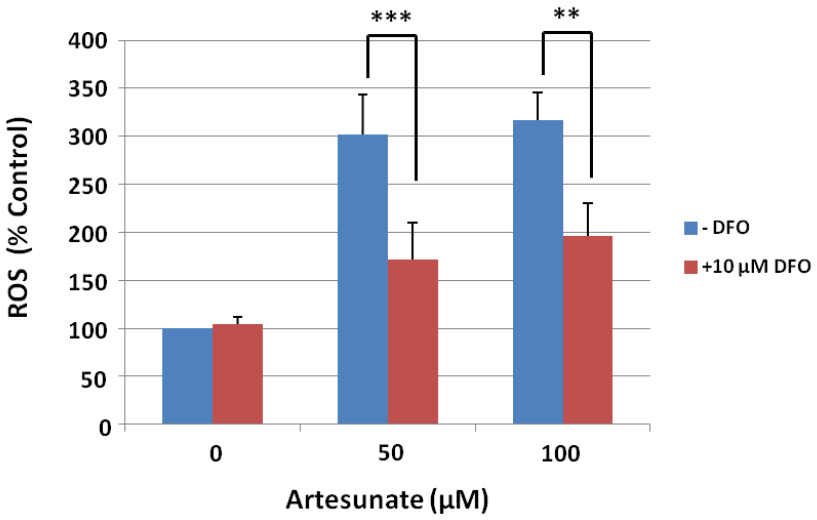

Figure 3.20. Impact of DFO upon artesunate-induced mitochondrial reactive oxygen species. HeLa cells were co-treated with 50 – 100 µM artesunate and 10 µM DFO for a period of 24 h. Mitochondrial ROS levels were determined through monitoring variation in MitoSOX fluorescence using flow cytometry. Values are expressed as percentage fold-increase relative to vehicle control, and are presented as the mean of three independent experiments, ± SD. ** represents $p < 0.01$ and *** represents $p < 0.001$, as determined through paired t-test.

3.3.4.4. Effect of DFO upon Artesunate-Induced Cellular Reactive Oxygen Species

The impact of DFO upon drug-stimulated cellular oxidative stress was examined using DHE. HeLa cells were dosed with 10 µM DFO alongside 50 and 100 µM artesunate, prior to 24 h incubation. The chelator was able to impart significant reductions in the prevalence of ROS (Fig 3.21.).

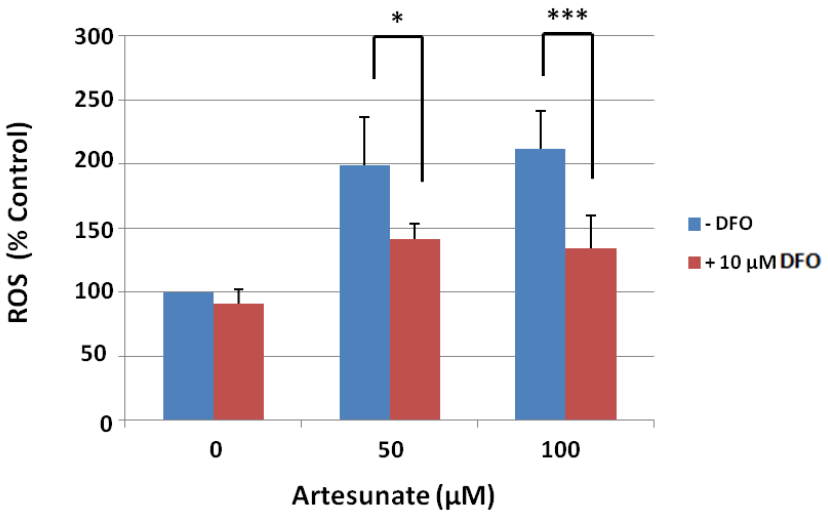

Figure 3.21. Effect of DFO upon artesunate-induced cellular reactive oxygen species. HeLa cells were co-treated with 50 – 100 µM artesunate and 10 µM DFO for a period of 24 h. Cellular ROS levels were determined through monitoring variation in DHE fluorescence using flow cytometry. Values are expressed as percentage fold-increase relative to vehicle control, and are presented as the mean of three independent experiments, ± SD. * represents $p < 0.05$ and *** $p < 0.001$, as determined through paired t-test.

3.3.4.5. Protective Effects of DFO against Artesunate Cytotoxicity

The cytoprotective potential of DFO against artesunate toxicity was examined using the MTT assay. HeLa cells were co-treated for 24 h with 50 and 100 µM artesunate and 10 µM DFO. The presence of DFO imparted significant reductions in levels of cell death arising from drug administration, with viability maintained at greater than 80% of control value (Fig 3.22.).

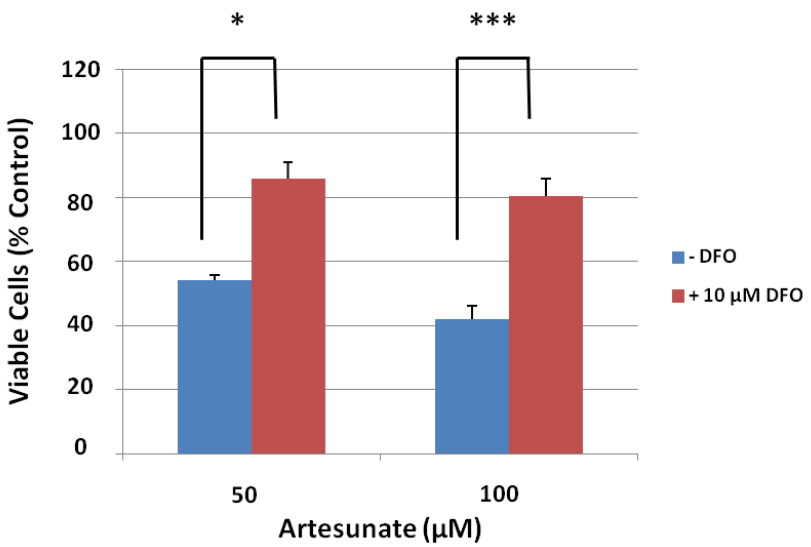

Figure 3.22. Protective effects of DFO against artesunate cytotoxicity. HeLa cells were co-treated with 50 – 100 µM artesunate and 10 µM DFO for a period of 24 h. Cytotoxicity was measured using the MTT assay. Values are expressed as percentage fold-change relative to vehicle control, and are presented as the mean of three independent experiments, ± SD. * represents $p < 0.05$ and *** $p < 0.001$, as determined through paired t-test.

3.3.4.6. Impact of DFO upon Artesunate-Induced Mitochondrial Dysfunction

Mitochondrial function was again assessed through use of the Seahorse XF stress test method. Co-treatment of HeLa cells with 10 µM DFO alongside 50 and 100 µM artesunate proceeded over 24 h. DFO demonstrated an ability to abrogate drug-induced impact upon coupling efficiency (Fig. 3.23. A) and reserve capacity (Fig. 3.23. B), restoring bioenergetic performance to levels commensurate with those apparent within vehicle controls.

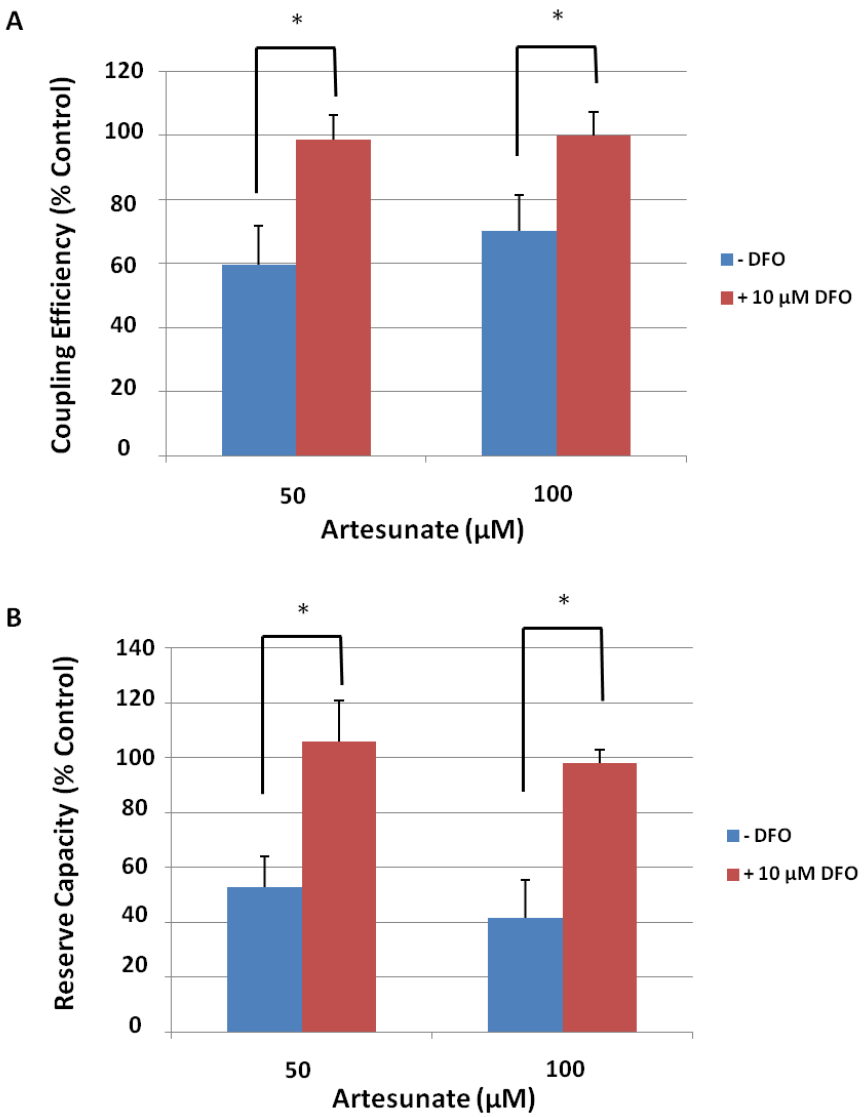

Figure 3.23. Impact of DFO upon artesunate-induced mitochondrial dysfunction. HeLa cells were treated for 24 h with 50 – 100 μM artesunate and 10 μM DFO, before coupling efficiency **(A)** and reserve capacity **(B)** were determined using the XF mitochondrial stress test. Values are expressed as percentage of normalised OCR relative to vehicle control, and are presented as the mean of three independent experiments, ± SD. * represents $p < 0.05$, as determined through paired t-test.

3.4. Discussion

The intention of the studies performed within this chapter has been to examine the hypothesis that iron-stimulated oxidative stress constitutes a central contributing factor towards the development of artemisinin-induced defects in mitochondrial bioenergetic functioning. Accordingly, the impact both of ROS scavenging antioxidants and the iron chelator DFO upon cellular response to artesunate treatment has been examined. Such investigations have been supplemented with assessment into the potential relevance of acknowledged superoxide-generating sources, including the substituent complexes of the electron transport chain, towards the emergence of oxidative stress.

In order that the importance of the contribution of artesunate-stimulated oxidative stress towards dysfunction across the cell could be ascertained, the impact of the antioxidant ROS scavengers tiron and TEMPOL upon the response of HeLa cells to drug treatment was first investigated. Although both compounds were able to exert significant cytoprotective effects against the artemisinin derivative, the effect of the former in preserving cell viability was notably more pronounced. Approaching 90% of treated cells exhibited evidence of survival in the presence of 2 mM tiron (Fig. 3.5.), as opposed to approximately 60% in response to an identical concentration of TEMPOL (Fig. 3.6.). In explaining the apparent greater impact of tiron in abrogating the cytotoxic effects of artesunate, it is necessary to consider the wider properties possessed by each compound, and the consequences that these might hold in determining the extent of any protective influence. Evidence suggests that tiron, unlike TEMPOL, contains the ability to permeate the mitochondrial outer membrane, and hence localise itself within the organelle (McArdle *et al.*, 2005; Supinski *et al.*, 1999). Whilst it appears rational, in light of the capacity of artemisinin derivatives to function as disruptors of mitochondrial function, to attribute the reduced susceptibility of cells towards drug effects solely upon an improved capability of the antioxidant to

neutralise mitochondrial ROS, it is apparent that further factors additionally influence such outcomes. It is observed that the impact of each compound upon the levels of artesunate-induced mitochondrial oxidative stress, as assayed through the flow cytometric MitoSOX protocol, is roughly equivalent, with fold changes in fluorescence detected relative to untreated controls decreasing to approximately 150% in both instances (Figs 3.3. and 3.4.). Studies have demonstrated that the protective impact of tiron against the deleterious effects of ROS is derived from actions imparted by the antioxidant across several aspects of cellular function (Ghosh *et al.*, 2002). Its ability to diminish oxidative damage towards mitochondrial and nuclear DNA sustained as a consequence of UV irradiation and hydrogen peroxide loading in dermal fibroblastic cells is witnessed to stand in excess of that possessed by the mitochondrially-targeted ubiquinone derivative MitoQ (Oyewole *et al.*, 2014). It is strongly implied, therefore, that the scope of its actions exceed merely those mediated within the mitochondrion. The capacity to function as a chelator for cellular transition and heavy metals has been suggested owing to outcomes obtained across a number of reports (Domingo *et al.*, 1997; Krishna *et al.*, 1992). As a result of the role possessed by free iron both in the propagation of ROS and in the progression of artemisinin-induced cell death, it is feasible that this capability might contribute towards its potential in abrogating toxicity.

Deficits in mitochondrial bioenergetic function stimulated through artesunate treatment were significantly minimised upon tiron co-administration. The presence of the antioxidant was observed to restore both the coupling efficiency and reserve capacity, as determined through the Seahorse XF stress test, to levels approaching those of control values (Fig. 3.9.). Such outcomes strongly suggest that oxidative damage is an essential causative factor in the emergence of impairment in the mitochondrion, serving furthermore to indicate that the formation of ROS constitutes an early event in the pathway towards cell death. A variety of systems within the organelle are susceptible to the disruptive impact of ROS.

Alongside their ability to cause insult to the structural integrity of DNA, their interactions culminating in the peroxidation of phospholipids and in the dismantling of Fe-S clusters are acknowledged as being central contributing factors towards interference with the machinery regulating energy production through oxidative phosphorylation (Cortes-Rojo *et al.*, 2011; Davies, 1990).

Investigation into formation of mitochondrial superoxide across HeLa and ρ^0 HeLa cells revealed, in line with the trends observed across previous whole-cell studies performed using DCFH-DA, that the presence of a functioning electron transport system contributes towards the emergence of elevated levels of oxidative stress (Fig. 3.10.) (Mercer *et al.*, 2011). Under physiological conditions, shuttling of electrons between operational complexes occurs continuously, with intermittent leak stimulating ROS formation. Damage to the integrity of this mechanism is associated with enhanced generation of superoxide, as compromised transport facilitates electron escape (Turrens, 2003). The ρ^0 line, owing to the characteristic depletion of mitochondrial DNA, expresses forms of the constituent units which exhibit incomplete assembly arising as a consequence of a variety of structural deficits imparted by the removal of relevant coding information (Chevallet *et al.*, 2006). The resulting inability of these cells to perform oxidative phosphorylation ensures that such an avenue towards the emergence of ROS generation is closed. In spite of these abnormalities, increases in superoxide levels detected within the ρ^0 line remain significant relative to control quantities upon artesunate dosing. The continued capacity for the drugs to stimulate substantial ROS production in the presence of a non-functioning respiratory chain serves to provide evidence that the primary mechanism through which the induction oxidative stress is imparted within these cell systems lies independent of the initiation of damage to the operation of the complexes constituting the electron transport arrangement. Accordingly, examination into the effects of artesunate upon the activity of these units within isolated mitochondria indicated that the presence of the compound

possesses no notable bearing upon the functioning of complexes I, III and IV. Significant but partial disruption to the operational capacity of complex II was observed, with the ability of the drug to reduce functioning of the enzyme to levels 60-65% of those in vehicle controls confirmed through two assay methods (Figs 3.11. and 3.12.). Investigations performed outlining the protective influence of tiron upon drug-stimulated mitochondrial respiratory dysfunction provide further evidence to support the assertion that the primary source of ROS-initiated damage to the organelle exists external to the system of electron transport. It can be hypothesised that the enhanced quantities of superoxide detected in the presence of an active respiratory chain arise as a function of defective operation imparted as a consequence of an initial oxidative injury. ROS-induced ROS release is identified as a phenomenon whereby ROS-stimulated mitochondrial damage proceeds to promote further, large-scale oxidative stress upsurge (Zorov *et al.*, 2014). It is believed that such a process is associated closely with the collapse of membrane potential and subsequent opening of the mitochondrial permeability transition pore, with the formation of ROS mediated as a consequence of defective functioning at the electron transport pathway. As such, the propagation of ROS about the whole cell might be readily facilitated.

In identifying an initial source for the formation of the ROS which ultimately stimulate mitochondrial damage, it was therefore necessary to consider the relevance of systems located outside of the organelle. Determination of the potential for the involvement of alternative ROS-generating enzymes in the emergence of artesunate-induced oxidative stress culminated in a series of investigations centred upon examining the contributions of NADPH oxidase, cytochrome P450, xanthine oxidase, and cyclooxygenase towards both cytotoxicity and levels whole-cell ROS. The rationale for the study was based upon the work performed by Lee *et al.* and Bobba *et al.,* in which delineation of the enzymatic sources behind ROS generation in tamoxifen treatment and in granulocyte apoptosis was achieved through assessing the impact of inhibitory agents upon cell response to stimuli (Bobba *et*

al., 2008; Lee *et al.*, 2000). A significant, albeit very limited cytoprotective effect towards artesunate was evident upon co-administration of the NADPH oxidase inhibitor DPI – an occurrence which was not mimicked across the other systems studied (Fig. 3.14.). Levels of drug-stimulated cellular ROS were similarly unaffected by inhibition of the examined enzymes (Fig. 3.15.). Such findings combined strongly indicate that the origin of oxidative stress in artemisinin treatment is not mediated through imparting changes to the functioning of these systems.

Further examinations of the pathways responsible for the formation and proliferation of the ROS which contribute ultimately towards the onset of artemisinin-stimulated mitochondrial injury considered the potential roles held by cellular free iron in the development of such phenomena. Unbound iron is strongly associated both with the enhanced formation of ROS arising through chemical mechanisms such the Fenton reaction, and furthermore with the initiation of radical formation courtesy of artemisinin endoperoxide bridge reduction (Dixon *et al.*, 2014; Mercer *et al.*, 2007; Thomas *et al.*, 2009). Pools of potentially reactive chelatable iron are found distributed at selected points within the cell, the most prominent of which lie within the lysosomal bodies (Kurz *et al.*, 2011). The impact of the lysosomal iron chelator DFO was examined with respect to its influence upon cell response to artesunate treatment. It was revealed that its co-administration alongside the artemisinin derivative had potential to elicit significant cytoprotective outcome, with cell viability restored to roughly 80% of control values following 24 h (Fig. 3.22.). This effect was accompanied by an ability to impart substantial decreases in quantities of drug-stimulated ROS detected both across the whole cell (Fig. 3.21.) and within the mitochondrion (Fig. 3.20.). Such findings indicate that the abrogation of cytotoxicity which occurs as a consequence of iron chelation is associated with diminution in oxidative stress. In delineating the events underpinning these observations, it was necessary to perform assessment into the capacity of DFO to impact upon

endoperoxide bridge bioactivation. Accordingly, this was achieved through the monitoring of decomposition of the artemisinin derivative PFDHA *via* the established LC-MS method (Mercer *et al.*, 2007). Outcomes indicated that the presence of the chelator imparted significant protective effect against the degradation of the parent compound following 24 h cell treatment, whilst simultaneously inhibiting the formation of its THF acetate isomer (Fig. 3.19.). The quantity of PFDHA recovered in DFO-treated cells stood at approximately 80% of that initially administered, strongly indicating that the ability of the chelator to abrogate bioactivation is not total. Previous studies have demonstrated that the recovery of the artemisinin derivative approaches totality following short incubation spans, hence suggesting that the recovered fraction in this assay is indeed not indicative of complete chelator-mediated prevention of Fe(II)-stimulated endoperoxide bridge reduction (Mercer *et al.*, 2011; Mercer *et al.*, 2007). Unfortunately, attempts to quantify cellular iron content using a ferrozine-based method were unsuccessful. Additional evidence has suggested that further DFO antioxidant capacity might derive from an ability to stimulate the expression of endogenous ROS-neutralising agents through activation of the nuclear factor erythroid 2-related factor (Nrf2) pathway (Chung *et al.*, 2014). The greater relevance of such an occurrence in the context of the systems examined remains uncertain.

In a manner similar to that of tiron, DFO was observed to exert significant protective effect against artesunate-induced mitochondrial dysfunction. At a concentration of 10 µM, the chelator raised coupling efficiency and reserve capacity to levels approximately commensurate with those in control cells (Fig. 3.23.). It can therefore be concluded that free iron plays an essential role in the progression of mitochondrial damage. Owing to the contribution of the unbound metal in propagating ROS, and to the efficacy of tiron in abrogating injury towards the processes of the organelle, it is rational to suggest that at least part of this association is attributable to antioxidant properties (Dixon *et al.*, 2014). It is, however, further plausible that protection might arise courtesy of the regulatory impact

of iron chelation upon alternative pathways, including drug bioactivation, in which the metal has involvement. Evidence exists to suggest that mobilisation of the unbound metal towards the mitochondrion occurs as a consequence of lysosomal dysfunction (Uchiyama *et al.*, 2008; Zhang *et al.*, 2013). It has been demonstrated that the employment of DFO has the potential to halt mitochondrial uptake of iron induced through bafilomycin-stimulated collapse of the lysosome membrane potential (Hung *et al.*, 2013). The outcomes of a further study, in which the relevance of lysosomal iron content towards the toxicity of artemisinin in breast cancer cells was investigated, have served to provide further indication of the importance of the chelatable pool towards the progression of cytotoxic effects (Hamacher-Brady *et al.*, 2011). These findings have prompted the authors to hypothesise that lysosomally-mediated programmed cell death occurs as an early stage during artemisinin-induced toxicity.

It can be concluded from the outcomes of the studies performed as part of this assessment that the emergence of artemisinin-induced mitochondrial dysfunction might be attributed primarily to the impact of oxidative damage upon the organelle. Abrogation of cellular and mitochondrial ROS levels has the effect of ameliorating drug-stimulated deficiency in bioenergetic activity, whilst simultaneously protecting against cytotoxic effects. Further evidence would appear to indicate that cellular free iron possesses roles both in the bioactivation of the drug and in the propagation of oxidative stress, with chelation associated with reduced prevalence of ROS and cessation in defective mitochondrial operation. The outcomes of examinations performed within ρ^0 HeLa cells attest that an operational electron transport chain, although contributing to the enhanced generation of ROS, does not function as an absolute requirement for their initiation. In combination with the apparently limited impact of the compound upon the activity of the substituent complexes within this system, such findings provide evidence that the initial source for ROS lies independent of the machinery of oxidative phosphorylation. The potential role of non-

mitochondrial ROS sources in the initiation of such effects is given examination, although with results proving ultimately inconclusive. The efficacy of the lysosomal iron chelator DFO in protecting against artesunate-induced cell termination provides tentative evidence that death pathways mediated through that body might influence treatment outcomes.

Chapter Four

Elucidation of the Role of Cardiolipin in the Progression of Artemisinin-Induced Cytotoxicity

4.1. Introduction

The ability of artemisinin derivatives to induce cell death through apoptosis forms an established feature of their mechanism of cytotoxicity (Firestone *et al.*, 2009; Mercer *et al.*, 2011). As understanding of the physiological processes underpinning mitochondrial function and the progression of programmed cell death continues to advance, the potential relevance of novel pathways and effectors grows more apparent. Recent research has revealed that the phospholipid cardiolipin performs numerous roles which are significant to both the respiratory functioning of the mitochondrion and to the regulation of apoptosis, transforming it into a growing focus of interest (Orrenius *et al.*, 2005). Despite great strides having been made in ascertaining its functions on a physiological level, its potential for a role in drug toxicity has yet to be explored.

It has been demonstrated that artemisinin derivatives can induce the peroxidation of phospholipids in both parasitic and mammalian systems (Berman *et al.*, 1997). Whilst this event may occur solely as a consequence of generalised damage associated with the presence of elevated levels of ROS within cells, it is alternatively hypothesised that the drugs might exert direct oxidising effects as a function of their chemical reactivity. Evidence from biomimetic studies attests to the capacity of artemisinin to stimulate substantial oxidative degradation of phospholipid structures (Kumura *et al.*, 2009). A proposed mechanism through which such effects might proceed, outlined in Section 1.3.4.6., Chapter 1, centres upon the postulated abstraction of protons from unsaturated fatty acid chains by reactive carbon radical species formed courtesy of the Fe(II)-mediated degradation of the parent compound (Mercer *et al.*, 2007; O'Neill *et al.*, 2004). This chapter shall seek to examine the potential relevance of this model with respect to the interaction between artesunate and cardiolipin, with studies focused upon investigating the impact of a

recently-developed small molecular inhibitor of physiological cardiolipin oxidation upon cellular response to the drug.

Cardiolipin is a unique phospholipid located almost exclusively within the mitochondrion (Houtkooper *et al.*, 2008). It possesses a characteristic diphosphatidylglycerol structure, consisting of a total of four fatty acyl chains bonded to a central glycerol-containing backbone. Although this assembly has the potential to lead to a great diversity of variant isoforms, it is arrangements containing the 18-carbon, doubly-unsaturated linoleic acid chain which are found to predominate overwhelmingly across mammalian tissues (Fig. 4.1.) (Schlame *et al.*, 2000). Tetralinoleoyl cardiolipin possesses heightened susceptibility towards lipid peroxidation mediated by free radical species, and it is hypothesised that it is this sensitivity which lends cardiolipin its key role in apoptotic progression.

The inner mitochondrial membrane accounts for the location of over 95% of cardiolipin, where it comprises roughly 25% of phospholipids present (Paradies et al., 2009). Cardiolipin possesses numerous roles critical to the maintenance of optimal mitochondrial bioenergetic function, derived primarily from interactions with the substituent proteins of complexes which form the electron transport chain (Pfeiffer *et al.*, 2003). The presence of cardiolipin is required for maximal activity in complexes I, III, and V, but it is its relationship with cytochrome c which has attracted most interest on account of its relevance during the early phases of apoptotic cell death (Crimi *et al.*, 2011).

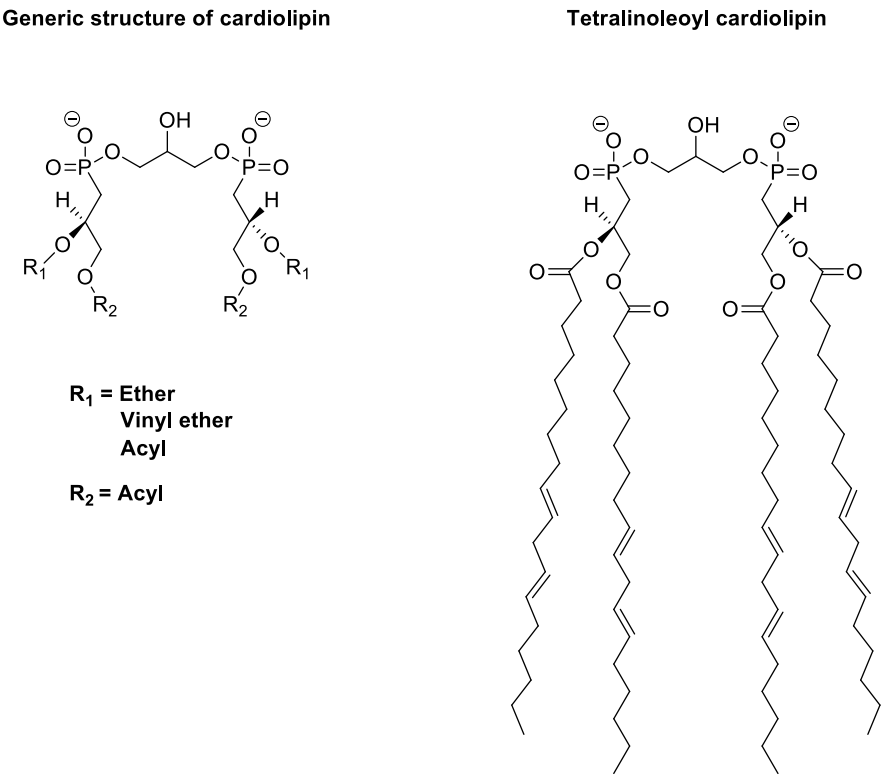

Figure 4.1. Generic structure of cardiolipin (left), and the structure of tetralinoleoyl cardiolipin, the most abundant form present in mammalian cells (right).

Cytochrome c, a haem-containing protein associated predominantly with the inner mitochondrial membrane, forms an essential constituent of complex III. During apoptosis, it migrates from its resting position, undergoing release into the cytosol, where it is found to activate caspase cleavage through binding of APAF-1 (Elmore, 2007). Recent research has uncovered that the regulation of cytochrome c motility during the early phases of apoptosis is heavily dependent upon its interaction with cardiolipin, with each protein possessing a significant influence over the positioning and the function of the other (Belikova *et al.*, 2006). In the absence of apoptotic stimuli, the primary function of cytochrome c as an electron transfer protein is maintained through its anchoring to the inner mitochondrial membrane, a process dependent upon cardiolipin association.

Evidence suggests that cytochrome c and cardiolipin are able to form specific complexes with one another, with two primary variant binding modes facilitated through the presence

electrostatic and hydrophobic interactions (Ott *et al.*, 2007). Loose binding is primarily hydrophobic in nature, and is observed between the lengthy acyl chains of cardiolipin, and the hydrophobic cleft present within cytochrome c (Belikova *et al.*, 2006). An alternative tight binding mode is the result of electrostatic attraction existing between the positively-charged cytochrome c, and the anionic head of cardiolipin. Loosely-bound complexes are associated with the electron-shuttling role of cytochrome c, whereas tightly-bound complexes have been shown to possess potent peroxidase activity. It is these which are heavily implicated during the process of cytochrome c release in early apoptosis (Kagan *et al.*, 2005).

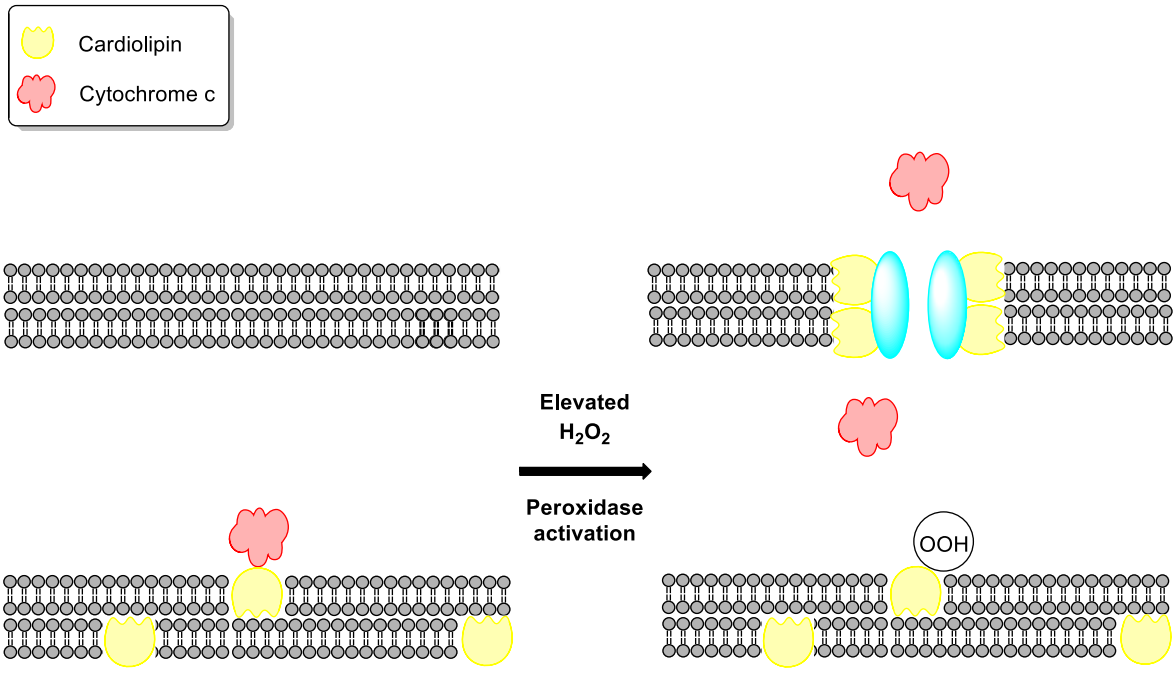

Figure 4.2. Cardiolipin is situated predominantly at the inner mitochondrial membrane, where it acts to anchor cytochrome c at its position within the electron transport chain. An elevated level of H_2O_2, which occurs as a by-product of ROS generation, triggers the peroxidation of cardiolipin. Cytochrome c is released from its resting position, diffusing into the intermembrane space. Transmembrane relocation of oxidised cardiolipin facilitates the binding of pro-apoptotic factors such as bax and t-bid, enabling pore formation and passage of cytochrome c into the cytosol.

The mechanism through which these peroxidase complexes mediate their effects has been ascertained primarily through molecular modelling studies, with the presence of tightly-

bound cardiolipin being found to exert a series of conformational changes upon cytochrome c which culminate in the exposure of its peroxidase active site (Kagan *et al.*, 2009b). Elevated levels of hydrogen peroxide, found accompanying a surge in ROS production during the early phases of apoptosis, spur these complexes to induce the direct, selective oxidation of cardiolipin. The phospholipid, in its oxidised state, develops a significantly reduced binding affinity for cytochrome c, facilitating its release from an anchored position at the inner mitochondrial membrane, and enabling its diffusion into the intermembrane space (Belikova *et al.*, 2006). It is additionally hypothesised that cardiolipin possesses a role in assisting the permeabilisation of the outer mitochondrial membrane, enabling the ultimate release of cytochrome c into the cytoplasm (Crimi *et al.*, 2011). Transmembrane relocation is believed to be initiated through the activity of scramblase enzymes, with the increased presence of oxidised cardiolipin in the outer membrane associated with a greater binding affinity for the apoptosis-promoting proteins bax and t-bid (Schlattner *et al.*, 2009). Through their action, pore formation across the membrane facilitates the passage of cytochrome c from the mitochondrion (Fig. 4.2.).

The studies presented within this chapter shall be centred upon examining the hypothesis that artemisinin-derived compounds possess a capacity to stimulate the direct oxidation of cardiolipin. Recently, the development of a series of compounds for the inhibition of peroxidase function in the cardiolipin-cytochrome c complexes has been reported (Atkinson *et al.*, 2011; Kagan *et al.*, 2009a). The employment of *in silico* modelling techniques has facilitated the rational design of a series of inhibitors which are intended to occupy the haem active-site of cytochrome c, thus preventing protein unfolding and impairing ability to induce cardiolipin peroxidation. These compounds, derived from unsaturated long-chained molecules such as ricinoleic and stearic acids, exert their activity primarily through their imidazole functionalities, which are able to act as ligands about the Fe(II) centre. Employment in an *in vitro* study performed across mouse embryonic cells has

demonstrated their ability to actively suppress peroxidase activity, resulting in the inhibition of cardiolipin oxidation and of accompanying apoptosis as part of a general cytoprotective effect. These outcomes have translated into *in vitro* models, with administration of the inhibitors being associated with greatly improved survival rates amongst mice subjected to radiation exposure.

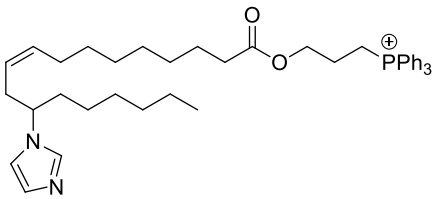

(12)

The impact of the ricinoleic acid-derived peroxidase inhibitor TPP-IOA **(12)** upon cellular response to artesunate treatment shall be examined. Its effects are ascertained through a range of assays, focusing upon two primary areas of investigation. Firstly, the capacity of the compound to induce reduction in drug-induced cardiolipin oxidation, and the consequences that this possesses regarding the progression of cytotoxic activity, shall be investigated. A second, parallel strand of study – spurred by evidence suggesting a potential role for microperoxidase-11 (MP-11) in the stimulation of endoperoxide bridge bioactivation – shall examine the effects of the peroxidase complex inhibition upon the structural integrity of the artemisinin derivative PFDHA (Rodriguez *et al.*, 2002). The development of an alternative route towards the chemical synthesis of the inhibitor is also given detailed description. Assessment of activity shall be performed across three cell types – the human promyelocytic leukaemia-derived HL-60 line, the HeLa and the HeLa ρ^0 variety. The latter of these forms has been depleted of mitochondrial DNA through prolonged culturing in the presence of ethidium bromide, and thus possesses no functional electron

transport chain. It is intended that this work shall allow for an initial examination into the potential for endoperoxides to directly alter the structure and activity of cardiolipin, ahead of any expansive future studies.

4.2. Materials and Methods

4.2.1. Materials

Roswell Park Memorial Institute (RPMI) medium, alongside all further chemicals and solvents, were purchased Sigma-Aldrich (Poole, Dorset, UK). HL-60 cells were acquired from the European Collection of Cell Cultures (Salisbury, UK).

4.2.2. Cell Culture and Experimental Preparation

HeLa and ρ^0 HeLa cells were cultured and maintained according to the protocols outlined respectively in Sections 2.2.2., Chapter 2 and 3.2.2., Chapter 3. HL-60 cells were maintained in RPMI 1640 medium, with the addition of supplemental FBS (10% v/v), L-glutamine (1% w/v) and penicillin/streptomycin solution (1% v/v). Cell density was maintained below $1x10^6$ cells/ml, in order to ensure exponential growth and to prevent differentiation.

4.2.3. Analysis through Flow Cytometry

Flow cytometric analysis was performed in accordance with the parameters described in Section 3.2.4., Chapter 3.

4.2.4. Determination of Cardiolipin Oxidation using Nonyl Acridine Orange

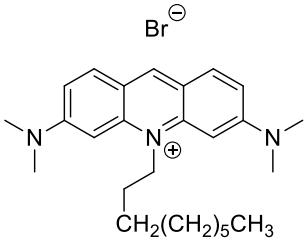

Nonyl acridine orange

Nonyl acridine orange (NAO) is a fluorescent dye possessing high affinity for cardiolipin. Decreases in fluorescence are associated with reduced cardiolipin presence within the mitochondrion (Kaewsuya *et al.*, 2007). Drug-treated HL-60, HeLa and HeLa ρ^0 cells (2 x 10^5) were washed with HBSS and centrifuged (1000*g*) to produce a pellet which was resuspended in 0.5 ml of 10 µM NAO solution. Following 15 minutes incubation at 37°C, cells were again centrifuged (1000*g*), before NAO solution was replaced by 0.5 ml HBSS. Cells (1x10^4 per sample) were analysed immediately through flow cytometry, with fluorescence monitored following excitation at a wavelength of 488 nm.

4.2.5. Analysis of Apoptotic Cell Population using Propidium Iodide

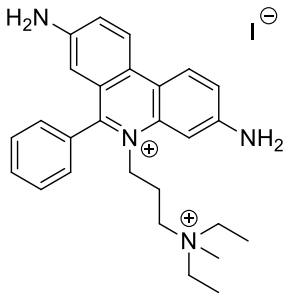

Propidium iodide

Propidium iodide (PI) acts as a DNA intercalator, having great affinity for binding within major grooves (Krishan, 1975). Following drug treatment, cells (2 x 10^5) were centrifuged (5 minutes, 1000*g*), and the resultant supernatant removed. Cells were washed with HBSS, before being fixed in 1 ml ice-cold 70% ethanol, and frozen at -20°C for a period of at least 2 h. The 70% ethanol was removed, and the cells washed again with HBSS, before they were re-suspended in 0.5 ml PI solution (40 µM, 1% RNAse, 1 % sodium citrate) and incubated at 37°C for 10 minutes. A minimum of 1x10^4 cells were analysed immediately upon the flow cytometer, with fluorescence monitored following 488 nm excitation.

4.2.6. Assessment of Cell Viability using the MTT Assay

Cell viability within the HeLa line was ascertained through use of the MTT assay, as detailed in Section 2.2.4., Chapter 2.

HL-60 cells (5 x 10^4/well) were plated, in triplicate, into flat-bottomed 96-well plates. They were subsequently exposed to concentrations of drug ranging from 0.1 µM to 100 µM, dependent upon the nature of the assay, and incubated for time periods of up to 24 h. Upon the completion of incubation, 20 µL of MTT solution (5 mg/ml in HBSS) was added to each well. Following a further 2 h incubation, 200 µL of a lysis buffer (20 % w/v SDS, 50 %

w/v DMF) was added to each well, and a further 4 h incubation at 37°C performed. Absorbance of each well was read on a plate reader (Dynex MRX, Magellan Bioscience, Worthing, UK), using a test wavelength of 570 nm and a reference wavelength of 590 nm. Results are expressed as a percentage of absorbance relative to untreated vehicle control, with IC_{50} derived from curves plotted using the GraFit Software.

4.2.7. Measurement of Mitochondrial Reactive Oxygen Species using MitoSOX

The specific formation of superoxide within the mitochondrion was quantified through use of the MitoSOX fluorescent dye, following the procedures described in Section 3.2.7., Chapter 3.

4.2.8. Analysis of Drug Bioactivation using an LC-MS Method

Bioactivation of the artemisinin derivative PFDHA was monitored according to the LC-MS method detailed in Section 3.2.10., Chapter 3.

4.2.9. Statistical Analysis

Data is presented and analysed in line with the protocols described in Section 2.2.10., Chapter 2.

4.2.10. Chemical Synthesis of TPP-IOA

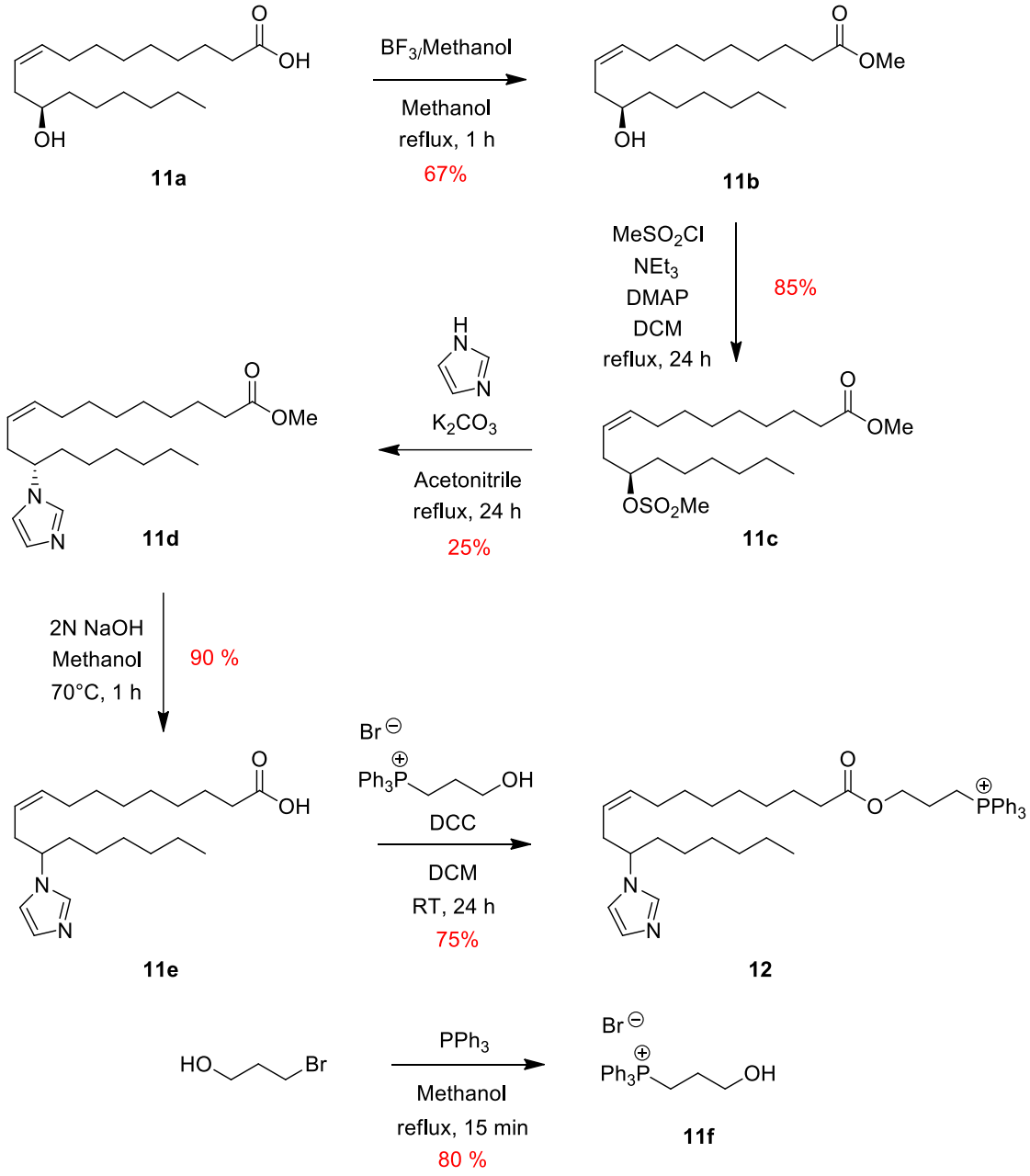

Figure 4.3. Scheme outlining the route towards synthesis of TPP-IOA.

Synthesis of the chemical cardiolipin/cytochrome c complex inhibitor TPP-IOA was achieved following a scheme derived from that employed by Atkinson *et al.* (Fig. 4.3.) (Atkinson *et al.*, 2011). Castor oil consists of a complex mixture of fatty acids, with approximately 90% of this content attributed to ricinoleic acid **(11a)** (Yang et al., 2002). Formation of the methyl ester of ricinoleic acid, (Z)-methyl 12-hydroxyoctadec-9-enoate **(11b)**, was effected through treatment of unpurified castor oil with the methylating agent boron trifluoride-methanol, with silica column chromatography facilitating the isolation of a pure product in 67% yield. Introduction of the methanesulphonyl (mesyl) leaving group produced (Z)-methyl 12-((methylsulphonyl)oxy)octadec-9-enoate **(11c)** at a yield of 85%. Substitution of this mesyl group with the imidazole functionality, in order to form (Z)-methyl 12-(1H-imidazol-1-yl)octadec-9-enoate **(11d)**, was facilitated through heating in the presence of the weak base potassium carbonate. Yields were held between 25-30%, owing to the preponderance of elimination side-products. Deprotection of the methyl ester was achieved through hydrolysis under basic conditions, with the presence of aqueous sodium hydroxide sufficient to produce (Z)-12-(1H-imidazol-1-yl)octadec-9-enoic acid **(11e)** at a yield of 90%. This compound was coupled with (3 hydroxypropyl)triphenylphosphonium bromide **(11f)** in the presence of *N,N*-dicyclohexylcarbodiimide (DCC) to furnish TPP-IOA **(12)** in 75% yield. Overall process yield, from starting material to the final product, stood at 9.6%. (3 hydroxypropyl)triphenylphosphonium bromide itself was formed through the heating of 3-bromopropanol alongside triphenylphosphine, with a yield 80% achieved.

4.2.10.1. (Z)-methyl 12-hydroxyoctadec-9-enoate (11b)

Castor oil (6.00 g), methanol (50 ml) and boron trifluoride-methanol (12 ml) were combined, with the resulting mixture stirred at 65°C for 1 h. Following extraction with ether (3 x 50 ml), the pooled organic layers were concentrated and purified through silica column

chromatography (3:7 ethyl acetate/petroleum ether) to yield (Z)-methyl 12-hydroxyoctadec-9-enoate as a light-yellow oil (4.2 g, 67%).

^{1}H NMR (400 MHz, $CDCl_3$); 0.9 (m, 3H), 1.2-1.7 (m, 22H), 2.0 (m, 2H), 2.2 (m, 2H), 2.4 (m, 2H), 3.6 (s, 1H) 3.7 (s, 1H), 4.6 (m, 1H), 5.4 (m, 1H), 5.6 (m, 1H); **^{13}C NMR (400 MHz, $CDCl_3$);** δ 174.7, 133.8, 125.6, 71.9, 53.8, 51.9, 37.3, 35.8, 34.5, 32.2, 30.0, 29.8, 29.5, 29.4, 27.8, 26.1, 25.3, 23.0, 14.5; **MS;** m/z 335.3 (M+Na)

4.2.10.2. (Z)-methyl 12-((methylsulphonyl)oxy)octadec-9-enoate (11c)

A stirred solution of (Z)-methyl 12-hydroxyoctadec-9-enoate (4.00 g, 1.3 x 10^{-2} mol), dimethylaminopyridine (0.313 g, 1.30 x 10^{-3} mol) and triethylamine (2.60 g, 2.6 x 10^{-2} mol) in anhydrous dichloromethane was cooled to 0°C, with methanesulphonyl chloride (2.93 g, 2.6 x 10^{-2} mol) introduced drop-wise over 5 minutes. The resulting mixture was allowed to warm to room temperature and stirred overnight, after which it was quenched with brine (50 ml) and 10% sulphuric acid (30 ml). Following extraction with dichloromethane (3 x 40 ml), organic phases were combined and concentrated to afford crude product. Purification through column chromatography was performed quickly, in order to minimise effects of product degradation upon silica. (Z)-methyl 12-((methylsulphonyl)oxy)octadec-9-enoate eluted at 3:7 ethyl acetate/petroleum ether (4.23 g, 85%), appearing as a yellow oil.

^{1}H NMR (400 MHz, $CDCl_3$); δ 0.9 (m, 3H), 1.2-1.5 (m, 16H), 1.7 (m, 4H), 2.0 (m, 2H), 2.2 (m, 2H), 2.4 (m, 2H), 3.0 (s, 3H), 3.7 (s, 3H), 4.6 (1H), 5.4 (m, 1H), 5.6 (m, 1H); **^{13}C NMR (400 MHz, $CDCl_3$);** δ 174.7, 134.8, 123.4, 84.0, 77.1, 51.8, 39.1, 34.6, 34.5, 32.9, 32.0, 29.8, 29.5, 29.5, 29.4, 27.8, 25.4, 25.3, 22.9, 14.4; **MS;** m/z 413.2 (M+Na)

4.2.10.3. (Z)-methyl 12-(1H-imidazol-1-yl)octadec-9-enoate (11d)

Imidazole (0.348 g, 5.10 x 10^{-3} mol) and potassium carbonate (0.707 g, 5.10 x 10^{-3} mol) were introduced to a stirred solution of (Z)-methyl 12-((methylsulphonyl)oxy)octadec-9-enoate (1.00 g, 2.60 x 10^{-3} mol) in acetonitrile. This mixture was heated overnight at a temperature of 80°C, before the addition of sodium bicarbonate (15 ml), brine (40 ml), and extraction with ethyl acetate (3 x 50 ml). The combined organic phases were concentrated to produce a crude product, which was purified through silica column chromatography (4:6 ethyl acetate/petroleum ether) to yield (Z)-methyl 12-(1H-imidazol-1-yl)octadec-9-enoate (0.227 g, 25%) as a pale yellow oil.

^{1}H NMR (400 MHz, $CDCl_3$); δ 0.9 (m, 3H), 1.2 (m, 16H), 1.5-1.8 (m, 6H), 2.2 (m, 2H), 2.4 (m, 2H), 3.7 (s, 3H), 3.8 (m, 1H) 5.1 (m, 1H), 5.3 (m, 1H), 6.8 (m, 1H), 7.0 (m, 1H), 7.4 (1H); **^{13}C NMR (400 MHz, $CDCl_3$);** δ 174.6, 136.5, 134.3, 129.5, 124.6, 117.0, 59.5, 51.8, 36.3, 35.8, 34.5, 33.7, 32.7, 32.0, 29.7, 29.4, 27.6, 26.8, 26.3, 25.6, 25.3, 14.5; **MS;** m/z 363.3 (M+)

4.2.10.4. (Z)-12-(1H-imidazol-1-yl)octadec-9-enoic acid (11e)

A solution containing (Z)-methyl 12-(1H-imidazol-1-yl)octadec-9-enoate (0.227 g, 6.50 x 10^{-4} mol) and aqueous sodium hydroxide (2N, 5 ml) in methanol was stirred for 1 h at 70°C. Upon completion, the reaction mixture was acidified with 2% aq. hydrochloric acid until a neutral PH had been acquired. Water was added, prior to extraction with ethyl acetate (3 x 30 ml). Combined organic phases were concentrated to yield (Z)-12-(1H-imidazol-1-yl)octadec-9-enoic acid (0.210 g, 80%) as a sticky, yellow oil.

^{1}H NMR (400 MHz, $CDCl_3$); δ 0.9 (m, 3H), 1.1-1.4 (m, 18H), 1.6 (m, 2H), 1.8 (m, 2H), 2.4 (m, 2H), 2.6 (m, 2H), 4.1 (m, 1H), 5.2 (m, 1H), 5.4 (m, 1H), 7.0 (m, 1H), 7.3 (m, 1H), 8.5 (1H), 11.0

(s, 1H); **^{13}C NMR (400 MHz, $CDCl_3$);** δ 178.0, 135.5, 135.1, 123.4, 123.1, 118.4, 61.2, 35.4, 34.8, 34.1, 31.9, 29.4, 29.2, 28.9, 27.5, 26.3, 25.3, 24.8, 24.1, 22.9, 14.4; **MS;** m/z 349.3 (M+)

4.2.10.5. TPP-IOA (12)

(Z)-12-(1H-imidazol-1-yl)octadec-9-enoic acid (0.210 g, 6.03 x 10^{-4} mol), (3-hydroxypropyl)triphenylphosphonium bromide (0.315 g, 7.84 x 10^{-4} mol) and DCC (0.162 g, 7.84 x 10^{-4} mol) were combined in dichloromethane. The resulting mixture was left to stir overnight, following which it was filtered through celite and concentrated to yield a crude product. Purification through silica chromatography (1:9 methanol/dichloromethane) furnished TPP-IOA (0.332 g, 75 %) as a thick, yellow-brown oil.

^{1}H NMR (400 MHz, $CDCl_3$); δ 0.9 (m, 3H), 1.2 (m, 16H), 1.4 (m, 2H), 1.6-2.0 (m, 6H), 2.2 (m, 2H), 2.4 (m, 2H), 3.7-4.0 (m, 2H), 4.3 (m, 1H), 5.1 (m, 1H), 5.3 (m, 1H), 6.8 (m, 1H), 7.0 (m, 1H), 7.4 (1H), 7.6-7.9 (m, 15H); **^{13}C NMR (400 MHz, $CDCl_3$);** δ 177.6, 135.9, 135.6, 134.9, 133.8, 132.7, 131.4, 123.6, 122.8, 118.0, 60.7, 35.9, 34.8, 32.2, 31.1, 29.6, 29.0, 28.1, 27.0, 25.3, 25.1, 24.9, 24.3, 22.6, 14.7; **MS;** m/z 651.4 (M+)

4.2.10.6. (3-hydroxypropyl)triphenylphosphonium bromide (11f)

Triphenylphosphine (4.35 x 10^{-3} mol, 1.13 g) was heated to 120°C, after which 1-bromo-3-propanol (3.60 x 10^{-3} mol, 0.5 g) was added. After being stirred for 15 minutes, a white precipitate appeared and ethanol (10 ml) was introduced. Heating was maintained for a further 10 minutes, during which the precipitate dissolved. The mixture was placed on ice, and ether added to induce the formation of (3-hydroxypropyl)triphenylphosphonium bromide as white crystals, with filtration yielding (0.985 g, 68%) of product.

^{1}H NMR (400 MHz, $CDCl_3$); δ 1.3 (m, 2H), 1.8-2.0 (m, 2H), 3.8-4.0 (m, 2H), 3.9 (s, 1H), 7.6-8.0 (m, 15H); **^{13}C NMR (400 MHz, $CDCl_3$);** δ 135.5, 133.9, 131.0, 118.7, 60.7, 26.3, 20.6; **MS;** m/z 321.2 (M+); **Elemental analysis;** Anal. calcd. $C_{21}H_{22}BrOP$: C, 62.86%, H, 5.53%; Found: C 62.75%, H, 5.55%.

4.3. Results

4.3.1. Effects of TPP-IOA upon Cell Viability

The impact of TPP-IOA upon viability was examined across each of the three cell types. IC_{50} values were obtained through use of the MTT assay, following 24 h incubation in HL-60 cells and following 48 h incubation in the HeLa and ρ^0 HeLa lines. Cytotoxic effects in the low micromolar range were evident in each instance, with greatest sensitivity exhibited within the HL-60 cells (Table 4.1.). As a consequence, the upper concentration limit at which the compound could be administered within each line corresponded to 1 µM within the HL-60 and 10 µM within HeLa and HeLa ρ^0 lines.

Cell Line	IC_{50} (µM)
HL-60	1.55 ± 0.71
HeLa	16.1 ± 3.69
HeLa ρ0	20.0 ± 4.73

Table 4.1. IC_{50} values of HL-60, HeLa and ρ^0 HeLa cells dosed with TPP-IOA. Cytotoxicity was measured using the MTT assay. Results are shown as the mean of three independent experiments, ± SD.

4.3.2. Impact of TPP-IOA upon Artesunate-Induced Cardiolipin Oxidation

Levels of oxidised cardiolipin within cells were determined through flow cytometry using NAO. NAO is a fluorescent dye which possesses affinity for cardiolipin, binding it in preference to other structurally related phospholipids. Intensity of fluorescence is generally proportional to the content of unoxidised cardiolipin present within the mitochondrion,

despite the existence of evidence suggesting that uptake of the compound within the organelle is influenced through membrane potential (Kaewsuya *et al.*, 2007).

Quantification of intact and oxidised cardiolipin was achieved through monitoring fluorescence following excitation at a wavelength of 488 nm. In Figure 4.4. A, a representative histogram in a sample of HeLa cells treated with vehicle control is outlined. An increase in the proportion of cells possessing the diminished fluorescence associated with cardiolipin oxidation is apparent following 24 h treatment with 25 µM artesunate (Fig. 4.4. B), as population within the gated area rises from 8.9% of total to 38.1%.

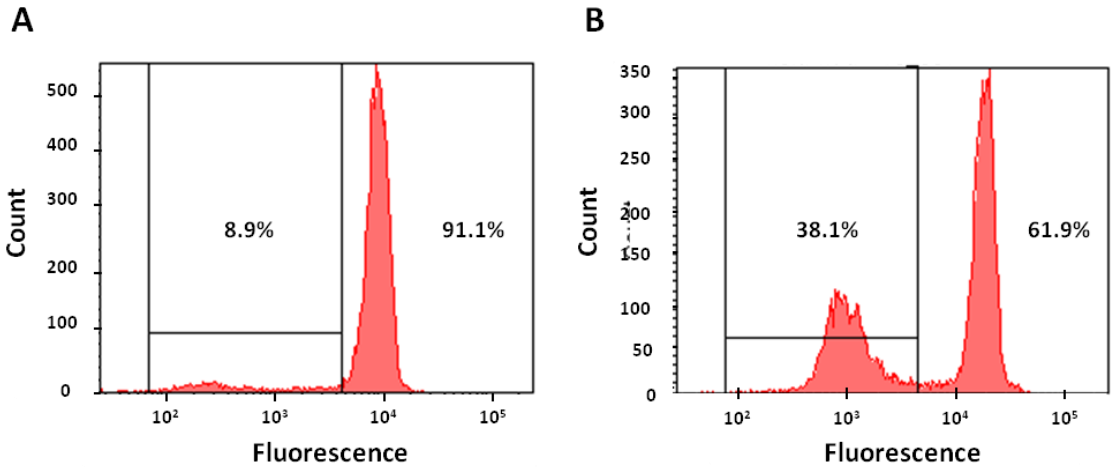

Figure 4.4. Representative histograms outlining variation in NAO fluorescence between control and drug-treated HL-60 cells. The distribution of NAO fluorescence is displayed in untreated control **(A)** and 25 µM artesunate-dosed HeLa cells **(B)** following 24 h incubation.

HL-60 cells were co-incubated with 0 – 10 µM artesunate and 0.5 µM TPP-IOA for a period of 24 h. The addition of the inhibitor was found to induce significant reductions in levels of cardiolipin oxidation with respect to those in cells administered solely with drug (Fig. 4.5. A). In HeLa (Fig. 4.5. B) and HeLa ρ^0 cells (Fig. 4.5. C) treated for 48 h with 0 – 50 µM artesunate, the presence of 10 µM TPP-IOA imparted no significant impact upon extent of cardiolipin oxidation relative to control.

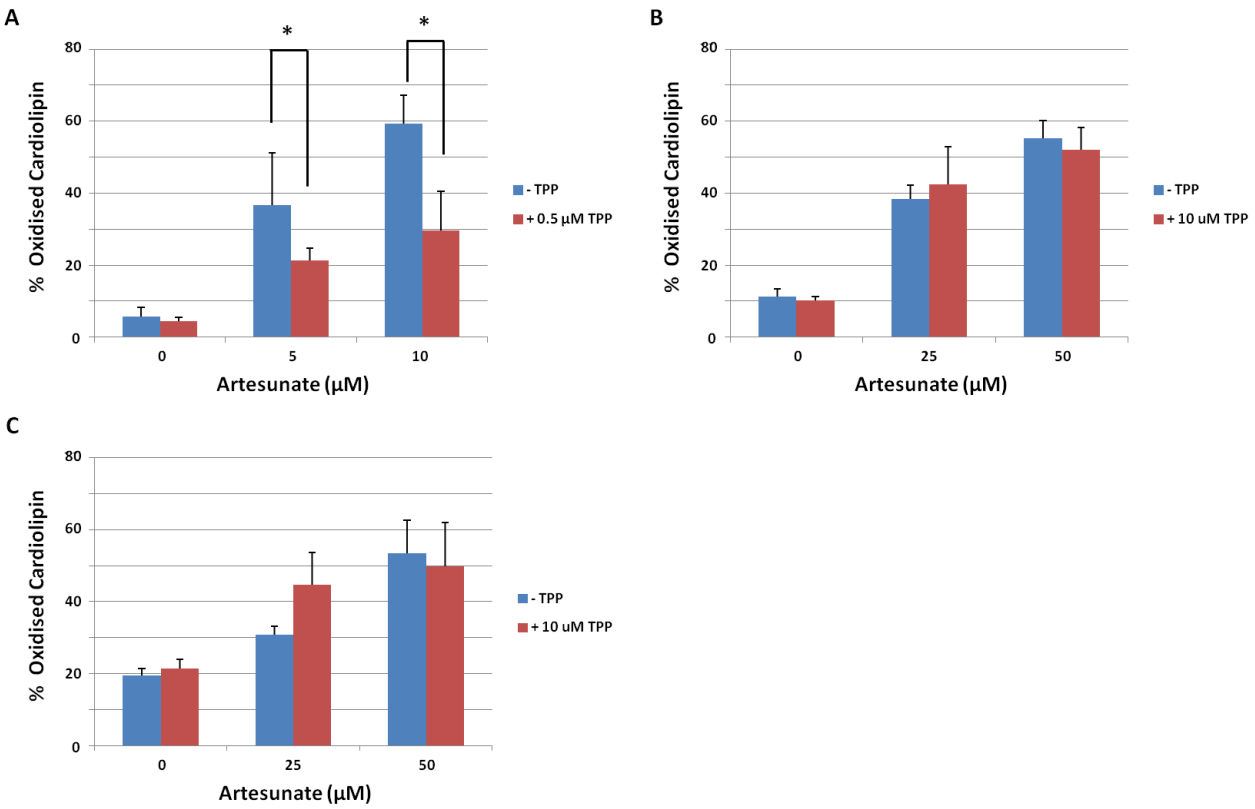

Figure 4.5. Impact of TPP-IOA upon artesunate-induced cardiolipin oxidation. HL-60 cells **(A)** were co-treated with 0 – 10 μM artesunate and 0.5 μM TPP-IOA for a period of 24 h. HeLa **(B)** and HeLa ρ^0 cells **(C)** were co-incubated with 0 – 50 μM artesunate and 10 μM TPP-IOA over 48 h. Cardiolipin oxidation was determined through measuring variation in NAO fluorescence using flow cytometry. Values are presented as the mean of three independent experiments, ± SD. * represents $p < 0.05$ as determined through paired t-test.

4.3.3. Cytoprotective Potential of TPP-IOA against Artesunate Treatment

The potential of TPP-IOA to ameliorate the toxicity of artesunate was investigated using the MTT assay. In HL-60 cells treated with 5 μM artesunate for 24 h, the co-administration of 1 μM TPP-IOA elicited a significant increase in cell viability (Fig. 4.6. A). Conversely, no significant cytoprotection was evident upon the co-incubation of 10 μM TPP-IOA alongside 25 μM artesunate in HeLa (Fig. 4.6. B) and HeLa ρ^0 cells (Fig. 4.6. C) following 48 h.

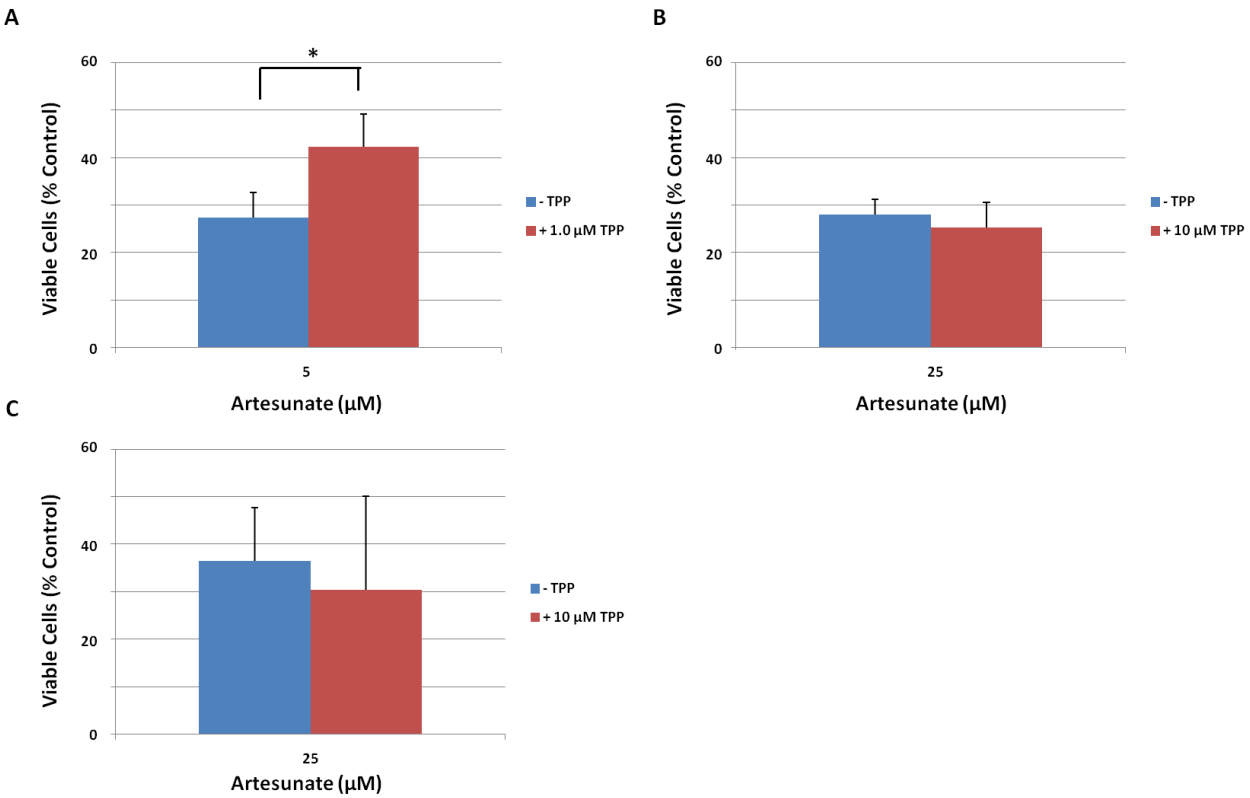

Figure 4.6. Cytoprotective potential of TPP-IOA against artesunate treatment. HL-60 cells **(A)** were co-treated with 5 µM artesunate and 1 µM TPP-IOA for a period of 24 h. HeLa **(B)** and HeLa ρ^0 cells **(C)** were co-incubated with 25 µM artesunate and 10 µM TPP-IOA over 48 h. Cell viability was determined using the MTT assay. Values are presented as the mean of three independent experiments, ± SD. * represents $p < 0.05$, as determined through the paired t-test.

4.3.4. Impact of TPP-IOA upon Artesunate-Induced Apoptosis

The emergence of an apoptotic cell population was quantified through flow cytometry using the DNA intercalator PI. PI fluoresces strongly upon formation of adducts alongside nuclear DNA, with the intensity of emission being proportional to the cellular DNA content. Through consideration of the relative abundance of DNA across its stages, measurement of fluorescence may be used in order to determine the progression of a cell population along the cell cycle. As a cell moves through this sequence, the process of DNA replication, which occurs during the S-phase, doubles content from 2n found in the G_0/G_1-phase to 4n at the G_2/M-phase. As a consequence of this growth, it is possible to infer from the plotting of

fluorescence intensity against cell count the relative proportion of cells present within each region (Fig. 4.7.). The apoptotic sub-G_0/G_1 population is characterised by its low apparent emission, which arises as a product of chromatin condensation and DNA degradation occurring during the enactment of programmed cell death.

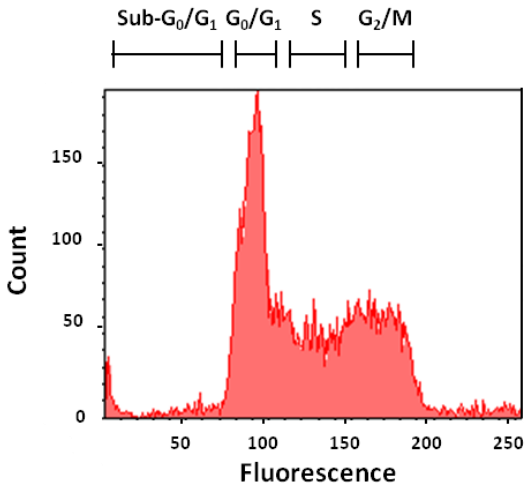

Figure 4.7. Representative histogram outlining fluorescence trace obtained in untreated cells upon PI staining. The locations of the regions which correspond to the sub-G_0/G_1, G_0/G_1, S and G_2/M cell cycle phases are detailed.

The accumulation of cells within the sub-G_0/G_1 region is indicative of the emergence of apoptotic death. Representative traces display alterations in PI fluorescence, stimulated through excitation at wavelength 488 nm, observed between vehicle control HL-60 cells (Fig. 4.8. A) and those treated with artesunate (Fig. 4.8. B) for a period of 24 h. The presence of drug leads to an increase in proportion of cells falling within this area, from 4.0% to 29.6% of total.

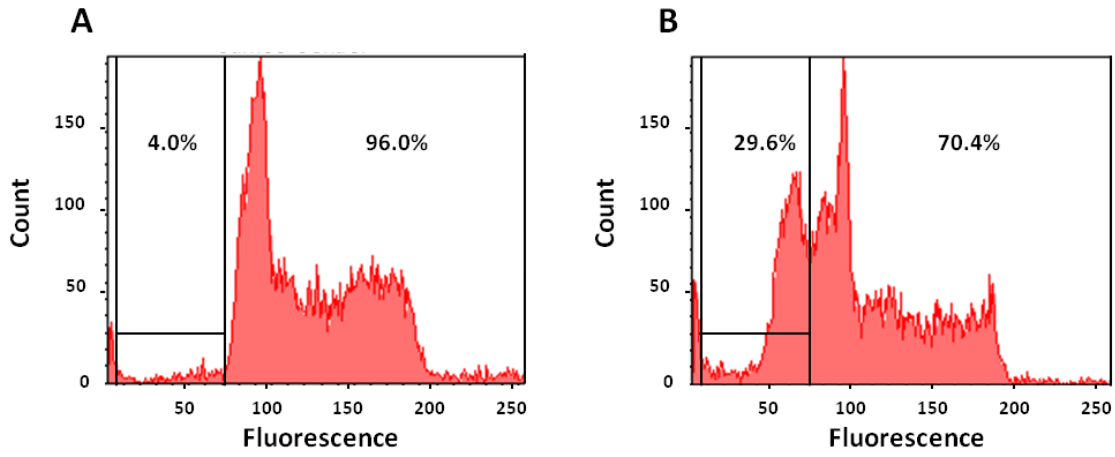

Figure 4.8. Representative histograms outlining variation in PI fluorescence between control and drug-treated HL-60 cells. The proportion of the population falling within the sub-G_0/G_1 cell cycle region, as highlighted within the gated area, is shown within untreated control **(A)** and artesunate-dosed cells **(B)** following 24 h incubation.

HL-60 cells were treated for 24 h with 5 µM artesunate. Co-administration of 1 µM TPP-IOA produced a mild but significant reduction in the proportion of cell appearing in the sub-G_0/G_1 cell cycle phase (Fig. 4.9.), indicating that the compound possesses potential to impart anti-apoptotic effects.

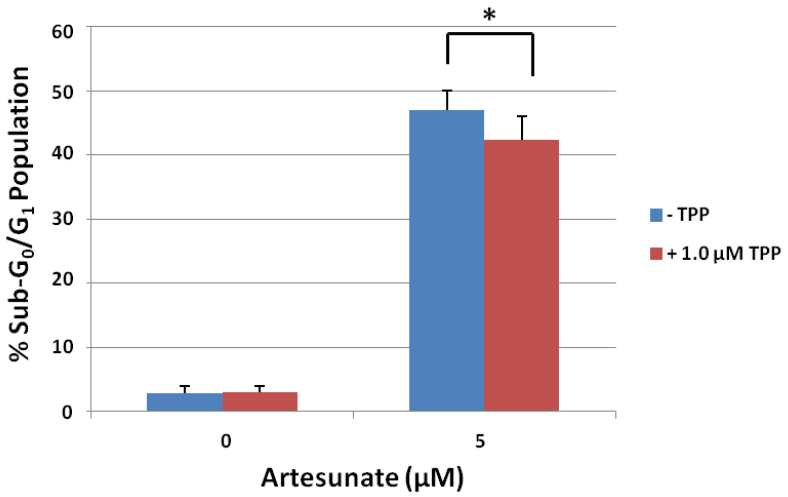

Figure 4.9. Impact of TPP-IOA upon artesunate-induced apoptosis. HL-60 cells were co-treated with 5 µM artesunate and 1 µM TPP-IOA for a period of 24 h. The proportion of cells undergoing apoptotic death was determined through quantification of sub-G_0/G_1 population using PI and flow cytometry. Results are presented as the mean of three independent experiments, ± SD. * represents $p < 0.05$, as determined through the paired t-test.

4.3.5. Modulatory Impact of TPP-IOA upon Artesunate-Induced Mitochondrial Superoxide Formation

The ability of TPP-IOA to impact upon levels of mitochondrial superoxide arising as an early feature of artesunate-induced toxicity was examined using MitoSOX. Specific detection of superoxide was facilitated through monitoring formation of the fluorescent hydroxyethidium product. Treatment of HL-60 cells with 1 µM TPP-IOA alongside 5 and 10 µM artesunate imparted general increases in the levels of drug-induced mitochondrial ROS following 16 h (Fig. 4.10. A). These effects were mirrored within HeLa line upon co-incubation for 24 h with 10 and 25 µM artesunate and 10 µM TPP-IOA (Fig. 4.10. B), but were less pronounced in the HeLa ρ^0 variety following an identical dosing plan (Fig. 4.10. C).

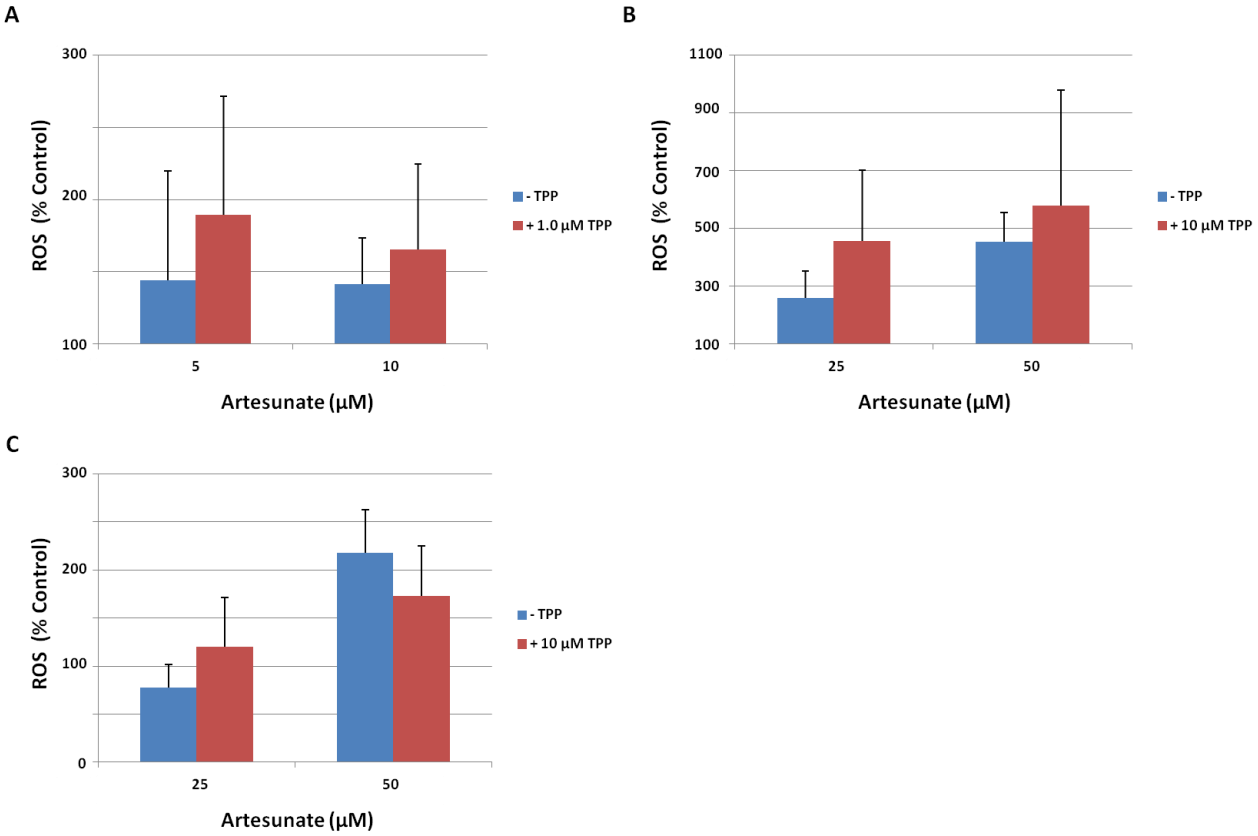

Figure 4.10. Modulatory impact of TPP-IOA upon artesunate-induced mitochondrial superoxide formation HL-60 cells **(A)** were co-treated with 5 and 10 µM artesunate and 1 µM TPP-IOA for a period of 16 h. HeLa **(B)** and HeLa ρ^0 cells **(C)** were co-incubated with 25 – 50 µM artesunate and 10 µM TPP-IOA over 24 h. ROS levels were determined through measurement of MitoSOX fluorescence. Values are expressed as percentage of ROS detected relative to vehicle control, and are presented as the mean of three independent experiments, ± SD.

4.3.6. Effects of TPP-IOA upon Artemisinin Bioactivation

The capacity of TPP-IOA to impact upon bioactivation of PFDHA was assessed using the LC-MS method detailed in Section 3.2.10., Chapter 3. HL-60 cells were incubated with 5 µM PFDHA and 1 µM TPP-IOA for a period of 24 hours prior to organic extraction (Fig. 4.11. A), whilst HeLa (Fig. 4.11. B) and HeLa ρ^0 cells (Fig. 4.11. C) were treated for 48 h with 25 µM PFDHA and 10 µM TPP-IOA. Across all cell lines, TPP-IOA was observed to have no significant impact upon the quantities of PFDHA and THF acetate recovered.

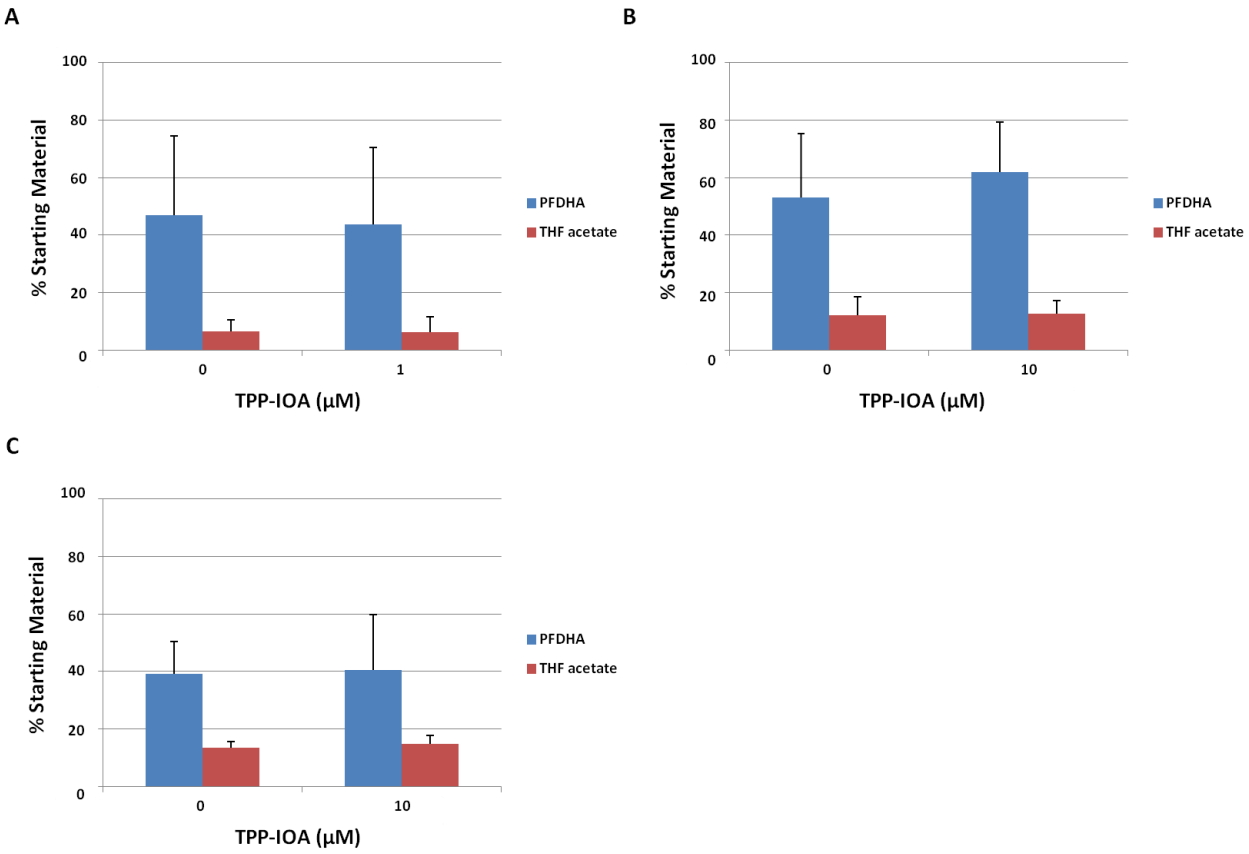

Figure 4.11. Effects of TPP-IOA upon artemisinin bioactivation. HL-60 cells **(A)** were co-treated with 5 µM PFDHA and 1 µM TPP-IOA for a period of 24 h. HeLa **(B)** and HeLa ρ^0 cells **(C)** were co-incubated with 25 µM PFDHA and 10 µM TPP-IOA over 48 h. Values are expressed in terms of the quantity of PFDHA and THF acetate recovered as a percentage of starting material, and are presented as the mean of three independent experiments, ± SD.

4.4. Discussion

The chemical synthesis of TPP-IOA proceeded broadly along the pathway outlined by Atkinson *et al*. (Atkinson *et al.*, 2011). A key variation with regards to this existing method was in the employment of castor oil as the source of methyl ricinoleate. Approximately 90% of the fatty acid content of this mixture is composed of ricinoleic acid triglyceride, ensuring that the desired methyl ester derivatives can be furnished readily with good yield and high purity upon chromatographic separation (Yang *et al.*, 2002). Although providing a further step to the synthetic pathway ahead of that reported in the literature, the use of inexpensive the castor oil circumvents the requirement for the employment of costly commercial sources of purified methyl ricinoleate and hence grants a greater cost-effectiveness to production. The overall product yield, from castor oil through five stages to TPP-IOA, was 9.6% (Fig. 4.3.).

The role of cardiolipin within the mechanism of artesunate-induced cytotoxicity was investigated through examining the impact of this inhibitor upon cell response to drug treatment. Studies into the effects of the compound were performed over three cell lines, with the HL-60 variety displaying greatest sensitivity towards its impact. A preliminary assessment of the activity of TPP-IOA alone within this line demonstrated an ability to induce cytotoxicity within the low micromolar range, with the upper concentration at which it could be used effectively limited to 1 μM (Table 4.1.). Increased resistance within the HeLa and HeLa ρ^0 varieties ensured that the employment up to a maximum concentration of 10 μM was permissible. In order to fully elucidate the route through which TPP-IOA induces the emergence of cell death, additional study shall be required. The outcomes of the examinations performed assessing impact upon artesunate-induced mitochondrial superoxide levels suggest that the inhibitor possesses a capacity to enhance oxidative stress

within the organelle (Fig. 4.10.). It is believed that the anti-peroxidase activity of TPP-IOA is derived from the strong ligand affinity of its imidazole functionality towards the haem-Fe(II) situated within cytochrome c (Atkinson *et al.*, 2011). Owing to the involvement of this unit within electron transport, it is feasible to hypothesise that disturbance to the coordination sites about the metal, arising from the presence of the additional ligand, might induce disruption to the redox processes mediated present and hence prevent passage through the electron transport chain.

Rationale for investigation into the potential for artemisinin derivatives to function as oxidants of cardiolipin has been provided through the outcomes of studies which have identified radical-initiated decomposition of the phospholipid as a key early stage in the progression of apoptosis (Fernandez *et al.*, 2002). Biomimetic examinations have allowed for the characterisation of numerous products emerging from the oxidative degradation of the common cardiolipin forms, enabling elucidation of the routes through which such transformations arise in physiological and pathological settings (Kim *et al.*, 2013; Kim *et al.*, 2011). The capacity of artemisinin to induce changes in the structures of related phospholipids has been demonstrated (Kumura *et al.*, 2009). It is thus theorised that carbon-centred radicals, formed courtesy of Fe(II)-mediated bioactivation of the artemisinin endoperoxide bridge, might initiate such peroxidation through direct abstraction at the unsaturated lipid chain.

Dose-dependent increases in levels of oxidised cardiolipin, as determined through use of a flow cytometric method reliant upon monitoring variation in NAO fluorescence, were witnessed following artesunate treatment across each of the three cell lines (Fig. 4.5.). The oxidation of cardiolipin, triggered through the induction of ROS formation, has been identified as a key stage mediating the release of cytochrome c and the progression of intrinsic apoptosis (Orrenius *et al.*, 2005). With existing evidence strongly suggesting the

ability for artemisinin-derived compounds to impart toxic effects through enhancing levels of oxidative stress and stimulating the onset of apoptotic cell death, such a finding is consistent with current understanding regarding their mechanism of action (O'Neill *et al.*, 2010b). It is interesting to note that great similarities in extent of cardiolipin oxidation were witnessed across HeLa and HeLa ρ^0 cells. Such an outcome serves to indicate that the influence held by an operational electron transport chain within the mediation of artemisinin-stimulated peroxidative effect is minimal.

The co-administration of TPP-IOA alongside artesunate in HL-60 cells induced significant reductions in levels of oxidised cardiolipin, as assayed using NAO (Fig. 4.5.). According to this metric, the addition of 0.5 μM inhibitor was sufficient to reduce drug-induced cardiolipin oxidation levels by half following 24 h incubation. Such effects were not evident within the HeLa cells, where TPP-IOA was unable to impact significantly upon phospholipid oxidation following 48 h artesunate treatment. Doubts over the suitability of NAO to function as a reliable determinant of cardiolipin oxidation status have been raised owing to concerns regarding the impact of mitochondrial membrane potential upon uptake of the compound within the organelle (Fernandez *et al.*, 2004; Rodriguez *et al.*, 2008). Hence, a collaborative venture with Huiyong Yin has sought the development of a more reliable mass spectrometric protocol for the assessment and quantification of oxidised cardiolipin levels. Previous research within this group has facilitated the LC-MS characterisation of molecular species formed through the oxidative decomposition of common cardiolipin isoforms (Liu *et al.*, 2011a; Yin *et al.*, 2012). Accordingly, monitoring the relative prevalence of these products against selected parent cardiolipin varieties has allowed for examination into the ability of artesunate and TPP-IOA to impact upon the oxidation state of the phospholipid. Co-treatment of HeLa cells with 50 μM artesunate and 10 μM TPP-IOA was performed over a period of 24 h. LC-MS quantification of cardiolipin oxidation product abundance following incubation confirmed the capacity of the drug to induce peroxidation, whilst simultaneously

illustrating the potential for the inhibitor to impart protective effect (Fig. 4.12.). Interestingly, the results accrued through use of the LC-MS method, which indicate that TPP-IOA possesses the capability to reduce levels of drug-induced cardiolipin oxidation within these cells, contrast with the outcomes obtained following the use of NAO. It would seem apparent, therefore, that NAO functions as an imperfect metric of cardiolipin oxidation within this cell type. Whilst the time-course of the LC-MS assessment, at 24 h, varied from that which was employed in the NAO studies, comparison between the two outcomes can be made. Extension of the scope of this study to include the HL-60 and ρ^0 HeLa lines would allow for the impact of TPP-IOA to be examined with much greater reliability, and would hence enable the validity of the both methods to be assessed more thoroughly.

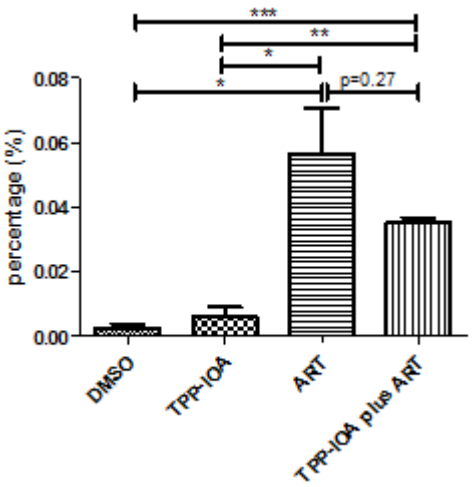

Figure 4.12. Impact of TPP-IOA upon artesunate-induced cardiolipin oxidation assayed using LC-MS. HeLa cells were co-incubated with 50 µM artesunate and 10 µM TPP-IOA for a period of 24 h. Ratio of oxidised to unoxidised cardiolipin was determined through an LC-MS method. Results are expressed as the mean of three independent experiments, ± SD.

In order to ascertain whether TPP-IOA exerted a cytoprotective effect against artesunate toxicity, the MTT assay was used in order to determine viability in co-treated cells.

Significant decreases in the levels of drug-induced cell death were apparent only within the HL-60 line, whilst no alteration in the susceptibility of both the HeLa and ρ^0 HeLa cells was evident (Fig. 4.6.). The capacity of the inhibitor to protect against the toxicity of artesunate within HL-60 cells mirrors the apparent reductions in cardiolipin oxidation levels detected through NAO. This correlation would suggest that an ability to restrain the oxidation of cardiolipin is associated with a reduced sensitivity towards the drug within this line. Examination of cell cycle population distribution using PI following artesunate treatment demonstrated a moderately decreased tendency for HL-60 cells to fall within the sub-G_0/G_1 region upon co-administration of the inhibitor (Fig. 4.9.). The mild anti-apoptotic effect would tally with the postulated relevance of cardiolipin oxidation within the progression of programmed cell death through the intrinsic pathway, whilst the continued impact of the endoperoxide upon viability indicates the inability of TPP-IOA to impart a complete suppression of peroxidation. Such observations stand in accordance with evidence derived from the early studies assessing the capacity of the inhibitor to mitigate the impact of pro-apoptotic and cytotoxic stimuli across *in vitro* and *in vivo* systems (Atkinson *et al.*, 2011). Through these investigations, it was witnessed that both radiation and rotenone-induced apoptotic cell death were diminished in mouse embryonic and lung epithelial cells upon administration of the compound, whilst the survival profiles of dosed, irradiated mice were further noted as favourable. However, concordant with the outcomes of the examinations performed within this chapter, whilst anti-apoptotic and cytoprotective effects were observed to be significant, in no system did they culminate in complete abrogation.

When viewed alongside data accrued from both the NAO and the collaborative LC-MS investigations, it becomes apparent that TPP-IOA is incapable of suppressing the drug-induced oxidation of cardiolipin in entirety. As such, the involvement of alternative pathways within the emergence of peroxidation becomes feasible. Direct, radical-mediated attack courtesy of the activated artemisinin derivative remains potentially a contributing

factor towards these effects. It is further acknowledged that, as in other phospholipids, peroxidase-independent modification of cardiolipin structure arises as a consequence of direct ROS-mediated attack occurring during instances of oxidative stress (Yin *et al.*, 2012). A chemical pathway through which such an effect might be mediated, by means of the hydroxyl radical, is outlined in Figure 4.13.

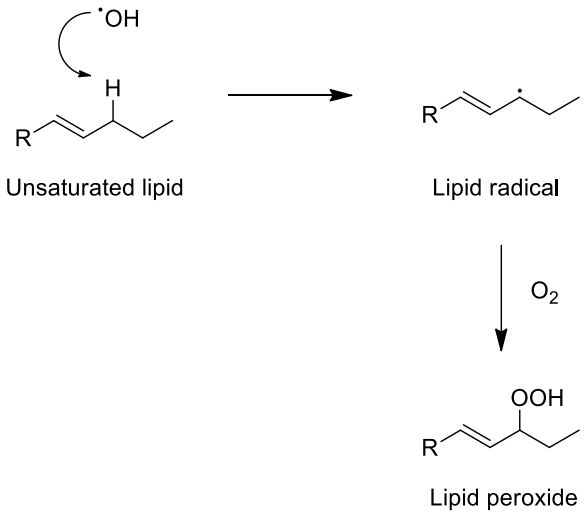

Figure 4.13. ROS-stimulated peroxidation of the unsaturated lipid chain.

Outcomes of the LC-MS assessment the capacity of the inhibitor to prevent PFDHA bioactivation indicate that any protective influence of the compound is unrelated to an ability to suspend peroxidase-mediated reduction of the endoperoxide bridge (Fig. 4.11.). It therefore appears implausible to hypothesise that the cytochrome c-cardiolipin complex functions as a significant site for drug activation.

The contrasting outcomes observed between cell models ensure that drawing definitive conclusions regarding the impact of TPP-IOA upon artesunate treatment is not possible in light of the evidence obtained. It is apparent that the inhibitor, which functions through suppressing the cytochrome c-peroxidase complex, is neither able to induce complete cessation in cardiolipin oxidation nor offer substantial cytoprotective effect. It follows that,

whilst investigation into the modulatory impact of the compound upon cell response to the drug has served to provide mechanistic insight into the activities of both, the precise mechanistic role of cardiolipin within the progression of artemisinin-induced cell death remains undetermined.

Chapter Five

Examination into the Cytotoxic Profiles of Novel Endoperoxide Compounds

5.1. Introduction

The great therapeutic efficacy of artemisinin derivatives has ensured that they have retained their role on the frontline of treatment against malaria. Whilst the value of the current set of clinically-employed compounds remains undoubted, the development of novel endoperoxide agents has continued to constitute an ongoing focus for research. In this chapter, a series of studies into the cytotoxic profiles of novel compounds from a host of recently developed synthetic and semi-synthetic endoperoxide classes is presented. Their number shall include both recently-developed antimalarial candidates and also experimental, anti-cancer drugs.

The search for new endoperoxide antimalarial agents is spurred on by concerns regarding the activity profiles and sustainability of the semi-synthetic, artemisinin-derived compounds currently in use (Ridley, 2002). Clinically, both their poor bioavailability and their short half-life form unfavourable aspects of their pharmacokinetic profiles. Whilst instance of toxicity in man is generally held to be absent under dosing protocols routinely employed, evidence accrued from *in vivo* and *in vitro* studies has been sufficient to cast doubts regarding their universal safety (Efferth *et al.*, 2010). An ability to induce the onset of embryotoxicity and neurotoxicity has been demonstrated consistently across animal models, influencing the WHO to recommend their contraindication in mothers during the opening trimester of pregnancy (WHO, 2006).

Alongside the issues surrounding safety, a growing body of evidence exists to suggest the emergence of artemisinin resistance amongst a subset of parasite strains within South-east Asia (O'Brien *et al.*, 2011). Although reduced susceptibility to drug effects has largely remained localised to regions surrounding the Thai-Cambodian border, a recent spread to neighbouring areas has been noted (Dondorp *et al.*, 2009; Noedl *et al.*, 2008). Whilst impact

upon the antimalarial efficacy of current combination therapy regimens has thus far remained minimal, it is conceivable that further extension might, with time, develop influence upon treatment outcomes. Additional concerns regarding drug affordability are derived from the costs associated with production of artemisinin (White, 2008). Extraction of the natural product from the leaves of *Artemisia annua* has remained the most economically viable route towards isolation, ensuring that supply has been dependent upon the commercial availability of the plant source. As a consequence of this, the typical market price for artemisinin derivatives has put them out of range in some of the world's poorest, neediest regions, necessitating the employment of older, less effective drug classes (Yeung *et al.*, 2008).

The shortfalls associated with the present stock of artemisinin-based compounds have stimulated interest in the development of wholly synthetic endoperoxide analogues. Research has demonstrated that antimalarial efficacy of the endoperoxide unit can be maintained, and even improved, outside of the artemisinin molecular framework (Opsenica *et al.*, 2009). A great number of peroxidic molecules, featuring a diverse array of structures, have been synthesised and examined for their activities, both *in vitro* and *in vivo*, over the preceding three decades (Jefford, 2007). Amongst these novel classes, compounds incorporating 1,2,4-trioxolane and 1,2,4,5-tetraoxane pharmacophores have displayed greatest promise regarding potential progression towards clinical use (Kumar *et al.*, 2011). Examination into structure activity relationship has determined that optimal antimalarial performance is ensured through the protection of the peroxide with adamantyl and cyclohexyl groups. Alongside OZ277, introduced in Section 1.7., Chapter 1, compounds such as OZ439 **(13)**, along with its tetraoxane isoform **(14)**, have displayed antiparasitic activities greater than those of the artemisinin derivatives in pre-clinical testing (Charman *et al.*, 2011).

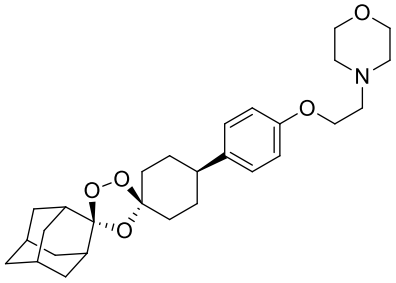

(13)

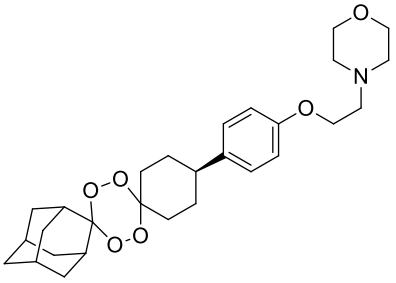

(14)

Whilst the cytotoxicity of endoperoxides within mammalian systems is an undesired feature of their activity profile during the course of antimalarial treatment, their enhanced sensitivity towards rapidly proliferating cancer cell lines *in vitro* has encouraged investigation into their potential for use as anticancer agents. A range of promising outcomes have been observed across a breadth of studies, with artemisinin derivatives including DHA and artesunate found to exert pro-apoptogenic and anti-proliferative effects against breast, prostate, lung, colon, and pancreatic cancer cells (Firestone *et al.*, 2009). Aside from direct action against cell viability, the impediment of cell metastasis through mechanisms dependent upon the suppression of matrix metalloproteinase (MMP) has been demonstrated across several lines (Weifeng *et al.*, 2011). It is theorised additionally that the ability of the drugs to initiate the downregulation of VEGF expression might lend them anti-angiogenic properties (Wartenberg *et al.*, 2003). Whilst evidence derived directly from clinical use remains limited, isolated studies attest to the therapeutic benefits of artesunate and artemether against a number of tumour types (Krishna *et al.*, 2008).

Research has thus sought the development of novel artemisinin derivatives providing enhanced potency and specificity towards rapidly proliferating cancer cells. Several strategies have been adopted in the design of these compounds, ranging from the creation of dimeric and trimeric artemisinin species to the construction of drug hybrids (Chaturvedi *et al.*, 2010; Xie *et al.*, 2011). Amongst these experimental classes, a number of which have been developed with the intention of offering improved activity against both the parasite

and against cancerous cells, there have been synthesised a variety of conjugates comprising DHA and an alternative active group. Within these categories have arisen combinations alongside thiazole, oxadiazole, caboxamide, spermidine and acridine moieties – the latter formed with the intention of enhancing toxicity through the provision of localisation towards DNA (Jones *et al.*, 2009; Kumar *et al.*, 2011). Many such derivatives have exhibited *in vitro* activities greater than that of DHA, and have hence been identified as promising potential leads for further trial. A further series of compounds, combining DHA with polypyrrole intercalators resembling those found upon antibiotics such a netropsin, have been designed rationally ahead of pre-clinical testing.

An examination into the *in vitro* activity of several newly-developed endoperoxide classes is reported in this chapter. Studies shall be focused upon assessing the toxicity of novel synthetic antimalarial compounds and semi-synthetic hybrid artemisinin derivatives against cancer cell lines. The group of Paul O'Neill has developed 1,2,4-trioxolane and 1,2,4,5-tetraoxane compounds which display great potency against parasite cultures (Ellis *et al.*, 2008; O'Neill *et al.*, 2010a). Trioxolane FBEG-100 **(15)** and 1,2,4,5-tetraoxane RKA-182 **(16)** are a pair of synthetic antimalarial candidates which differ structurally only in their pharmacophores. Assessment of their cytotoxic properties in cancer cells, including investigation into their impact upon mitochondrial function, shall allow not only for an evaluation of their potential safety within mammalian systems, but also for direct comparison of the impact of any variations in activity arising from differences between the three-oxygen and four-oxygen peroxidic groups. The time-dependence of the activity of the novel tetraoxane E-209 **(17)** shall also be examined across several cell lines, so that a more complete image of its activity profile across a greater array of systems might be obtained.

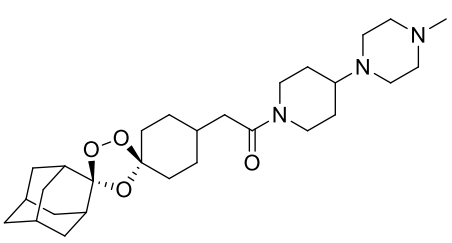

(15)

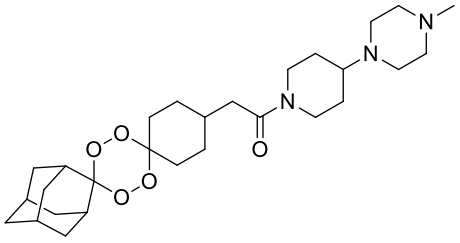

(16)

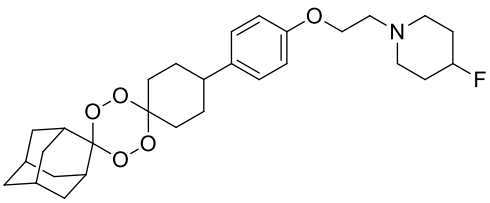

(17)

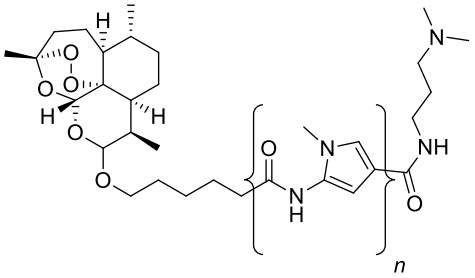

(18): *n* = 2
(19): *n* = 3

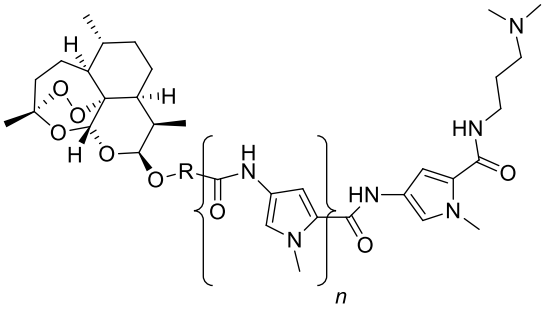

(20): R = *m*-Ph, *n* = 2
(21): R = *p*-Bn, *n* = 1
(22): R = *p*-Bn, *n* = 2

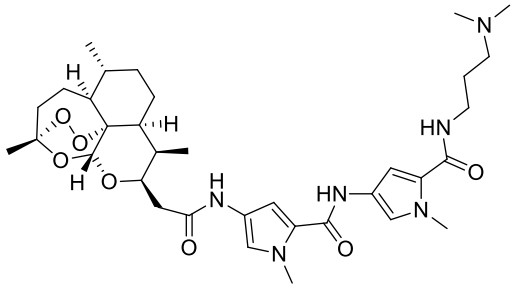

(23)

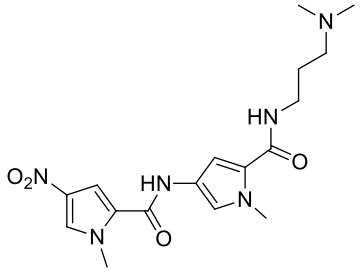

(24)

Alongside these studies, the toxic profile of a series of anticancer artemisinin-polypyrrole hybrids is investigated. As alluded to earlier, it is intended that the conjugation of the DNA intercalator shall allow for the localisation of the compounds within the nucleus, where their proximity to DNA might enhance cell killing ability. Amongst the candidates examined shall be the related pair dipyrrole LLP-271 **(18)** and tripyrrole LLP-272 **(19)**, the aryl-linked

NET-4, NET-5 and NET-6 (**20-22**) and non-ether linked NET-7 **(23)**. Demonstration of enhanced cytotoxic activity within these compounds relative to established artemisinin derivatives shall provide indication of their potential suitability for progression into further trial. Both the conjugates and the synthetic antimalarials will be compared against DHA for their performance.

5.2. Materials and Methods

5.2.1. Materials

TMRE was purchased from Sigma-Aldrich (Poole, Dorset, UK). All compounds tested were synthesised by the group of Prof. Paul O'Neill (University of Liverpool, Liverpool, UK).

5.2.2. Cell Culture and Experimental Preparation

HeLa and Hep G2 cells were cultured and maintained according to protocols outlined in Section 2.2.2., Chapter 2. HL-60 cells were handled as in Section 4.2.2., Chapter 4.

5.2.3. Analysis through Flow Cytometry

Flow cytometric analysis was performed according to the parameters described in Section 3.2.4., Chapter 3.

5.2.4. Measurement of Mitochondrial Depolarisation using TMRE

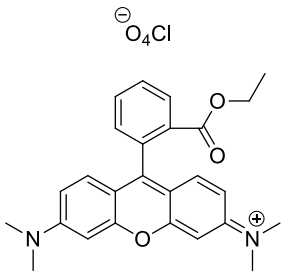

TMRE

Tetramethylrhodamine ethyl ester (TMRE) is a fluorescent compound which is taken up into the mitochondrion to an extent proportional with the magnitude of the membrane

potential (Scaduto *et al.*, 1999). Drug-treated HL-60 cells (2.5 x 10^5) were centrifuged (1000*g*) and washed with HBSS, before the cell pellet was resuspended in TMRE solution (50 nM in HBSS). Samples were incubated for 10 minutes at 37°C, prior to analysis (minimum 1 x 10^4 cells) through flow cytometry. Fluorescence was monitored following excitation at 488 nm. Parameters were assessed in non-quenching mode.

5.2.5. Determination of Apoptotic Cell Population using Propidium Iodide

The ability of drugs to exert influence upon the proportion of HL-60 cells falling within the sub-G_0/G_1 cycle phase was assessed using PI, following the protocol described in Section 4.2.5., Chapter 4.

5.2.6. Assessment of Cell Viability using the MTT Assay

Cell viability within the HeLa and Hep G2 lines was ascertained through use of the MTT assay, as detailed in Section 2.2.4., Chapter 2. For HL-60 cells, the slightly modified protocol of Section 4.2.6., Chapter 4 was employed.

5.2.7. Statistical Analysis

Data is presented and analysed in line with the protocols described in Section 2.2.10., Chapter 2.

5.3. Results

5.3.1. Cytotoxic Activities of Novel Endoperoxide Compounds against Cancer Cells

5.3.1.2. 1,2,4-Trioxolane and 1,2,4,5-Tetraoxane Antimalarials

5.3.1.2.1. FBEG-100 and RKA-182

The cytotoxicity of the 1,2,4-trioxolane FBEG-100 and the 1,2,4,5-tetraoxane RKA-182 was assessed in HL-60 cells using the MTT assay. IC_{50} values, obtained following 24 h incubation, are listed in Table 5.1. Both compounds displayed activities within the low micromolar range, indicating reduced toxicity relative to the artemisinin derivative DHA. It is apparent that cell sensitivity towards the tetraoxane is greater than that towards the trioxolane.

Compound	IC_{50} (μM)
DHA	0.39 ± 0.11
FBEG-100	23.6 ± 1.57
RKA-182	5.07 ± 0.72

Table 5.1. IC_{50} values of HL-60 cells dosed with FBEG-100 and RKA-182. Cytotoxicity was measured using the MTT assay. Results are shown as the mean of three independent experiments, ± SD.

5.3.1.2.2. E-209

An assessment of the time-dependence of response towards tetraoxane E-209 was performed in HL-60 cells. Using the MTT assay, IC_{50} values were determined over time-

courses ranging from 6 to 72 h (Table 5.2.). A rapid onset of cytotoxicity was observed, with low micromolar activity evident after only 6 h treatment.

T (h)	IC_{50} (µM)
6	13.7 ± 1.67
16	4.63 ± 1.44
24	2.85 ± 0.988
48	1.59 ± 0.324
72	1.28 ± 0.382

Table 5.2. IC_{50} values of HL-60 cells dosed with E-209. Cytotoxicity was measured using the MTT assay. Results are shown as the mean of three independent experiments, ± SD.

5.3.1.3. Artemisinin-Polypyrrole Anticancer Conjugates

5.3.1.3.1. LLP 271 and LLP-272

The activity of the artemisinin-dipyrrole conjugates LLP-271 and LLP-272 was examined in HL-60 cells. Following 24 h incubation, the MTT assay was employed in order to determine IC_{50} values for both the compounds and for an unconjugated control dipyrrole moiety (Table 5.3.). Although LLP-271 displayed the greater potency of the two, neither possessed activity greater than that of DHA. The observed inertness of the dipyrrole unit **(24)** demonstrates that it exerts no cytotoxic effects in isolation.

Compound	IC_{50} (µM)
LLP-271	2.16 ± 0.52
LLP-272	15.5 ± 1.32
Dipyrrole	> 100

Table 5.3. IC_{50} values of HL-60 cells dosed with LLP-271, LLP-272 and dipyrrole. Cytotoxicity was measured using the MTT assay. Results are shown as the mean of three independent experiments, ± SD.

5.3.1.3.2. NET-4, NET-5, NET-6 and NET-7

A further selection of polypyrrole compounds were examined for their cytotoxic properties in HL-60 cells. Again, IC_{50} values were obtained following 24 h incubation using the MTT assay (Table 5.4). Activity was observed within the low micromolar range, but no compound exhibited cell killing ability greater than that possessed by DHA.

Compound	IC_{50} (μM)
NET-4	6.35 ± 2.93
NET-5	1.42 ± 0.66
NET-6	4.60 ± 1.40
NET-7	11.7 ± 4.38

Table 5.4. IC_{50} values of HL-60 cells dosed with NET-4, NET-5, NET-6 and NET-7. Cytotoxicity was measured using the MTT assay. Results are shown as the mean of three independent experiments, ± SD.

5.3.2. Mechanistic Aspects of Novel Endoperoxide Activity in Cancer Cells

Having examined the cytotoxic potentials of the novel antimalarial and anticancer candidates, further investigations centred upon determining the mechanistic routes through which impact towards the viability of cells might potentially be mediated were performed with selected compounds.

5.3.2.1. FBEG-100 and RKA-182

5.3.2.1.1. Effects upon Mitochondrial Membrane Potential

The impact of drug treatment upon mitochondrial membrane potential was determined through use of TMRE. TMRE is a fluorescent rhodamine derivative, which owing to its

lipophilic cationic properties, accumulates readily within the mitochondrion (Scaduto *et al.*, 1999). The extent to which it is taken up into the organelle is determined by the magnitude of the membrane potential, with increased presence within the matrix correlating with greater fluorescence. It is the relationship between mitochondrial membrane potential, mitochondrial uptake and compound fluorescence which allows for assessment of membrane depolarisation. A fall in fluorescence, as measured following 488 nm excitation, is associated with diminished potential within non-quenching mode. Representative traces displayed in Figure 5.1. outline the variation between high-potential, untreated control cells (Fig. 5.1. A), and low-potential cells dosed for 24 h with 100 µM DHA (Fig. 5.1. B). The shift in distribution from upper to lower quadrants is readily apparent.

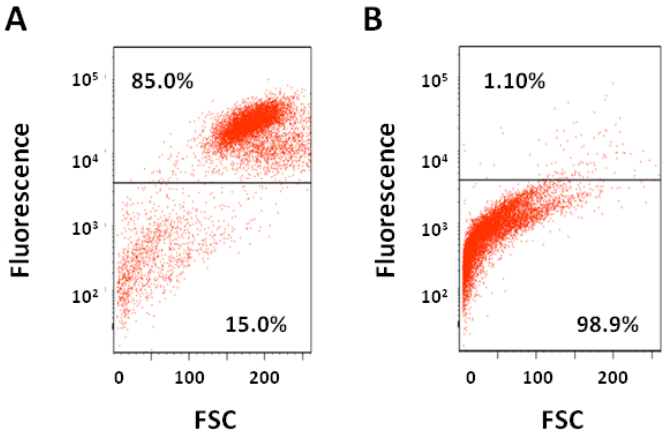

Figure 5.1. Representative dotplots outlining variation in TMRE fluorescence between control and drug-treated HL-60 cells. TMRE fluorescence in control **(A)** and 100 µM DHA-treated HL-60 cells **(B)** following 24 h incubation.

HL-60 cells were treated for 24 h with 0 – 100 µM DHA, 0 – 30 µM FBEG-100 and 0 – 10 µM RKA-182. Mitochondrial membrane potential was subsequently measured using TMRE. A significant, dose-dependent increase in the proportion of depolarised cells was witnessed with each compound, with DHA exerting greater impact than either synthetic variety (Fig. 5.2.).

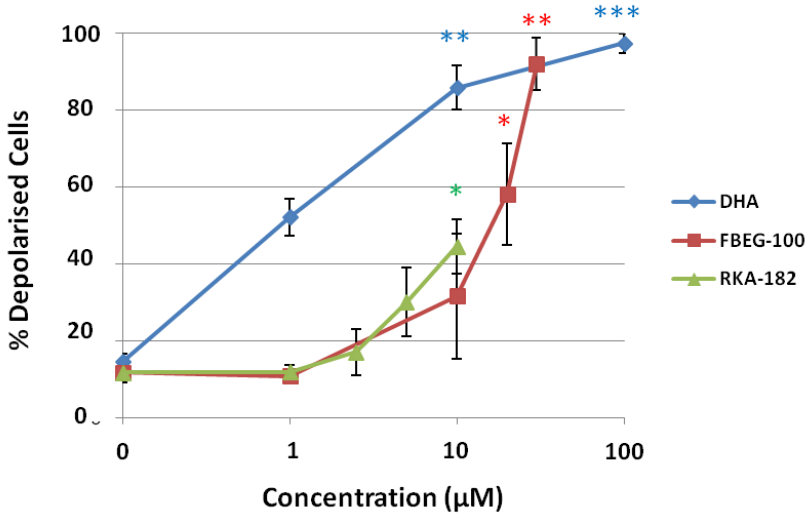

Figure 5.2. Effects of trioxolane and tetraoxane antimalarials upon mitochondrial membrane potential. HL-60 cells were treated with 0 – 100 µM DHA 0 – 30 µM FBEG-100 and 0 – 10 µM RKA-182 for a period of 24 h. Mitochondrial membrane potential was determined through flow cytometry using the TMRE dye. Results are shown as the mean of three independent experiments, ± SD. * represents $p < 0.05$, ** $p < 0.01$ and *** $p < 0.001$ as determined through paired t-test.

5.3.2.1.2. Ability to Induce Cell Death through Apoptosis

The presence of apoptotic cells was detected using propidium iodide staining through the method described in Section 4.2.5., Chapter 4. HL-60 cells were treated with 0 – 100 µM DHA, 0 – 30 µM FBEG-100 and 0 – 10 µM RKA-182 for a period of 24 h, prior to flow cytometric analysis. Dose-dependent increases in the proportion of cells falling in the sub-G_0/G_1 cycle region were apparent with each drug, with neither synthetic class displaying potency greater than DHA (Fig. 5.3.).

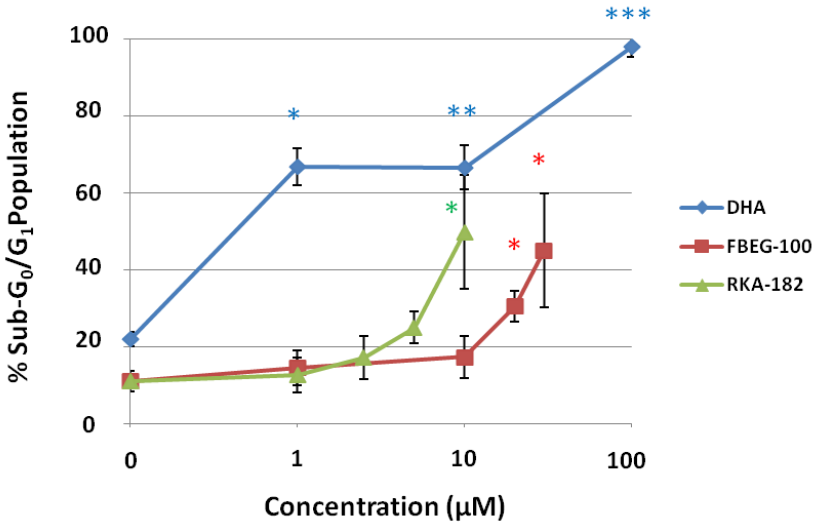

Figure 5.3. Ability of trioxolane and tetraoxane antimalarials to induce cell death through apoptosis. HL-60 cells were treated with 0-100 µM DHA 0 – 30 µM FBEG-100 and 0 – 10 µM RKA-182 for 24 h. The proportion of cells undergoing apoptotic death was determined through quantification of sub-G_0/G_1 population using PI and flow cytometry. Results are shown as the mean of three independent experiments, ± SD. * represents $p < 0.05$, ** $p < 0.01$ and *** $p < 0.001$ as determined through paired t-test.

5.3.2.2. E-209

5.3.2.2.1. Further Impact upon the Viability of Cancer Cells

Investigation into the cytotoxic impact of 1,2,4,5-tetraoxane E-209 was expanded to include assessment of its activity against cells belonging to both the HeLa and Hep G2 lines. Using the MTT assay, IC_{50} values were determined over time-courses ranging from 6 – 72 h in the former and 24 – 72 in the latter (Table 5.5.). Whilst Hep G2 cells were shown to exhibit greater sensitivity towards the effects of the drug relative to those of the HeLa variety, neither line displayed responsiveness comparable to that observed within the HL-60 type (recorded in Table 5.2).

T (h)	IC_{50} (μM)	
	HeLa	Hep G2
6	445 ± 85.4	Not determined
16	83.3 ± 7.60	Not determined
24	57.3 ± 20.7	13.4 ± 1.70
48	45.6 ± 8.90	10.5 ± 3.34
72	38.2 ± 16.5	8.20 ± 3.72

Table 5.5. IC_{50} values of Hep G2 and HeLa cells dosed with E-209. Cytotoxicity was measured using the MTT assay. Results are shown as the mean of three independent experiments, ± SD.

5.3.2.3. LLP 271 and LLP-272

5.3.2.3.1. Effects upon Mitochondrial Membrane Potential

HL-60 cells were treated with DHA, LLP-271, LLP-272 and dipyrrole in concentrations ranging from 0 – 100 μM for a period of 24 h, before mitochondrial membrane potential was determined through flow cytometry using TMRE. Significant, dose-dependent increases in the proportion of depolarised cells were witnessed with each of the artemisinin-dipyrrole conjugates, although with neither exhibiting potency comparable to DHA at lower concentrations (Fig. 5.4.). Unconjugated dipyrrole displayed no activity.

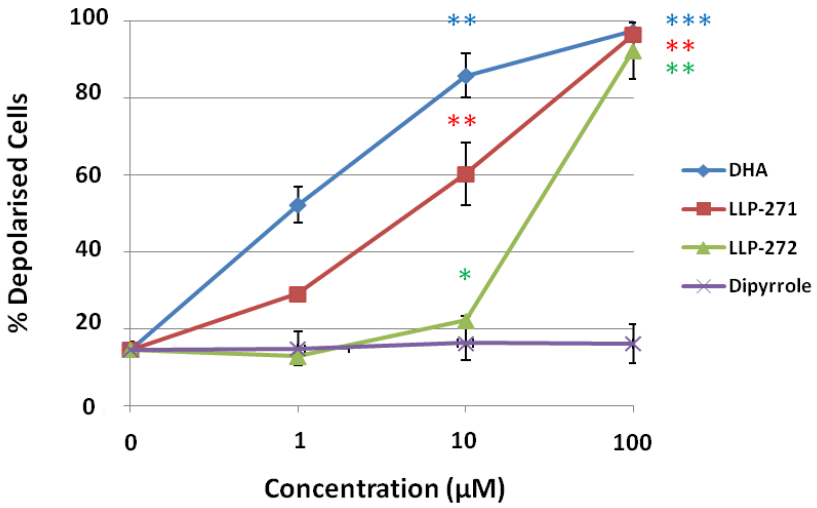

Figure 5.4. Effects of artemisinin-dipyrrole conjugates upon mitochondrial membrane potential. HL-60 cells were treated with 0 – 100 µM DHA, LLP-271, LLP-272 or dipyrrole for 24 h. Mitochondrial membrane potential was determined through flow cytometry using the TMRE dye. Results are shown as the mean of three independent experiments, ± SD. * represents $p < 0.05$, ** $p < 0.01$ and *** $p < 0.001$ as determined through paired t-test.

5.3.2.3.2. Ability to Induce Cell Death through Apoptosis

HL-60 cells were treated for 24 h with DHA, LLP-271, LLP-272 and dipyrrole in concentrations ranging from 0 – 100 µM. Apoptotic cell population was determined through PI staining. Significant, dose-dependent increases in the number sub-G_0/G_1 cells were witnessed through each compound, with DHA providing the greatest effect and the unconjugated dipyrrole appearing inactive (Fig. 5.5.).

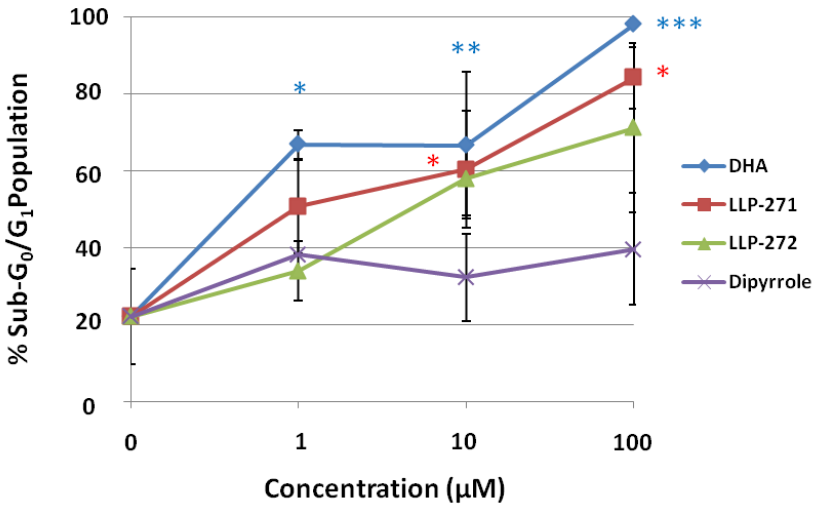

Figure 5.5. Ability of artemisinin-dipyrrole conjugates to induce cell death through apoptosis. HL-60 cells were treated with 0 – 100 µM DHA, LLP-271, LLP-272 or dipyrrole for a period of 24 h. The proportion of cells undergoing apoptotic death was determined through quantification of sub-G_0/G_1 population using PI and flow cytometry. Results are shown as the mean of three independent experiments, ± SD. * represents $p < 0.05$, ** $p < 0.01$ and *** $p < 0.001$ as determined through paired t-test.

5.4. Discussion

The cytotoxic activities of novel endoperoxide derivatives belonging to several experimental drug classes were investigated within cancer cell lines. Broadly, the intentions of these assessments have been to determine the suitability of drug candidates for further development towards clinical use. 1,2,4-trioxolane and 1,2,4,5-tetraoxane antimalarial compounds were examined so that their toxicity in mammalian systems might be inferred ahead of their employment as therapy against parasitic infection. Similarly, study into the direct impact of the anticancer polypyrrole compounds upon cancer cell viability aimed to deduce the early feasibility for their potential use as disease treatment within a clinical setting. The model cell line employed across these investigations, the HL-60, has been chosen for its heightened sensitivity towards the effects of artemisinin derivatives and related endoperoxide compounds.

Studies assessing the cytotoxic profiles of 1,2,4-trioxolane FBEG-100 and 1,2,4,5-tetraoxane RKA-182 have demonstrated that, whilst such synthetic agents display reduced levels of toxicity in HL-60 cells relative to that of the artemisinin derivative DHA, characteristic features of the mechanism through which death is imparted remain conserved across class. Dose-dependent collapse of the mitochondrial membrane, inferred through flow cytometric monitoring of TMRE fluorescence, is witnessed universally. This is accompanied by increases in the proportion of cells appearing in the sub-G_0/G_1 region of the cell cycle. Accordingly, it can be theorised that the route towards toxicity in the novel varieties proceeds, as it does in artemisinin derivatives, through induction of mitochondrial dysfunction and the emergence of apoptotic cell death.

Further assessment of the activity of these compounds has provided additional mechanistic insight into the means by which such events might arise (Copple *et al.*, 2012). These studies constituted an overall extension of the work reported within this chapter. In common with

the artemisinin-derived artesunate, it was revealed that toxicity proceeds through the induction of oxidative stress and the stimulation of caspase activation mediated courtesy of a mechanism reliant upon haem and cellular iron. In spite of these shared characteristics, it is apparent that there are variations in the manner by which the artemisinin-based and novel drug classes interact with cells. Onset of cytotoxicity is observed to occur rapidly in the synthetic compounds, with substantial impact upon the viability of cells evident within 2 h of treatment. This contrasts greatly to the more delayed response to artesunate administration, by which significant levels of cell death are not noted until after approximately 12 h incubation. LC-MS studies have suggested key differences in the chemistry underpinning activity between classes, with the absence of observed structural degradation in the novel compounds, even following incubation periods at which cytotoxic effects are pronounced, contrasting with the well-characterised time-dependent and dose-dependent fragmentation of PFDHA reported in other sources. Owing to the necessity of the endoperoxide bridge for pharmacological and toxicological functions, it has been suggested that bioactivation in these agents must proceed along an alternative route.

It is noted that, whilst cytotoxicity is dependent upon the presence of haem and cellular iron, sensitivity of FBEG-100 and RKA-182 to the effects of iron and haem content modulation differ relative to that of artesunate. Whilst imparting cytoprotective effects across all classes, haem synthesis inhibitors and free iron chelators were shown to exert a more pronounced effect in diminishing the toxicity of the artemisinin derivative. Alternatively, it was observed that iron loading through holotransferrin instead served to preferentially enhance the impact of the novel compounds. Findings such as this suggest that a differential in sensitivity towards iron concentration exists between the synthetic and semi-synthetic varieties, with the former possessing greater toxicity when levels are elevated to supra-physiological, and the latter being more active when content is closer to basal quantities. It is hypothesised that this relationship might offer explanation for the

greater toxicity of artesunate and DHA across cell lines studied, whilst simultaneously enabling rationalisation for the increased antiparasitic effects reported in FBEG-100 and RKA-182.

Owing to their otherwise identical structures, explanation for the variation between the cytotoxic profiles of the 1,2,4,5-tetraoxane RKA-182 and the 1,2,4-trioxolane FBEG-100 must be sought through reference to the properties of their respective pharmacophores. RKA-182 is witnessed to exhibit four-fold greater activity relative to its trioxolane counterpart within HL-60 cells (Table 5.1.), whilst simultaneously demonstrating greater mitochondrial liability (Fig. 5.2.) and enhanced stimulation of apoptotic death (Fig. 5.3.). It has been demonstrated previously, through studies assessing the activities of related compounds from both classes, that the presence of the four-oxygen 1,2,4,5-tetraoxane functional group imparts greater stability to the molecule compared to that which arises from incorporation of the three-oxygen 1,2,4-trioxolane equivalent (Ellis *et al.*, 2008). As a consequence, it is noted that degradation of such compounds occurs at a greatly reduced rate, with lengthened half-lives and increased antimalarial potency following concurrently (Opsenica *et al.*, 2009). It is feasible that the greater toxicity of RKA-182 relative to FBEG-100 might arise as a consequence its comparative resistance to decomposition. Accordingly, it has been demonstrated that the rate of recovery for the tetraoxane following 24 h incubation in cell-free media is greater than that of the trioxolane analogue (Copple *et al.*, 2012). In spite of the initial promise attributed to RKA-182 as a consequence of its performance *in vitro*, further progression towards clinical use was halted owing to the discovery of its potential to induce the acute onset of neurotoxicity upon administration in dogs.

In light of the unfavourable activity of RKA-182 *in vivo*, the development of novel 1,2,4,5-tetraoxane derivatives has proceeded. Attempts to improve metabolic stability have led to

the testing of a new generation of compounds which dispense with the requirement for incorporation of the potentially labile amide side linkage (Marti *et al.*, 2011). One such candidate, E-209 was tested for its toxicity across HL-60, Hep G2 and HeLa cells (Table 5.2. and 5.5). As anticipated owing to the enhanced general sensitivity of the cells towards endoperoxide activity, the effects of the drug were most pronounced within the HL-60 line. It is generally believed that this greater susceptibility derives from the presence of elevated intracellular iron content (Mercer *et al.*, 2011). The low micromolar activity of the drug observed within this system is comparable to that witnessed in RKA-182 and DHA. Similarly, a rapid onset of cell death in common with that witnessed upon treatment with FBEG-100 and RKA-182 is shown to occur, suggesting that such activity is a feature shared across these synthetic classes (Copple *et al.*, 2012). Interestingly, the cytotoxicity within Hep G2 cells was witnessed to be more pronounced than that noted within the HeLa variety. This trend stands in contrast to the pattern observed across the studies reported in Section 2.3.1., Chapter 2, where treatment with artesunate had greater impact upon the viability of the HeLa line. Whereas previous studies have identified correlations between the sensitivity of cancer cells towards artemisinin derivatives and their expression of genes involved in the regulation of areas such as cell cycle progression, antioxidant response, iron uptake and the performance of apoptosis, the scope of these assessments has included neither the novel synthetic compounds nor the lines in question. It is feasible, however, that relative susceptibility is dictated likewise through the unique pattern of gene expression characteristic to each cell type. The disparity in response between classes could arise as a product of suggested mechanistic variation between their modes of activity.

The potential for clinical utility in E-209, and indeed all other novel endoperoxides compounds, cannot be reliably ascertained until both their antiparasitic activity and toxicity have been assessed further across more representative systems *in vivo*. As has been witnessed in the instance of RKA-182, reduced apparent toxicity relative to the artemisinin

derivatives *in vitro* does not necessarily translate to an improved safety profile within more complex settings. Nevertheless, the promise of these classes remains owing to their strong antiparasitic properties, and to the relative ease with which novel agents can be developed and functionalised.

It was determined that conjugation of polypyrrole units to the DHA moiety did not have the effect of increasing cytotoxicity to levels exceeding that of the parent compound within HL-60 cells. Dipyrrole LLP-271 and tripyrrole LLP-272 exhibited cell killing ability which was reduced five-fold and forty-fold respectively relative to the artemisinin derivative (Table 5.3.). Cytotoxic effects were mediated through the common artemisinin mechanism of mitochondrial dysfunction (Fig. 5.4.) preceding apoptosis (Fig. 5.5.), and not, as the inactivity of **(24)** attests, through the specific actions of the polypyrrole unit. Investigation of the activities of the dipyrrole hybrids NET-5 and NET-7, and of the tripyrrole compounds NET-4 and NET-6, outlined that the attachment of the groups produced a similar diminution in the ability to induce toxic effects (Table 5.4.).

Assessment of the properties of the NET series of conjugates formed one aspect of a larger study which aimed to ascertain the cytotoxic potential and mechanistic profiles of a broader range of related compounds (La Pensee *et al.*, 2013). Rationale for the incorporation of the polypyrrole units was derived from the ability of these structures, as a consequence of their affinity for DNA conjugation, to impart the localisation of pyrrole-amidine antibiotic agents, such as netropsin and distamycin, towards the nucleus. It is theorised that the presence of such groups would enhance the targeting of the artemisinin moiety towards DNA, hence aiding in the induction of fragmentation and the subsequent emergence of cell death. It was in fact revealed that the majority of the other compounds examined, in common with those assessed as part of the work presented within this chapter, exhibited reduced cytotoxicity relative to unmodified DHA. A single dipyrrole

compound, NET-2 **(25)**, was found to exhibit preferable activity across both the HL-60 and intestinal HT-29 cell lines in which such effects were studied. The variability in the response imparted by the presence of the intercalators has been rationalised in terms of their structures, with the interplay between apparent binding affinity and the relevance of steric effects believed to be determinant of their ultimate impact upon the fate of cells. It is hypothesised that steric hindrance of the endoperoxide bridge, arising from occlusion of the group courtesy of the bulky polypyrrole chain, might inhibit drug bioactivation and hence reduce efficacy. It has thus been posited that the improved activity of NET-2 owes itself both to the apparent flexibility of the intercalator unit present, and to its proposed affinity towards the binding of DNA as inferred through molecular modelling studies.

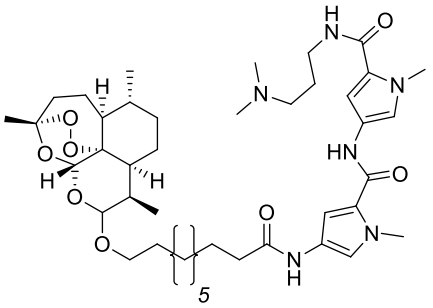

(25)

Further *in vivo* and clinical study would be required before the suitability of these compounds as anticancer agents could be adequately determined. Evidence for the anti-tumour efficacy of traditional artemisinin derivatives in a clinical setting has been obtained in a small number of studies (Ho *et al.*, 2014). Owing to the as yet limited scope of these assessments, it remains unclear precisely how performance against cell lines *in vitro* translates into a direct therapeutic utility. Artemisinin dimers have been shown to demonstrate improved activity relative to DHA in the reduction of breast tumour size in rats, in a manner which correlates with their cytotoxicity *in vitro* (Singh et al., 2011). Again,

studies would have to be extended to include a more diverse array of drugs and systems before the universality of such a relationship could be established.

Chapter Six

Final Discussion

The capacity for endoperoxide antimalarial compounds to impart cytotoxic effects within mammalian systems is attested across an extensive body of literature. Studies have demonstrated that drugs belonging to both the semi-synthetic artemisinin-derived and rationally-designed synthetic drug classes possess an ability to stimulate the emergence of developmental and neurological toxicity across within animal models, whilst further initiating death in sensitive, proliferating cell lines (Crespo-Ortiz *et al.*, 2012; Mercer *et al.*, 2010; O'Neill *et al.*, 2010b). Although the evidence for the direct clinical relevance of these outcomes remains inconclusive, their persistence has prompted the WHO to recommend the contraindication of all routinely employed artemisinin-based therapies for use in mothers during the opening trimester of pregnancy (WHO, 2006).

Prior mechanistic examinations into the routes through which these compounds induce cell death have elucidated aspects related both to the deficiencies in physiological functioning arising as a consequence of their administration, and to the chemical characteristics which underpin the emergence of such events (Lai *et al.*, 2013; Mercer *et al.*, 2011; O'Neill *et al.*, 2004). It is thus generally theorised that the activity of the drugs is derived from the Fe(II)-dependent reduction of the endoperoxide bridge moiety, culminating in the formation of reactive carbon-centred radical species which proceed to impart structural modifications upon cellular proteins (Denisov *et al.*, 2010; Mercer *et al.*, 2007). Whilst the identity of relevant sites which may potentially function as targets for these products remain unknown, it has been demonstrated across studies performed in immortalised cancer lines that the generation of ROS and the initiation of mitochondrial dysfunction occur both as early phases in a cell death pathway which terminates with the stimulation of intrinsic apoptosis (Efferth *et al.*, 2007; Mercer *et al.*, 2011). Haem-iron has been associated with possessing an important role in the progression of this sequence, thus implicating proteins containing such units in functioning both as points of drug bioactivation and as targets for activity.

Whilst it is strongly implied that oxidative stress and mitochondrial dysfunction act as key stages in the route through which the endoperoxide compounds convey their cytotoxic impact, comparatively little has been determined regarding the mechanisms through which these occurrences arise following drug treatment, and of the relevance which they ultimately possess towards the progression of cell death. It has thus been the intention of the studies performed within this thesis to examine in greater detail the influence imparted by artemisinin derivatives upon the functioning of the mitochondrion, giving focus both to the characteristics of the deficits induced, and to the factors responsible for mediating their emergence. Accordingly, investigation into drug impact upon cellular bioenergetics has been supplemented by assessment into the importance of oxidative stress in affecting the progression of cytotoxicity. Accompanying examinations have focused upon assessing the potential capacity of the compounds to behave as direct phospholipid oxidants, and furthermore upon the activity profiles of novel, experimental derivatives.

Primary examination into the capacity of the compounds to exert mitochondrial liability was performed utilising a method adapted from that developed by Marroquin *et al.* (Marroquin *et al.*, 2007). The culturing of cancer cells in galactose-supplemented medium devoid of glucose has the effect of promoting oxidative ATP generation within the organelle, halting glycolysis and imparting cell sensitisation towards the effects of mitochondrially toxic agents (Dykens *et al.*, 2008b). Whilst no significant variation in susceptibility towards artesunate was apparent between glucose and galactose-cultured Hep G2 lines following 24, 48 and 72 h treatment, substantial differences within the more sensitive HeLa cells were apparent upon identical periods of administration. The magnitude of this disparity is such that it is rational to suggest, in accordance with literature reports relating to alternative mitochondrially-active compounds, that the artemisinin derivatives exert toxicity through means which are at least partially reliant upon disruption to the functioning of the organelle (Swiss *et al.*, 2013). Further assessment indicated that

decreases in ATP content within this line preceded falls in cell viability, providing evidence that interference with the machinery of oxidative phosphorylation forms an early stage in the pathway through which death is stimulated. A more thorough analysis of bioenergetic function, obtained through employment of the Seahorse XF analyser, revealed that the compound does indeed possess the ability to exert deleterious effects upon the efficiency of oxidative coupling, whilst simultaneously reducing the reserve respiratory capacity and enhancing reliance upon glycolytic ATP synthesis.

In elucidating the factors associated with mediating artemisinin-induced impact upon the health of the mitochondrion, it was necessary to examine the contributory roles played by ROS and cellular Fe(II) in the emergence of any observed functional deficiencies. Reduction in artesunate-stimulated whole-cell and mitochondrial ROS levels through co-administration of the mitochondrially-localised antioxidant tiron had the effect of substantially reducing the bearing of the drug upon the viability of HeLa cells, whilst simultaneously restoring bioenergetic capacity assayed through the Seahorse stress test. Such outcomes strongly indicate that oxidative damage to the mitochondrion forms a central facet of the respiratory dysfunction which is ultimately causative of cell death. Following on from these findings, the utilisation of the Fe(II) chelator DFO permitted mechanistic assessment of the influence of free iron upon the progression of cytotoxicity. Reduction in the content of the unbound metal was shown to produce partial diminution in the extent of PFDHA bioactivation, whilst further reducing artesunate-stimulated oxidative stress both across the whole-cell and within mitochondrion, imparting cytoprotective effect and precluding the onset of mitochondrial respiratory injury. It is apparent that the consequences of Fe(II) chelation regarding artemisinin toxicity are multifaceted, with the metal implicated in possessing contributions towards both the propagation of drug-induced oxidative stress and also in the potential formation of active radical species. Examinations performed within ρ^0 HeLa line served to indicate that initial generation of ROS occurs

through mechanisms independent of the electron transport chain. Accordingly, investigation into the impact of the drug upon the complexes constituting this system revealed that it held only minimal bearing. Further attempts to establish the potential roles of the non-mitochondrial ROS-producing enzymes xanthine oxidase, NADPH oxidase, cytochrome c and COX in the routes towards oxidative stress arising from artesunate treatment produced results suggesting that inhibition of neither enzyme imparts substantial influence towards cell survival.

Based upon the sum of this evidence, it would appear rational to hypothesise that damage towards the respiratory functioning of the mitochondrion, arising through means dependent upon the emergence of oxidative stress, acts as an essential stage in the pathway along which the endoperoxide antimalarials exert toxicity within cancer cells. It is apparent, therefore, that delineation of the source by which ROS formation is stimulated – be it as a function of carbon-centred radical formation, Fenton chemistry, lipid peroxidation or specific enzyme inhibition – must constitute a central facet of any attempt to construct a thorough mechanistic understanding of the route through which these cytotoxic effects materialise. It is interesting to note that, whilst both prevalence of mitochondrial ROS and the susceptibility of cells towards the cytotoxic impact of artesunate are diminished within the ρ^0 HeLa line, formation of superoxide continues to proceed in significant quantities. Such an outcome would suggest that, although a functioning electron transport chain holds a contributory role towards the enhancement of oxidative stress, its presence does not stand as a requirement for primary initiation. Investigations assessing the impact of artesunate upon the activity of the units constituting the electron transport chain within isolated mitochondria reveal that artesunate possesses no capacity to impart functional defects within the primary superoxide-generating sites at complex I and complex III. It is hence feasible that the presence of oxidative stress within the organelle might be attributable to damage sustained towards the body as a consequence ROS generated at

alternative sites within the cell. ROS-induced ROS release is a phenomenon whereby mitochondria subject to oxidative damage are liable to exhibit greatly enhanced ROS production, accompanied by permeability transition and collapse of membrane potential (Zorov *et al.*, 2014). The release of ROS from impacted mitochondria may serve to initiate damage within neighbouring organelles, hence perpetuating a chain sequence capable of propagating injury throughout the cell. It follows naturally that the dysfunction of the respiratory chain, the oxidative degradation of phospholipids such as cardiolipin and the initiation of apoptotic death would form the consequences of this series of events.

The possibility that oxidative stress stimuli located external to the electron transport chain might be of central importance within mediation of the mechanisms through which artemisinin derivatives initiate cytotoxic impact prompts consideration into the significance of alternative pathways upon which the drugs may have potential to exert influence. Outcomes of the assessments performed within this body of work indicate strongly that Fe(II) exerts substantial influence upon the progression of drug-induced deficiencies in cellular functioning. Chelation of free iron is associated with imparting reduction in levels of oxidative stress, whilst simultaneously exhibiting capacity to inhibit bioactivation of the endoperoxide bridge. Viewed from the perspective of the carbon-centred radical hypothesis, it is plausible to suggest that the prevention of iron activation leads to a curtailment in the generation of ROS as a function of the capacity to promote reduction in the formation of the reactive radical fragments postulated as having a central role within the induction of cellular injury (Mercer *et al.*, 2011). The inability of the chelator to stimulate complete cessation of bioactivation would, however, appear to indicate that its protective influence extends beyond such a faculty. Accordingly, it follows that capacity to stimulate abrogation of oxidative stress and reduction in incidence of cell death is associated with the facility to bind labile iron. Thus, it can be reliably concluded that the contribution of the metal towards the procession of cytotoxicity is multifactorial.

Evidence has suggested that interaction with the lysosomal bodies, notable for possessing elevated content of labile iron, might potentially function as an early mediator both of mitochondrial and greater cellular response towards artemisinin administration (Hamacher-Brady *et al.*, 2011). Owing to the liability of the unbound metal towards participation in Fenton chemistry reactions, the often excessive concentrations of Fe(II) contained within the lysosome grant it particular relevance as a site for ROS formation (Kurz *et al.*, 2008; Thomas *et al.*, 2009). Associated closely with the emergence of oxidative stress within these bodies is the phenomenon of lysosomal membrane depolarisation – a process akin to that witnessed within the mitochondrion upon the induction of internal stress – whereby permeabilisation of the outer membrane culminates in the cytosolic release of cathepsins and related death-promoting factors (Aits *et al.*, 2013). It is these which progress to stimulate depolarisation of the mitochondrion, promoting release of pro-apoptotic initiators ahead of subsequent cell termination. The impact of lysosomal dysfunction upon the progression of artemisinin-stimulated toxicity has been examined in detail (Hamacher-Brady *et al.*, 2011). In line with the outcomes of the assays reported within this thesis, depletion of free iron content was associated with an abrogation in drug impact upon ROS formation and subsequent cell survival. It is therefore rational to postulate that the capacity of the artemisinin derivatives to exert initial injury to the mitochondrion is at least partially upon reliant upon the influence of lysosomally-stimulated oxidative stress and resultant programmed cell death. A scheme outlining a hypothesised pathway along which artesunate-stimulated cell death might proceed is displayed in Figure 6.1.

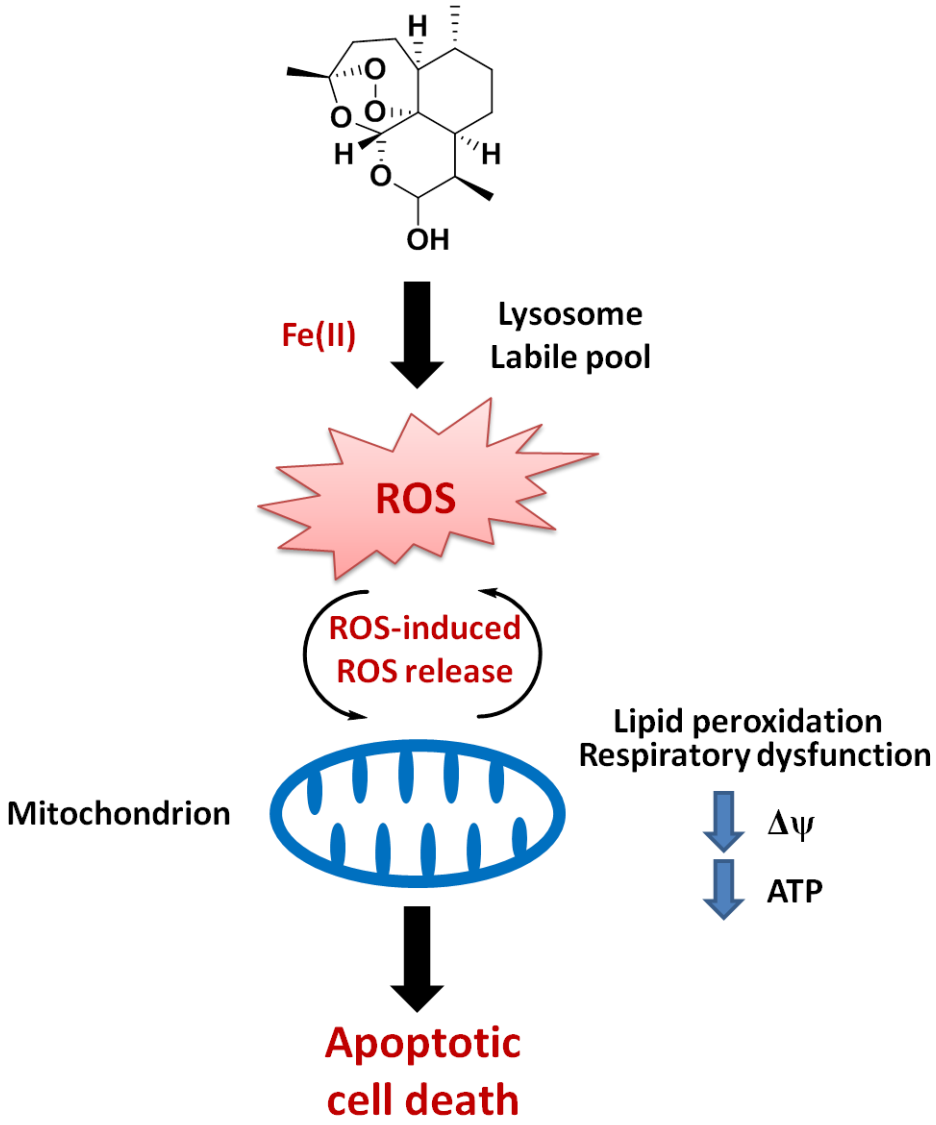

Figure 6.1. Representation of the proposed route towards the induction of cell death through ROS-stimulated mitochondrial bioenergetic dysfunction.

A further factor related to lysosomal functioning which may possess relevance towards the mechanism of artemisinin-induced ROS generation derives from the interplay which exists between iron pools located both within those bodies and within mitochondria. The motility of Fe(II) towards the mitochondrion is acknowledged to arise subsequent to the onset of damage to lysosome structural integrity (Uchiyama *et al.*, 2008). It is plausible, therefore, that this loading of the organelle with the unbound metal might form a key determinant in the progression of response to drug treatment. Mechanisms through which such impact

might be mediated may be postulated as being related both to the increased potential for the body to operate as a site for generation of ROS, and furthermore to the enhancement in its capacity to serve as a location for drug bioactivation (Mercer *et al.*, 2011; Thomas *et al.*, 2009). Studies have indicated that bafilomycin and paracetamol-induced mitochondrial Fe(II) uptake might be inhibited through the co-administration of free iron chelators, abrogating ROS formation and imparting cytoprotective effect (Hung *et al.*, 2013; Kon *et al.*, 2010). As such, so that it may be possible to discern the relevance of such a connection, it would be beneficial to monitor, in a similar manner, the occurrence of any redistribution of Fe(II) content related to artemisinin dosing. Repetition of the assessments performed monitoring the impact of mitochondrial iron transporter mitoferrin-2 knockdown upon the progression of cell response to the drugs would be greatly beneficial towards this end.

Whilst iron-stimulated pathways towards the formation of ROS might appear to be of primary importance as regards to the activity of the drugs within cancer cells, it remains further plausible that enhancements in oxidative stress may have origins in alternative interactions occurring directly between the endoperoxide bridge and other cellular substituents. It has been posited, owing to outcomes obtained across a series of biomimetic examinations, that the artemisinin derivatives may, as a function of the chemistry of the endoperoxide bridge, possess capacity to behave as direct oxidants of reduced cofactors crucial for the maintenance of redox homeostasis (Haynes *et al.*, 2012). It is held, specifically, that oxidation of $FADH_2$, a molecule essential within the pathway mediating the generation of reduced glutathione equivalents, impairs the facility for cells to neutralise the emergence of ROS, and hence contributes towards the observed growth in the incidence of oxidative stress (Haynes *et al.*, 2011). Such a sequence of reactions remains largely conserved within mammalian environments, ensuring the theoretical translatability of this hypothesised mode of action between pharmacological and toxicological settings. FAD, and related units, are identified as possessing roles within electron transport across a diverse

range of systems – including those related to the oxidative generation of ATP (Huttemann *et al.*, 2008). It is feasible, therefore, that if such an oxidant capacity for the endoperoxide compounds holds relevance within living organisms, that the impact wrought upon cellular bioenergetic function could be substantial. The outcomes of the examinations performed within this body of work – particularly those detailing the importance of oxidative stress and mitochondrial respiratory dysfunction towards the progression of toxicity – are explicable in terms of a cofactor oxidation pathway. Nevertheless, despite the promise of this model, the paucity of evidence for its applicability outside of biomimetic chemical settings ensures that the nature of its clinical relevance remains undetermined. Extension of the scope of examination to include investigation into its presence across *in vitro* and *in vivo* cellular and parasitic environments shall constitute an essential stage in the establishment of its wider bearing, although owing to generality of the cofactors within the regulation of a varied selection of redox processes, elucidation of the precise pathways impacted as a consequence of drug treatment may prove experimentally challenging.

Investigation into the capacity for endoperoxide compounds to function as direct oxidants of lipids focused upon assessing their influence upon the integrity of the mitochondrial phospholipid cardiolipin. Studies were based around examining the impact of artesunate upon cardiolipin oxidation in HL-60, HeLa and HeLa ρ^0 cells whilst in the presence of the cytochrome c-cardiolipin peroxidase inhibitor, TPP-IOA. Outcomes indicated that this inhibitor produced influences upon the prevalence of drug-stimulated oxidised cardiolipin, which were variable dependent upon the nature of the cell line examined, and also upon the method employed in the quantification of the parameter. Accordingly, owing to the inability of the compound to induce complete cessation in oxidation of the phospholipid, reliable conclusions as to the mechanism through which the artemisinin derivatives exert such effects cannot be drawn from the evidence accrued. It cannot be ruled out, therefore, that the lipid peroxidation emerges merely as factor secondary to the generalised increases

in ROS stimulated by the actions of the drugs. It is interesting to note that extent of oxidation is observed to be substantial across both the HeLa and the HeLa ρ^0 lines. The apparent lack of dependence upon the electron transport chain within the mediation of such an effect acquires further significance when viewed alongside the data outlining the variation in ROS formation evident between the two cell varieties. It is feasible that this observation might function as indirect evidence supporting the relevance of a ROS-independent pathway towards peroxidation emergence, and that this drug class might possess a role as a direct oxidant of the phospholipid.

A primary aim of the research performed within this thesis has been to elucidate the mechanisms through which endoperoxide antimalarials impart cell death in mammalian systems, in order that a clearer understanding of the interactions underpinning drug activity might ultimately inform the development both of novel synthetic compounds which display cleaner safety profiles, and also of hybrid artemisinin derivatives which exhibit clinical utility as anticancer agents. Assessments into the cytotoxic profiles of novel experimental synthetic antimalarial 1,2,4-trioxoloane and 1,2,3,5-tetraoxane compounds revealed apparent mechanistic commonality with the activities of the artemisinin derivatives across cancer cell lines, with similarities evident within both their capacity to impart mitochondrial dysfunction, and also within their ability to stimulate the emergence of apoptotic death. Semi-synthetic artemisinin-polypyrolle conjugates, functionalised with the intent of enhancing cytotoxic capacity for potential anti-cancer utility, were furthermore shown to exhibit a similar toxic capacity to that of their parent compound. Additional investigation has demonstrated that drugs belonging to the synthetic 1,2,4-trioxoloane and 1,2,3,5-tetraoxane classes exert a series of developmental defects *in vivo* which closely mimic those reported to occur alongside the artemisinin agents (Copple *et al.*, 2012). The precise mechanism through which the emergence of mitochondrial dysfunction, as noted within the *in vitro* cancer studies, relates to the pattern of abnormalities

characteristic over embryonic maturity – namely the depletion of immature erythrocyte stock and the subsequent impacting of haematopoiesis, the onset of anaemia and the emergence of structural deficiencies within cardiovascular and skeletal growth – awaits definitive establishment (Efferth *et al.*, 2010). It is pertinent to note that, at such a stage within their development, extrusion of the mitochondrial body from the growing erythrocytic cell has yet to occur (Mortensen *et al.*, 2010). Studies have demonstrated that DHA possesses the capacity to produce significant anti-angiogenic impact, stimulating downregulation in VEGF receptor expression and furthermore promoting the arrest of growth in vascular endothelial cell lines (Chen *et al.*, 2003; D'Alessandro *et al.*, 2007). Such effects are witnessed to occur alongside an increased formation of ROS, and are further associated with death arising through apoptotic routes. Interestingly, it has been shown that the sensitivity of these systems towards the toxicity of the artemisinin derivatives may be enhanced under conditions of hypoxia (D'Alessandro *et al.*, 2011). Whilst the mechanistic rational for this observation remains to be elucidated, it is notable that early embryonic development, particularly that which occurs during the relatively narrow window at which susceptibility towards the effects of the drugs is at its most heightened, proceeds under conditions of reduced oxygen tension (Dunwoodie, 2009). It is therefore rational to posit the existence of a relationship between the hypoxic nature of the environment present, the ensuing enhanced potency of artemisinin-stimulated toxicity, and the genesis of developmental dysfunction.

Interestingly, evidence has indicated that, unlike their artemisinin-derived counterparts, the activity of the examined candidates FBEG-100 and RKA-182 does not bear correlation with extent of structural decomposition. It is further observed that the onset of impact towards cell viability imparted by drugs belonging to the novel classes proceeds at a rate which displays relative acceleration (Copple *et al.*, 2012). Concordant discrepancies relating to pharmacokinetic parameters have been observed within related compounds, with 1,2,4-

trioxoloane and 1,2,3,5-tetraoxane agents typically exhibiting enhanced elimination half-lives in comparison with the traditional treatments (Wang *et al.*, 2013). It would be beneficial in future study to examine in greater detail the origins of such variation, in order that further insight into relationships underpinning the functioning of all classes might be attained. It has been posited that the independence of the cellular toxicity of FBEG-100 and RKA-182 upon chemical degradation might stand in support of the aforementioned direct cofactor oxidation model (Haynes *et al.*, 2012).

Whilst the experimental outcomes obtained from the research performed within this body of work have attended to expand existing knowledge of the mechanistic routes through which endoperoxide compounds, both artemisinin-derived and synthetic, proceed to induce cellular dysfunction and toxicity, there remains substantial scope for further investigation into the nature of the interactions which underpin such observations. The practical applications of such improved understanding within the development of novel drug analogues and safer, more effective therapeutic routines are areas additionally in need of development. Although the evidence provided serves strongly to indicate the presence of a non-mitochondrial, iron-dependent source for the ROS ultimately causative of cell death, identification of the cellular substituents central to their emergence, and definition of the precise influence of endoperoxide chemistry upon the progression of response, remain both incomplete.

Recognition of the importance of the lysosome within the initiation of oxidative stress occurring subsequent to the administration of these drugs has developed as a consequence of recent research. Despite such advancements, the process of characterising specific properties related to the impacts exerted upon the activity of constituent networks within these organelles remains grounded at an early phase. It would accordingly be beneficial to examine the factors underlying their sensitivity to the actions of the endoperoxides, with

focus given to aspects influencing the uptake and distribution of the compounds inside the bodies. Whilst it is plausible that their status as sites for iron accumulation might form the solitary factor responsible for their apparent roles in the stimulation of ROS generation, little has yet been ascertained regarding potential capacity of the drug to impart direct dysfunction or activation to proteins regulating pathways mediated within. As such, a further assessment into the facility of the artemisinin derivatives to induce alterations within processes such as iron motility, acidification, cathepsin-dependent apoptosis and membrane structural integrity would enable a more thorough understanding to be attained.

Appreciation of the causative factors underlying the initiation of artemisinin-induced cytotoxicity would be incomplete without thorough distinction of the chemical mechanisms through which the activity of the compounds is mediated. Despite the existence of numerous plausible theories regarding the nature of the reactivity of the endoperoxide bridge, and the consequences which these ultimately possess towards the onset and progression of defective cell functioning, the identity of the definitive pathways relating drug activation to pharmacological and toxicological outcome has yet to be conclusively established. Observations that endoperoxide activity retains dependence upon interaction with iron sources, and that ROS generation is an essential feature for biological activity, remain explicable in terms of several common postulates. Accordingly, additional research would be required before the applicability of free radical and direct oxidant models could be applied with certainty to draw a complete image of the route through which cytotoxicity proceeds.

In the functionalisation of endoperoxide hybrids for the enhancement of anticancer activity, it would appear that consideration of the outcomes obtained within this thesis might potentially prove beneficial towards the development of compounds displaying

enhanced activity over pre-existing artemisinin derivatives. Should the lysosomal action of the drugs be essential in mediating the progression of cytotoxicity, it is rational to theorise that targeting of the agents towards that body might enable a greater cell killing capacity. The influence of the lysosome upon the mediation of programmed cell death has led to its identification in the holding of roles contributory towards the abnormalities in cellular function characteristic of cancer (Kirkegaard *et al.*, 2009). Accordingly, it has been suggested that the deployment of drugs exhibiting lysosomal liability might constitute a focus for the development of future anticancer treatment (Fehrenbacher *et al.*, 2005; Saftig *et al.*, 2013). It is noted that molecules displaying a particular affinity towards accumulation within these bodies typically possess cationic amphiphilic properties, hence enabling sequestration as a function of ion trapping imparted due to the acidic nature of the environment therein. Owing to concerns regarding toxicity related to the lack of specificity of such compounds towards cancerous cells – and in light of further evidence detailing potential localisation issues related to acidification abnormalities in the lysosomes of selected cancer models – it is apparent that further investigation would be required before the functionalisation of artemisinin derivatives to display such characteristics would be feasible in regards to the enhancement of therapeutic benefit (Ndolo *et al.*, 2012). Several strategies for the localisation of compounds towards the lysosome have instead been posited based upon the putative efficacy of experimental polymeric conjugate delivery systems (Binauld *et al.*, 2013; Chiang *et al.*, 2014). As a consequence of the relative novelty of such technology, it is yet not possible to assess with reliability its potential relevance towards improvement of artemisinin-based anticancer treatment outcome.

By way of conclusion, it can be stated that the studies performed within this thesis have served to elucidate the essential contribution of mitochondrial dysfunction towards the progression of cytotoxicity induced through the endoperoxide class of antimalarial drugs. Defective respiratory and bioenergetic operation, emerging subsequent to damage

imparted through Fe(II)-associated oxidative stress, are identified as primary mechanisms through which cell death is stimulated. Consideration of these outcomes facilitates the identification of further pathways which might potentially be of relevance in informing understanding of the activity associated with the compounds. It is intended the establishment of such relationships shall enable eventual determination of the factors associated with the mediation of toxic impact, so that the development of safer treatment regimens might proceed with greater theoretical grounding.

Bibliography

Aits S, Jaattela M (2013). Lysosomal cell death at a glance. *Journal of Cell Science* **126**(9)**:** 1905-1912.

Andreyev AI, Kushnareva YE, Starkov AA (2005). Mitochondrial metabolism of reactive oxygen species. *Biochemistry-Moscow* **70**(2)**:** 200-214.

Anyasor G, Ajayi E, Saliu J, Ajagbonna O, Olorunsogo O (2009). Artesunate opens mitochondrial membrane permeability transition pore. *Annals of Tropical Medicine and Public Health* **2**(2)**:** 37-41.

Apel K, Hirt H (2004). Reactive oxygen species: Metabolism, oxidative stress, and signal transduction. *Annual Review of Plant Biology* **55:** 373-399.

Armstrong C, Staples JF (2010). The role of succinate dehydrogenase and oxaloacetate in metabolic suppression during hibernation and arousal. *Journal of Comparative Physiology B-Biochemical Systemic and Environmental Physiology* **180**(5)**:** 775-783.

Arnou B, Montigny C, Morth JP, Nissen P, Jaxel C, Moller JV*, et al.* (2011). The Plasmodium falciparum Ca2+-ATPase PfATP6: insensitive to artemisinin, but a potential drug target. *Biochemical Society Transactions* **39:** 823-831.

Atkinson J, Kapralov AA, Yanamala N, Tyurina YY, Amoscato AA, Pearce L*, et al.* (2011). A mitochondria-targeted inhibitor of cytochrome c peroxidase mitigates radiation-induced death. *Nature Communications* **2**.

Aweeka FT, German PL (2008). Clinical pharmacology of artemisinin-based combination therapies. *Clinical Pharmacokinetics* **47**(2)**:** 91-102.

Bedard K, Krause K-H (2007). The NOX family of ROS-generating NADPH oxidases: Physiology and pathophysiology. *Physiological Reviews* **87**(1)**:** 245-313.

Beekman AC, Barentsen ARW, Woerdenbag HJ, VanUden W, Pras N, Konings AWT*, et al.* (1997). Stereochemistry-dependent cytotoxicity of some artemisinin derivatives. *Journal of Natural Products* **60**(4)**:** 325-330.

Beekman AC, Woerdenbag HJ, Kampinga HH, Konings AWT (1996). Cytotoxicity of artemisinin, a dimer of dihydroartemisinin, artemisitene and eupatoriopicrin as evaluated by the MTT and clonogenic assay. *Phytotherapy Research* **10**(2)**:** 140-144.

Belikova NA, Vladimirov YA, Osipov AN, Kapralov AA, Tyurin VA, Potapovich MV*, et al.* (2006). Peroxidase activity and structural transitions of cytochrome c bound to cardiolipin-containing membranes. *Biochemistry* **45**(15)**:** 4998-5009.

Benakis A, Paris M, Loutan L, Plessas CT, Plessas ST (1997). Pharmacokinetics of artemisinin and artesunate after oral administration in healthy volunteers. *Am. J. Trop. Med. Hyg.* **56**(1)**:** 17-23.

Berman PA, Adams PA (1997). Artemisinin enhances heme-catalysed oxidation of lipid membranes. *Free Radical Biology and Medicine* **22**(7)**:** 1283-1288.

Binauld S, Stenzel MH (2013). Acid-degradable polymers for drug delivery: a decade of innovation. *Chemical Communications* **49**(21)**:** 2082-2102.

Bobba A, Atlante A, Petragallo VA, Marra E (2008). Different sources of reactive oxygen species contribute to low potassium-induced apoptosis in cerebellar granule cells. *International Journal of Molecular Medicine* **21**(6)**:** 737-745.

Boya P, Kroemer G (2008). Lysosomal membrane permeabilization in cell death. *Oncogene* **27**(50)**:** 6434-6451.

Bradford MM (1976). Rapid and sensitive method for quantitation of microgram quantities of protein utilizing principle of protein-dye binding. *Analytical Biochemistry* **72**(1-2)**:** 248-254.

Brewer TG, Peggins JO, Grate SJ, Petras JM, Levine BS, Weina PJ*, et al.* (1994). Neurotoxicity in animals due to arteether and artemether. *Transactions of the Royal Society of Tropical Medicine and Hygiene* **88:** 33-36.

Cairo G, Bernuzzi F, Recalcati S (2006). A precious metal: Iron, an essential nutrient for all cells. *Genes and Nutrition* **1**(1)**:** 25-39.

Cazelles J, Robert A, Meunier B (2001). Alkylation of heme by artemisinin, an antimalarial drug. *Comptes Rendus De L Academie Des Sciences Serie Ii Fascicule C-Chimie* **4**(2)**:** 85-89.

Charman SA, Arbe-Barnes S, Bathurst IC, Brun R, Campbell M, Charman WN*, et al.* (2011). Synthetic ozonide drug candidate OZ439 offers new hope for a single-dose cure of uncomplicated malaria. *Proceedings of the National Academy of Sciences of the United States of America* **108**(11)**:** 4400-4405.

Chaturvedi D, Goswami A, Saikia PP, Barua NC, Rao PG (2010). Artemisinin and its derivatives: a novel class of anti-malarial and anti-cancer agents. *Chemical Society Reviews* **39**(2)**:** 435-454.

Chen HH, Zhou HJ, Fan X (2003). Inhibition of human cancer cell line growth and human umbilical vein endothelial cell angiogenesis by artemisinin derivatives in vitro. *Pharmacological Research* **48**(3)**:** 231-236.

Chevallet M, Lescuyer P, Diemer H, van Dorsselaer A, Leize-Wagner E, Rabilloud T (2006). Alterations of the mitochondrial proteome caused by the absence of mitochondrial DNA: A proteomic view. *Electrophoresis* **27**(8)**:** 1574-1583.

Chiang Y-T, Lo C-L (2014). pH-Responsive polymer-liposomes for intracellular drug delivery and tumor extracellular matrix switched-on targeted cancer therapy. *Biomaterials* **35**(20)**:** 5414-5424.

Chung JH, Kim YS, Noh K, Lee YM, Chang SW, Kim EC (2014). Deferoxamine promotes osteoblastic differentiation in human periodontal ligament cells via the nuclear factor erythroid 2-related factor-mediated antioxidant signaling pathway. *Journal of Periodontal Research* **49**(5)**:** 563-573.

Clark RL, Arima A, Makori N, Nakata Y, Bernard F, Gristwood W*, et al.* (2008). Artesunate: Developmental toxicity and toxicokinetics in monkeys. *Birth Defects Res. Part B-Dev. Reprod. Toxicol.* **83**(4)**:** 418-434.

Clark RL, White TEK, Clode SA, Gaunt I, Winstanley P, Ward SA (2004). Developmental toxicity of artesunate and an artesunate combination in the rat and rabbit. *Birth Defects Res. Part B-Dev. Reprod. Toxicol.* **71**(6)**:** 380-394.

Copple IM, Mercer AE, Firman J, Donegan G, Herpers B, Wong MHL*, et al.* (2012). Examination of the cytotoxic and embryotoxic potential and underlying mechanisms of next-generation synthetic trioxolane and tetraoxane antimalarials. *Molecular Medicine* **18**(7)**:** 1045-1055.

Cortes-Rojo C, Rodriguez-Orozco AR (2011). Importance of oxidative damage on the electron transport chain for the rational use of mitochondria-targeted antioxidants. *Mini-Reviews in Medicinal Chemistry* **11**(7)**:** 625-632.

Crespo-Ortiz MP, Wei MQ (2012). Antitumor activity of artemisinin and its derivatives: From a well-known antimalarial agent to a potential anticancer drug. *Journal of Biomedicine and Biotechnology*.

Crimi M, Degli Esposti M (2011). Apoptosis-induced changes in mitochondrial lipids. *Biochimica Et Biophysica Acta-Molecular Cell Research* **1813**(4)**:** 551-557.

Cui W, Zhou Y (2009). Ancient Chinese anti-fever cure becomes panacea for malaria. *Bulletin of the World Health Organization* **87**(10)**:** 743-744.

D'Alessandro S, Basilico N, Corbett Y, Scaccabarozzi D, Omodeo-Sale F, Saresella M*, et al.* (2011). Hypoxia modulates the effect of dihydroartemisinin on endothelial cells. *Biochemical Pharmacology* **82**(5)**:** 476-484.

D'Alessandro S, Gelati M, Basilico N, Parati EA, Haynes RK, Taramelli D (2007). Differential effects on angiogenesis of two antimalarial compounds, dihydroartemisinin and artemisone: Implications for embryotoxicity. *Toxicology* **241**(1-2)**:** 66-74.

Dakubo GD (2010). *The Warburg Phenomenon and Other Metabolic Alterations of Cancer Cells*. edn.

Davies KJA (1990). Oxidative Damage and Repair: Chemical, Biological and Medical Aspects.

del Pilar Crespo M, Avery TD, Hanssen E, Fox E, Robinson TV, Valente P*, et al.* (2008). Artemisinin and a series of novel endoperoxide antimalarials exert early effects on digestive vacuole morphology. *Antimicrobial Agents and Chemotherapy* **52**(1)**:** 98-109.

Denisov ET, Solodova SL, Denisova TG (2010). Radical chemistry of artemisinin. *Russian Chemical Reviews* **79**(11)**:** 981-1003.

Diepart C, Verrax J, Calderon PB, Feron O, Jordan BF, Gallez B (2010). Comparison of methods for measuring oxygen consumption in tumor cells in vitro. *Analytical Biochemistry* **396**(2)**:** 250-256.

Divakaruni AS, Brand MD (2011). The regulation and physiology of mitochondrial proton leak. *Physiology* **26**(3)**:** 192-205.

Dixon SJ, Stockwell BR (2014). The role of iron and reactive oxygen species in cell death. *Nature Chemical Biology* **10**(1)**:** 9-17.

Domingo JL, delaTorre A, Belles M, Mayayo E, Llobet JM, Corbella J (1997). Comparative effects of the chelators sodium 4,5-dihydroxybenzene-1,3-disulfonate (Tiron) and diethylenetriaminepentaacetic acid (DTPA) on acute uranium nephrotoxicity in rats. *Toxicology* **118**(1)**:** 49-59.

Dondorp AM, Nosten F, Yi P, Das D, Phyo AP, Tarning J*, et al.* (2009). Artemisinin resistance in plasmodium falciparum malaria. *New England Journal of Medicine* **361**(5)**:** 455-467.

Dranka BP, Benavides GA, Diers AR, Giordano S, Zelickson BR, Reily C*, et al.* (2011). Assessing bioenergetic function in response to oxidative stress by metabolic profiling. *Free Radical Biology and Medicine* **51**(9)**:** 1621-1635.

Dranka BP, Hill BG, Darley-Usmar VM (2010). Mitochondrial reserve capacity in endothelial cells: The impact of nitric oxide and reactive oxygen species. *Free Radical Biology and Medicine* **48**(7)**:** 905-914.

Dunwoodie SL (2009). The role of hypoxia in development of the mammalian embryo. *Developmental Cell* **17**(6)**:** 755-773.

Dykens JA, Jamieson J, Marroquin L, Nadanaciva S, Billis PA, Will Y (2008a). Biguanide-induced mitochondrial dysfunction yields increased lactate production and cytotoxicity of aerobically-poised HepG2 cells and human hepatocytes in vitro. *Toxicology and Applied Pharmacology* **233**(2)**:** 203-210.

Dykens JA, Jamieson JD, Marroquin LD, Nadanaciva S, Xu JJ, Dunn MC*, et al.* (2008b). In vitro assessment of mitochondrial dysfunction and cytotoxicity of nefazodone, trazodone, and buspirone. *Toxicological Sciences* **103**(2)**:** 335-345.

Dykens JA, Will, Y. (2008). *Drug-Induced Mitochondrial Dysfunction*. 10th edn. John Wiley and Sons.

Eastman RT, Fidock DA (2009). Artemisinin-based combination therapies: a vital tool in efforts to eliminate malaria. *Nat. Rev. Microbiol.* **7**(12)**:** 864-874.

Eckstein-Ludwig U, Webb RJ, van Goethem IDA, East JM, Lee AG, Kimura M*, et al.* (2003). Artemisinins target the SERCA of Plasmodium falciparum. *Nature* **424**(6951)**:** 957-961.

Efferth T (2006). Molecular pharmacology and pharmacogenomics of artemisinin and its derivatives in cancer cells. *Current Drug Targets* **7**(4)**:** 407-421.

Efferth T, Dunstan H, Sauerbrey A, Miyachi H, Chitambar CR (2001). The anti-malarial artesunate is also active against cancer. *International Journal of Oncology* **18**(4)**:** 767-773.

Efferth T, Giaisi M, Merling A, Krammer PH, Li-Weber M (2007). Artesunate induces ROS-mediated apoptosis in doxorubicin-resistant T leukemia cells. *Plos One* **2**(8).

Efferth T, Kaina B (2010). Toxicity of the antimalarial artemisinin and its dervatives. *Critical Reviews in Toxicology* **40**(5)**:** 405-421.

Ellis GL, Amewu R, Sabbani S, Stocks PA, Shone A, Stanford D*, et al.* (2008). Two-step synthesis of achiral dispiro-1,2,4,5-tetraoxanes with outstanding antimalarial activity, low toxicity, and high-stability profiles. *Journal of Medicinal Chemistry* **51**(7)**:** 2170-2177.

Elmore S (2007). Apoptosis: A review of programmed cell death. *Toxicologic Pathology* **35**(4)**:** 495-516.

Faurant C (2011). From bark to weed: The history of artemisinin. *Parasite-Journal De La Societe Francaise De Parasitologie* **18**(3)**:** 215-218.

Fehrenbacher N, Jaattela M (2005). Lysosornes as targets for cancer therapy. *Cancer Research* **65**(8)**:** 2993-2995.

Fernandez MG, Troiano L, Moretti L, Nasi M, Pinti M, Salvioli S*, et al.* (2002). Early changes in intramitochondrial cardiolipin distribution during apoptosis. *Cell Growth & Differentiation* **13**(9)**:** 449-455.

Fernandez MIG, Ceccarelli D, Muscatello U (2004). Use of the fluorescent dye 10-N-nonyl acridine orange in quantitative and location assays of cardiolipin: a study on different experimental models. *Analytical Biochemistry* **328**(2)**:** 174-180.

Fiers W, Beyaert R, Declercq W, Vandenabeele P (1999). More than one way to die: apoptosis, necrosis and reactive oxygen damage. *Oncogene* **18**(54)**:** 7719-7730.

Firestone GL, Sundar SN (2009). Anticancer activities of artemisinin and its bioactive derivatives. *Expert Reviews in Molecular Medicine* **11**(e32).

Foley M, Tilley L (1998). Quinoline antimalarials: Mechanisms of action and resistance and prospects for new agents. *Pharmacology & Therapeutics* **79**(1)**:** 55-87.

Fosslien E (2001). Review: Mitochondrial medicine - Molecular pathology of defective oxidative phosphorylation. *Annals of Clinical and Laboratory Science* **31**(1)**:** 25-67.

Frazier AE, Thorburn DR (2012). Biochemical analyses of the electron transport chain complexes by spectrophotometry. *Mitochondrial Disorders: Biochemical and Molecular Analysis*, edn, Vol. 837. p^pp 49-62.

Freedman DO (2008). Malaria prevention in short-term travelers. *New England Journal of Medicine* **359**(6)**:** 603-612.

Galaris D, Pantopoulos K (2008). Oxidative stress and iron homeostasis: Mechanistic and health aspects. *Critical Reviews in Clinical Laboratory Sciences* **45**(1)**:** 1-23.

Ghosh M, Wang HD, McNeill JR (2002). Tiron exerts effects unrelated to its role as a scavenger of superoxide anion: effects on calcium binding and vascular responses. *Canadian Journal of Physiology and Pharmacology* **80**(8)**:** 755-760.

Golenser J, Waknine JH, Krugliak M, Hunt NH, Grau GE (2006). Current perspectives on the mechanism of action of artemisinins. *International Journal for Parasitology* **36**(14)**:** 1427-1441.

Golstein P, Kroemer G (2007). Cell death by necrosis: towards a molecular definition. *Trends Biochem.Sci.* **32**(1)**:** 37-43.

Green JD, Narahara HT (1980). Assay of succinate-dehydrogenase activty by the tetrazolium method – evaluation of an improved technique in skeletal-muscle fractions. *Journal of Histochemistry & Cytochemistry* **28**(5)**:** 408-412.

Halliwell B (2007). Biochemistry of oxidative stress. *Biochemical Society Transactions* **35:** 1147-1150.

Hamacher-Brady A, Stein HA, Turschner S, Toegel I, Mora R, Jennewein N*, et al.* (2011). Artesunate activates mitochondrial apoptosis in breast cancer cells via iron-catalyzed lysosomal reactive oxygen species production. *Journal of Biological Chemistry* **286**(8)**:** 6587-6601.

Haynes RK, Chan W-C, Wong H-N, Li K-Y, Wu W-K, Fan K-M*, et al.* (2010). Facile oxidation of leucomethylene blue and dihydroflavins by artemisinins: Relationship with flavoenzyme function and antimalarial mechanism of action. *Chemmedchem* **5**(8)**:** 1282-1299.

Haynes RK, Chan WC, Lung C-M, Uhlemann A-C, Eckstein U, Taramelli D*, et al.* (2007). The Fe2+-mediated decomposotion, PfATP6 binding, and antimalarial activities of artemisone and other arteminisins: The unlikehood of C-centered radicals as bioactive intermediates. *Chemmedchem* **2**(10)**:** 1480-1497.

Haynes RK, Cheu K-W, Chan H-W, Wong H-N, Li K-Y, Tang MM-K*, et al.* (2012). Interactions between artemisinins and other antimalarial drugs in relation to the cofactor model – a unifying proposal for drug action. *Chemmedchem* **7**(12)**:** 2204-2226.

Haynes RK, Cheu K-W, N'Da D, Coghi P, Monti D (2013). Considerations on the mechanism of action of artemisinin antimalarials: Part 1-The 'carbon radical' and 'heme' hypotheses. *Infectious Disorders - Drug Targets* **13**(4)**:** 217-277.

Haynes RK, Cheu K-W, Tang MM-K, Chen M-J, Guo Z-F, Guo Z-H*, et al.* (2011). Reactions of antimalarial peroxides with each of leucomethylene blue and dihydroflavins: Flavin reductase and the cofactor model exemplified. *Chemmedchem* **6**(2)**:** 279-291.

Haynes RK, Ho WY, Chan HW, Fugmann B, Stetter J, Croft SL*, et al.* (2004). Highly antimalaria-active artemisinin derivatives: Biological activity does not correlate with chemical reactivity. *Angewandte Chemie-International Edition* **43**(11)**:** 1381-1385.

Haynes RK, Pai HHO, Voerste A (1999). Ring opening of artemisinin (qinghaosu) and dihydroartemisinin and interception of the open hydroperoxides with formation of N-oxides - A chemical model for antimalarial mode of action. *Tetrahedron Letters* **40**(25)**:** 4715-4718.

Haynes RK, Vonwiller SC (1996). The behaviour of qinghaosu (artemisinin) in the presence of heme Iron(II) and (III). *Tetrahedron Letters* **37**(2)**:** 253-256.

He Q, Shi J, Shen X-L, An J, Sun H, Wang L*, et al.* (2010). Dihydroartemisinin upregulates death receptor 5 expression and cooperates with TRAIL to induce apoptosis in human prostate cancer cells. *Cancer Biology & Therapy* **9**(10)**:** 819-824.

Hentze MW, Muckenthaler MU, Andrews NC (2004). Balancing acts: Molecular control of mammalian iron metabolism. *Cell* **117**(3)**:** 285-297.

Hill BG, Benavides GA, Lancaster JR, Jr., Ballinger S, Dell'Italia L, Zhang J*, et al.* (2012). Integration of cellular bioenergetics with mitochondrial quality control and autophagy. *Biological Chemistry* **393**(12)**:** 1485-1512.

Hill BG, Dranka BP, Zou L, Chatham JC, Darley-Usmar VM (2009). Importance of the bioenergetic reserve capacity in response to cardiomyocyte stress induced by 4-hydroxynonenal. *Biochemical Journal* **424:** 99-107.

Ho WE, Peh HY, Chan TK, Wong WSF (2014). Artemisinins: Pharmacological actions beyond anti-malarial. *Pharmacology & Therapeutics* **142**(1)**:** 126-139.

Hou J, Wang D, Zhang R, Wang H (2008). Experimental therapy of hepatoma with artemisinin and its derivatives: In vitro and in vivo activity, chemosensitization, and mechanisms of action. *Clinical Cancer Research* **14**(17)**:** 5519-5530.

Houtkooper RH, Vaz FM (2008). Cardiolipin, the heart of mitochondrial metabolism. *Cellular and Molecular Life Sciences* **65**(16)**:** 2493-2506.

Hung H-I, Schwartz JM, Maldonado EN, Lemasters JJ, Nieminen A-L (2013). Mitoferrin-2-dependent mitochondrial iron uptake sensitizes human head and neck squamous carcinoma cells to photodynamic therapy. *Journal of Biological Chemistry* **288**(1)**:** 677-686.

Hutagalung R, Htoo H, Nwee P, Arunkamomkiri J, Zwang J, Carrara VI*, et al.* (2006). A case-control auditory evaluation of patients treated with artemether-lumefantrine. *Am. J. Trop. Med. Hyg.* **74**(2)**:** 211-214.

Huttemann M, Lee I, Pecinova A, Pecina P, Przyklenk K, Doan JW (2008). Regulation of oxidative phosphorylation, the mitochondrial membrane potential, and their role in human disease. *Journal of Bioenergetics and Biomembranes* **40**(5)**:** 445-456.

Huttemann M, Lee I, Samavati L, Yu H, Doan JW (2007). Regulation of mitochondrial oxidative phosphorylation through cell signaling. *Biochimica Et Biophysica Acta-Molecular Cell Research* **1773**(12)**:** 1701-1720.

Hyde JE (2002). Mechanisms of resistance of Plasmodium falciparum to antimalarial drugs. *Microbes and Infection* **4**(2)**:** 165-174.

Imlay JA (2003). Pathways of oxidative damage. *Annual Review of Microbiology* **57:** 395-418.

Jastroch M, Divakaruni AS, Mookerjee S, Treberg JR, Brand MD (2010). Mitochondrial proton and electron leaks. *Essays in Biochemistry: Mitochondrial Function*, edn, Vol. 47. p^pp 53-67.

Jefford CW (2007). New developments in synthetic peroxidic drugs as artemisinin mimics. *Drug Discovery Today* **12**(11-12)**:** 487-495.

Jiang JB, Jacobs G, Liang DS, Aikawa M (1985). Qinghaosu-induced changes in the morphology of plasmodium-inui. *Am. J. Trop. Med. Hyg.* **34**(3)**:** 424-428.

Jones-Brando L, D'Angelo J, Posner GH, Yolken R (2006). In vitro inhibition of Toxoplasma gondii by four new derivatives of artemisinin. *Antimicrobial Agents and Chemotherapy* **50**(12)**:** 4206-4208.

Jones M, Mercer AE, Stocks PA, La Pensee LJI, Cosstick R, Park BK*, et al.* (2009). Antitumour and antimalarial activity of artemisinin-acridine hybrids. *Bioorganic & Medicinal Chemistry Letters* **19**(7)**:** 2033-2037.

Kaewsuya P, Danielson ND, Ekhterae D (2007). Fluorescent determination of cardiolipin using 10-N-nonyl acridine orange. *Analytical and Bioanalytical Chemistry* **387**(8)**:** 2775-2782.

Kagan VE, Bayir A, Bayir H, Stoyanovsky D, Borisenko GG, Tyurina YY*, et al.* (2009a). Mitochondria-targeted disruptors and inhibitors of cytochrome c/cardiolipin peroxidase complexes: A new strategy in anti-apoptotic drug discovery. *Molecular Nutrition & Food Research* **53**(1)**:** 104-114.

Kagan VE, Bayir HA, Belikova NA, Kapralov O, Tyurina YY, Tyurin VA*, et al.* (2009b). Cytochrome c/cardiolipin relations in mitochondria: a kiss of death. *Free Radical Biology and Medicine* **46**(11)**:** 1439-1453.

Kagan VE, Tyurin VA, Jiang JF, Tyurina YY, Ritov VB, Amoscato AA*, et al.* (2005). Cytochrome c acts as a cardiolipin oxygenase required for release of proapoptotic factors. *Nature Chemical Biology* **1**(4)**:** 223-232.

Kakhlon O, Cabantchik ZI (2002). The labile iron pool: Characterization, measurement, and participation in cellular processes. *Free Radical Biology and Medicine* **33**(8)**:** 1037-1046.

Kim J, Hoppel CL (2013). Comprehensive approach to the quantitative analysis of mitochondrial phospholipids by HPLC-MS. *J. Chromatogr. B* **912:** 105-114.

Kim J, Minkler PE, Salomon RG, Anderson VE, Hoppel CL (2011). Cardiolipin: characterization of distinct oxidized molecular species. *Journal of Lipid Research* **52**(1)**:** 125-135.

Kirkegaard T, Jaattela M (2009). Lysosomal involvement in cell death and cancer. *Biochimica Et Biophysica Acta-Molecular Cell Research* **1793**(4)**:** 746-754.

Kirkinezos IG, Moraes CT (2001). Reactive oxygen species and mitochondrial diseases. *Seminars in Cell & Developmental Biology* **12**(6)**:** 449-457.

Klayman DL (1985). Qinghaosu (artemisinin) - an antimalarial drug from China. *Science* **228**(4703)**:** 1049-1055.

Kon K, Kim J-S, Uchiyama A, Jaeschke H, Lemasters JJ (2010). Lysosomal iron mobilization and induction of the mitochondrial permeability transition in acetaminophen-induced toxicity to mouse hepatocytes. *Toxicological Sciences* **117**(1)**:** 101-108.

Kowaltowski AJ, Vercesi AE (1999). Mitochondrial damage induced by conditions of oxidative stress. *Free Radical Biology and Medicine* **26**(3-4)**:** 463-471.

Krishan A (1975). Rapid flow cytofluorometric analysis ofmammalian-cell cycle by propidium iodide staining. *Journal of Cell Biology* **66**(1)**:** 188-193.

Krishna CM, Liebmann JE, Kaufman D, Degraff W, Hahn SM, McMurry T*, et al.* (1992). The catecholic metal sequestering agent 1,2-dihydroxybenzene-3,5-disulfonateE confers protection against oxidative cell-damage. *Archives of Biochemistry and Biophysics* **294**(1)**:** 98-106.

Krishna S, Bustamante L, Haynes RK, Staines HM (2008). Artemisinins: their growing importance in medicine. *Trends in Pharmacological Sciences* **29**(10)**:** 520-527.

Krysko DV, Vanden Berghe T, D'Herde K, Vandenabeele P (2008). Apoptosis and necrosis: Detection, discrimination and phagocytosis. *Methods* **44**(3)**:** 205-221.

Kumar N, Sharma M, Rawat DS (2011). Medicinal chemistry perspectives of trioxanes and tetraoxanes. *Current Medicinal Chemistry* **18**(25)**:** 3889-3928.

Kumura N, Furukawa H, Onyango AN, Izumi M, Nakajima S, Ito H*, et al.* (2009). Different behavior of artemisinin and tetraoxane in the oxidative degradation of phospholipid. *Chemistry and Physics of Lipids* **160**(2)**:** 114-120.

Kurz T, Eaton JW, Brunk UT (2011). The role of lysosomes in iron metabolism and recycling. *Int. J. Biochem. Cell Biol.* **43**(12)**:** 1686-1697.

Kurz T, Terman A, Gustafsson B, Brunk UT (2008). Lysosomes in iron metabolism, ageing and apoptosis. *Histochemistry and Cell Biology* **129**(4)**:** 389-406.

Kwok JC, Richardson DR (2002). The iron metabolism of neoplastic cells: alterations that facilitate proliferation? *Crit. Rev. Oncol./Hematol.* **42**(1)**:** 65-78.

La Pensee L, Sabbani S, Sharma R, Bhamra I, Shore E, Chadwick AE*, et al.* (2013). Artemisinin-polypyrrole conjugates: Synthesis, DNA binding studies and preliminary antiproliferative evaluation. *Chemmedchem* **8**(5)**:** 709-718.

Lai H, Singh NP (1995). Selective cancer cell cytotoxicty from exposure to dihydroartemisinin and holotransferrin. *Cancer Letters* **91**(1)**:** 41-46.

Lai HC, Singh NP, Sasaki T (2013). Development of artemisinin compounds for cancer treatment. *Invest. New Drugs* **31**(1)**:** 230-246.

Le Bras M, Clement MV, Pervaiz S, Brenner C (2005). Reactive oxygen species and the mitochondrial signaling pathway of cell death. *Histology and Histopathology* **20**(1)**:** 205-219.

Lee YS, Kang YS, Lee SH, Kim JA (2000). Role of NAD(P)H oxidase in the tamoxifen-induced generation of reactive oxygen species and apoptosis in HepG2 human hepatoblastoma cells. *Cell Death and Differentiation* **7**(10)**:** 925-932.

Li W, Mo WK, Shen D, Sun LB, Wang J, Lu S*, et al.* (2005). Yeast model uncovers dual roles of mitochondria in the action of arternisinin. *Plos Genetics* **1**(3)**:** 329-334.

Li X, Fang P, Mai J, Choi ET, Wang H, Yang X-f (2013). Targeting mitochondrial reactive oxygen species as novel therapy for inflammatory diseases and cancers. *Journal of Hematology & Oncology* **6**.

Lill R, Kispal G (2000). Maturation of cellular Fe-S proteins: an essential function of mitochondria. *Trends Biochem.Sci.* **25**(8)**:** 352-356.

Liu W, Porter NA, Schneider C, Brash AR, Yin HY (2011a). Formation of 4-hydroxynonenal from cardiolipin oxidation: Intramolecular peroxyl radical addition and decomposition. *Free Radical Biology and Medicine* **50**(1)**:** 166-178.

Liu Y, Cui KQ, Lu WQ, Luo W, Wang J, Huang J*, et al.* (2011b). Synthesis and antimalarial activity of novel dihydro-artemisinin derivatives. *Molecules* **16**(6)**:** 4527-4538.

Longo M, Zanoncelli S, Manera D, Brughera M, Colombo P, Lansen J*, et al.* (2006). Effects of the antimalarial drug dihydroartemisinin (DHA) on rat embryos in vitro. *Reproductive Toxicology* **21**(1)**:** 83-93.

Loria P, Miller S, Foley M, Tilley L (1999). Inhibition of the peroxidative degradation of haem as the basis of action of chloroquine and other quinoline antimalarials. *Biochemical Journal* **339:** 363-370.

Marroquin LD, Hynes J, Dykens JA, Jamieson JD, Will Y (2007). Circumventing the crabtree effect: Replacing media glucose with galactose increases susceptibility of HepG2 cells to mitochondrial toxicants. *Toxicological Sciences* **97**(2)**:** 539-547.

Marti F, Chadwick J, Amewu RK, Burrell-Saward H, Srivastava A, Ward SA*, et al.* (2011). Second generation analogues of RKA182: synthetic tetraoxanes with outstanding in vitro and in vivo antimalarial activities. *Medchemcomm* **2**(7)**:** 661-665.

McArdle F, Pattwell DM, Vasilaki A, McArdle A, Jackson MJ (2005). Intracellular generation of reactive oxygen species by contracting skeletal muscle cells. *Free Radical Biology and Medicine* **39**(5)**:** 651-657.

McGready R, Cho T, Cho JJ, Simpson JA, Luxemburger C, Dubowitz L*, et al.* (1998). Artemisinin derivatives in the treatment of falciparum malaria in pregnancy. *Transactions of the Royal Society of Tropical Medicine and Hygiene* **92**(4)**:** 430-433.

McGready R, Cho T, Keo NK, Thwai KL, Villegas L, Looareesuwan S*, et al.* (2001). Artemisinin antimalarials in pregnancy: A prospective treatment study of 539 episodes of multidrug-resistant Plasmodium falciparum. *Clinical Infectious Diseases* **33**(12)**:** 2009-2016.

Mercer AE (2009). The role of bioactivation in the pharmacology and toxicology of the artemisinin-based antimalarials. *Current Opinion in Drug Discovery & Development* **12**(1)**:** 125-132.

Mercer AE, Copple IM, Maggs JL, O'Neill PM, Park BK (2011). The role of heme and the mitochondrion in the chemical and molecular mechanisms of mammalian cell death induced by the artemisinin antimalarials. *Journal of Biological Chemistry* **286**(2)**:** 987-996.

Mercer AE, Copple IM, Maggs JL, Park BK (2010). The chemical and molecular basis of mammalian cell susceptibility to cell death induced by the artemisinin antimalarials. *Toxicology* **278**(3)**:** 358-359.

Mercer AE, Maggs JL, Sun X-M, Cohen GM, Chadwick J, O'Neill PM*, et al.* (2007). Evidence for the involvement of carbon-centered radicals in the induction of apoptotic cell death by artemisinin compounds. *Journal of Biological Chemistry* **282**(13)**:** 9372-9382.

Meshnick SR, Taylor TE, Kamchonwongpaisan S (1996). Artemisinin and the antimalarial endoperoxides: From herbal remedy to targeted chemotherapy. *Microbiol. Rev.* **60**(2)**:** 301-+.

Moreno-Sanchez R, Rodriguez-Enriquez S, Marin-Hernandez A, Saavedra E (2007). Energy metabolism in tumor cells. *Febs Journal* **274**(6)**:** 1393-1418.

Morrissey C, Gallis B, Solazzi JW, Kim BJ, Gulati R, Vakar-Lopez F*, et al.* (2010). Effect of artemisinin derivatives on apoptosis and cell cycle in prostate cancer cells. *Anti-Cancer Drugs* **21**(4)**:** 423-432.

Mortensen M, Ferguson DJP, Edelmann M, Kessler B, Morten KJ, Komatsu M*, et al.* (2010). Loss of autophagy in erythroid cells leads to defective removal of mitochondria and severe anemia in vivo. *Proceedings of the National Academy of Sciences of the United States of America* **107**(2)**:** 832-837.

Mosmann T (1983). Rapid colorimetric assay for cellular growth and survival – application to proliferation and cyto-toxicity assays. *Journal of Immunological Methods* **65**(1-2)**:** 55-63.

Murphy MP (2009). How mitochondria produce reactive oxygen species. *Biochemical Journal* **417:** 1-13.

Nathan AT, Singer M (1999). The oxygen trail: tissue oxygenation. *British Medical Bulletin* **55**(1)**:** 96-108.

Ndolo RA, Luan YP, Duan SF, Forrest ML, Krise JP (2012). Lysosomotropic properties of weakly basic anticancer agents promote cancer cell selectivity in vitro. *Plos One* **7**(11).

Neustadt J, Pieczenik SR (2008). Medication-induced mitochondrial damage and disease. *Molecular Nutrition & Food Research* **52**(7)**:** 780-788.

Newmeyer DD, Ferguson-Miller S (2003). Mitochondria: Releasing power for life and unleashing the machineries of death. *Cell* **112**(4)**:** 481-490.

Newton C, Hien TT, White N (2000). Cerebral malaria. *Journal of Neurology Neurosurgery and Psychiatry* **69**(4)**:** 433-441.

Newton PN, Barnes KI, Smith PJ, Evans AC, Chierakul W, Ruangveerayuth R*, et al.* (2006). The pharmacokinetics of intravenous artesunate in adults with severe falciparum malaria. *European Journal of Clinical Pharmacology* **62**(12)**:** 1003-1009.

Noedl H, Se Y, Schaecher K, Smith BL, Socheat D, Fukuda MM*, et al.* (2008). Evidence of artemisinin-resistant malaria in western Cambodia. *New England Journal of Medicine* **359**(24)**:** 2619-2620.

Nosten F, White NJ (2007). Artemisinin-based combination treatment of falciparum malaria. *Am. J. Trop. Med. Hyg.* **77**(6)**:** 181-192.

O'Brien C, Henrich PP, Passi N, Fidock DA (2011). Recent clinical and molecular insights into emerging artemisinin resistance in Plasmodium falciparum. *Current Opinion in Infectious Diseases* **24**(6)**:** 570-577.

O'Neill PM, Amewu RK, Nixon GL, ElGarah FB, Mungthin M, Chadwick J*, et al.* (2010a). Identification of a 1,2,4,5-tetraoxane antimalarial drug-development candidate (RKA 182) with superior properties to the semisynthetic artemisinins. *Angewandte Chemie-International Edition* **49**(33)**:** 5693-5697.

O'Neill PM, Barton VE, Ward SA (2010b). The molecular mechanism of action of artemisinin – the debate continues. *Molecules* **15**(3)**:** 1705-1721.

O'Neill PM, Bishop LPD, Searle NL, Maggs JL, Storr RC, Ward SA*, et al.* (2000). Biomimetic Fe(II)-mediated degradation of arteflene (Ro-42-1611). The first EPR spin-trapping evidence for the previously postulated secondary carbon-centered cyclohexyl radical. *J. Org. Chem.* **65**(5)**:** 1578-1582.

O'Neill PM, Posner GH (2004). A medicinal chemistry perspective on artemisinin and related endoperoxides. *Journal of Medicinal Chemistry* **47**(12)**:** 2945-2964.

Olliaro PL, Haynes RK, Meunier B, Yuthavong Y (2001). Possible modes of action of the artemisinin-type compounds. *Trends in Parasitology* **17**(3)**:** 122-126.

Opsenica DM, Solaja BA (2009). Antimalarial peroxides. *Journal of the Serbian Chemical Society* **74**(11)**:** 1155-1193.

Orient A, Donko A, Szabo A, Leto TL, Geiszt M (2007). Novel sources of reactive oxygen species in the human body. *Nephrology Dialysis Transplantation* **22**(5)**:** 1281-1288.

Orrenius S, Zhivotovsky B (2005). Cardiolipin oxidation sets cytochrome c free. *Nature Chemical Biology* **1**(4)**:** 188-189.

Ott M, Zhivotovsky B, Orrenius S (2007). Role of cardiolipin in cytochrome c release from mitochondria. *Cell Death and Differentiation* **14**(7)**:** 1243-1247.

Oyewole AO, Wilmot M-C, Fowler M, Birch-Machin MA (2014). Comparing the effects of mitochondrial targeted and localized antioxidants with cellular antioxidants in human skin cells exposed to UVA and hydrogen peroxide. *Faseb Journal* **28**(1)**:** 485-494.

Papi A, Contoli M, Gasparini P, Bristot L, Edwards MR, Chicca M*, et al.* (2008). Role of xanthine oxidase activation and reduced glutathione depletion in rhinovirus induction of inflammation in respiratory epithelial cells. *Journal of Biological Chemistry* **283**(42)**:** 28595-28606.

Paradies G, Petrosillo G, Paradies V, Ruggiero FM (2009). Role of cardiolipin peroxidation and Ca2+ in mitochondrial dysfunction and disease. *Cell Calcium* **45**(6)**:** 643-650.

Park BK, O'Neill PM, Maggs JL, Pirmohamed M (1998). Safety assessment of peroxide antimalarials: clinical and chemical perspectives. *British Journal of Clinical Pharmacology* **46**(6)**:** 521-529.

Pedersen PL (1978). Tumor mitochondria and the bioenergetics of cancer cells. *Progress in experimental tumor research* **22:** 190-274.

Perron NR, Beeson C, Rohrer B (2013). Early alterations in mitochondrial reserve capacity; a means to predict subsequent photoreceptor cell death. *Journal of Bioenergetics and Biomembranes* **45**(1-2)**:** 101-109.

Peshavariya HM, Dusting GJ, Selemidis S (2007). Analysis of dihydroethidium fluorescence for the detection of intracellular and extracellular superoxide produced by NADPH oxidase. *Free Radical Research* **41**(6)**:** 699-712.

Pfeiffer K, Gohil V, Stuart RA, Hunte C, Brandt U, Greenberg ML*, et al.* (2003). Cardiolipin stabilizes respiratory chain supercomplexes. *Journal of Biological Chemistry* **278**(52)**:** 52873-52880.

Ridley RG (2002). Medical need, scientific opportunity and the drive for antimalarial drugs. *Nature* **415**(6872)**:** 686-693.

Rizzo AM, Berselli P, Zava S, Montorfano G, Negroni M, Corsetto P*, et al.* (2010). Endogenous antioxidants and radical scavengers. *Bio-Farms for Nutraceuticals: Functional Food and Safety Control by Biosensors*. **698**: 52-67.

Robert A, Benoit-Vical F, Claparols C, Meunier B (2005). The antimalarial drug artemisinin alkylates heme in infected mice. *Proceedings of the National Academy of Sciences of the United States of America* **102**(38)**:** 13676-13680.

Robert A, Cazelles J, Meunier B (2001). Characterization of the alkylation product of heme by the antimalarial drug artemisinin. *Angewandte Chemie-International Edition* **40**(10)**:** 1954-1957.

Robinson KM, Janes MS, Pehar M, Monette JS, Ross MF, Hagen TM*, et al.* (2006). Selective fluorescent imaging of superoxide in vivo using ethidium-based probes. *Proceedings of the National Academy of Sciences of the United States of America* **103**(41)**:** 15038-15043.

Rodriguez M, Claparols C, Robert A, Meunier B (2002). Alkylation of microperoxidase-11 by the antimalarial drug artemisinin. *Chembiochem* **3**(11)**:** 1147-1149.

Rodriguez ME, Azizuddin K, Zhang P, Chiu S-M, Lam M, Kenney ME*, et al.* (2008). Targeting of mitochondria by 10-N-alkyl acridine orange analogues: Role of alkyl chain length in determining cellular uptake and localization. *Mitochondrion* **8**(3)**:** 237-246.

Rossignol R, Gilkerson R, Aggeler R, Yamagata K, Remington SJ, Capaldi RA (2004). Energy substrate modulates mitochondrial structure and oxidative capacity in cancer cells. *Cancer Research* **64**(3)**:** 985-993.

Saftig P, Sandhoff K (2013). Cancer killing from the inside. *Nature* **502**(7471)**:** 312-313.

Scaduto RC, Grotyohann LW (1999). Measurement of mitochondrial membrane potential using fluorescent rhodamine derivatives. *Biophysical Journal* **76**(1)**:** 469-477.

Schlame M, Rua D, Greenberg ML (2000). The biosynthesis and functional role of cardiolipin. *Progress in Lipid Research* **39**(3)**:** 257-288.

Schlattner U, Tokarska-Schlattner M, Ramirez S, Brueckner A, Kay L, Polge C*, et al.* (2009). Mitochondrial kinases and their molecular interaction with cardiolipin. *Biochimica Et Biophysica Acta-Biomembranes* **1788**(10)**:** 2032-2047.

Schmuck G, Roehrdanz E, Haynes RK, Kahl R (2002). Neurotoxic mode of action of artemisinin. *Antimicrobial Agents and Chemotherapy* **46**(3)**:** 821-827.

Segal BH, Grimm MJ, Khan ANH, Han W, Blackwell TS (2012). Regulation of innate immunity by NADPH oxidase. *Free Radical Biology and Medicine* **53**(1)**:** 72-80.

Selmeczi K, Robert A, Claparols C, Meunier B (2004). Alkylation of human hemoglobin A(0) by the antimalarial drug artemisinin. *Febs Letters* **556**(1-3)**:** 245-248.

Sidhu JS, Ashton M (1997). Single-dose, comparative study of venous, capillary and salivary artemisinin concentrations in healthy, male adults. *Am. J. Trop. Med. Hyg.* **56**(1)**:** 13-16.

Sinclair D, Zani B, Donegan S, Olliaro P, Garner P (2009). Artemisinin-based combination therapy for treating uncomplicated malaria. *Cochrane Database of Systematic Reviews*(3).

Singh NP, Lai H (2001). Selective toxicity of dihydroartemisinin and holotransferrin toward human breast cancer cells. *Life Sciences* **70**(1)**:** 49-56.

Singh NP, Lai HC (2004). Artemisinin induces apoptosis in human cancer cells. *Anticancer Research* **24**(4)**:** 2277-2280.

Singh NP, Lai HC, Park JS, Gerhardt TE, Kim BJ, Wang S*, et al.* (2011). Effects of artemisinin dimers on rat breast cancer cells in vitro and in vivo. *Anticancer Research* **31**(12)**:** 4111-4114.

Steegmann-Olmedillas JL (2011). The role of iron in tumour cell proliferation. *Clin. Transl. Oncol.* **13**(2)**:** 71-76.

Steinbrueck L, Pereira G, Efferth T (2010). Effects of artesunate on cytokinesis and G(2)/M cell cycle progression of tumour cells and budding yeast. *Cancer Genomics & Proteomics* **7**(6)**:** 337-346.

Stocks PA, Bray PG, Barton VE, Al-Helal M, Jones M, Araujo NC*, et al.* (2007). Evidence for a common non-heme chelatable-iron-dependent activation mechanism for semisynthetic and synthetic endoperoxide antimalarial drugs. *Angewandte Chemie-International Edition* **46**(33)**:** 6278-6283.

Supinski G, Nethery D, Stofan D, DiMarco A (1999). Extracellular calcium modulates generation of reactive oxygen species by the contracting diaphragm. *Journal of Applied Physiology* **87**(6)**:** 2177-2185.

Swiss R, Niles A, Cali JJ, Nadanaciva S, Will Y (2013). Validation of a HTS-amenable assay to detect drug-induced mitochondrial toxicity in the absence and presence of cell death. *Toxicology in Vitro* **27**(6)**:** 1789-1797.

Tahara EB, Navarete FDT, Kowaltowski AJ (2009). Tissue-, substrate-, and site-specific characteristics of mitochondrial reactive oxygen species generation. *Free Radical Biology and Medicine* **46**(9)**:** 1283-1297.

Tait SWG, Green DR (2010). Mitochondria and cell death: Outer membrane permeabilization and beyond. *Nature Reviews Molecular Cell Biology* **11**(9)**:** 621-632.

Taylor RC, Cullen SP, Martin SJ (2008). Apoptosis: Controlled demolition at the cellular level. *Nature Reviews Molecular Cell Biology* **9**(3)**:** 231-241.

Thomas C, Mackey MM, Diaz AA, Cox DP (2009). Hydroxyl radical is produced via the Fenton reaction in submitochondrial particles under oxidative stress: Implications for diseases associated with iron accumulation. *Redox Report* **14**(3)**:** 102-108

Toovey S (2006). Are currently deployed artemisinins neurotoxic? *Toxicology Letters* **166**(2)**:** 95-104.

Tu Y (2011). The discovery of artemisinin (qinghaosu) and gifts from Chinese medicine. *Nature Medicine* **17**(10)**:** 1217-1220.

Turrens JF (2003). Mitochondrial formation of reactive oxygen species. *Journal of Physiology-London* **552**(2)**:** 335-344.

Uchiyama A, Kim J-S, Kon K, Jaeschke H, Ikejima K, Watanabe S*, et al.* (2008). Translocation of Iron from lysosomes into mitochondria is a key event during oxidative stress-induced hepatocellular injury. *Hepatology* **48**(5)**:** 1644-1654.

Uhlemann A-C, Wittlin S, Matile H, Bustamante LY, Krishna S (2007). Mechanism of antimalarial action of the synthetic trioxoane RBX11160 (OZ277). *Antimicrobial Agents and Chemotherapy* **51**(2)**:** 667-672.

Vanlangenakker N, Vanden Berghe T, Krysko DV, Festjens N, Vandenabeele P (2008). Molecular mechanisms and pathophysiology of necrotic cell death. *Current Molecular Medicine* **8**(3)**:** 207-220.

Vertuani S, Angusti A, Manfredini S (2004). The antioxidants and pro-antioxidants network: An overview. *Current Pharmaceutical Design* **10**(14)**:** 1677-1694.

Wang C, Youle RJ (2009). The role of mitochondria in apoptosis. *Annual Review of Genetics*, Vol. 43: 95-118.

Wang J, Huang LY, Li J, Fan QW, Long YC, Li Y*, et al.* (2010). Artemisinin directly targets malarial mitochondria through its specific mitochondrial activation. *Plos One* **5**(3)**:** A158-A169.

Wang X, Dong Y, Wittlin S, Charman SA, Chiu FCK, Chollet J*, et al.* (2013). Comparative antimalarial activities and ADME profiles of ozonides (1,2,4-trioxolanes) OZ277, OZ439, and their 1,2-dioxolane, 1,2,4-trioxane, and 1,2,4,5-tetraoxane isosteres. *Journal of Medicinal Chemistry* **56**(6)**:** 2547-2555.

Warren MJ, Smith AG (2009). *Tetrapyrroles: Birth, Life and Death*. 9th edn. Landes Bioscience.

Wartenberg M, Wolf S, Budde P, Grunheck F, Acker H, Hescheler J*, et al.* (2003). The antimalaria agent artemisinin exerts antiangiogenic effects in mouse embryonic stem cell-derived embryoid bodies. *Laboratory Investigation* **83**(11)**:** 1647-1655.

Weifeng T, Feng S, Xiangji L, Changqing S, Zhiquan Q, Huazhong Z*, et al.* (2011). Artemisinin inhibits in vitro and in vivo invasion and metastasis of human hepatocellular carcinoma cells. *Phytomedicine : international journal of phytotherapy and phytopharmacology* **18**(2-3)**:** 158-162.

White NJ (2008). Qinghaosu (artemisinin): The price of success. *Science* **320**(5874)**:** 330-334.

White TEK, Bushdid PB, Ritter S, Fan SBL, Clark RL (2006). Artesunate-induced depletion of embryonic erythroblasts precedes embryolethality and teratogenicity in vivo. *Birth Defects Res. Part B-Dev. Reprod. Toxicol.* **77**(5)**:** 413-429.

WHO (2006). World Health Organisation Assessment of the Safety of Artemisinin Compounds in Pregnancy.

WHO (2010). World Health Organisation Guidelines for the Treatment of Malaria, Second edn.

Will Y, Dykens J (2014). Mitochondrial toxicity assessment in industry - a decade of technology development and insight. *Expert Opinion on Drug Metabolism & Toxicology* **10**(8)**:** 1061-1067.

Will Y, Hynes J, Ogurtsov VI, Papkovsky DB (2006). Analysis of mitochondrial function using phosphorescent oxygen-sensitive probes. *Nature Protocols* **1**(6)**:** 2563-2572.

Woerdenbag HJ, Moskal TA, Pras N, Malingre TM, Elferaly FS, Kampinga HH*, et al.* (1993). Cytotoxicty of artemisinin-related endoperoxides to Ehrlich ascites tumor-cells. *Journal of Natural Products* **56**(6)**:** 849-856.

Wu WM, Wu YK, Wu YL, Yao ZJ, Zhou CM, Li Y*, et al.* (1998). Unified mechanistic framework for the Fe(II)-induced cleavage of qinghaosu and derivatives/analogues. The first spin-trapping evidence for the previously postulated secondary C-4 radical. *Journal of the American Chemical Society* **120**(14)**:** 3316-3325.

Wu YK, Liu HH (2003). Probing the possible molecular origin of the highly selective toxicity of antimalarial peroxide Qinghaosu (artemisinin). *Chemical Research in Toxicology* **16**(10)**:** 1202-1206.

Xie LJ, Zhai X, Ren LX, Meng HY, Liu C, Zhu WF*, et al.* (2011). Design, synthesis and antitumor activity of novel artemisinin derivatives using hybrid approach. *Chemical & Pharmaceutical Bulletin* **59**(8)**:** 984-990.

Xu RH, Pelicano H, Zhou Y, Carew JS, Feng L, Bhalla KN*, et al.* (2005). Inhibition of glycolysis in cancer cells: A novel strategy to overcome drug resistance associated with mitochondrial respiratory defect and hypoxia. *Cancer Research* **65**(2)**:** 613-621.

Yang L, Huang Y, Wang HQ, Chen ZY (2002). Production of conjugated linoleic acids through KOH-catalyzed dehydration of ricinoleic acid. *Chemistry and Physics of Lipids* **119**(1-2)**:** 23-31.

Yang YZ, Asawamahasakda W, Meshnick SR (1993). Alkylayion of human albumin by the antimalarial artemisinin. *Biochemical Pharmacology* **46**(2)**:** 336-339.

Yang YZ, Little B, Meshnick SR (1994). Alkylation of proteins by artemisinin – effects of heme, pH, and drug structure. *Biochemical Pharmacology* **48**(3)**:** 569-573.

Yeung S, Van Damme W, Socheat D, White NJ, Mills A (2008). Cost of increasing access to artemisinin combination therapy: The Cambodian experience. *Malaria Journal* **7**.

Yin H, Zhu M (2012). Free radical oxidation of cardiolipin: chemical mechanisms, detection and implication in apoptosis, mitochondrial dysfunction and human diseases. *Free Radical Research* **46**(8)**:** 959-974.

Zhang S, Gerhard GS (2009). Heme Mediates Cytotoxicity from artemisinin and serves as a general anti-proliferation target. *Plos One* **4**(10).

Zhang X, Lemasters JJ (2013). Translocation of iron from lysosomes to mitochondria during ischemia predisposes to injury after reperfusion in rat hepatocytes. *Free Radical Biology and Medicine* **63:** 243-253.

Zhao HT, Kalivendi S, Zhang H, Joseph J, Nithipatikom K, Vasquez-Vivar J*, et al.* (2003). Superoxide reacts with hydroethidine but forms a fluorescent product that is distinctly different from ethidium: Potential implications in intracellular fluorescence detection of superoxide. *Free Radical Biology and Medicine* **34**(11)**:** 1359-1368.

Zielonka J, Kalyanaraman B (2010). Hydroethidine- and MitoSOX-derived red fluorescence is not a reliable indicator of intracellular superoxide formation: Another inconvenient truth. *Free Radical Biology and Medicine* **48**(8)**:** 983-1001.

Zorov DB, Juhaszova M, Sollott SJ (2014). Mitochondrial reactive oxygen species (ROS) and ROS-induced ROS release. *Physiological Reviews* **94**(3)**:** 909-950.

Zorov DB, Juhaszova M, Sollott SJ (2006). Mitochondrial ROS-induced ROS release: An update and review. *Biochimica Et Biophysica Acta-Bioenergetics* **1757**(5-6)**:** 509-517.